HEINRICH HEINE
UNIVERSITÄT DÜSSELDORF

Interleukin-26

A cytokine at the interface between innate and adaptive immunity

Inaugural dissertation

for the attainment of the title of doctor

in the Faculty of Mathematics and Natural Sciences

at the Heinrich Heine University Düsseldorf

presented by

Heike Carolin Hawerkamp

from Schwäbisch Hall

Düsseldorf, November 2018

From the Department of Dermatology, Heinrich Heine University Hospital
at the Heinrich Heine University Düsseldorf

Published by permission of the
Faculty of Mathematics and Natural Sciences at
Heinrich Heine University Düsseldorf

Supervisor: PD Dr. Stephan Meller

Co-supervisor: Univ.-Prof. Dr. Johannes Hegemann

Day of the oral examination: 24th April 2019

Table of content

Abstract

Interleukin-26 (IL-26) is a cytokine mainly secreted from T_H17 cells with multifaceted characteristics. IL-26 signals through a receptor heterodimer consisting of IL-20R1 and IL-10R2. This unique heterodimeric combination is only found on a few cell types, such as epithelial cell. In these cells, such as keratinocytes or colon cells, IL-26 signals via the STAT pathway and elicits the secretion of pro-inflammatory IL-8. Investigating the molecular properties of IL-26, it was revealed that IL-26 is highly cationic and has an amphipathic structure, a phenomenon where charged amino acids cluster within the molecule. This amphipathic structure is common among antimicrobial peptides. Similar to antimicrobial peptides, IL-26 is able to directly kill microorganisms. Besides this impact on innate immunity, IL-26 also plays a role in autoimmunity. IL-26's cationic surface allows for binding to human self-DNA, which then gets transferred into immune cells that erroneously induce an antiviral immune response.

In this project, we characterize the role of IL-26 in different skin diseases via gene expression analysis. Furthermore, we closely investigate the binding partners of IL-26 on the surface of different microbes, such as LPS and LTA, using microscale thermophoresis, including a broad investigation of IL-26's potential in killing mycobacteria, as well as its role in tuberculosis. Additionally, the investigation on the binding of IL-26 to anionic compounds is extended to RNA, and the subsequent effects of IL-26/RNA complexes on the respective immune cells, such as dendritic cells, were elucidated. As immune cells need to be attracted to such inflammatory sites, we set off to uncover some chemokine ligand and receptor patterns involved in immune cell recruitment in the presence of IL-26 and IL-26 nucleic acid complexes. Seeing that immune cells respond to IL-26 in absence of the IL-26 receptor, we investigate suitable surface molecules that might transmit signals upon IL-26 binding. Another part of this project aims to unveil the effects of IL-26 under reducing conditions that resemble the physiological state during inflammation. Here, we compare the oxidized IL-26 to its reduced counterpart without disulphide bonds, and examined the effects on protein binding partners as well as on stimulatory capacity of immune cells.

Abstract in German

Interleukin-26 (IL-26) ist ein Zytokin, das hauptsächlich von T_H17 Zellen sekretiert wird und vielseitige Charakteristika aufweist. IL-26 vermittelt seine Signale durch ein Rezeptorheterodimer bestehend aus IL-20R1 und IL-10R2. Diese spezifische Heterodimer-Kombination ist nur auf wenigen Zelltypen wie zum Beispiel Epithelzellen zu finden. In diesen Epithelzellen, zu denen Keratinozyten oder auch Kolonzellen gehören, überträgt IL-26 seine Signale mithilfe des STAT-Signalweges und löst die Sekretion von pro-inflammatorischem IL-8 aus. Bei Untersuchungen der molekularen Eigenschaften des IL-26 zeigte sich, dass das Protein stark kationisch ist und eine amphipatische Struktur aufweist. Hierbei finden sich geladene Aminosäuren in Gruppen an verschiedenen Seiten des Moleküls zusammen. Diese amphipatische Struktur ist sehr verbreitet unter antimikrobiellen Peptiden. Ähnlich wie antimikrobielle Peptide ist IL-26 in der Lage Mikroorganismen direkt abzutöten. Neben diesem Einfluss in der angeborenen Immunität, spielt IL-26 auch eine Rolle in der Autoimmunität. Die kationische Oberfläche des IL-26 erlaubt die Bindung an humane DNA, die dann wiederum in Immunzellen eingeschleust werden kann und dort fälschlicherweise eine antivirale Immunreaktion hervorruft.

In diesem Projekt wurde die Rolle des IL-26 in verschiedenen Hautkrankheiten als auch in der Infektionskrankheit Tuberkulose untersucht. Des Weiteren wurde die Bindung des IL-26 gegenüber Oberflächenmolekülen wie LPS oder LTA, die sich auf unterschiedlichen Mikroben befinden, untersucht. In diesem Rahmen wurde auch die ermittelt in welchem Umfang IL-26 in der Lage ist das Mycobacterium tuberculosis, den Erreger der Tuberkulose abzutöten. Es wurde zudem weitere Untersuchungen betreffend der Rolle des IL-26 in der angeborenen Immunität unternommen und hierbei die Binding des IL-26 an RNA überprüft und Effekte dieser IL-26/RNA-Komplexe auf dendritische Zellen beleuchtet. Da Immunzellen mithilfe sogenannter Chemokine an Entzündungsherde gelockt werden, wurde untersucht ob IL-26 hier eine direkte Funktion hat oder in Komplex mit Nukleinsäuren diese Rezeptoren oder Liganden auf entsprechenden Immunzellen regulieren kann. In einem anderen Aspekt dieses Projekts wurde das IL-26 unter reduzierenden Bedingungen getestet, welche dem physiologischen Zustand während einer Entzündung ähnlich sind. Dazu wurde das oxidierte IL-26 mit seinem reduzierten Gegenstück ohne Disulphidbrücken bezüglich Bindungsaffinitäten und Effekte auf Immunzellen untersucht.

Publications

Publications and manuscripts

Publication

Stephan Meller, Jeremy Di Domizio, Kui S. Voo, **Heike C. Friedrich,** Georgios Chamilos, Dipyaman Ganguly, Curdin Conrad, Josh Gregorio, Didier Le Roy, Thierry Roger, John E. Ladbury, Bernhard Homey, Stanley Watowich, Robert L. Modlin, Dimitrios P. Kontoyiannis, Yong-Jun Liu, Stefan T. Arold and Michel Gilliet:

Th17 cells promote microbial killing and innate immune sensing of DNA via IL-26, Nat Immunol. 2015 Sep;16(9):970-9. doi: 10.1038/ni.3211

Impact Factor: 19.381

Contribution to the publication: 5 %

- prepared skin specimen and performed ELISAs
- wrote part of the manuscript

Manuscript in revision

Heike C. Hawerkamp, Lasse van Geelen, Jan Korte, Marc Swidergall, Joachim Ernst, Rainer Kalscheuer, Bernhard Homey, Stephan Meller:

Interleukin-26 activates macrophages and facilitates killing of *Mycobacterium tuberculosis*

For publication in *Scientific Reports*

First author

Contribution to the publication: 85 %

- planned, performed, and analyzed most experiments
- generated figures
- wrote large parts of the manuscript

Meeting abstracts

Presentation

Stephan Meller, Jeremy Di Domizio, **Heike C. Friedrich**, Marc Swidergall, Laura Gayk, Lothar Gremer, Bernhard Homey, Michel Gilliet:

Interleukin-26 and its role in inflammatory conditions of the skin;

43rd Scandinavian Society for Immunology Meeting 2016, Turku, Finland

Poster

Laura Gayk, **Heike C. Friedrich**, Alessio Mylonas, Curdin Conrad, Michel Gilliet, Bernhard Homey, Stephan Meller:

Reduktion der Disulfidbrücken des IL-26 erleichtert Immunreaktionen in Rosazea;

Symposium der medical Research School Düsseldorf (medRSD) 2016, Düsseldorf

Index of abbreviations

AD	Atopic dermatitis
ADS	Albumin, D-glucose, Salt
AMP	Antimicrobial peptide
APC	Antigen-presenting cells
BCA	Bicinchoninic acid
β-ME	β-mercaptoethanol
BSA	Bovine serum albumin
BSL	Biosafety level
BPE	Bovine pituitary extract
CD	Cluster of differentiation
cDNA	Complementary DNA
CFU	Colony forming units
CO_2	Carbon dioxide
CRF2	Cytokine class II receptor family
CPD	Critical point drying
DAPI	4′,6-diamidin-2-phenylindol
DC	Dendritic cell
DMEM	Dulbecco’s Modified Eagle's Medium
DMSO	Dimethyl sulphoxide
DNA	Deoxyribonucleic acid
dNTP	Deoxy nucleoside triphosphate
DTBA	Dithiobutylamine
DTT	Dithiothreitol
ECM	Extracellular matrix
EDTA	Ethylenediaminetetraacetic acid
EGF	epidermal growth factor
ELISA	Enzyme linked immunoassay
ESI-MS	Electrospray ionization mass spectrometry
FAM	Fluorescein amidite
FCS	Fetal calf serum
FFPE	Formalin-fixed paraffin-embedded (tissue)
FITC	Fluorescein isothiocyanate

FLS	Fibroblast-like synoviocyte
GM-CSF	Granulocyte-macrophage colony-stimulating factor
hBD	Human β-defensin
HCl	Hydrogen chloride
HIF	Hypoxia-inducible factor
HPLC	High performance liquid chromatography
HRP	Horseradish peroxidase
ICAM	Intercellular adhesion molecule 1
IF	Immunofluorescence
IFN	Interferon
IHC	Immunohistochemistry
IL	Interleukin
ILC	Innate lymphoid cell
IR	Infrared
KH_2PO_4	Potassium dihydrogen phosphate
K_2HPO_4	Dipotassium hydrogen phosphate
LAM	Lipoarabinomannan
LED	Light-emitting diode
LN	Lymph node
LPS	Lipopolysaccharide
LTA	Lipoteichoic acid
MAPK	Mitogen-activated protein kinase
M-CSF	Macrophage colony-stimulating factor
MF	Mycosis fungoides
$MgCl_2$	Magnesium chloride
MIC	Minimal inhibitory concentration
moDC	Monocyte-derived dendritic cell
MΦ	Macrophage
MST	Microscale Thermophoresis
MTT	3-(4,5-dimethylthiazol-2-yl)-2,5-diphenyltetrazolium bromide
NaCl	Sodium chloride
NADPH	Nicotinamide adenine dinucleotide phosphate
NF-κB	nuclear factor kappa-light-chain-enhancer of activated B cells

NH_4Cl	Ammonium chloride solution
NK cell	Natural killer cell
OD	Optical density
O_2	Oxygen
PBMC	Peripheral mononuclear cells
PBS	Phosphate buffered saline
PCR	Polymerase chain reaction
pDC	Plasmacytoid dendritic cell
PMA	Phorbol 12-myristate 13-acetate
Poly (I:C)	Polyinosinic:polycytidylic acid
PRR	Pattern-recognition receptor
PV	Psoriasis vulgaris
RA	Rheumatoid arthritis
RNA	Ribonucleic acid
RORγt	Retinoic acid related orphan receptor gamma transcription
RPMI	Roswell Park Memorial Institute (medium)
RT	Room temperature
SCC	Squamous cell carcinoma
SDS	Sodium dodecyl sulphate
SDS-PAGE	Sodium dodecyl sulfate polyacrylamide gel electrophoresis
SEAP	Secreted embryonic alkaline phosphatase
SEM	Scanning electron microscopy
SFM	Serum-free medium
TCEP	Tris(2-carboxyethyl)phosphine
TFA	Trifluoraocetic acid
T_H cell	T helper cell
TLR	Toll-like receptor
TNF	Tumor necrosis factor
TSB	Tryptic soy broth
TXN	Thioredoxin
TXNRD1	Thioredoxin reductase

1 Introduction

1.1 Healthy human skin

The human skin is one of the largest and most important immunologic organs[1,2]. The skin can roughly be divided into three layers: the epidermis, which is the outermost layer consisting mainly of keratinocytes in various differentiation states, the dermis, which is the middle layer of the skin where blood and lymphatic vessels are found and the majority of immune cells reside, and finally a subcutaneous fatty layer[3,4]. The epidermis can further be divided into the stratum corneum, stratum granulosum, stratum spinosum, and stratum basale. The epidermis is separated from the dermis via the basement membrane[3,4]. The dermis is further separated into two compartments: the papillary dermis located at the basement membrane and the much thicker reticular dermis[5]. Large and important skin structures such as hair (follicle and roots), glands (sebaceous and sweat), nerve fibers, and different vessels are found within the dermis[5]. The main cells in this layer are dermal fibroblasts that produce collagen and thereby provide the skin with flexibility, and also structure[5]. Due to its location as the outer surface of the body, the skin needs to be able to protect the body against all sorts of environmental threats. Thus, the skin is populated with a variety of immune cells. Some immune cells reside in the epidermis: mainly Langerhans cells (specialized epidermal dendritic cells (DC)), but also T cells that carry a protein named cluster of differentiation (CD) 8 on their surface, and so are referred to as $CD8^+$ T cells. The majority of immune cells are found in the dermis, where they enter the tissue from the vessels. These specialized cells are plasmacytoid DCs, dermal DCs, tissue macrophages, different subtypes of $CD4^+$ T helper (T_H) cells, namely T_H1 cells, T_H2 cells, and T_H17 cells, but also natural killer (NK) T cells and innate lymphocytic cells (ILC)[4].

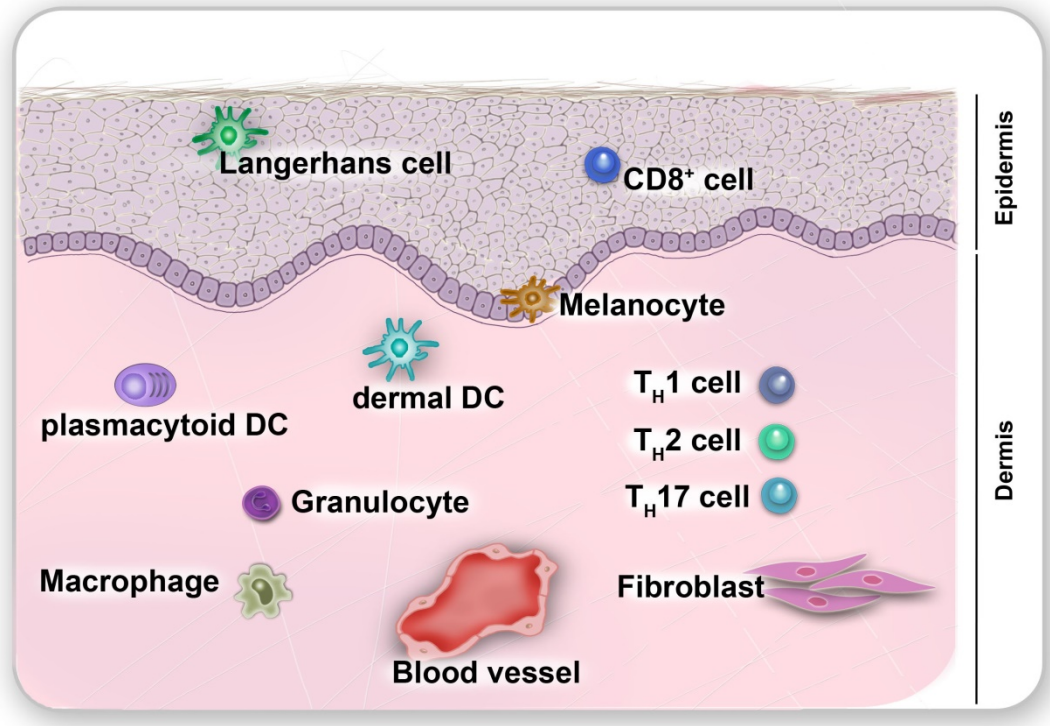

FIGURE 1: Human skin, its two outermost layers and the skin-residing immune cells. Scheme with modifications adapted from: Nestle *et al.* 2013[3].

1.1.1 Structural skin cells

1.1.1.1 Keratinocytes

Keratinocytes are the cells that form the epidermal skin layer and are found in various shapes[3,4,6]. Starting from the inner epidermal layer, one finds rapidly proliferating, undifferentiated keratinocytes, referred to as basal keratinocytes. These keratinocytes then differentiate, change their shape, divide further, move to the stratum spinosum, and start the production of proteins and lipids[3]. Reaching the stratum granulosum, the keratinocytes are at their maximum production of lipids and proteins. The outermost layer of the epidermis, the stratum corneum, is characterized by corneocytes. These are dead keratinocytes without organelles, and they are playing a huge role in the skin barrier as they prevent external substances from entering and water from leaving the skin[3].

1.1.1.2 Fibroblasts

Dermal fibroblasts provide their respective skin layer with extracellular matrix (ECM) and thereby generate a flexible structure[5,7,8]. Generally, depending on

the localization within the dermis, different fibroblasts can be defined as either upper papillary or lower reticular fibroblasts[7]. Some progenitor fibroblasts can also differentiate into intradermal adipocytes[5]. Fibroblasts produce collagens, different elastic fibers such as elastin for skin stability, a diverse range of proteoglycans, and fiber-forming proteins that play an important role in wound healing[8].

1.2 Immune system

The immune system is the entirety of all immune cells and immune effectors, for example cytokines or antimicrobial proteins. This system is our powerful weapon against all sorts of intruders, be it environmental toxins or microorganisms such as fungi, bacteria, or viruses. The immune system also controls the body cells and eliminates diseased or dead cells.

The immune system can be divided into the innate and the adaptive immune system, which both work together[9-11]. The innate immune system – as the name implies – is fully functional at birth. It is fast acting and broad in its responses, but very effective in fighting intruding microorganisms[9,10]. The adaptive immune system is very precise, as it acts after an antigen encounter with antibody production only against the specific antigen. After an antigen encounter, memory cells will be generated to fight the antigen faster in a second encounter[10,11].

1.3 Immune cells

The majority of our immune cells are T lymphocytes and B lymphocytes in various subtypes belonging to the lymphoid lineage[11]. Their names refer to the organ where they develop: T cells in the thymus and B cells in the bone marrow[11]. As both thymus and bone marrow are organs where immune cells develop, they are called primary lymphoid organs. During the maturation and differentiation, the immune cells move to the secondary lymphoid organs. such as the spleen and lymph nodes, but also the respiratory tract and skin[11].

Another immune cell lineage is the myeloid lineage. This group consists of blood monocytes that differentiate into macrophages inside tissues and granulocytes, which are divided again into neutrophils (also called: neutrophilic granulocytes), eosinophils, and basophils[12]. A third group belonging to this

lineage are the dendritic cells (DCs), which are further classified into myeloid DCs or plasmacytoid DCs[12].

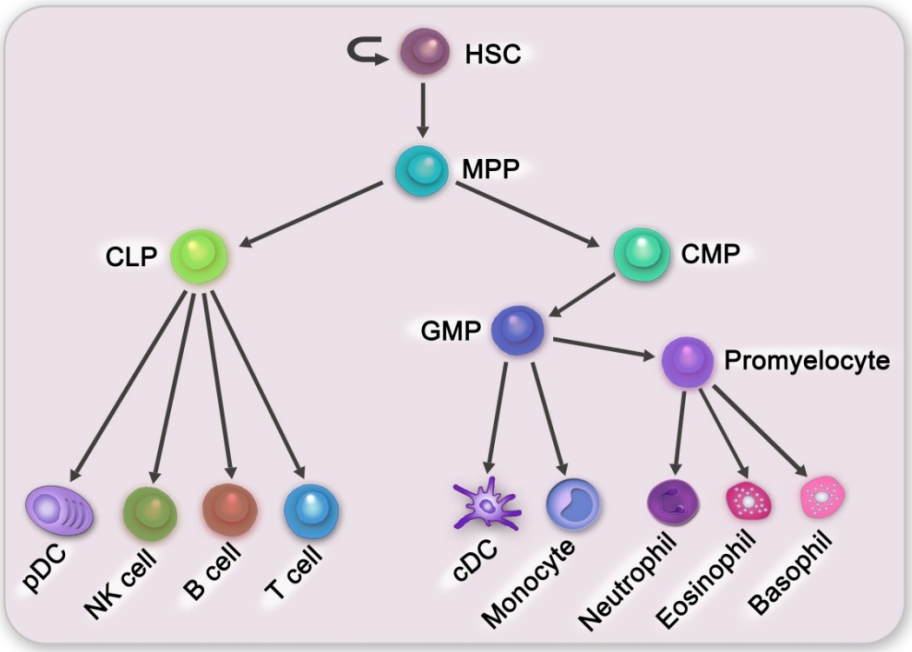

FIGURE 2: The immune cells derive from two different lineages: the lymphoid and the myeloid lineage. Lymphoid cells derive from a common lymphoid precursor (CLP) and myeloid cells derive from a common myeloid precursor (CMP). Abbreviations: HSC; hematopoietic stem cell, MPP; multipotent progenitor, GMP; granulocyte- monocyte progenitor, pDC; plasmacytoid dendritic cell, cDC; classical dendritic cell. Image with modifications from: Luis. 2012[13].

1.3.1 T cells

T cells are divided into two main subgroups: cytotoxic $CD8^+$ T cells and helper $CD4^+$ T cells (T helper (T_H) cells)[11].

$CD4^+$ T_H cells are further divided into four main populations: T_H1, T_H2, T_H17 cells, and induced regulatory T cells (iTregs)[14,15]. Each population has its role within the adaptive immune system.

T_H1 cells develop in the presence of interferon (IFN)-γ and interleukin (IL)-12 from naïve $CD4^+$ T cells[16]. T_H1 cells are characterized by the transcription factors T-bet and signal transducer and activator of transcription (STAT) 4[14]. After differentiation, they produce cytokines such as IL-2, IFN-γ, and lymphotoxin (LT)-α. This cytokine portfolio makes them perfectly suitable to fight intracellular pathogens, but they also play a role in autoimmunity when deregulated[14].

T_H2 cells need a combination of IL-4 and IL-2 for their differentiation and express the STAT5 and the GATA3 transcription factor[14]. The name of the latter refers to its DNA binding sequence (A/T)GATA(A/G)[17]. The characteristic cytokines produced by T_H2 cells are IL-4, IL-5, IL-9, IL-13, IL-25 (also known as IL-17E), and IL-10. Producing IL-5, which attracts eosinophils, and IL-13, which helps in banishing – for example – worms, makes T_H2 cells the guardians against extracellular parasites. But they also play a role in asthma and allergies[14].

The presence of IL-6, IL-21, IL-23, and transforming growth factor (TGF)-β leads to the differentiation from naïve $CD4^+$ T cells into T_H17 cells[14,15]. This T cell subpopulation is defined by the transcription factors STAT3 and retinoic acid related orphan receptor gamma transcription (RORγt)[18]. T_H17 cells produce IL-21, IL-17A, IL-17F, and IL-22[14]. Recently, the production of IL-26 and IL-29 by T_H17 cells has been described[19,20]. These cytokines are useful in the defense against extracellular bacteria and fungi. A deregulation here will eventually lead to autoimmunity.

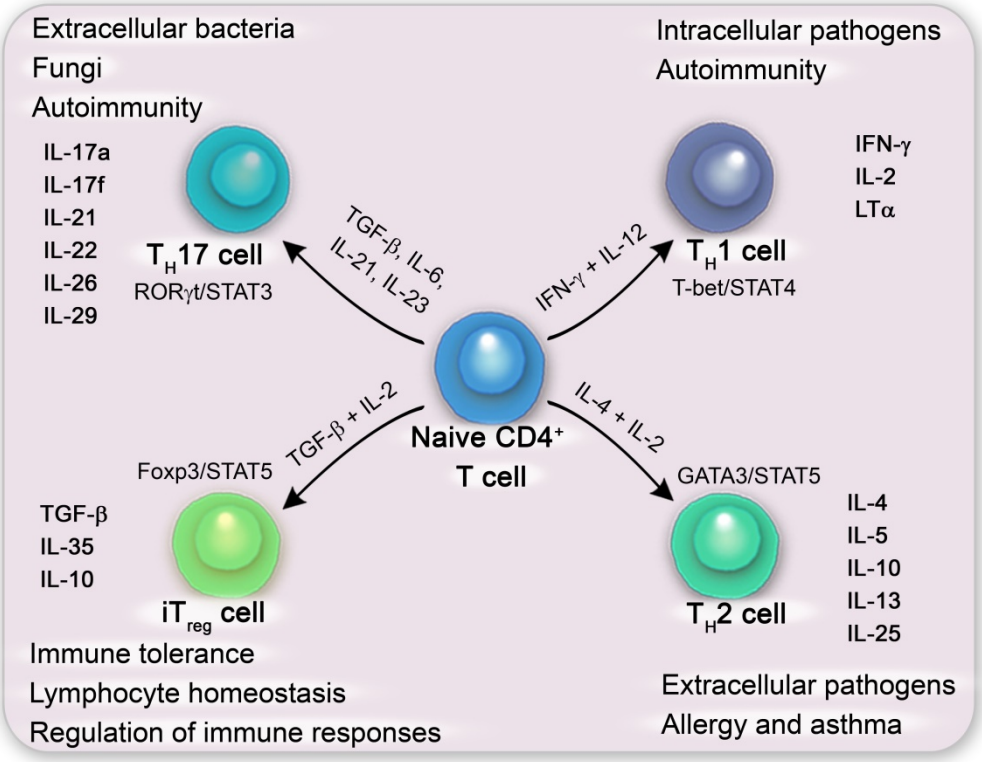

FIGURE 3: Naïve $CD4^+$ T cells can differentiate into four main subsets. These subsets are classified according to the cytokines needed for their differentiation, their transcriptions factors, and the cytokines they produce. The cytokine pattern of the respective subsets determines their task within the immune system. Illustration modified from: Zhu. 2008[14].

Besides T_H17 cells, there are two more T cells populations that are named after their signature cytokine: IL-9 producing T cells (T_H9 cells) and IL-22 producing T cells (T_H22 cells)[15]. T_H9 cells were initially identified as a subpopulation of T_H2 cells[21-23]. T_H22 cells are found to express the unique transcription factors basonuclein (BNC)-2 and forkhead box (Fox) O4, and play an important role in skin immunity[24]. Unlike T_H17 cells, T_H22 cells are not able to produce IL-17[24,25].

Coming to immune regulation, the specialized T cell population that fulfill this task are Tregs[14], Treg development needs IL-2 and TGF-β, and their distinguishing transcription factors are STAT5 and Foxp3[18]. The cytokines produced by Tregs comprise TGF-β for maintenance of a positive feedback loop, but also IL-10 and IL-35. Besides the regulation of immune responses, Tregs are additionally involved in immune tolerance and lymphocyte homeostasis[14].

1.3.2 Monocytes

Monocytes are blood-circulating immune effector cells that are characterized by a high expression of CD14[12,26]. Furthermore, monocytes can be divided into ‘classical monocytes’, lacking expression of CD16, and ‘(tissue) resident macrophages’, showing expression of CD16[26]. Monocytes arise in the bone marrow from myeloid progenitor cells and circulate in the blood some time before they enter the tissue and differentiate into DCs or macrophages[26-28]. Considering this differentiation, some researchers see monocytes as “DC precursors”[29]. In order to facilitate the migration into tissues, monocytes are decorated with adhesion molecules and express a number of chemokines[26,28]. Monocytes are capable of producing inflammatory cytokines, and are capable of phagocytosis of cells or various substances that they then intracellularly process to antigens that are presented to T cells[28].

In vitro monocytes can be differentiated into so called monocyte-derived DCs (moDCs) in the presence of granulocyte-macrophage colony-stimulating factor (GM-CSF) and IL-4. To generate monocyte-derived macrophages *in vitro*, monocytes need to be cultured with GM-CSF or M-CSF[27].

1.3.3 Dendritic cells (DCs)

Classical dendritic cells (cDCs) or DCs act at the border between the innate and adaptive immune systems[30,31]. They are antigen-presenting cells (APC) that are able to take up intruding microorganisms and viruses, process them, and present them to T cells to activate an adaptive immune response. Furthermore, the DCs carry different pattern-recognition receptors (PRR), such as Toll-like receptors (TLRs), that recognize conserved patterns found on microorganisms and viruses[31].

The specific skin DCs, so called Langerhans cells, express TLR1, TLR2, and TLR6 together with low amounts of TLR3[31]. More about TLRs is found in the designated chapter (chapter 1.7).

1.3.4 Macrophages

Macrophages are phagocytic APCs that arise from monocytes and reside in tissues[28]. Macrophages are a high heterogeneous group of cells: depending on the organ they are residing, in they display different phenotypes. Based on these phenotypes, they have been classified into Langerhans cells, which are found in the epidermal layer of the skin, or Kupffer cells found in the liver. Furthermore, there are alveolar macrophages in the lung and splenic macrophages found in the spleen[26].

1.3.5 Plasmacytoid dendritic cells (pDCs)

Plasmacytoid dendritic cells (pDCs) are from cDCs, as they arise from a different progenitor cell[13]. They are a rare cell population found in the blood stream (0.3 to 0.5% of human peripheral blood) and different organs, such as the skin[28,32,33]. PDCs are highly specialized cells for viral defense as they are able to secrete a vast amount of type I interferons upon viral infection[28]. PDCs have an exclusive TLR expression pattern as, except for TLR6, the other TLRs (TLR1, TLR7 and TLR9) are not expressed in cDCs[31]. Due to their high expression of endosomal TLR7 and 9, pDCs are able to detect intracellular foreign, bacterial, and viral nucleic acids[34,35]. PDCs can be detected in tissues via the marker anti-CD303[36].

1.4 Interleukins

Interleukins are secreted proteins specific to the (adaptive) immune system and promote *inter*action between *leuk*ocytes by binding to the receptor on the target cells (white blood cells). In 1977 the first interleukin was described as produced by monocytes[37]. The list of interleukins is continuously growing, and recently IL-39 and IL-40 were described[38,39].

1.4.1 Interleukin-26

The IL-26 protein was originally named AK155, and was discovered and cloned by Knappe and colleagues in the year 2000[40]. The *IL26* gene is found on the long arm of chromosome 12q15 close to the Interferon (IFN)-γ gene. There is no homologues *IL26* gene in mice, but there was an extensive study published on chicken IL-26[41].

1.4.1.1 Protein properties of IL-26

The IL-26 protein is composed of 171 amino acids (see below) that build six alpha helices[40]. Additionally, there are five highly conserved cysteines (Table 1), of which four build two intramolecular disulphide bonds and the fifth cysteine is predicted to pair with the fifth cysteine from a second IL-26 protein to form a homodimer[40]. As IL-26 shares high amino acid identity (24.7%) and similarity (47%) with human IL-10, it was classified to be a member of the human IL-10 family[40]. Another similarity of IL-26 to IL-10 is the ability to form the above-mentioned homodimers[40].

Recombinant oxidized IL-26 monomeric protein has a total of 151 amino acids, starting from lysine (three-letter code: Lys; one-letter code: K) at position 22 and ending with glutamine (Gln; Q) at position 171, together with an N-terminal methionine (Met) according to the corresponding datasheet. The recombinant IL-26 protein lacks a signal peptide. The disulphide bond forming cysteines (cys11 - cys100 (1st cys - 4th), cys58 – cys103 (2nd - 5th)) were marked turquoise and the free cysteine (pos: 81(3rd)) was marked magenta[19]. This means the recombinant IL-26 one-letter amino acid code reads as follows:

MKHKQSSFTKSCYPRGTLSQAVDALYIKAAWLKATIPEDRIKNIRLLKKKTKKQ
FMKNCQFQEQLLSFFMEDVFGQLQLQGCKKIRFVEDFHSLRQKLSHCISCAS
SAREMKSITRMKRIFYRIGNKGIYKAISELDILLSWIKKLLESSQ

The physiological IL-26 protein with signal peptide (coloured green) reads as follows:

MLVNFILRCGLLLVTLSLAIA_KHKQSSFTKSCYPRGTLSQAVDALYIKAAWLKA TIPEDRIKNIRLLKKKTKKQFMKNCQFQEQLLSFFMEDVFGQLQLQGCKKIRFV EDFHSLRQKLSHCISCASSAREMKSITRMKRIFYRIGNKGIYKAISELDILLSWIK KLLESSQ

The molecular weight of recombinant IL-26 (including N-terminal methionine) is 17,714.0 Daltons (http://web.expasy.org/protparam/). The larger physiological IL-26 protein, including signal peptide, weighs 19,842.7 Daltons. The IL-26 protein has an isoelectric point at pH 10.81, and a strong positive charge of +18.2 at neutral pH was predicted for IL-26[19,40]. This high cationicity is generally a hallmark of antimicrobial peptides (AMP, see chapter 1.6). After the generation of a computational model where IL-26 was compared to the known IL-22[19]. it was found that IL-26 possesses a so-called amphipathic structure. This means that positively or negatively charged amino acids cluster together on different sides of the protein. This amphipathic structure again resembles AMPs.

1.4.1.2 IL-26 receptor complex

For IL-26, there are two processes of cell activation described: one is the signal transduction into cells via binding the IL-26 receptor complex and the other signaling pathway is receptor independent (chapter 1.4.1.3). The IL-26 receptor complex consists of the IL-20 receptor 1 (IL-20R1) and the IL-10 receptor 2 (IL-10R2)[42]. This receptor combination seems to be unique for IL-26, as none of IL-10, IL-19, nor IL-22 are able to signal through this heterodimeric receptor[42,43]. The IL-26 receptor belongs to the cytokine class II receptor family (CRF2)[44] and, considering CRF nomenclature, IL-20R1 is designated CRF2-8 and IL-10R2 is designated CRF2-4[42]. IL-20R1 can additionally dimerize with IL-20R2 in order to form the receptor complex for IL-19, IL-20, and IL-24. IL-10R2 in turn can obviously also dimerize with IL-20R1 forming the complex for IL-10 signaling[42]. Furthermore, IL-10R2 dimerizes with IL-22R1 and thereby provides the receptor for IL-22, and finally IL10R2 can also form a receptor heterodimer with IFN-λR1 and in this way allows IFN-λ signal transduction into the receptor

bearing cells[42]. Signaling via the IL-26 receptor induces the phosphorylation of STAT 1 and 3.

Interestingly, the IL-10R2 is ubiquitously expressed in various tissue and cell types, including immune cells[42,45], while IL-20R1 is expressed only on a small number of tissues and cells. IL-20R1 is only found on epithelial cells/tissues (keratinocytes[46,47], synovial cells[48], skin[42], colon[49] or lung[42]) or epithelial cell lines, such as HaCaT keratinocytes[50]. Further, various colon carcinoma cell lines express IL-20R1[51]. Immune cells generally seem to lack the IL-20R1. In contrast, a single publication by Bech and colleagues[52] stated that monocyte-derived dendritic cells (moDCs) also express very low amounts of IL-20R1, making them a target of IL-20. Besides moDCs, neutrophilic granulocytes also seem to express the IL-20R1[53].

1.4.1.3 IL-26´s effects on tissues and cell types

IL-26 mediates its effects via the receptor complex of IL-20R1 and IL-10R2, as described above, which is mainly found on cells from epithelial tissues.

Looking at the skin, keratinocytes are possibly the main targets of IL-26[50]. Using a keratinocyte cell line, namely HaCaT keratinocytes, Hör *et al.* showed that IL-26 induces a strong secretion of CXCL8 (IL-8) in this cell line. Intracellularly, IL-26 leads to a phosphorylation of STAT3[50].

Looking at the colon, and especially at a carcinoma cell line named Colo-205, here IL-26 again provokes high secretion of IL-8, but also IL-10 and additionally, it leads to the phosphorylation of both STAT1 and STAT3[50]. Furthermore, an increased expression of intercellular adhesion molecule 1 (ICAM1; CD54) is detected on Colo-205 cells after IL-26 stimulation[50]. So far, all tested colon cancer cell lines express IL-20R1[54]. It has further been found that IL-26 slightly inhibits proliferation in these cell lines, but drives TNF-α and suppressor of cytokine signaling 3 (SOCS3) mRNA expression. IL-26 has been shown to be associated with increased inflammatory bowel diseases, such as Crohn's disease[54,55] and ulcerative colitis[55]. Besides colon carcinoma cell lines, primary human colonic subepithelial myofibroblasts (SEMF) also express the IL-26 receptor and respond to IL-26 with IL-8 and IL-6 secretion[55]. In SEMF, IL-26 signals via the mitogen-activated protein kinase (MAPK) pathway, a common

cytokine signaling pathway. Further, the transcription factor nuclear factor kappa-light-chain-enhancer of activated B cells (NF-κB), which plays a role in the expression of proinflammatory cytokines, is involved in IL-26-induced cytokine secretion by SEMFs[55]. The above mentioned phosphorylation of STAT3 associated with IL-26 has also been seen for gastric cancers, where increased IL-26 was detected in sera[56]. Gastric cancers also express higher levels of IL-20R1 compared to the respective healthy control[56].

Alveolar macrophages in human airways express the *IL26* gene and also release IL-26, the same applies for bronchial epithelial cells[53]. Furthermore, Che and colleagues found that neutrophils also express the IL-26 heterodimeric receptor at a very low level. Adding recombinant IL-26 to cells isolated from bronchoalveolar lavage (BAL), a slightly increased secretion of CXCL8, IL-1β, TNF-α and GM-CSF was detected. Here in turn, CXCL8 is especially important as it is also an important chemokine attracting neutrophils. Looking at bronchial epithelial cells, they express the IL-26 receptor and they secrete IL-26 themselves after stimulation with IL-17A and IL-22, both in combination or alone[57].

Osteoclasts are differentiated cells belonging to the monocyte/macrophages lineage and their task is to demolish bone cells[58]. It has been found that IL-26 strongly decreases this demolishment[59]. Osteoclasts express IL-20R1 and are, as a consequence, able to respond to IL-26[60]. The counteracting cells to osteoclasts are osteoblasts that synthesize bones. Osteoblasts respond to IL-26 with greatly increased bone mineralization[61]. In a normal steady-state, both cell types are balanced and the bones are healthy. A disease where osteoclasts cause severe damage through bone destruction is rheumatoid arthritis (RA). In the reverse case, the osteoblasts are dysregulated and produce large quantities of bone, a disease called spondyloarthritis develops. In both diseases, high levels of IL-26 were detected (in sera from RA patients and in synovial fluids from patients suffering from spondyloarthritis)[61,62]. Looking at other joint cells. such as fibroblast-like synoviocytes (FLS), they express the rare second part of the IL-26 receptor, namely IL-20R1, but they do not respond to recombinant IL-26[62]. On the other hand, stimulating FLS with IL-1β or TNF-α does lead to IL-26 production by FLS[61].

Besides the above described IL-26 receptor-dependent effects on epithelial cells, IL-26 also exerts effects on immune cells without the IL-20R1/IL-10R2 receptor complex. In a study from Corvaisier *et al.* about RA, they also investigated monocytes and found that they respond to IL-26 with IL-6, TNF-α, and IL-1β secretion[62]. Also, when treating macrophages, myeloid DCs and moDCs with IL-26 and IL-6 secretion are detected. Furthermore, stimulating memory $CD4^+$ T cells with IL-26 in the presence of monocytes results in the $CD4^+$ T cells differentiating towards IL-22 producing T_H17 cells[62].

1.5 Chemokines

Chemokines are cytokines that attract immune cells to inflammation sites by a movement process called chemotaxis[63,64]. Chemokines possess three to four cysteine amino acids and are divided into four subgroups depending on the cysteine motif in a conserved region. The two major groups either have a C-X-C motif, where another amino acid is found between the cysteines, or the C-C motif without an amino acid separating the cysteines. The third chemokine group is characterized by only one cysteine in this conserved region, and the fourth group even has three amino acids separating the cysteines in the conserved region (C-X_3-C motif)[63]. Chemokines transmit their signal via seven-transmembrane, G-protein coupled receptors on the corresponding cell surface[64].

Looking at structural skin cells such as keratinocytes, they express CCL20, which is a ligand for CCR6 that is found on T_H17 cells but also on immature DCs, to recruit them to the epithelial tissue[65,66]. Furthermore, it has been shown that the T_H17 cytokines IL-17 and IL-22 induce the expression of CCL20 in keratinocytes. With this positive feedback loop, T_H17 cells are forced to stay in the skin in an inflammatory capacity, further enhancing the inflammation[65,67]. Besides CCL20, keratinocytes secrete CXCL8, CXCL9, and CXCL10 – especially upon stimulation with polyinosinic:polycytidylic acid (poly (I:C)), a synthetic analog of dsRNA and known as a ligand for TLR3[68]. Furthermore, the chemokines CCL2, CCL22, CCL27, and CXCL1 are expressed by keratinocytes and the chemokine receptor CXCR2 is found on their surface[69,70].

Monocytes express high levels of the chemokine receptor CCR2 and are therefore mainly attracted by CCL2 (also named: monocyte chemoattractant protein-1 (MCP-1)[71,72]. CCL2 mediates the migration and infiltration from monocytes in the blood stream into the tissue. This chemokine ligand is produced by a large number of cells, including epithelial and endothelial cells but also monocytic cells[71,72]. Besides CCL2, CCL7 also binds to CCR2 and subsequently impacts monocyte recruitment[73].

Having attracted CCR6-expressing immature DCs to epithelial tissues via CCL20, the maturating DCs need to be able to migrate to the lymph nodes in order to present an up taken antigen to T cells. A key chemokine receptor in DCs, CCR7, fulfills this task and is crucial for DCs to be able to migrate into skin lymphatic tissue[74,75]. This receptor is upregulated under DC maturation, for example in the presence of microbial components, and leads them to migrate from the organs to the secondary lymphoid tissues[75,76].

In macrophages, commonly expressed chemokines are CCL3 (macrophage inflammatory protein (MIP) -1α), CCL4 ((MIP-1β), and CCL5 (RANTES)[77,78]. Additionally, macrophages secrete CXCL2 (MIP-2) that in turn attracts neutrophils to the site of inflammation[79]. Macrophages also express CXCL8 upon stimulation, for example with components from *Mycobacterium tuberculosis* (Mtb)[80]. CXCL8 attracts neutrophilic granulocytes[81]. It has also been shown that CXCL8 plays a pivotal role in enhancing mycobacterial killing within macrophages[82].

1.6 Antimicrobial Peptides (AMP)

Antimicrobial peptides (AMPs) protect epithelial surfaces and are part of the innate immune system. Defensins and cathelicidins represent the major classes of AMP in mammals[83]. Nevertheless, several other proteins showing antimicrobial activities such as psoriasins have been described. Most AMPs are cationic peptides sharing the affinity for negatively charged molecules that are part of the cell envelope of many germs. Briefly, the binding of AMP to a negatively charged microbial cell envelope component thins the outer layer, finally leading to a pore formation and microbial death by disrupting the cell membrane[83]. AMPs have a very broad antimicrobial spectrum as they inhibit

both gram-positive and gram-negative bacteria, but also yeasts like *Candida* types[84].

Defensins from humans are divided into the subgroups α and β, characterized by β-sheet folding, three disulphide bridges within the molecules and molecular masses between 3.5 and 6 kDa, where the smaller masses belong to α-defensins and the bigger ones to β-defensins[84-86]. The defensins display sequence lengths between 30 and 47 amino acids. Four α-defensins are produced by neutrophils to kill incorporated microorganisms and two further α-defensins are secreted by cells of the small intestine or urogenital tract[84]. There are also six β-defensins described in humans (hBD-1 to hBD-6) that can be split between two further subgroups: hBD-1 to hBD-3 are expressed by epithelial tissues and hBD-4 to hBD-6 are only expressed in the epididymis.

The only cathelicidin found in humans is cathelicidin antimicrobial peptide (CAMP) or LL37. It is derived from the human CAP18 protein and has a specific length of 37 amino acids with two leucines at the end[84,87]. LL37 does not have cysteines and therefore has a linear structure. LL37 is expressed in epithelial cells from the skin and intestinal tract, but also in a wide range of leukocytes (e.g. neutrophils, monocytes or T cells)[84,87]. Like the other AMPs, LL37 has inhibitory effects on both gram-negative and gram-positive bacteria[84]. Furthermore, LL37 affects yeast growth, as it has been shown to inhibit growth of *Candida albicans* at a minimal inhibitory concentration (50% killing; MIC50) between 12 and 25 µM depending on the growth medium used and its pH[88]. LL37 is capable of killing *Staphylococcus aureus*, both extra- and intracellularly[89]. Interestingly, LL37 has an affinity towards lipopolysaccharides (LPS), a surface molecule of gram-negative bacteria, but it simultaneously neutralizes LPS and in this way blocks TNF-α secretion from (mouse) macrophages at the site of infection[90]. This neutralization in mouse macrophages has also been demonstrated following stimulation with lipoteichoic acid (LTA) found on gram-positive germs, as well as lipoarabinomannan (LAM) found on *Mycobacterium tuberculosis* (Mtb)[90]. Besides the antimicrobial properties, LL37 also impacts viruses. LL37 doesn´t show direct antiviral effects, but it effects the viral replication of human immunodeficiency virus (HIV) -1[91].

LL37 is not only directly active against microorganisms, yeasts, and viruses, it also stimulates the expression of chemokines and chemokine receptors on other immune cells[90]. It induces the expression of CCL2 on macrophages and CXCL8 on epithelial cells[90]. Alongside these functions, being part of the innate immune system, LL37 also fulfils key roles in adaptive immunity and has negative impacts in autoimmunity[92]. Considering adaptive immunity, LL37 provokes a high surface expression of the costimulatory molecule CD86 on DCs[93]. Furthermore, LL37 leads to increased secretion of IL-12 and IL-6 from DCs and decreased secretion of IL-4[93].

The cationic LL37 is capable of binding to extracellular DNA due to its cationic charge. This LL37/DNA complex can then be transferred inside eukaryotic cells. Mechanistically, LL37 binds to proteoglycans on the cell surface and the LL37/DNA complex is then taken up via endocytosis[94]. The initial binding of LL37 to the cell surface can again be explained by its cationicity, as proteoglycans are highly negatively charged[95]. In a healthy state, free human self-DNA released after cell death is rapidly degraded by DNases, and so only foreign viral or microbial DNA is recognized inside immune cells via the respective endosomal TLRs[96,97]. LL37 is able to bind to free human DNA and form complexes that are not degradable with DNases[96]. These complexes are then taken up by pDCs, transmit signals via TLR9, and subsequently stimulate the pDCs to secrete IFNs for a falsely triggered defense against viral/microbial entry[96]. This LL37/DNA transport has also been described for monocytes that also respond with IFN-α secretion[97]. It seems that the transport into monocytes is even more efficient than to pDCs. In addition, the activation of monocytes by LL37/DNA complexes is independent from TLRs, as a blockade does inhibit IFN-α secretion[97]. Similarly to the complex formation with DNA, LL37 also forms complexes with RNA, which in turn activate monocyte-derived DCs that express endosomal TLR8 and leads to the secretion of TNF-α and IL-6[98]. LL37/RNA complexes also activate pDCs, here via TLR7, but as with LL37/DNA complexes IFN-α secretion is induced.

1.6.1 Antimicrobial features of IL-26

As described in chapter 1.4.1, IL-26 is characterized by an amphipathic structure that resembles the hallmark feature typically found in antimicrobial

peptides (chapter 1.6). Having this feature, the question arose if IL-26 is able to kill bacteria? Indeed, IL-26 is able to directly kill both gram-positive and gram-negative germs[19,99]. In contrast to LL37, IL-26 is not able to kill the yeast *Candida albicans* at concentrations below 25 µM. In addition to its direct antimicrobial effects, IL-26 also exerts indirect antimicrobial effects as it is able to attract neutrophils[19,53].

IL-26 also displays effects on viruses, but these could not be more divergent as reports vary between an improvement or worsening of viral infectivity in the presence of IL-26[100]. Looking at the vesicular stomatitis virus (VSV), IL-26 enhances the infection effectivity of the virus. Contrasting to this finding, IL-26 treated human fibroblasts are protected against human cytomegalovirus infection. It has been found that IL-26 is overexpressed in hepatitis C virus (HCV) infected patients[101]. Here it was demonstrated that IL-26 enhanced the expression of tumor necrosis factor (TNF)-related apoptosis-inducing ligand (TRAIL) on NK cells, which in turn made them effective in killing HCV-infected cells. Added to this, IL-26 induced antiviral interferons such as IFN-β and IFN-γ[101]. Investigation of IL-26 in poly (I:C)-treated bronchial epithelial cells revealed an increased IL-26 expression after TLR3-stimulation and additive effects after co-stimulation of poly (I:C) with IL-17 or the combination of both IL-17 and IL-22[57].

Another attribute that IL-26 shares with LL37 is the cationicity enabling IL-26 to bind to nucleic acids. Identically to LL37/DNA complexes, IL-26/DNA complexes further activate pDC to secrete type I interferons[19], monocytes to express IL-6 and IL1-β, as well as neutrophils to secrete CXCL8[102]. If IL-26 forms complexes with RNA, this has not been reported yet.

1.7 Toll-like receptors (TLRs)

Toll-like receptors (TLRs) in mammals are the homologues to the earlier found Toll receptors described in the fruit fly *Drosophila melanogaster*[103]. Today there are 10 TLRs (TLR1 to TLR10) described in humans and 12 TLRs (TLR1 to TLR9 and TLR11 to 13) in mice[104,105]. TLRs belong to the category of PRRs, which are key proteins in the detection of molecules specific for a variety of intruding microbes. These receptors are mainly found on different immune cells but also on vascular endothelial cells, adipocytes and intestinal epithelial

cells[106], and keratinocytes[107]. TLRs are generally found in two different compartments of the cells: either on the surface or intracellularly in the endosomes[108]. The TLRs on the surface are TLR1, TLR2, TLR4, TLR5, and TLR6. TLR1 only acts when complexed with TLR2, and recognizes lipopeptides like LTA on gram-positive bacteria[109]. LTAs from different bacteria display different stimulatory intensities on TLR2[110]. TLR2 is also able to form complexes with TLR6. TLR4 binds LPS found on gram-negative bacteria[111]. TLR5 recognizes flagellin, a major component of the flagella-bearing bacteria. The intracellular TLRs in the endosomal compartment exclusively recognize nucleic acids. TLR3 identifies dsRNA commonly found in viruses and poly (I:C), which is an artificial RNA analog[112]. Looking at TLR7, it also binds RNA but the single-stranded type, whereas for TLR8 the ssRNA needs to be rich in guanidine and uridine[113]. TLR9 is the receptor for DNA, usually from bacteria[108,114]. TLR9 together with TLR7 are exclusively expressed on pDCs[108]. One TLR that has not been listed here is TLR10. It is regarded as an orphan receptor, as respective ligands have not yet been found. Like TLR1 and TLR6, TLR10 complexes with TLR2[115]. Interestingly, investigations on this complexation revealed that TLR10 is the only TLR that has inhibitory properties[116].

Primary keratinocytes express TLR1, 2, 3, 4, 6, 9, and comparably higher levels of TLR5[68]. The expression of TLR10 has also been described, but TLR7 and 8 are not expressed[117]. The expression of both TLR2 and TLR4 on keratinocytes is significantly increased after stimulation with a mixture of LPS and IFN-γ[118]. The actual functionality of the receptors TLR2, 3, 4, 5, and 9 has been demonstrated[117,119,120]. Looking at other epithelial cells, such as intestinal epithelial cells, it was shown that even though they express TLR2 mRNA, they are unresponsive towards TLR2 ligands such as LTA[121].

1.8 Physiological skin conditions

1.8.1 Physiological conditions for reduction of disulphides

The breakage of disulphide bonds has physiological relevance since approximately 20% of all human proteins contain cysteine residues forming disulphide bonds[122]. There are two types of disulphide bonds: the ones that are stably connected to support the final protein structure and the ones that are able to switch from reduced to oxidized states[122].

Recently, it has been demonstrated that a reduction of disulphide-bridges dramatically enhances the antimicrobial activity of human β-defensin 1 (hBD-1)[123]. HBD-1 is not very active against microbes under normal conditions, when compared to hBD-3. Moreover, Schröder *et al.* demonstrated that hBD-1 is a substrate of thioredoxin (TXN)[123]. TXN is a ubiquitously expressed enzyme that regulates physiological redox-reactions[124]. The importance of this finding relies on the fact that infectious sites, such as chronic inflamed tissues, wounds or mucosal epithelia within the gut, display a hypoxic or even an anaerobic microenvironment[124].

1.8.2 Chemical disulphide reduction

Disulphide bonds can be broken up chemically using agents such as dithiothreitol (DTT) or Tris(2-carboxyethyl)phosphine (TCEP). DTT has first been described and developed by Cleland[125], therefore it's sometimes called Cleland's reagent. The chemical formula of DTT is $C_4H_{10}O_2S_2$, which forms an inactive ring structure when oxidized. The molecular weight of DTT is 154.25 (Product Information Sheet; Sigma-Aldrich). DTT reveals its highest reducing power above pH 7.0, preferably at pH 8.0[125]. This reagent is commonly used in many protein research applications, such as sodium dodecyl sulfate polyacrylamide gel electrophoresis (SDS-PAGE).

Tris(2-carboxyethyl)phosphine (TCEP) has been introduced some 25 years ago by Burns *et al.*[126]. It is an alternative to DTT due to its higher stability and its high reducing power over a wide pH range, specially below pH 7.0[127].

Only recently, another reducing agent has been developed that is active at a physiological pH of 7.0, unlike DTT[128]. This potent reducing agent, named (2S)-2-amino-1,4-dimercaptobutane (dithiobutylamine or DTBA), can be synthesized from aspartic acid.

1.8.3 Hypoxia

The atmospheric oxygen content is about 21%[129]. Looking at skin, the partial oxygen pressure is much below the atmospheric oxygen pressure reaching a maximum of about5% in the sub-papillary plexus[129,130]. In superficial skin regions, the partial oxygen pressure is even lower with about 1%[130]. An oxygen pressure of 1% is generally considered as hypoxia[131]. The most important factor

during hypoxia is the hypoxia-inducible factor 1 alpha (HIF1α)[131]. Under normoxic conditions, this factor is immediately degraded by prolyl hydroxylases, which themselves require oxygen for their actions[132,133]. When oxygen is lacking and the conditions are hypoxic, the prolyl hydroxylases are unable to degrade HIF1α, which in turn migrates into the nucleus and exerts its actions by modifying the transcription of different genes[132].

Hypoxia is linked to disulphide bond reduction, as some steps of disulphide bond formation rely on the presence of enough oxygen[134]. Furthermore, another cellular redox protein, the so-called protein-disulphide isomerase, has been shown to be upregulated in hypoxia[135]. Hypoxia is also directly linked to the described physiological thioredoxin system, as TXN upregulates HIF1α[136]. TXN and HIF1α also seem to be associated in other pathologies, such as cerebral arteriovenous malformations[137].

1.9 Infectious skin disorders

1.9.1 Skin-infecting bacteria and mycobacteria

Mycobacterium tuberculosis (Mtb)[138-140] is the agent that causes tuberculosis in humans. Tuberculosis is among the top 10 causes of death worldwide, infecting 10.4 million people and causing 1.3 million deaths in 2016 according to the World Health Organization's Global Tuberculosis report[141]. Strikingly, only five countries are covering 56% of all tuberculosis incidences: China, India, Indonesia, Pakistan, and the Philippines[141]. Tuberculosis is transmitted via airborne droplets that infect the alveolar macrophages in the lung. There are two stages of the disease: the latent stage where the mycobacterium is tightly controlled by the immune system and the active disease stage where the spreading of the infection takes place. The only vaccine against tuberculosis available today is the *Mycobacterium bovis Bacille de Calmette et Guérin (M. bovis BCG)*[142].

A rare appearance of tuberculosis is as an infection of the skin[143,144]. About 4% of tuberculosis patients present cutaneous manifestations[145]. Cutaneous tuberculosis is mainly caused by Mtb, but also *M. bovis* or the vaccine strain *M. bovis BCG* might be causative[143].

Tuberculosis is curable but there are only a few treatment options available: among those is isoniazid[146], to which patients often develop resistant mycobacteria[147], or rifampicin (sometimes also named rifampin)[148], which is used as second line treatment in patients resistant to isoniazid. Rifampicin inhibits bacterial DNA polymerase[146] and is further used as positive control in the performed experiments. Three endogenous agents that are able to kill Mtb *in vitro* are granulysin[149], hBD2[150,151], and LL37[152,153]. All three kill Mtb extracellularly but they also decrease the viability of Mtb within macrophages. LL37 and hBD2 belong to the group of cationic antimicrobial peptides defined by their peptide properties and their ability to kill bacteria (chapter 1.6).

1.9.1.1 Immunogenic patterns on bacteria and mycobacteria

The human immune system has co-evolved with intruding microorganisms in order to effectively combat them. The described TLRs (chapter 1.7) are one of the immune system's ways to recognize different bacterial and mycobacterial cell wall components.

Gram-negative bacteria, such as *Pseudomonas aeruginosa*, carry LPS on their outer membrane, which is recognized via TLR4[111,154]. Gram-positive bacteria that are characterized by a thick peptidoglycan cell wall layer, such as *Staphylococcus aureus*, express different teichoic acids and LTA on their surface[154]. The respective receptor on immune cells to recognize LTA is TLR2[109]. Mycobacteria have a thin layer of peptidoglycan outside the cell membrane, somewhat resembling the one from gram-negative bacteria (Fig. 4)[154]. Outside of the peptidoglycan layer, arabinoglycan and mycolic acids covered with glycolipids are found. The outermost structure in mycobacteria is LAM[154]. LAMs are also recognized via TLR2[155,156], and especially in the TLR1/TLR2 complex[157]. The activation of TLR2 in turn leads to a production of nitric oxide within macrophages, and subsequent enhanced killing of the intracellular mycobacteria[158].

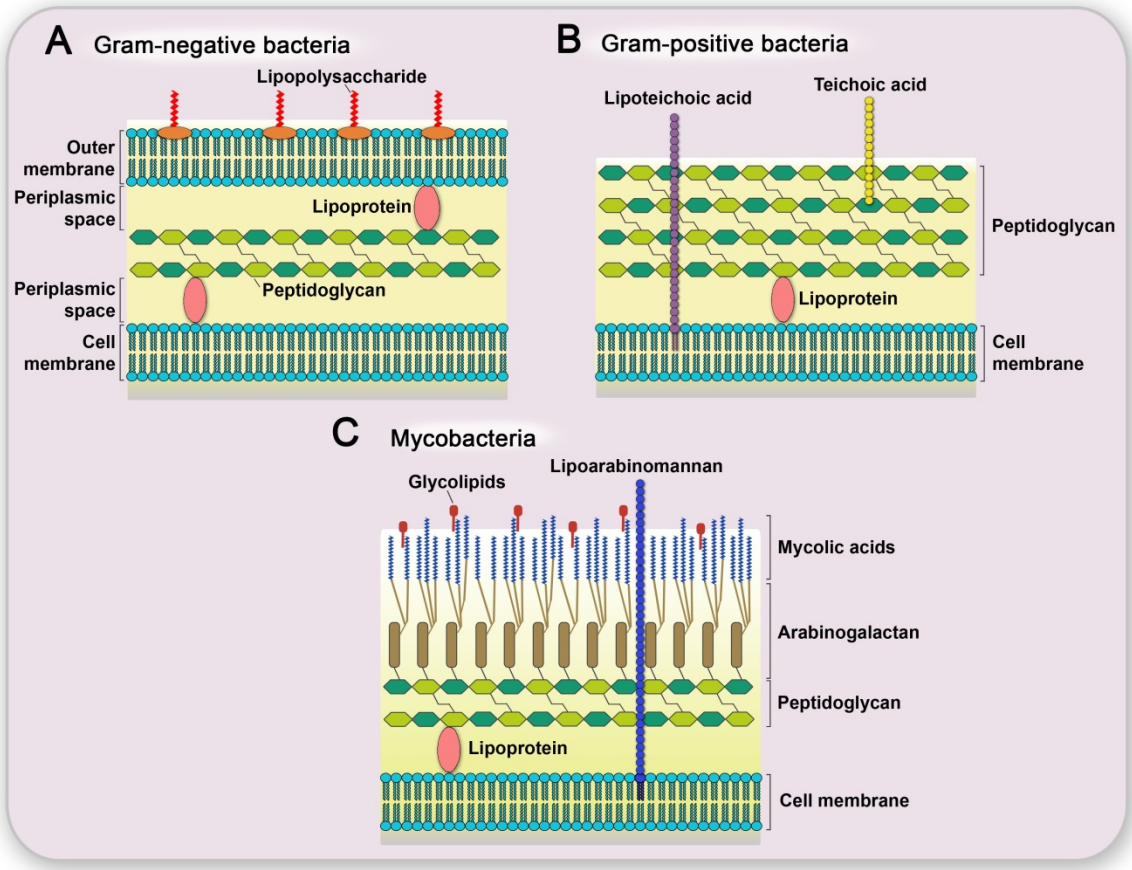

FIGURE 4: Schematic depiction of bacterial cell surface molecules. The surface structures and molecules from gram-negative bacteria (A), gram-positive bacteria (B), and mycobacteria (C) are compared. Illustration modified from: Brown *et al.* 2015[154].

1.10 Inflammatory skin disorders

1.10.1 Psoriasis

Psoriasis is a common chronic inflammatory skin disease characterized by red scaly plaques[159-161]. Histologically, a drastically thickened epidermis is found, together with deep epidermal ridges reaching into the dermis[159]. In psoriatic lesions, T_H1 and T_H17 cells are predominantly found together with an increased expression of IL-17 and IL-22[162]. An increased number of T_H1 and T_H17 cells furthermore result in increased secretion of IL-26 in psoriatic lesions[19,163]. A key player accountable for the thickened epidermis is IL-22, which promotes proliferation of keratinocytes[164-166]. Additionally, Wilson *et al.*[163] demonstrated that an increased amount of IL-23 and IL-1β produced by DCs drives the T_H17 cell differentiation and thereby accelerates the progression of the psoriatic phenotype.

1.10.2 Atopic dermatitis

Atopic dermatitis (AD) is a chronic inflammatory skin disorder characterized by severe itching (medically termed pruritus)[167-170] The prevalence is about 10-20% in developed countries and in approximately 60% of the cases the diseases onset is in the first years of life[171]. In contrast to psoriasis, AD has been proposed to display a T_H2 cell-associated phenotype with increased expression of IL-4 and IL-5[172]. However, chronic AD also displays IFN-γ, the signature cytokine for T_H1 cells[173,174]. In line with the finding that AD appears to be a disease associated with a mix of T_H1 and T_H2 cells, IL-26 is found more highly expressed in AD than in psoriasis, while it is not found at all in healthy skin[47]. Patients suffering from AD are prone to skin infections with *S. aureus* but also viral infections caused by the herpes simplex virus (HSV)[169,175]. A reason for this might be that there are lower levels of antimicrobial peptides in atopic dermatitis as in psoriasis[176,177].

1.10.3 Mycosis fungoides

Mycosis fungoides (MF) is a form of cutaneous non-Hodgkin T cell lymphoma. Together with the Sézary syndrome (a leukemic form of MF), MF belongs to the most common cutaneous T cell lymphoma[178,179]. It is a rare disease predominantly found in elderly males with an onset at the age of 55 years[180]. MF is characterized by an overproduction of T lymphocytes, mainly $CD4^+$ T cells from the T_H2 subtype[179]. Besides the skin, MF also generally spreads to lymph nodes, lung, spleen, and liver, but in general all organs can be affected[181].

Patients suffering from MF are also more prone to infections, similar to AD patients. In MF, it has been found that the production of antimicrobial peptides is very limited[182]. Looking at LL37, the levels in MF are nearly as low as in healthy individuals[182]. When focusing on IL-17A, a key cytokine for the induction of antimicrobial peptides, it revealed that IL-17 is increased in MF lesions compared to healthy skin but by far less than in psoriatic lesions[182]. The other T_H17 cytokines IL-22 and IL-26 were as highly expressed in MF lesions as in psoriatic lesions[182,183].

1.10.4 Rosacea

Another common skin disease is rosacea[184,185]. It mainly affects the central areas of the face around the nose, but eye involvements also occur[184-186]. The disease is characterized by facial erythema and rashes that can be enhanced by environmental factors such as UV radiation and spicy foods[186]. The prevalence of rosacea in females is higher than in males. The onset of the disease has been found to be in the ages between 30 and 50 years. There are four subtypes of rosacea, which in turn can be divided into mild, moderate, and severe disease[186].

The role of microorganisms in rosacea is discussed intensively[187]. Microorganisms increasingly found in rosacea are a mite named *Demodex folliculorum*, and bacteria such as *Helicobacter pylori*, *Staphylococcus epidermidis*, and *Chlamydophila pneumoniae*[187]. In line with high bacterial load, an enhanced expression of TLR2 has also been reported[188,189]. Surprisingly, other inflammatory skin diseases such as psoriasis and AD did not show an altered TLR2 expression. Given the large amount of microorganisms, antimicrobial peptides, especially LL37, are also highly expressed in rosacea[190]. A recent study from Buhl *et al.*[191] investigating the T_H1/T_H17 pathway in different subtypes of rosacea found an upregulated expression of IL-26 in all subtypes compared to healthy skin in the performed microarrays.

1.11 Aim of the study

In this study we want to broaden our knowledge regarding the physiological and pathophysiological roles of IL-26. First, we will study the involvement of IL-26 in infectious as well as chronic inflammatory skin disorders, and we will get a closer insight into the physiological role of IL-26 by investigating receptor-mediated effects of IL-26 on epithelial cells, namely keratinocytes. Second, we want to examine the binding of IL-26 to different microbial surface molecules that potentially explain the antimicrobial effects of IL-26 on a molecular level. Third, the investigation of the antimicrobial activity of IL-26 will be expanded to mycobacteria, which can – in general – be targeted by antimicrobial peptides. Fourth, we aim to investigate pathophysiological mechanisms, such as IL-26/nucleic acid-complex mediated immune cell and resident skin cell activation, with a focus on IL-26/RNA complexes and chemokine patterns. Finally, we will

unmask the effects of IL-26 under reducing conditions, which are typical for wounds or infectious sites, and therefore compare the oxidized and the reduced form of the IL-26 protein in terms of bacterial killing and nucleic acid complex formation as well as subsequent immune stimulation.

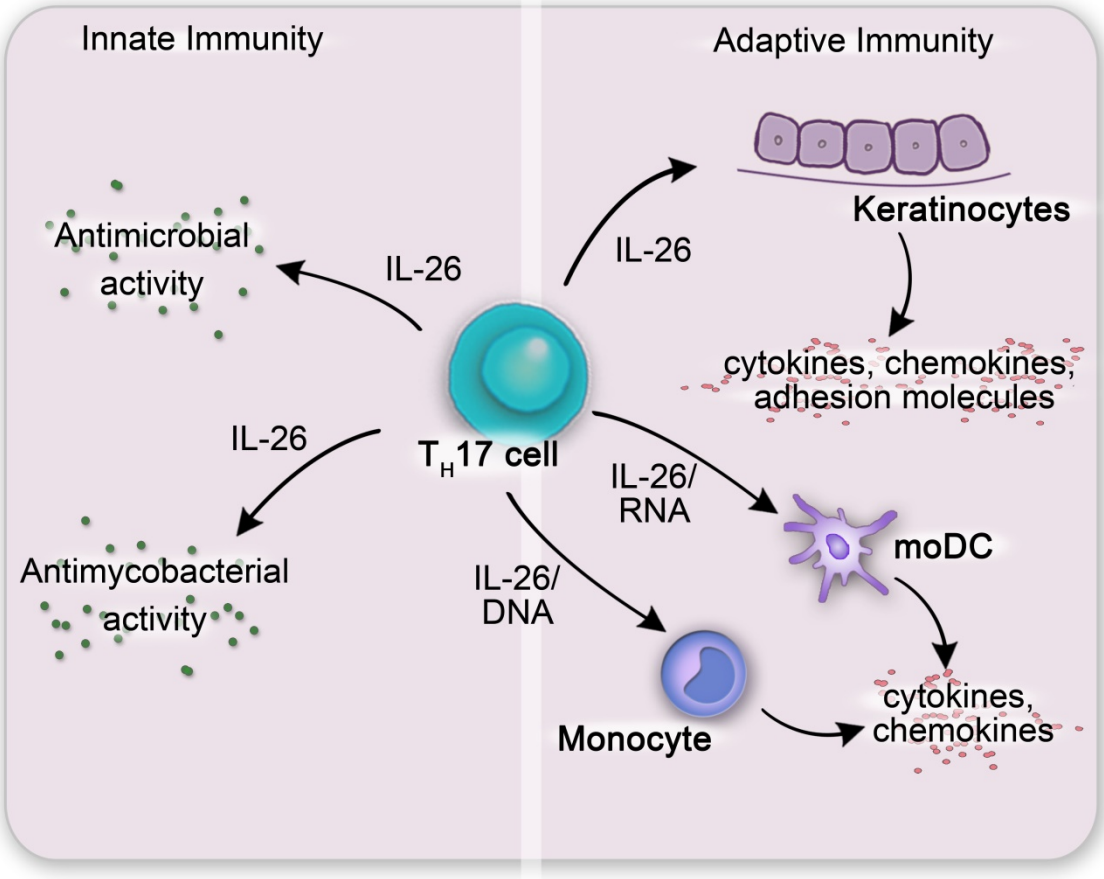

FIGURE 5: Schematic depiction of the aims of the study.

2 Material and methods

The study was approved by the local ethics committee (approval number: 4028). The ethics approval was extended by two amendments: one approves the usage of biopsies and blood samples from a large number of skin diseases and the other one includes the utilization of tissues from tuberculosis-infected patients.

2.1 Human samples

Buffy Coats from healthy human individuals were obtained from the central blood donor unit at the University Hospital Düsseldorf.

Skin punch biopsies from different skin diseases, as well as from healthy skin, were taken after informed consent and snap-frozen in liquid nitrogen before storage at -80°C.

Paraffin-sections (10 µm thick), mainly from lymph nodes, but also lung and skin tissue from healthy subjects as well as from patients suffering from tuberculosis, were provided by Dr. Henry Mayringer, PD Dr. Nektaria Simiantonaki and Prof. Irene Esposito from the Institute of Pathology at the University Hospital Düsseldorf. These samples are covered by the second amendment of the ethics approval number 4028.

For the rosacea samples, about half of them were collected at the Department of Dermatology in Duesseldorf and complementary DNA (cDNA) from the other half was obtained from Dr. Curdin Conrad from the Department of Dermatology, University Hospital CHUV, Lausanne, Switzerland. The Swiss study was approved by the local ethics committee, protocol number 265/12 (Commission cantonale d'éthique de la recherche sur l'être humain, Canton Vaud, Suisse).

2.2 Reagents

Recombinant human IL-26 (carrier-free) and recombinant human IL-22 (carrier-free) were obtained from biotechne (previous: R&D Systems). LL37 and lipoteichoic acid (LTA, from *Staphylococcus aureus*) were obtained from InvivoGen. Lipopolysacharide (LPS; from *Escherichia coli O26:B6*) was purchased from Sigma-Aldrich.

TABLE 1: List of cDNA synthesis reagents

Reagent	Content/Concentration	Company
SuperScript II Reverse Transcriptase	SuperScript® II Reverse Transcriptase 200 U/µl (10000 U total)	Invitrogen, Carlsbad (US)
	First-strand buffer (5x)	
	Dithiothreitol (DTT) (100 mM)	
RNasin® Plus RNase Inhibitor	40 U/µl (10000 U total)	Promega, Madison (US)
DNase I recombinant	10 U/µl (10000 U total)	Roche, Basel (CH)
Oligo deoxythymidine (dT) 12-18 Primer	0.5 µg/ml (25 µg total)	Invitrogen, Carlsbad (US)
Random Primers	500 µg/ml (20 µg total)	Promega, Madison (US)
deoxy nucleoside triphosphate (dNTP)	2.5 mM (1 ml total)	Bioline, London (UK)
Nuclease-free H_2O	-	Roth, Karlsruhe (DE)

TABLE 2: List of qPCR reagents and material

Reagent	Content/Concentration	Company
Ribosomal RNA Control Reagents (VIC ™ Probe)	Ribosomal Probe (VIC) 40 µM	Life technologies, Austin (US)
	Ribosomal Forward Primer 10 µM	
	Ribosomal Reverse Primer 10 µM	
Power SYBR ® Green PCR Master Mix	5 ml	Applied Biosystems, Warrington (UK)
TaqMan ® 2X Universal PCR Master Mix	5 ml	Applied Biosystems, Warrington (UK)
Nuclease-free H_2O	-	Roth, Karlsruhe (DE)
CELLSTAR 96 Well round-bottom Cell Culture Plate		Greiner Bio-One, Frickenhausen (DE)
Plate seal for 96 well plate		NUNC, Roskilde (Denmark)
MicroAmp Optical 96-Well Reaction Plate with Barcode		Applied Biosystems, Warrington (UK)
StarSeal Advanced Polyolefin Film		STARLAB, Hamburg (DE)

TABLE 3: List of TaqMan Assay and orther qPCR primers

Gene	TaqMan Assay number	Cat. number:	Company
18S	-	4308329	Applied Biosystems
CCL20	Hs00171125_m1		Thermo Fisher
CCR7	Hs00171054_m1		Thermo Fisher
CXCL2	Hs00601975_m1		Thermo Fisher
CXCL8	Hs00174103_m1		Thermo Fisher
IL20R1	Hs00205346_m1		Thermo Fisher
IL17A	Hs00174383_m1		Thermo Fisher
IL22	Hs00220924_m1		Thermo Fisher
IL26	Hs00218189_m1		Thermo Fisher

TABLE 4: List of SYBR qPCR primers

Gene	Sequence forward	Sequence reverse	Ref.
CCR6	agctcaagccccaacatcag	gtgtgaacccaagtaccagactgt	
HIF1A	ccagcagactcaaatacaagaacc	tgtatgtgggtaggagatggagat	[192]
ICAM1	gggcagtcaacagctaaacctt	cacctggcagcgtagggtaa	
IL10	tcctgactggggtgagggcc	ggcaggttgcctgggaagtgg	
IL10R2	gctgtggtgcgtttacaaga	gaggatggcccaaaaactct	
TLR2	cgttctctcaggtgactgctc	cctttggatcctgcttgc	
TXN	tggtgtgggccttgcaaaatga	ttcacccacctttgtcccttc	[123]
TXNRD1	tgaggagaaagctgtggagaa	ccattccaatggccaaaa	

FAM-labeled DNA and RNA for Microscale thermophoresis measurements were obtained from MWG Eurofins (Ebersberg, Germany). The sequences were for single-stranded (ss) and double-stranded (ds) DNA:

AGAGGTCATCTCTCCTGTGGAGTTCCAGACACTCCTCCTAGCTTGACTTTC TCAGGAAAACCTTACACATTCCAAGCAGC,

for ssRNA: AGAGGUCAUCUCUCCUGUGGAGUUCCAGACACUCCUCCUAG CUUGACUUUCUCAGGAAAACCUUACACAUUCCAAGCAGC.

For dsDNA the FAM-labeled sense-strand was annealed to the unlabeled anti-sense strain, by incubating them at a ratio of 1:1 for five minutes at 65°C and subsequently 20 minutes at 37°C.

2.3 Buffers and solutions

PBS (phosphate buffer saline), 20 x	160 g NaCl 4 g KCl 28.8 g Na_2HPO_4 + 2 H_2O 4.8 g KH_2PO_4	
	ad 1000 ml ddH_2O	pH 7.4
Ammonium chloride lysis buffer	8.29 g NH_4Cl 1 g $KHCO_3$ 0.0375 g Na_2-EDTA	
	ad 1000 ml ddH_2O	pH 7.4
MTT stop solution	49.7 ml DMSO 0.3 ml HCl 5 g SDS	
	50 ml solution	
Potassium phosphate buffer (1M)	K_2HPO_4 (1 M; Merck) KH_2PO_4 (1 M; Merck)	pH 7.4
Fixation solution (2,5% glutaraldehyde + 4% PFA)	2 g paraformaldehyde 18 ml ddH_2O 5 ml 25% glutaraldehyde 25 ml PBS	
	ad 50 ml ddH_2O	pH 7.4

2.4 RNA Isolation

RNA Isolation was performed using the RNeasy Mini Kit from Qiagen (Venlo, Netherlands) or the RNeasy Plus Micro Kit according to the manufacturer's protocol. Before the RNA isolation could be done, the cells needed to be lysed with 350 µl or 700 µl RLT Buffer, including β-mercaptoethanol (10 µl β-ME in 1 ml RLT Buffer) for the RNeasy Mini Kit or 350 µl RLT Plus Buffer including β-ME for the RNeasy Plus Micro Kit.

In the following paragraph, the general RNA isolation procedure using the RNeasy Mini Kit is described. The cell lysate was mixed with an equal volume (350 µl) of 70% ethanol and completely transferred onto a RNeasy Mini Column. This mixture was then centrifuged for 15 seconds at 8,000 × *g* before the flow-through was discarded. Thereafter, 700 µl of buffer RW1 were put onto the column and again centrifuged for 15 second at 8,000 × *g*. Again, the flow-

through was discarded and 500 µl of Buffer RPE were added. Subsequently, the column was centrifuged at 8,000 × *g* for 15 seconds again. The flow-through was again discarded and another 500 µl of Buffer RPE was transferred onto the column. After this step, the column was first centrifuged for 2 min at 8,000 × *g* and then 1 min at full speed. In order to elute the RNA from the column, 30 to 50 µl RNAse-free water was transferred directly onto the column membrane and incubated for 3 min at room temperature (RT). In the last step the column was centrifuged for 1 min at 8,000 × *g* before the RNA concentration at 280 nm was determined using a NanoDrop 2000 Spectrophotometer (Thermo Scientific, USA).

2.5 RNA Isolation from Paraffin-embedded tissue sections

For RNA Isolation from formalin-fixed, paraffin-embedded, tissue sections, the RNeasy FFPE Kit from Qiagen was used, according to the manufacturer's handbook.

In the first step, the two paraffin-sections (10 µm each) were carefully removed from the object slide and transferred into a 2 ml reaction tube (Eppendorf) using a razor blade. The following deparaffinization was then performed by adding 1 ml xylene (VWR Chemicals) to the paraffin-sections. This mixture was then vortexed vigorously for 10 seconds and centrifuged at full speed for 2 minutes. The supernatant was then carefully removed and 1 ml ethanol (100%) was added to the pellet. After vortexing, another centrifugation step at full speed was conducted for 2 min. Again, the supernatant was carefully removed and discarded. The reaction tubes were then left for about ten minutes to incubate at RT for remaining ethanol to evaporate. Then 150 µl of Buffer PKD were added and vortexed. After the addition of 10 µl proteinase K, two incubation steps were performed. The first incubation was 15 min at 56°C and thereafter 15 min at 80°C. The samples were then immediately transferred on ice and incubated for 3 min. After the incubation on ice the samples were centrifuged for 15 min at 20,000 × g (13,500 rpm) before the supernatant was carefully transferred to a new reaction tube. Now, DNase Booster Buffer at a tenth of the sample volume (16 µl) and 10 µl DNase I stock solution was added to the tube, mixed by carefully inverting the tube, and then incubated for 15 min at RT. Thereafter, 320 µl Buffer RBC was added to the samples and mixed thoroughly followed by

an addition of 720 µl ethanol (100%) and mixing by pipetting. From this mixture, 700 µl were transferred onto a RNeasy MinElute spin column placed in a 2 ml collection tube and centrifuged for 15 sec at ≥ 8,000 × g (≥ 10,000 rpm). After centrifugation the flow-through was discarded and the remaining sample was transferred onto the RNeasy MinElute spin column and the centrifugation repeated.

From here the protocol resembles the one from the RNeasy Mini Kit described in the previous paragraph. After the centrifugation 500 µl Buffer RPE was transferred onto the column and centrifuged for 15 sec at ≥ 8,000 × g (≥ 10,000 rpm). The flow-through was discarded and another 500 µl RPE was added to the column and centrifuged for 2 min at ≥ 8,000 × g (≥ 10,000 rpm). Then the lid of the RNeasy MinElute spin column opened and the column was placed in a new collection tube and centrifuged at full speed for 5 min. The RNeasy MinElute spin column was then placed on a 1.5 ml reaction tube. Finally, 25 µl RNase-free water was pipetted directly on the spin column membrane and centrifuged 1 min at full speed in order to elute the RNA. The RNA concentration was determined using a NanoDrop 2000 Spectrophotometer (Thermo Scientific). If the RNA concentration was much higher than 400 ng/µl, the sample was further diluted in RNase-free water and measured again.

2.6 Reverse transcriptase-PCR

In order to obtain complementary DNA (cDNA) for subsequent quantitative PCR, the isolated RNA (previous paragraphs) needs to be transcribed into cDNA.

All of the following steps have been performed on ice. Details about the reagents used are found in the table, “List of cDNA synthesis reagents”, in paragraph 2.2. First, 4 µg of RNA was diluted in nuclease-free H_2O (Roth) to a final volume of 10 µl if necessary and transferred into a 0.5 ml thin-walled PCR tube (Eppendorf). Then 1.5 µl 5 × first strand buffer (Invitrogen), 1 µl RNasin® Plus (Promega), 1 µl DNase I recombinant (Roche) and 2.5 µl nuclease-free H_2O were added per RNA sample, mixed well and placed into a thermal cycler (TRIO Thermoblock with heated lid, Biometra). The first incubation was 20 min at 37°C, followed by 10 min at 70°C before the samples were cooled to 4°C.

After that 1 µl Oligo dT (Invitrogen), 0.4 µl Random Primer (Promega), and 2.6 µl water was transferred to each tube. Incubation in the thermal cycler for 10 min at 70°C was the conducted, before cooling to 4°C. Finally, 4.5 µl 5 × first strand buffer, 1.5 µl dNTP Mix (Bioline), 1 µl DTT (Invitrogen), 0.5 µl RNasin® Plus, 1 µl SuperScript ® II Reverse Transcriptase (Invitrogen) as well as 1.5 µl nuclease-free water was added to each sample. The samples were then transferred into the thermal cycler again and incubated for 50 min at 42°C, followed by 10 min at 70°C before cooling to 4°C. The final cDNA was now diluted to a concentration of 10 µg/ml, which implies the addition of 370 µl nuclease-free H_2O to reach a final volume of 400 µl. If the amount of 4 µg RNA was not available in the beginning of the reverse transcription, accordingly less water is added to reach the final concentration of 10 µg/ml. The cDNA was subsequently diluted 1:4 (50 µl cDNA plus 150 µl H_2O) into a round-bottom 96-well cell culture plate (Greiner Bio-One) resulting in a final concentration of 250 ng/ml cDNA. The remaining cDNA in the tubes as well as the diluted cDNA in the 96 well-plate were stored at -20°C until further usage.

2.7 Quantitative PCR

Quantitative (q)-PCR was performed to investigate the amount of expression of various genes after cell stimulation or in different diseases compared to the healthy or untreated control. Gene specific primers were designed using the “assay design center” from Roche, which can be found online at: http://lifescience.roche.com/webapp/wcs/stores/servlet/CategoryDisplay?catalogId=10001&tab=Assay+Design+Center&identifier=Universal+Probe+Library&langId=-1 or taken from publications as indicated in the primer table (Table 4). The primer sequences are listed in table 4 for SYBR Green primers and obtained from MWG Eurofins. For assays on demand (AOD) from Applied Biosystems the catalogue number is listed in table 3.

The specific details for the qPCR reagents are found in paragraph 2.2 in the table “List of qPCR reagents and material”. The first step was the preparation of PCR primer mixes. The mix for the ribosomal 18 S control gene contained per sample 12.5 µl TaqMan Master Mix (Applied Biosystems), 0.15 µl Ribosomal Probe (life technologies), 0.15 µl Forward Primer (life technologies), 0.15 µl Reverse Primer (life technologies), and 2.05 µl nuclease-free water. This results

in a final volume of primer mix of 15 µl per sample. These 15 µl of primer mix were then transferred into a specific 96 well MicroAmp Optical qPCR plate before 10 µl of cDNA (25 ng) was transferred from the round-bottom 96 well-plate to the primer mix. An additional 10 µl nuclease-free H_2O were added to a separate well and served as negative control. The 96-well-plate containing the cDNA stocks were sealed with a NUNC plate seal and stored again at -20°C. The MicroAmp 96 well plate containing the qPCR mixtures was sealed with a StarSeal Advanced Polyolefin Film (STARLAB), centrifuged for 2 min at 1200 rpm in a Labofuge 400 (Heraeus by Thermo Scientific), and subsequently placed in the QuantStudio™ 6 Flex real-Time PCR System (Applied Biosystems by ThermoFisher Scientific, Waltham, US). The settings of the qPCR machine were adjusted to a VIC reporter and a TAMRA quencher. Furthermore, the machine was set to 40 cycles, starting off with a 2 min heating at 50°C followed by a temperature increase to 95°C for 10 min. Thereafter, the first cycle started with 15 seconds at 95°C and then 1 min at 60°C. This cycle was then repeated 39 times.

For TaqMan primers other than the ribosomal 18S control gene, the primer mix contained, per sample, 12.5 µl TaqMan Master Mix, 0.75 µl specific target probe (10 µM), 0.6 µl specific target forward primer (45 µM), 0.6 µl specific target reverse primer (45 µM), and 0.55 µl nuclease-free water. For AOD primers, 10 µl TaqMan Master Mix and 1 µl AOD primer was added to the cDNA. Here the qPCR machines detection was set to a FAM reporter without quencher and the cycles were as described above.

For SYBR Green primers, the primer mix contained 12.5 µl SYBR Green Master Mix and 2.5 µl of a 2 µM mix containing forward and reverse primer of the specific target gene. Using SBYR Green reagents the qPCR machine was set to a SYBR reporter without quencher. Additionally, a melt curve stage is included in the qPCR cycles. The cycles were identical to the ones with TaqMan primers described above, but a melt curve stage including 15 seconds at 95°C, followed by 1 min at 60°C and final heating to 95°C for 15 seconds is added to every cycle. Having this melt curve stage, one can easily evaluate the quality of the primer, when looking at the melt curve plot. If this plot depicts a single peak for all samples, the primer was working well and no primer dimers have been

formed. On the other hand, if there are two peaks that even reach the same height, then the samples need to be excluded from analysis and a new primer design should be considered. Furthermore, a very low gene expression might result in a plot without a precise peak.

2.8 Tissue homogenization for IL-26 ELISA

The skin biopsies were first transferred from the cryo-preservation tubes into polypropylene tubes containing 1 ml buffer consisting of PBS supplemented with 1 M NaCl and protease inhibitor (Protease Inhibitor Cocktail Set III, Merck Millipore). Subsequently, the homogenization was performed using a Polytron PT 2500 E (Kinematica). The homogenates were then transferred into Protein Low Bind Tubes (Eppendorf) and centrifuged at 5,000 × *g* for 5 min at 4 °C in a Centrifuge 5415 R (Eppendorf). The supernatant was taken and transferred into new Protein Low Bind tubes, which were then stored at −20°C until further usage. The remaining cell debris was discarded. Next, the Pierce™ BCA Protein Assay Kit (ThermoFisher Scientific) was used according to the manufacturer's protocol to determine the concentration of total protein. Finally, the samples' total protein concentration was adjusted to 100 µg/ml and thereafter IL-26 protein concentrations were determined by ELISA (Cusabio Biotech).

2.9 Enzyme linked immunoassay

Interleukin-26 protein content in human skin punch biopsies was determined using the commercially available enzyme linked Immunoassay (ELISA) kit for Interleukin-26 from CusaBio Biotech. The ELISA was implemented according to the manufacturer's instructions.

Cytokine levels in supernatants from monocyte-derived dendritic cells (moDCs) and macrophages were identified with DuoSet ELISA kits for IL-6 (moDCs only) and TNF-α (both biotechne) following the manufacturer's instructions.

IL-1β levels in supernatants from $CD14^+$ Monocytes were measured with the respective DuoSet ELISA from biotechne.

CXCL8 and IL-10 in supernatants from keratinocytes were also analysed with the respective DuoSet ELISA (biotechne) according to the manufacturer's handbook.

2.10 Immunofluorescence with cryo-preserved tissue sections

The cryo-cutted skin sections were first air-dried and subsequently fixed in acetone for 10 min at 4°C. The slides were then marked with fat-pen before they were washed twice for 3 min in PBS. The slides were then transferred into a moist chamber and incubated for 30 min at RT with a blocking buffer consisting of PBS with 2% goat serum, 0.1% fish gelatin (Sigma), and 0.05% Tween-20. After the incubation time, the blocking buffer was removed and unlabeled anti-IL-26 antibody or isotype control antibody (mouse IgG1, Dako Agilent Technologies) was diluted in a blocking buffer to a final concentration of 10 µg/ml and transferred onto the respective cryo-section. The skin sections were then incubated with the unlabeled primary antibodies at 4°C overnight. The slides were then washed three-times for 3 min with PBS, before they were covered with 2 µg/ml AlexaFluor555 donkey anti-mouse secondary antibody (Invitrogen Molecular Probes) for 45 min at RT. Thereafter, the sections were washed again three-times with PBS. Then the samples were covered with 10 µg/ml 4′,6-diamidin-2-phenylindol (DAPI; Molecular Probes) and incubated for 10 min at RT. After this incubation time, the sections were washed twice for 3 min with PBS before they were mounted (Fluoromount-G; eBioscience), covered with coverslip, and stored at 4°C until fluorescence microscopy.

2.11 Immunohistochemistry with FFPE tissue sections

In the first step of immunohistochemistry (IHC), the slides with the paraffin-sections (10 µm per section) were incubated vertically overnight at 60°C or 80°C. The slides were then washed in an alcohol series starting with 99% isopropanol, followed by 96% isopropanol and finished with 70% isopropanol. The slides were then incubated for 20 min with a demasking solution (Dako Target Retrieval Solution, ph9; Dako Agilent Technologies) in a steam cooker, and subsequently the slides were washed for 5 min in PBS. After marking the slides with a fat-pen they were incubated with 0.6 % H_2O_2 for 10 min. The slides were then washed for 5 min three times in PBS. Next, the sections were incubated with 10% human serum and Streptavidin (4 drops/ml; from the Streptavidin/Biotin Blocking Kit, Vector Laboratories) in a moisty dark chamber for 30 min at RT. After the incubation time, the serum and Streptavidin was removed.

Then the primary antibodies: anti-IL-26 (Clone: 197505 unconjugated, biotechne) and mouse isotype (BD Pharmingen™ Purified Mouse IgG2b, κ Isotype Control, BD Biosciences), were diluted in 1% human serum/PBS and Biotin (from the Streptavidin/Biotin Blocking Kit) and adjusted to a final concentration of 2 µg/ml before distribution on the slides. In a different IHC experiment, the primary antibodies, anti-TXN (clone: polyclonal goat IgG unconjugated, biotechne) and its corresponding goat isotype ChromPure Goat IgG (Jackson ImmunoResearch Laboratories), were diluted to a final concentration of 2 µg/ml in 1% human serum/PBS and Biotin. The slides were incubated in the moisty dark chamber overnight at 4°C. Subsequently, the antibodies were removed, and the slides were washed three times for 5 min in PBS. Now, the slides were incubated with 10% horse serum diluted in PBS for 15 min at RT and then washed again three times for 5 min in PBS

After the last washing step, the secondary antibody (biotinylated anti-mouse IgG from VectaStain) was diluted 1:200 in PBS, transferred onto the slides and incubated for 30 min at RT. Then another set of three 5 min washes with PBS was conducted before Streptavidin horseradish peroxidase (HRP; Dako Agilent Technologies) diluted 1:500 in PBS was added on the slides and incubated for 45 min at RT. The sections were then washed twice for 5 min in PBS and once for 5 min in distilled H_2O. After these washing steps, the sections were incubated with the AEC 2 Components Kit (DCS Chromokine) at RT and the time point to stop the reaction was monitored frequently under the microscope. After about eight to ten minutes the reaction was stopped by transferring the slides into distilled H_2O. After the filtration of hematoxylin, the sections were counterstained with the freshly filtered hematoxylin for 15 sec. The counterstaining was stopped using tap water and the slides were then washed twice more in tap water. To finally stop the reaction, the slides were incubated in citrate for two minutes. The sections were then covered with mounting medium (DCS Labline, DCS) and coverslips. The sections were stored at RT until microscopy using a Nikon ECLIPSE Ni microscope together with a Nikon DS-Ri1 camera and the program NIS-elements BR Version 4.20 (Nikon Instruments Europe B.V.).

2.12 NADPH consumption assay

This assay was used to indirectly determine the reduction of monomeric IL-26 using the Thioredoxin system composed of nicotinamide adenine dinucleotide phosphate (NADPH), rat thioredoxin reductase 1 (ratTXNRD1), and human Thioredoxin (TXN). The consumption of NADPH is thereby indicated by a decrease of absorption at 340nm. The protocol implemented was analogous to that in Holmgren et.al.[193] and Schroeder *et al.*[123].

This assay was performed in 0.1 M potassium phosphate buffer with 2 mM EDTA in a final volume of 60 µl. The reaction compounds were 0.2 µM TXN (Sigma-Aldrich), 10 nM TXNRD (Sigma-Aldrich) and 32 µM NADPH (biomol), which were preincubated for 30 min at RT before the addition of 2.5 µM IL-26. These incubation mixtures were then immediately transferred into cuvettes (UVette, Eppendorf) and the absorbance at 340 nm was measured with a NanoDrop 2000 Spectrophotometer (Programm UV-Vis; ThermoScientific) repetitively every 5 min for at least 1.5 hours. Insulin (2.5 µM; Insuman Rapid, Sanofi), the antimicrobial peptide LL37 (2.5 µM) or the Thioredoxin system alone were used as controls.

2.13 RNA generation from the U937 cell line

The human monocytic U937 cells were UVB-irradiated and the supernatants, as well as the RNA isolated from the cells, were used for different IL-26/RNA complex experiments, e.g. stimulation of moDCs.

The U937 cell line was maintained in RPMI 1640 medium (Gibco, life technologies) supplemented with 10 % fetal calf serum (FCS), 10.000 units/ml Penicillin and 10.000 µg/ml Streptomycin at 37°C and 5% CO_2. The cell culture was maximally grown to a density of 2×10^6 cells per ml.

Half of the cells were UV-irradiated with 60mJ/cm^2 to induce apoptosis and subsequently incubated for 4h at a density of 1×10^6 cells per ml. The other half was irradiated with 480 mJ/cm^2 and incubated for 24h at high density (50×10^6 cells/ml)[98]. This procedure leads the cells into necrosis. With the end of the respective incubation times the cells were pelleted and resuspended in RLT buffer (supplied with the RNeasy Mini Kit).

2.14 Nucleic acid condensation assay

The DNA condensation assay was performed analogous to Ganguly *et al.* [98]. Human genomic DNA (3 µg/ml; InVivoGen) was incubated with human monomeric IL-26 in different concentrations up to 2 µM for 30 min at RT in a final volume of 60 µl in Eppendorf tubes. The samples were then stained with PicoGreen (Quant-iT PicoGreen dsDNA kit, Invitrogen) according to the manufacturer's protocol and transferred into a black half-area 96-well-plate (Corning). The specimen was then measured fluorometrically with an excitation at 485 nm and a measured emission at 538nm using a Fluoroskan Ascent (Thermo Scientific).

The massive drop in nucleic acid staining results from the IL-26/DNA complex formation and denotes the DNA condensation. This observation is explained by dye exclusion.

In some experiments, IL-26 was incubated with 2 mM DTT for 30 min at RT to reduce the disulphides before human DNA was added.

The IL-26/RNA complex assay was implemented identically as describe above with only the exceptions that the RNA was generated from the monocytic cell line U937 (see paragraphs 2.4 RNA isolation and 2.13) and stained with RiboGreen (Quant-iT RiboGreen RNA kit, Invitrogen).

2.15 Cell isolation from Buffy Coat

Buffy Coats obtained from the blood donor centre were transferred into a cell culture bottle and diluted with PBS to a volume around 125 ml. Subsequently the blood-PBS-mixture was very carefully transferred to 50 ml-Falcon tubes that already contained 15 ml Ficoll-Paque PLUS (GE Healthcare). The total four tubes were now centrifuged at 1150 rpm for 20 min at RT (without brake and speed-up) using a Rotanta 46 RC centrifuge (Hettich). Thereafter the lymphocyte layer was collected and transferred into a new tube pooling two original tubes. The Falcon tubes were then filled up to 50 ml with room-tempered PBS before another centrifugation step (970 rpm, 10 min, RT, no brake, no speed-up) was performed. After discarding the supernatant, the remaining two Falcon tubes were pooled, 25 ml lysis buffer (isotonic ammonium chloride solution {NH_4Cl}) was added and incubated for 10 min at 4°C. To stop

the lysis reaction, 25 ml PBS was appended. The cell solution was now centrifuged again using the same conditions as described above. The supernatant was again discarded, and the remaining cell pellet was suspended in 50 ml PBS before the number of cells was determined. The cell suspension containing peripheral mononuclear cells (PBMCs) was now ready for further procedures, such as the isolation of $CD14^+$ cells using the MagCellect Kit (biotechne).

2.16 Cell culture

2.16.1 HaCaT and primary keratinocytes

HaCaT keratinocytes are a cell line created from human adult skin keratinocytes by Boukamp *et al.*[194]. The cells, a kind gift from Norbert Fusenig (Deutsches Krebsforschungszentrum (DKFZ), Heidelberg, Germany), were cultured as described[194], maintained in Dulbecco's modified Eagle medium (DMEM) supplemented with 10 % fetal calf serum (FCS), 1% Pencillin and Streptomycin as well as L-glutamine and used in early passages (ca. 30 to 40). Even though HaCaT keratinocytes arose from spontaneous transformation and are considered immortal and non-tumorigenic, they do not differ much from primary keratinocytes in terms of morphology as well as differentiation and cytokine expression patterns [194]. Due to their high similarity to their human origin, HaCaT are well suitable as model cell line for primary keratinocytes.

Primary human normal keratinocytes were obtained from human foreskin. The keratinocytes were then grown in Keratinocyte-serum free medium (Keratinocyte-SFM, Gibco by Thermo Fisher Scientific) together with supplements for keratinocyte-SFM (contains Bovine Pituitary Extract (BPE) and human recombinant epidermal growth factor (EGF), Gibco) until sub-confluence.

2.16.2 Monocyte-derived dendritic cells

The first step to monocyte-derived dendritic cells (moDCs) was the isolation of $CD4^+$ monocytes from PBMCs. This was done using the MagCellet Human CD14+ cell Isolation Kit (biotechne) or alternatively using the human Monocyte Isolation Kit II (Miltenyi Biotec) according to the instructions provided by the manufacturer. After the last isolation step, the cells were suspended in 10 ml

cell culture media (RPMI 1640 GlutaMAX (Gibco), supplemented with 10% FCS as well as penicillin and streptomycin) and counted. The cell concentration was then adjusted to 1 × 10^6 cells per ml, and 100 ng/ml GM-CSF as well as 50 ng/ml IL-4 (final concentrations, respectively) were added to the cell suspension. Finally, the cell suspension was distributed 2 ml per well into 12-well-plates and incubated for 3 days at 37°C and 5% CO_2 in an INCO2 incubator (Memmert GmbH + Co.KG).

After 3 days of incubation the medium was renewed by carefully removing 1 ml and subsequently adding 1 ml fresh medium supplemented with 100 ng/ml GM-CSF and 50 ng/ml IL-4 to each well. The medium change was followed by an additional incubation time of 3 days. On the 6^{th} day the cells, now exhibiting small dendrites, were suspended, transferred into a Falcon tube and centrifuged at 1150 rpm for 10 min at RT. The cell pellet was suspended in a 10 ml warmed RPMI and counted. Thereafter, 100 ng/ml GM-CSF and 50 ng/ml IL-4 were appended and the cell concentration was adjusted to have 200.000 cells/175 µl/well in a round-bottomed 96-well-plate. The different stimulating agents, such as LPS (final: 100ng/ml), LL37 (final: 10 µM), IL-26 (final: 2 µM), and LL37/RNA complexes as well as IL-26/RNA complexes, were added in a final volume of 25 µl. Additionally, the LL37/RNA or IL-26/RNA complexes were incubated for 30 min at RT before appending to the cells. Cells stimulated only with RNA (3 µg/ml and 10 µg/ml) or 25 µl H_2O were used as negative controls.

In some experiments, IL-26 was incubated for 30 min at 37°C with RNAse A (final: 50 µg/ml) and DNase I (final: 2000 U/ml) before appending to the cells. Furthermore, sometimes cells were treated with chloroquine (5 µM, InvivoGen) or bafilomycin (100 nM; InvivoGen) for 30 min at 37°C prior to the addition of IL-26/RNA complexes. The supernatants were collected and stored at -20°C for ELISAs and the cells were analysed via flow cytometry (paragraph 2.21).

2.16.3 Monocyte-derived macrophages

Monocyte-derived macrophages (Mϕ) were generated similarly to moDCs as described in the paragraph above, but their cell culture media was only supplemented with 100 ng/ml GM-CSF. Briefly, the $CD14^+$ monocytes were adjusted to a concentration of 1 × 10^6 cells per ml and 100 ng/ml GM-CSF was

added. The cell suspension was then transferred into a flat-bottom 96-well-plate (200 µl per well) and incubated from 3 days before the first medium change. On the 6th day, the medium was completely removed, and the cell stimulation was performed.

2.16.4 THP1 Macrophages

Experiments with THP1 macrophages were performed in cooperation with the group of Prof. Rainer Kalscheuer from the Institute of Pharmaceutical Biology at the Heinrich-Heine-University Düsseldorf. The THP1 monocytic cell line was cultured in RPMI 1640 supplemented with 10% FCS (without antibiotics). The cells were adjusted to 1 × 10^6 cells per ml and 100 µl cell suspension was transferred into each well of a 96-well-plate. Subsequently, the cells were stimulated with 50 nM phorbol 12-myristate 13-acetate (PMA) overnight in order to generate macrophages. After the incubation time with PMA, the medium was completely removed and the cells were washed twice with PBS.

For stimulation experiments using different reagents, such as IL-26, LL37, or LPS, the cells were subjected to the respective reagent diluted in medium to a final volume of 100 µl per well. The stimulated cells were then incubated at 37°C and 5% CO_2 for 24 hours.

For infection experiments to investigate the intracellular killing capacity of IL-26, see paragraph 2.20.

2.16.5 HEK-Blue™ hTLR2 cells

HEK-Blue™ hTLR2 cells are obtained from InvivoGen, derived from a HEK293 cells line and are specially engineered human TLR2 and secreted embryonic alkaline phosphatase (SEAP) co-expressing cells. The SEAP reporter gene is under the control of a promotor fused to NF-κB and AP-1 binding sites. The stimulation of TLR2 can then be evaluated via the activation of NF-κB and subsequent induction of SEAP. Using the suitable HEK-Blue™ Detection medium, the amount of SEAP secretion can easily be observed by the naked eye and measured using a spectrophotometer at 620 (to 655) nm.

HEK-Blue™ hTLR2 cells were cultured and maintained according to manufacturer's instructions in DMEM (Gibco) supplemented with 4.5 g/l glucose, 10% FCS, 50 U/ml penicillin, 50 µg/ml streptomycin, 100 µg/ml

Normocin™ (InvivoGen), and 2 mM L-glutamine. In this media, the cells were cultured for two passages until 1× HEK-Blue™ Selection (a selective antibiotics cocktail) was added to the cell culture medium. The cell culture medium was changed twice a week and the cells were passaged after a confluency of 70 to 80% was reached. For passaging, the cell media was removed completely, PBS was added, and the cells were detached by tapping against the cell culture flask.

2.16.6 Mycobacteria

Experiments with *Mycobacterium tuberculosis H37Rv* (Mtb, virulent strain) were performed in cooperation with the group of Prof. Rainer Kalscheuer from the Institute of Pharmaceutical Biology at the Heinrich-Heine-University Düsseldorf. Mtb was cultured in Difco™ Middlebrook 7H9 Broth (BD Biosciences) supplemented with 10 % ADS (5% bovine serum albumin (BSA), 2% D(+) glucose and 0.85% NaCl) as well as 0.05% Tween-20. The mycobacteria were incubated at 37°C and continuously lightly shaken.

Furthermore, *Mycobacterium bovis BCG*, which is classified into biosafety level 2, were cultured in Middlebrook's 7H9 Broth as described above.

2.16.7 Pseudomonas aeruginosa

Experiments with *Pseudomonas (P.) aeruginosa* have been performed in collaboration with the group of Prof. Brötz-Oesterhelt and the group of Prof. Däubener at biosafety level 2. *P. aeruginosa ATCC 27853* was cultured in tryptic soy broth (TSB) until mid-logarithmic growth with was monitored at an optical density (OD) of 600 nm. For P. aeruginosa an OD_{600nm} of 0.1 resembles a bacterial concentration of 1.1×10^8 colony forming units (CFU) per ml. The bacteria were then subjected to microbroth dilution assays similar as described in chapter 2.18. In contrast, here the bacterial cells were adjusted to 1×10^5 CFU/ml and incubated for 18n before the OD at 600nm was measured.

2.17 Secreted embryonic alkaline phosphatase reporter assay

HEK-Blue™ hTLR2 cells needed to be at 70 to 80% confluency.

To start off, 20 µl of each sample or control were added per well in a flat-bottom 96-well-plate (Greiner Bio-One) with some exceptions, e.g. where a pre-

incubation with cells was necessary. In different experiments, LL37 (10 µM), IL-22 (2 µM), IL-26 (2 µM), IL-26 in combination with 10 µg/ml anti-hTLR2-IgA (Invivogen), and IL-26 in combination with DNAse I (2000 U/ml) and RNAse A (50 µg/ml) have been used. Anti-hTLR2-IgA and DNAse I/RNAse A have been added 45 min prior to the addition of IL-26. Positive controls were LPS (100 ng/ml) and LTA (100 ng/ml; InvivoGen). As negative controls, water, medium only, and PBS were used.

After the HEK-Blue™ hTLR2 cells have been removed from the incubator, their growth medium was discarded and 2 ml pre-warmed PBS was added to the flasks. The cells were then detached by tapping against the flask and possible cell clumps were dissociated by pipetting up and down. The cells were then counted and adjusted to a concentration of 0.28×10^6 cells per ml in HEK-Blue™ Detection medium. An amount of 180 µl of cell suspension was then added to each well of the 96-well-plate, resulting in 50,000 cells per well. The cells were then pre-incubated for 45 min at 37°C and 5% CO_2 before finally IL-26 and other reagents (as named above) were added. The cells were then again transferred into an INCO2 incubator (Memmert GmbH + Co.KG) at 37°C, 5% CO_2 for 24 hours. After the incubation time, the SEAP secretion turned the HEK-Blue™ Detection medium from a reddish colour into a blue colour that was then measured using a spectrophotometer Multiskan Ascent (ThermoFisher Scientific) or an Infinite® M200 (TECAN) at 620 nm.

2.18 Microbroth dilution assay

Microbroth dilution assays or “killing assays” with *Mycobacterium tuberculosis* (Mtb) and *M. bovis BCG* were performed to determine if IL-26 is capable of killing mycobacteria, and if yes, which minimal inhibitory concentration can be obtained.

This assay was performed in a round-bottom polypropylene 96-well-plate (Corning Costar) as IL-26 is very prone to bind to the polystyrene that is used in regular 96-well plates. This binding would lead to less bacterial killing and thereby falsifying the results.

In the first step, the mycobacteria, which have been incubating at 37°C with light shaking, were transferred into a cuvette together with an equal amount of 10%

formaldehyde (Sigma-Aldrich) in order to deactivate the culture. The cuvette was then used to measure the optical density (OD) of the culture at 600 nm. An OD_{600nm} of 1 equals 3×10^8 colony forming units (CFU) per ml. The cells were then diluted to a final concentration of 1×10^6 CFU/ml in RPMI medium diluted 1:4 in ddH2O. Now, 50 µl of diluted RPMI medium was transferred into all wells of the polypropylene 96-well-plate except the first column. In each well of the first column, the reagents to test (e.g. IL-26, LL37 as well as Rifampicin, which served as positive control, and DMSO and PBS, which were negative controls) were diluted in a final volume of 100 µl with diluted RPMI medium to the double concentration as the highest concentration was supposed to be. Thereafter, a serial dilution was performed using a multichannel pipette and transferring 50 µl from wells of the first column to the second. Then the components of the second column were pipetted up and down and finally 50 µl were again transferred to the third row. This procedure was repeated until the second last row was reached, then the remaining 50 µl in the multichannel pipette were discarded and the last row was kept untouched.

Now, as all wells had a content of 50 µl serially diluted components, the mycobacteria were added in a volume of 50 µl reaching a final volume of 100 µl. The bacterial concentration was now 0.5×10^5 CFU per well. The 96-well-plate was incubated for 5 days at 37°C without shaking. After the incubation time, 10 µl resazurin was added to all wells and incubated for another 24 hours at RT. Resazurin is blue dye that is metabolized by living and active cells to a pinkish dye called resorufin. The change in color is then measured with a fluorescence reader (Infinite® 200, TECAN) using an excitation wavelength at 540 nm and an emission wavelength at 590 nm. For some experiments with *M. bovis BCG* a BakTiter-Glo™ Microbial Cell Viability Assay (Promega) was performed according to the manufacturer's instructions.

2.19 Scanning Electron Microscopy

Sample preparation with critical point drying (CPD) and following scanning electron microscopy (SEM) of treated and untreated *Mycobacterium tuberculosis H37Rv* were performed by Steffen Köhler from the Center of Advanced Imaging (CAi) at the Heinrich-Heine-University Düsseldorf.

Mycobacteria were adjusted to a concentration of 5 × 10^5 mycobacteria/ml in a diluted RPMI medium without supplements and transferred to a 24 well plate containing a round cover glass, which was pre-coated with poly-L-lysine (PLL; Sigma-Aldrich) according to the manufacturer's poly-L-lysine cell attachment protocol. After addition of the reagents, with potential anti-mycobacterial activity, such as in the case of IL-26 or LL37, and positive controls, such as rifampicin or isoniazid, the mycobacteria were incubated for 24 hours or 5 days. Isoniazid is a potent anti-mycobacterial agent inducing bleb-formation in the mycobacteria and is therefore used as suitable positive control.

After incubation, the mycobacteria were fixed with a fixation solution consisting of glutaraldehyde and paraformaldehyde (PFA) in a phosphate buffer (PBS). In order to prepare this fixation solution, PFA was dissolved in distilled water at 60°C to a concentration of 11 %. To this, 25% glutaraldehyde and PBS was added to create a solution with 8% PFA and 5% glutaraldehyde. The addition of glutaraldehyde to PFA needs to be freshly prepared every time. An equal amount of fixation solution as mycobacteria suspension was added to the chambers resulting in a final fixation concentration of 2.5% glutaraldehyde and 4% PFA. Both of those substances in the concentrations used would separately kill the mycobacteria. After incubation, with the fixation solution refrigerated for at least 16 hours, the chamber slide was intensely disinfected on its surface and then taken out of the S3 laboratory for further procedures such as dehydration.

The media and fixation solution were carefully removed completely from the wells containing the cover glasses. Then 200 µl PBS was carefully added to the wells and incubated for some minutes. The PBS was then carefully removed and the lowest concentration of ethanol (EtOH, 50%) was transferred to each chamber and incubated at RT for five minutes. The 50% ethanol was then carefully removed and 70% EtOH were added with care. This serial dehydration series was repeated with increasing EtOH concentrations (80%, 90%, and 96%) until pure (100%) EtOH was transferred onto the cover glasses. After removal of the 100% EtOH, the cover glasses were washed twice with 100% acetone for final complete drying. The dehydrated samples were then subjected to CPD.

The dried cover glasses were sputtered with gold using a Manual Sputter Coater (Agar Scientific). Scanning electron microscopy was performed using a Leo 1430 VP (Zeiss).

2.20 Intracellular killing assay (Mycobacteria in THP1 macrophages)

PMA-stimulated THP1 macrophages were washed twice with PBS as described in paragraph 2.16.4. After washing with PBS, RPMI medium was added to the THP1 macrophages and they were rested for 3 hours. In these experiments it is crucial that the macrophages have been growing confluent in order to obtain good results in fluorescent microscopy. The rested macrophages were then transferred into the biosafety level 3 (BSL3 or S3) laboratory where they were infected with a *Mycobacterium tuberculosis H37Rv* reporter strain (Mtb pBEN::mCherry (Hsp60)), that expresses mCherry under a promotor of heat shock protein 60 (Hsp60). With this reporter gene construct mycobacteria inside, the macrophages are easily evaluated via fluorescent microscopy. The THP1 macrophages were infected with a MOI (molecules of infection) rate of 3, meaning there were 3 mycobacteria per cell. As there were 1×10^5 macrophages per well, the number of mycobacteria was adjusted to a concentration of 3×10^5 mycobacteria per well and added a final volume of 20 µl to the cells. Mycobacteria and macrophages were now incubated for 3 h, before all medium was removed and the cells were washed once with PBS. Subsequently, fresh medium, including gentamycin (5 µg/ml), was added to all wells. Gentamycin kills all extracellular mycobacteria and is not able to pass the macrophage membrane. At this point the reagents such as IL-26 (final: 2 µM), LL37 (final: 10 µM), Rifampicin (final: 10 µM) and controls were added. The infected THP1 macrophages were incubated at 37°C for 5 days, before fluorescent microscopy was performed.

2.21 Flow cytometry

Flow cytometry was performed to detect specific surface proteins. First, immune cells were isolated from the buffy coat, e.g. $CD14^+$ monocytes were isolated from PBMCs using the earlier described MagCellect $CD14^+$ Cell Isolation Kit (biotechne). The cells were then transferred into specific flow cytometry tubes and centrifuged for 1250 rpm for 5 min at 4°C. The supernatant was then

discarded, the cells suspended in 1 ml cold PBS and divided in further flow cytometry tubes for unstained and stained cells and for cells treated with isotype control. Then three drops of human serum were added to each tube and incubated on ice for 15 min before 1 ml cold PBS was added to each tube. Subsequently, the tubes were centrifuged again at 1250 rpm, 5 min at 4°C. The supernatant was discarded, the pellet was suspended and 0.5 µg/ml antibody (anti-IL-20RA or mouse IgG1 isotype control, see *table 5*) was added and incubated for 45 min on ice in the dark. After the incubation, 2 ml cold PBS were added to each tube and centrifuged again at 1250 rpm for 5 min at 4°C. After discarding the supernatant and resuspension of the cell pellet, 500 µl 10% donkey serum was added for 15 min while the sample was on ice, before another 1ml cold PBS was transferred into the flow cytometry tubes. The samples were then centrifuged again. After the supernatant was again discarded, 10 µg/ml anti-mouse IgG1 AlexaFluor555 secondary antibody was added and incubated for 20 min on ice in the dark. 2 ml cold PBS were added and the sample was centrifuged, for the last time, as before. The supernatant was again removed, and the cell pellet was resuspended and fixed in 250 µl 1% PFA. The analysis was done using a FACS Calibur flow cytometer (BD Biosciences) together with the corresponding CellQuest software (BD Biosciences).

TABLE 5: List of flow cytometry antibodies.

Antibody	**Clone**	**Company**
Human IL-20RA antibody	173707	Biotechne
Mouse IgG_1 Isotype Control	11711	Biotechne
CD83-FITC (IgG_1, BD)	HB15e	Biotechne
CCR7-PE(IgG_{2a}-PE, BD)	150503	Biotechne
CD86-PE-Cy5 (IgG_{2b}-PE-Cy5, BD)	IT2.2	eBioscience

2.22 MTT cell viability assay

Cell viability was evaluated using an MTT assay. In this colorimetric assay, viable cells convert MTT (3-(4,5-dimethylthiazol-2-yl)-2,5-diphenyltetrazolium bromide; Sigma) into formazan, an insoluble component with a purple colour[195].

A subsequently added solution containing sodium dodecyl sulphate is then dissolving the formazan obtaining a coloured solution of which the absorbance is then measured.

The cells (e.g. keratinocytes) were cultured in a flat bottom 96-well-plate and the medium was adjusted to 100 µl per well. Fifty µl of the MTT solution (5 mg/ml, in PBS) were added to the wells and incubated for two hours at 37°C. The medium was then decanted completely by inverting the 96-well-plate or alternatively via careful removal if non-adherent cells were in the plate. Thereafter, 100 µl MTT Stop Solution (described above) was added and incubated for 20 min at RT before the absorbance was measured at 570 nm in a spectrophotometer.

2.23 Microscale Thermophoresis

Microscale thermophoresis (MST) analysis was performed in cooperation with the working group of Prof. Joachim Ernst from the Institute of Molecular Mycology at the Heinrich-Heine-University Düsseldorf. A NanoTemper Monolith NT.115 apparatus[196] was used to perform the experiments.

A constant amount of FITC-labeled LPS (45 nM; Sigma) and Alexa488-labeled lipoteichoic acid (LTA, 38 nM; InvivoGen) was incubated for 15 min at 37°C in the dark with different concentrations of IL-26 or IL-22 (serially diluted) in MST binding buffer (50 mM Tris-HCl, pH 7.6, 150 mM NaCl, 10 mM $MgCl_2$, 0.05 % Tween-20) containing 0.005% SDS for IL-26/LTA measurements. LTA was labelled with the Alexa Fluor 488 ® Microscale Protein Labeling Kit from life technologies according to the manufacturer's instructions. Ten µl of the samples were loaded into standard glass capillaries (Monolith NT Capillaries) and thermophoresis analysis was performed (settings for the light-emitting diode (LED) and infrared (IR) laser were 80% and 70%, respectively).

For DNA and RNA binding experiments, single-stranded and double-stranded FAM-DNA as well as FAM-RNA (all: 10 nM; MWG Eurofins Genomics) were incubated analogously to LPS and LTA. The sequences of the FAM-DNA as well as FAM-RNA are indicated in the reagents section in paragraph 2.2. The MST buffer used here contained 50 mM Tris, 0.05% Tween 20, and 0.005% SDS. For measurements with nucleic acids and LL37, the MST binding buffer

did not contain SDS. For experiments that involved reduced IL-26, 1mM TCEP was added to the MST buffer in order to maintain a reducing environment.

In order to investigate the potential binding of IL-26 to lipoarabinomannan (LAM), a surface molecule found on mycobacteria, purified LAM from Mycobacterium smegmatis, and purified LAM from Mycobacterium tuberculosis H37Rv was obtained through BEI Resources, NIAID, NIH. Subsequently, LAM was labelled with the previously described Alexa Fluor 488 ® Microscale Protein Labeling Kit according to manufacturer's instructions. AlexaFluor488-labeled LAM was adjusted to a constant concentration of 200 nM for following MST measurements. The MST buffer used here contained 50 mM Tris and 0.05% Tween 20. For measurements with LAM and reduced IL-26 the MST binding buffer did additionally contain 1mM TCEP and 0.005% SDS. MST measurements were performed with LED power set to 100% and IR laser to 70%.

For graphical depiction of the results, the K_D values and other information was provided to NanoTemper's homepage: http://www.nanotemper-technologies.com/get-it-all/tools/concentration-finder/. The homepage then provides the data that were used for GraphPad Prism analysis.

2.24 Reduction of IL-26 and HPLC Purification

Experiments involving protein reduction and the purification via HLPC were either done in cooperation with Prof. Jens-Michael Schröder from the Department of Dermatology, Kiel or Dr. Lothar Gremer from the Institute of Biophysics at the Heinrich-Heine-University Düsseldorf. To obtain reduced IL-26, recombinant human IL-26 was incubated in low-bind tubes with 20 mM DTT at 37°C for 4h. As this high concentration of DTT would negatively impact all further experiments, the reduced IL-26 needed to be purified. The reduction of IL-26 with DTT frequently leads to precipitation and therefore the reduced IL-26 was first centrifuged at 8000 rpm for 8 min at RT. The supernatant was removed, and the resulting pellet was dissolved by the addition of 40 µl methanol, 80 µl 80% acetonitrile in 0.1% trifluoraocetic acid (TFA), and 460 µl 0.1% TFA in H_2O. The dissolved, reduced IL-26 was then subjected to reversed phase-HPLC. The HPLC column used was a Zorbax 300 SB C8 column (9.4 ×

200 mm, 1 ml/min, 1000 µl loop) together with an Agilent HPLC machine (Agilent, Santa Clara, USA). The collected, purified, and reduced IL-26 was then transferred into low-bind tubes and snap-frozen in liquid nitrogen. In order to narrow down the volume and increase the concentration of the reduced IL-26, the open tubes were placed in a Speedvac vacuum concentrator (Savant, Thermo Scientific) and centrifuged at 1000 rpm. The concentration of the reduced IL-26 was finally determined using a NanoDrop spectrophotometer with the programme “Protein A280” and the selection “type: other protein” and “ε/1000: 16.96” and “MW (kDa): 17.72” specifically for the reduced IL-26.

2.25 Circular dichroism

Circular dichroism (CD) experiments were performed in cooperation with Dr. Lothar Gremer from the Institute of Biophysics at the University Düsseldorf. The measurements were performed on a JASCO J-815 spectropolarimeter (Jasco Corporation) at a temperature of 25°C.

In the first step, 20 mM sodium phosphate (NaH_2PO_4 × H_2O, AppliChem PANCREAC) buffer was prepared with double distilled H_2O. The buffer was adjusted to a pH of 6.5. Oxidized IL-26 needed to be transferred into this buffer since its original stock solution contains glycerol, which negatively effects CD spectrum measurements.

IL-26 (stock: 75 µM) was transferred onto a 0.5 ml Amicon Ultracel 10K Membrane filter (Millipore) together with 20 mM sodium phosphate. The mixture was then centrifuged at 12300 rpm for 8 min at 4°C. The eluent was discarded and new sodium phosphate buffer was transferred onto the Amicon filter, before it was centrifuged again. This procedure was repeated four times. Then the Amicon was placed upside down on a collection tube and centrifuged at 3300 rpm for 2 min at 4°C. The IL-26 was eluted with 4-times 50 µl 20 mM sodium phosphate and centrifugation steps into the collection tube. The volume was then adjusted to 250 µl, which is needed for the CD cuvette. Subsequently, the final concentration of IL-26 was determined using a NanoDrop 2000 spectrophotometer.

2.26 Hypoxia treatment

Experiments where hypoxia was induced in cells were performed in cooperation with the group of Prof. Joachim Ernst from the Institute of Molecular Mycology at the University Duesseldorf. Skin cells and immune cells were cultivated in their respective standard culture medium and stimulated with different reagents, e.g. IL-26. The cells were then placed in an InVivoO_2 200 hypoxia chamber (Ruskinn) under 1% O_2 and 5% CO_2 and 37°C. In order to compare the results, some cells were treated under standard normoxic conditions (atmospheric O_2 (20%), 5% CO_2 and 37°C) in a separate incubator.

2.27 Calculations and statistical analysis

All analyses were done using GraphPad Prism Version 5.03 (GraphPad Software, Inc.).

In the NADPH consumption assay, the data from NADPH alone was subtracted from the actual sample (IL-26, insulin or CAMP) to achieve delta (∆) values. These values were then adjusted to the initial value (start value equals 0).

For sample group sizes larger than 10, D'Agostino and Pearson normality testing was performed first. If the samples did not pass normality testing, the non-parametric Kruskal-Wallis test with Dunn's post-hoc testing was performed if more than two groups were compared. For statistical analysis of two groups without guaranteed normal distribution or sample sizes less than 10, non-parametric Mann Whitney *U* test was applied.

In cases with a strong variation in the control samples and between experiments, Wilcoxon matched-pairs signed rank test was applied and used to compare two groups.

Statistical significances are depicted as follows; * equals $P \leq 0.05$, ** equals $P \leq 0.01$ and *** equals $P \leq 0.001$. P-values > 0.05 were considered non-significant.

3 Results

3.1 Disease associations of Interleukin-26

3.1.1 Skin disease association

Interleukin-26 gene expression was investigated in several different skin conditions and is seen to be upregulated in a large number of the screened skin disorders. Here we show a significant upregulation in *IL26* gene expression in psoriasis vulgaris (PV), rosacea, atopic dermatitis (AD), mycosis fungoides (MF), and cutaneous sarcoidosis (*Fig. 6A*). The gene expression is displayed in relative units (RU) compared to 18S ribosomal RNA. The most significant upregulation of *IL26* is found in both PV and rosacea. Two of the highest detected *IL26* gene expression values are found within the MF cohort. Atopic dermatitis (AD) showed a trend towards higher *IL26* gene expression. Other tested skin disease samples that did not show any *IL26* upregulation on the RNA level were: seborrheic keratosis, actinic keratosis, squamous cell carcinoma (SCC), basal cell carcinoma (BCC), condyloma acuminatum, lichen planus, cutaneous lupus erythematosus, prurigo nodularis, as well as acne inversa (*Supplemental figure 1*).

To confirm the gene expression results on the protein level, we performed an IL-26 ELISA with supernatants from homogenized skin punch biopsies. A small amount of IL-26 protein was found in healthy skin, but the concentrations of IL-26 in psoriasis vulgaris, psoriasis pustulosa (a variant of psoriasis vulgaris; sometimes also defined as different entity), and rosacea were significantly increased. The highest amount of IL-26 protein was found within the psoriasis pustulosa group. Looking at rhinophyma, a subtype of rosacea, we did not detect significant higher levels of IL-26 protein (*Fig. 6B*).

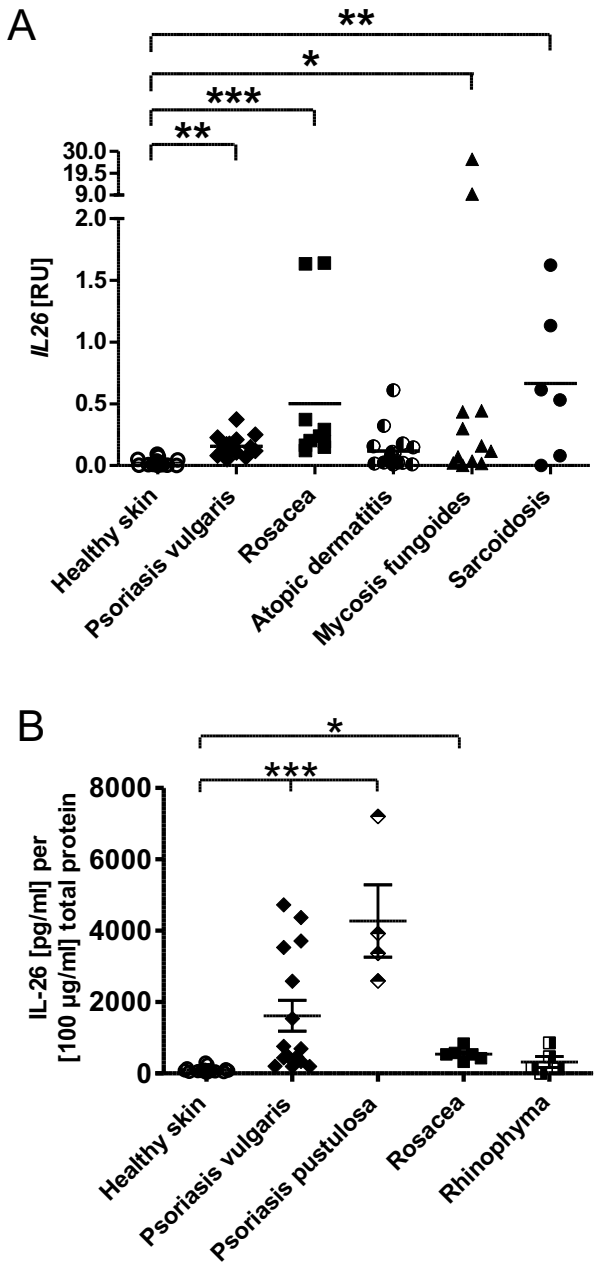

FIGURE 6: Interleukin-26 in different skin diseases compared to healthy skin. A) *IL26* gene expression in different skin diseases. Psoriasis vulgaris (n=16), rosacea (n=10), atopic dermatitis (AD, n=16), mycosis fungoides (MF, n=12) and sarcoidosis (n=6) were compared to healthy skin (n=15) Data depicted in relative expression units (RU) compared to 18S ribosomal RNA. B) IL-26 protein levels measured by IL-26 ELISA are increased analogously to gene expression. Psoriasis vulgaris (n=15), psoriasis pustulosa (n=4), rosacea (n=5) and rhinophyma (n=5) were compared with healthy skin (n=15). Statistical analysis was done using Kruskal-Wallis test with Dunn's post-hoc test and significances are depicted as follows; * equals $P \leq 0.05$, ** equals $P \leq 0.01$ and *** equals $P \leq 0.001$.

We further examined cryoconserved skin sections via immunofluorescence (IF) to identify the localization of IL-26 protein in skin tissue. The skin sections were

stained with DAPI and anti-IL-26 antibody (clone: 13). In healthy skin sections (*Fig. 7A-C*), nearly no staining with anti-IL-26 antibody could be seen. Looking at PV (*Fig. 7D-F*), psoriasis pustulosa (*Fig. 7G-I*) and rosacea (*Fig. 7J-L*) a clear red fluorescence can be observed. Staining for IL-26 in these diseases is lightly seen in the epidermal skin layer but more prominently in the dermal skin closely located to blood vessels and cells in the dermis, most likely infiltrating immune cells such as blood lymphocytes including T cells.

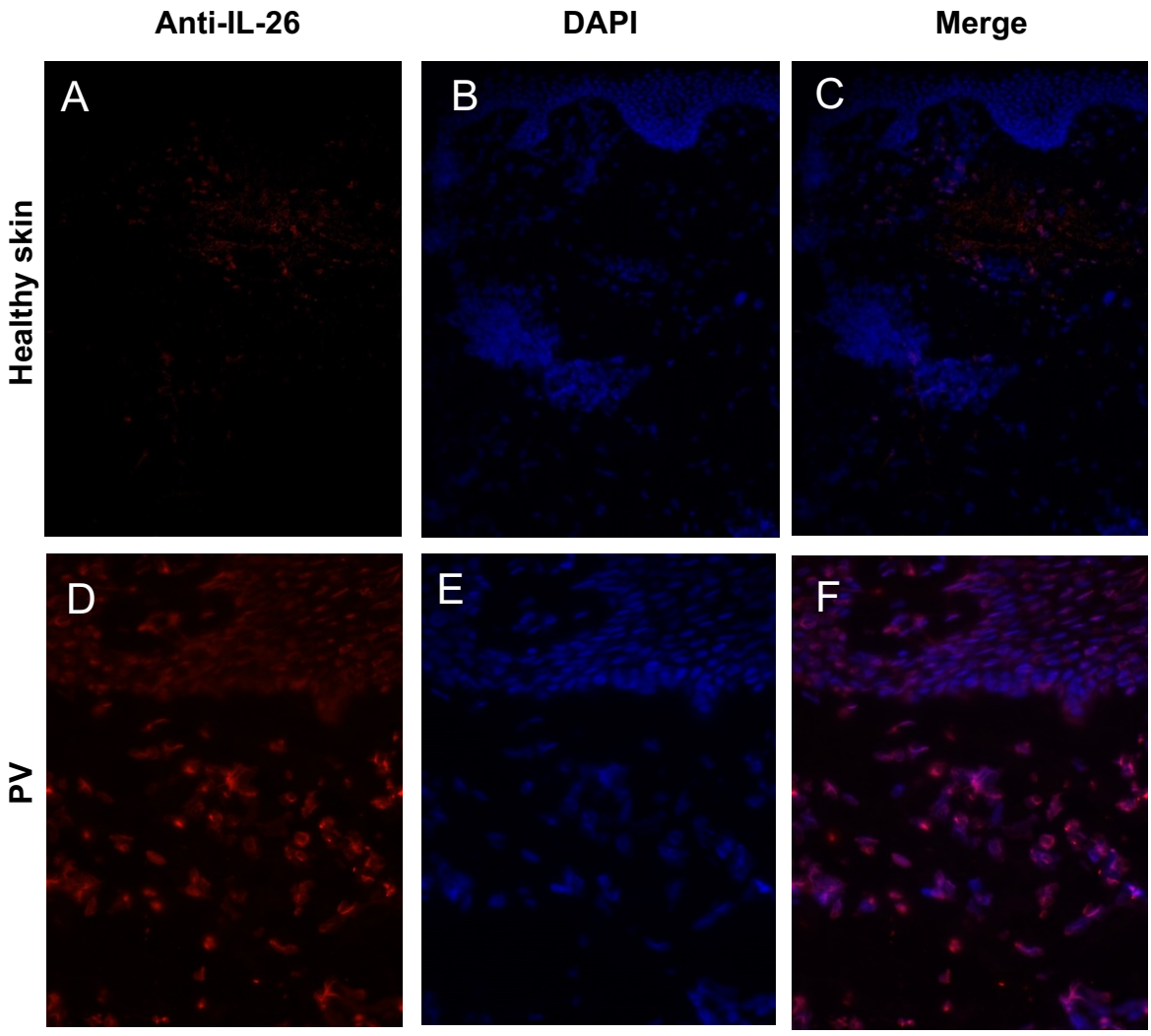

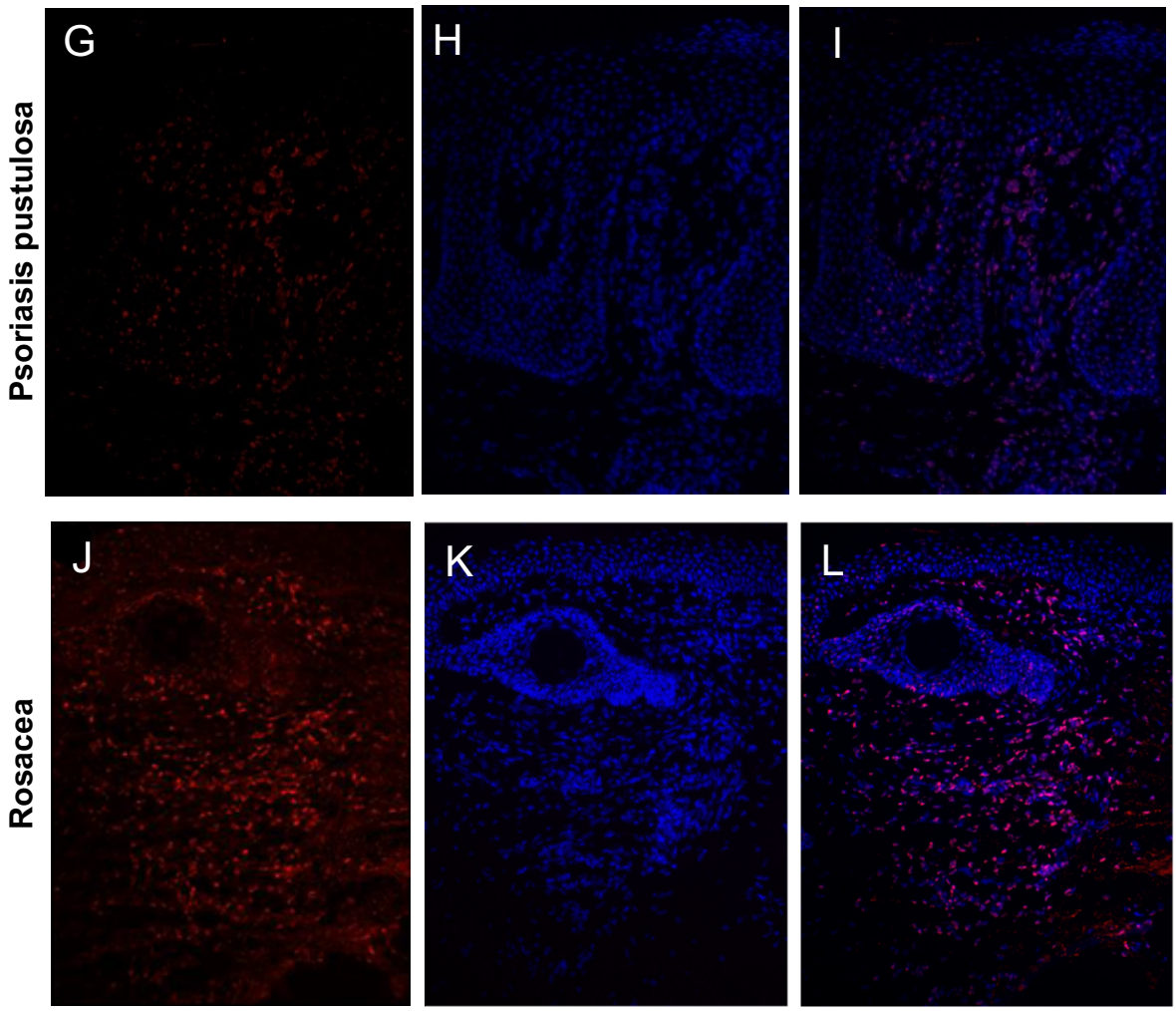

FIGURE 7: Interleukin-26 staining in different skin diseases and healthy skin. The first column represents the staining with anti-IL-26 alone, the second column shows the DAPI stain, while the last column shows images where anti-IL-26 staining is merged with DAPI staining. A-C) healthy skin, D-F) psoriasis vulgaris (PV), G-I) psoriasis pustulosa and J-L) rosacea. Representative pictures are shown (Magnification: 40×).

Furthermore, we performed IHC with FFPE skin sections to detect anti-IL-26 specific staining. In healthy skin sections (*Fig 8A-C*) we did not detect any or only little staining of IL-26, while in PV we found very strong specific staining mainly associated with infiltrating immune cells (*Fig. 8D and E*). Furthermore, the epidermal keratinocyte layer displays very homogenous staining. In psoriasis pustulosa the keratinocyte layer seems to be less intensively stained as in psoriasis vulgaris (comparing *Fig. 8E and H)*. The staining appears to be concentrated around the pustules. In rosacea (*Fig. 8J-L*), we also see a prominent IL-26 staining in the keratinocytes layer and additionally in the epidermal layers around blood vessels.

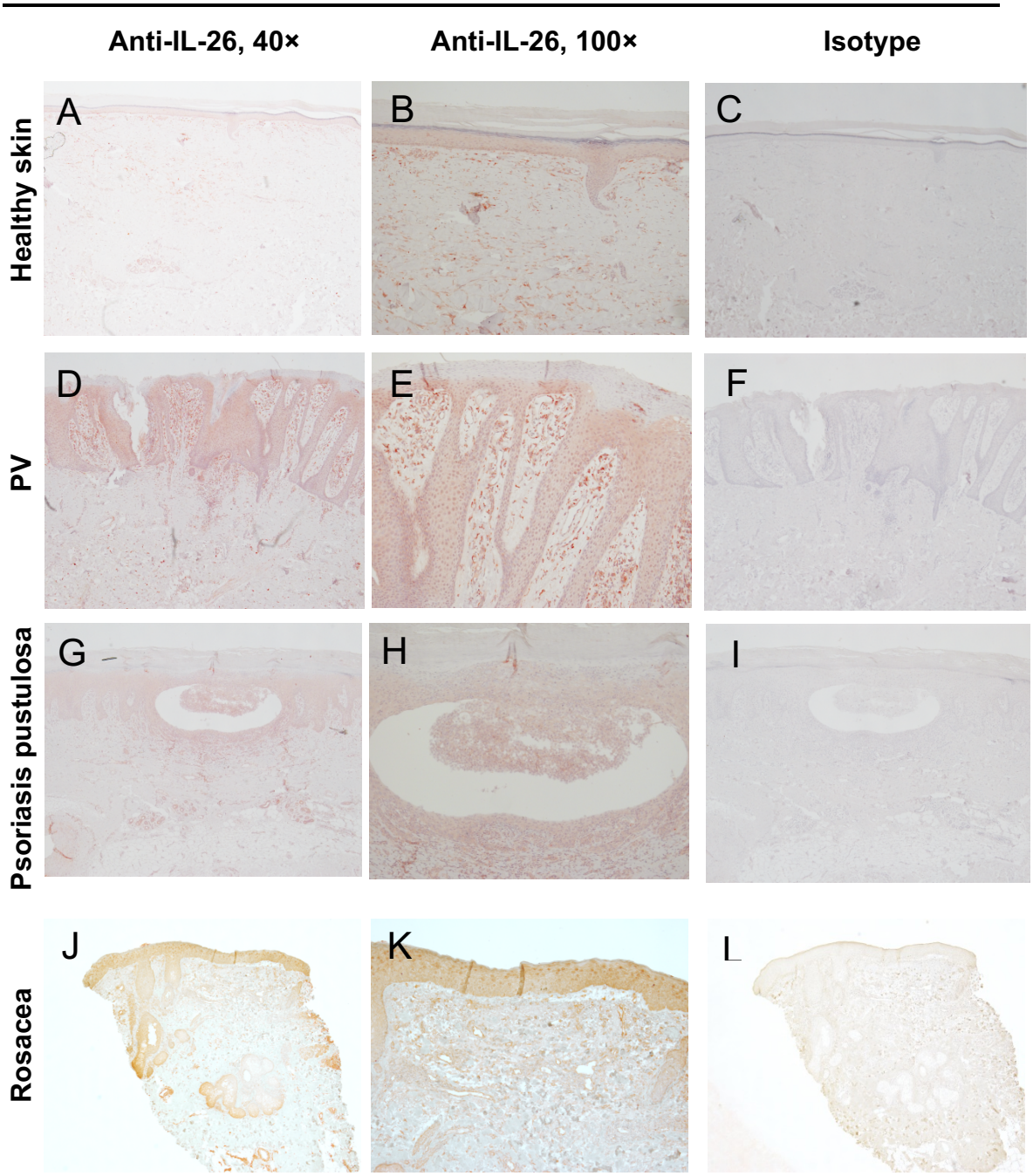

FIGURE 8: Interleukin-26 staining in skin diseases in comparison to healthy skin. The first column represents the IHC staining with anti-IL-26 at a magnification of 40, the second column shows anti-IL-26 at a magnification of 100, while the last column shows images of the isotype control (Magnification: 40×). A-C) healthy skin, D-F) psoriasis vulgaris, G-I) psoriasis pustulosa and J-L) rosacea. Representative pictures are shown.

In order to evaluate our results for IL-26, we searched the open FANTOM5 database within the ZENBU browser (http://fantom.gsc.riken.jp/zenbu/gLyphs/#config=ONHzqgf2E5Xtmnpsh2gURB;loc=hg19::chr12:68589018..68625682) generated by an international research consortium around Dr. Hayashizaki from the RIKEN Center for Life Science Technology in Japan. The FANTOM5

database aims to comprise data on transcriptomal expression of all cell types found within the human body. The most prominent expression of *IL26* is found in a T cell lymphoma cell line of mycosis fungoides (*Table 6*). This correlates with the high *IL26* gene expression levels of our own samples depicted in Fig. 6A. Furthermore, a cell line from chronic T cell lymphocytic leukemia appears (position 4), but also other types of T cells or different T cell donors appear in the top 30 hits. Skin tissue itself is also found at position 17.

TABLE 6: Table shows top 30 results on *IL26* distribution in FANTOM5 database.

	IL26	neg_strand _value	pos_strand _value
#	**experiment_name**		
1	mycosis fungoides, T cell lymphoma cell line	74.4	0
2	anaplastic large cell lymphoma cell line	61.97	0
3	osteoclastoma cell line	46.15	0
4	chronic lymphocytic leukemia (T-CLL) cell line	36.79	0
5	Synoviocyte, donor3	32.93	0
6	mesenchymal precursor cell - bone marrow, donor2	23.4	0
7	Perineurial Cells, donor1	17.15	0
8	cholangiocellular carcinoma cell line	14.24	0
9	rhabdomyosarcoma cell line	2.43	8.35
10	CD4+CD25+CD45RA- memory regulatory T cells expanded, donor2	8.97	0
11	CD4+CD25+CD45RA- memory regulatory T cells expanded, donor3	8.32	0.13
12	Chondrocyte - de diff, donor1	8.31	0
13	CD4+CD25+CD45RA- memory regulatory T cells expanded, donor1	8.02	0
14	Ewing's sarcoma cell line	5.96	0
15	CD4+CD25-CD45RA- memory conventional T cells expanded, donor1	5.55	0
16	mesenchymal precursor cell - bone marrow, donor3	5.34	0
17	Skin - palm, donor1	2.34	2.34
18	mesenchymal precursor cell - bone marrow, donor1	4.55	0
19	Multipotent Cord Blood Unrestricted Somatic Stem Cells, donor1	4.07	0.24
20	CD4+CD25-CD45RA- memory conventional T cells, donor1	4.22	0
21	Smooth Muscle Cells - Brachiocephalic, donor2	3.97	0
22	Sertoli Cells, donor2	3.79	0
23	duodenum, fetal, donor1, tech rep1	3.63	0
24	CD8+ T Cells, donor2	1.07	2.14
25	CD19+ B Cells, donor2	0	2.94
26	optic nerve, donor1	0	2.86
27	Smooth Muscle Cells - Prostate, donor3	2.78	0
28	tenocyte, donor2	2.77	0
29	CD4+CD25-CD45RA+ naive conventional T cells expanded, donor3	2.76	0
30	CD4+CD25-CD45RA- memory conventional T cells, donor3	0.76	1.77

3.1.2 Infectious disease association

During the screening of different skin diseases for *IL26* gene expression, we found that *IL26* is upregulated in sarcoidosis. As sarcoidosis is characterized by the formation of granulomas that resemble the ones seen in tuberculosis, we wondered about the role of *IL26* in tuberculosis, the disease caused by *Mycobacterium tuberculosis*.

The FFPE-tissue samples comprised mainly lymph node tissue but also lung tissue and tuberculosis skin samples from subcutaneous tissue without the epidermal layer of keratinocytes. From the tissues, the RNA was extracted in order to perform subsequent qPCR. Using only lymph node samples, we found that the *IL26* gene is increasingly expressed in tuberculosis lymph nodes (*Fig. 9A*). *IL22* expression is also increased in some tuberculosis samples compared to healthy lymph nodes (*Fig. 9B*), while an *IL17A* expression could not be detected at all (*Fig. 9C*).

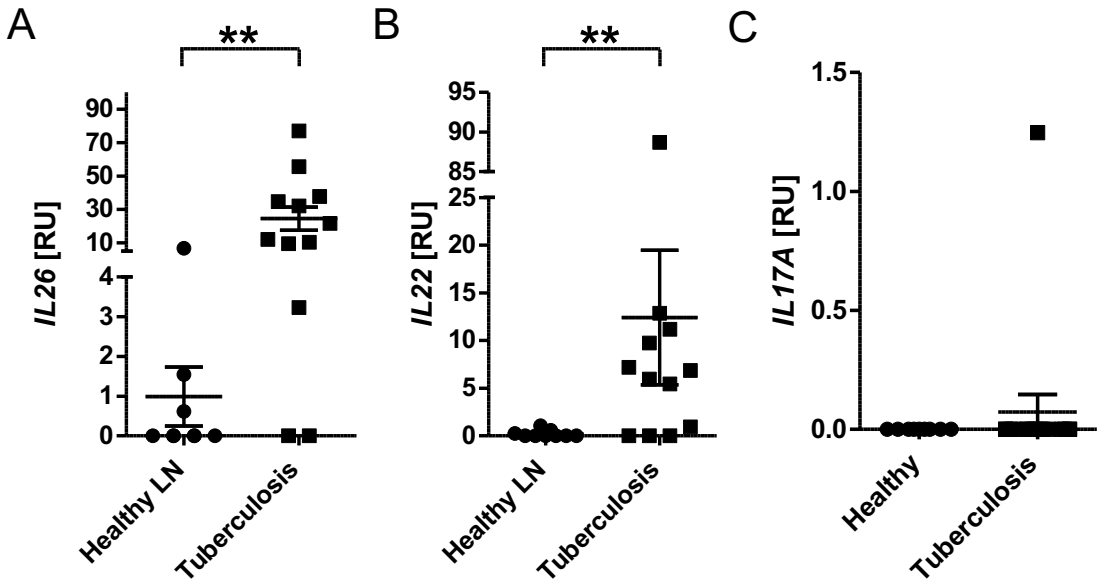

FIGURE 9: T_H17-associated gene expression is increased in patients suffering from tuberculosis. A) *IL26* gene expression in tuberculosis lymph nodes (n=12) compared to healthy lymph nodes (n=9). B) *IL22* gene expression. C) *IL17A* gene expression. Data depicted in relative expression units compared to 18S ribosomal RNA. Statistical analysis was done using Mann Whitney U test and shown as ** equals $P \leq 0.01$ and *** equals $P \leq 0.001$.

Finding an increased expression of the *IL26* gene in both sarcoidosis and tuberculosis, we performed IHC staining with anti-IL-26 antibody to prove the results on the protein level. Healthy skin was basically unstained (*Fig. 8A-C and Fig. 10A-C*). The granulomatous structures in the sarcoidosis skin are very

strongly stained with anti-IL-26 (*Fig. 10D-F*). The epidermal layer in sarcoidosis is compared to the granulomatous structures only weakly stained by anti-IL-26 antibody. In contrast the dermal granulomatous structures of sarcoidosis were strongly and homogenously stained. When comparing the staining in a healthy lymph node (*Fig. 10H-I*) to a lymph node from a tuberculosis patient (*Fig. 10J-L*), there is again no staining in healthy lymph node, while the lymph node from the tuberculosis patient can be considered homogenously stained for IL-26. This observation resembles the gene expression data observed by qPCR.

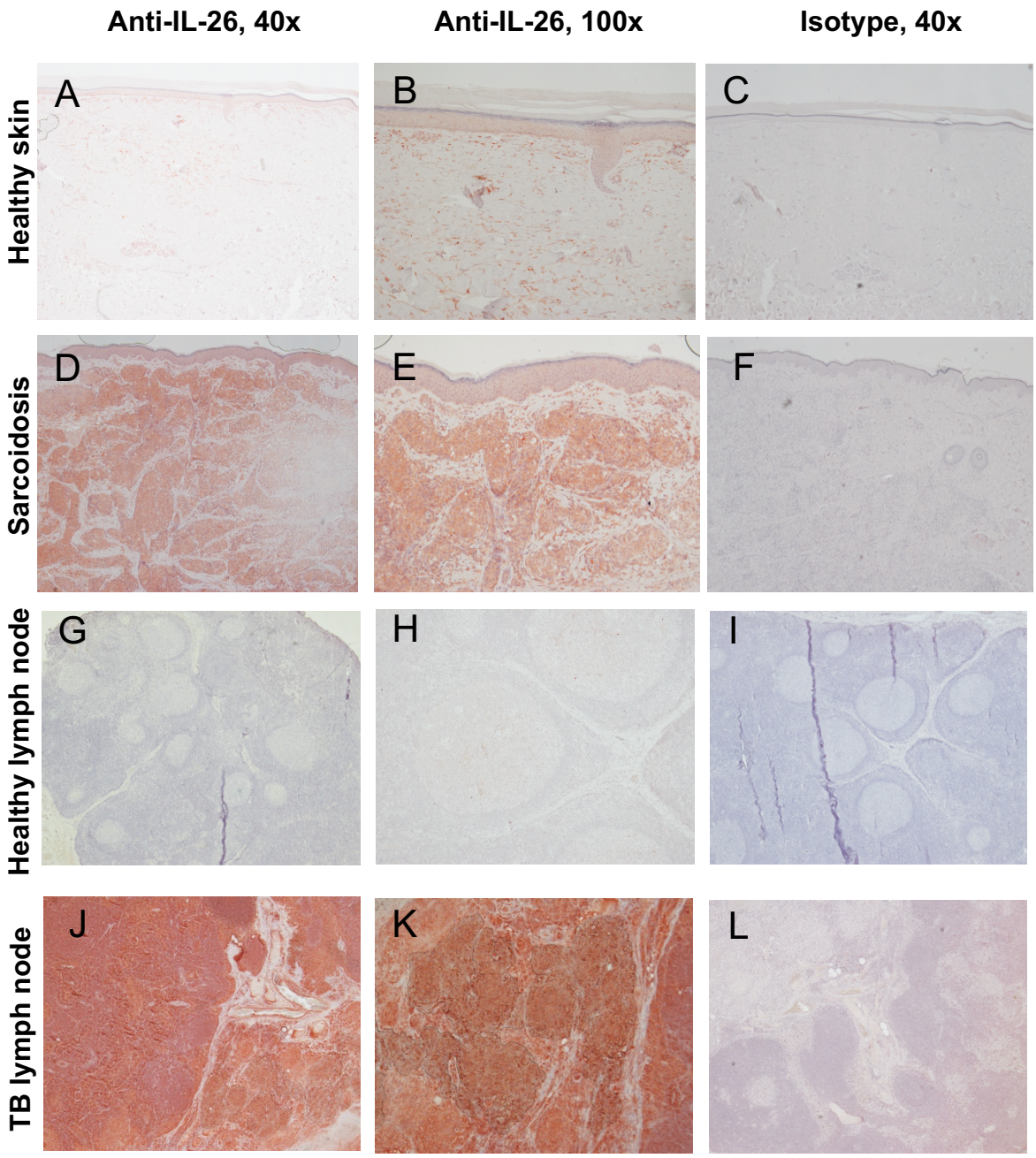

FIGURE 10: Immunohistochemistry of IL-26 in sarcoidosis and tuberculosis. The first column represents the staining with anti-IL-26 (Magnification: 40×), the second column shows a higher

magnification of anti-IL-26 staining (Magnification: 100×), while the last column shows images of the isotype control (Magnification: 40×). A-C) healthy skin, D-F) sarcoidosis, G-I) healthy lymph node and J-L) tuberculosis lymph node. Representative pictures are shown.

To validate the results from sarcoidosis and tuberculosis, a database search using the GEO profiles provided by the National Center for Biotechnology Information (NCBI, https://www.ncbi.nlm.nih.gov/geoprofiles/?term=IL-26+tuberculosis) was performed. One promising entry comprised a dataset with healthy lung tissue compared to pulmonary sarcoidosis (*Fig. 11A*) (Original publication:[197]). Another dataset from microarrays using PBMCs from patients suffering from tuberculosis and healthy donors showed an increased IL-26 expression in active tuberculosis PBMCs compared to healthy PBMCs and latently tuberculosis infected PBMCs (*Fig. 11B*) (Original publication:[198]). Comparing *IL26* expression in latently infected PBMCs with healthy ones, there was nearly no difference in *IL26* expression, it even appears as if latently infected PBMCs showed less *IL26* expression. Looking at the *IL26* expression in the active tuberculosis PBMCs from Fig. 11B, under anti-tuberculosis chemotherapy in a time interval of three months, it appeared as if *IL26* expression slightly decreases during the treatment (*Fig. 11C*).

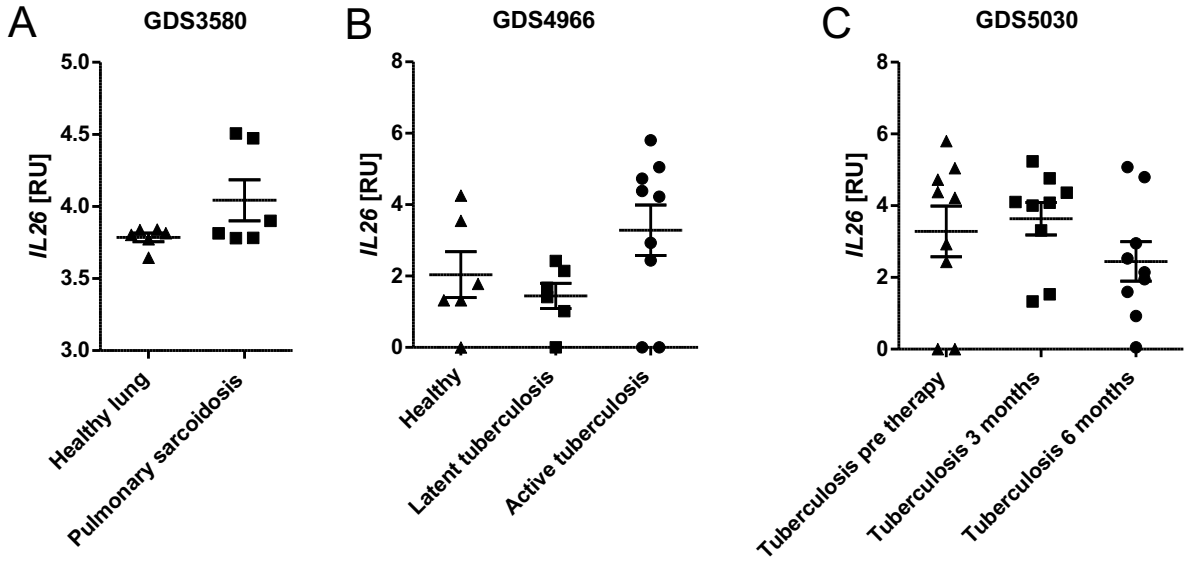

FIGURE 11: *IL26* expression in microarray data (GEO Profiles) from sarcoidosis and tuberculosis found in the literature. A) Healthy lung tissue (n=6) compared to pulmonary sarcoidosis (n=6). B) *IL26* gene expression in peripheral blood mononuclear cells (PBMCs) comparing healthy (n=6) to latent (n=6) and active tuberculosis (n=9), and C) *IL26* expression in

PBMCs during anti-TB chemotherapy (n=9) at different time points compared to pre-therapy (n=9).

3.2 IL-26 in structural skin cells

3.2.1 Effects on keratinocytes

The proposed IL-26 receptor heterodimer consisting of IL-20R1 and IL-10R2 is expressed on epithelial cells such as keratinocytes (*Fig. 12*). The baseline *IL20R1* expression in untreated keratinocytes (control) was around 0.3 relative units (RU), while the expression of *IL10R2* was around 2 RU. The addition of recombinant human (rh) IL-26 to the keratinocyte culture tendentially increased the expression of *IL20R1* (*Fig. 12A*) and *IL10R2* (*Fig. 12B*).

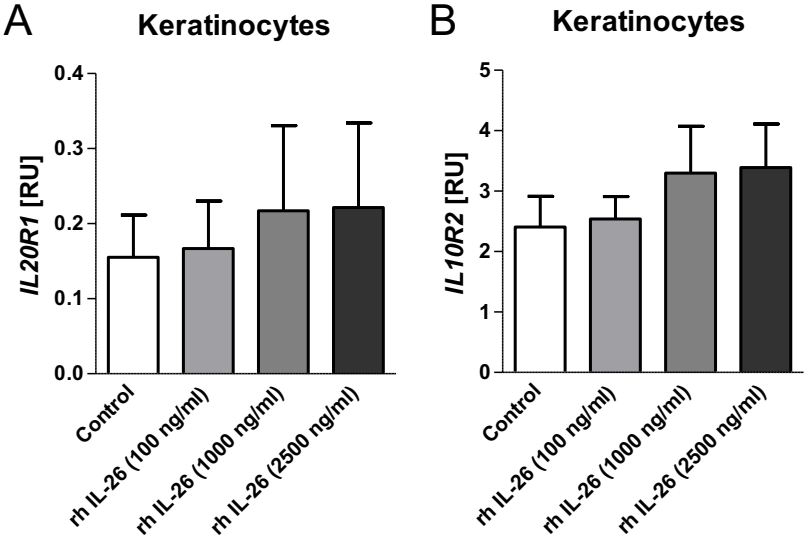

FIGURE 12: Gene expression of *IL20R1* and *IL10R2* in primary human keratinocytes detected via RT-qPCR. A) *IL20R1* gene expression appears to be slightly induced when recombinant human (rh) IL-26 is added (n=5-6). B) *IL10R2* gene expression is also slightly induced in keratinocytes in the presence of IL-26 for 24h (n=5-6).

Seeing that the IL-26 receptor was indeed expressed by the primary human keratinocytes in our hands, we further investigated the receptor-mediated effects of IL-26 on these skin cells. As other T_H17-cell derived interleukins, such as IL-17 or IL-22, unleash effects on target cells at concentrations ranging around 100 ng/ml, we stimulated the keratinocytes accordingly. It has been shown that CXCL8 is upregulated after IL-26 stimulation in the HaCaT keratinocyte cell line and CXCL8, IL-10, and ICAM1 (CD54) are upregulated in

Colo-205 cells[50]. We started testing these genes in our IL-26 treated normal human primary keratinocytes. Both *CXCL8* and *IL10* showed very low expression levels in keratinocytes. Adding IL-26, gene expression of *IL10* was even slightly downregulated (*Fig. 13A*). *CXCL8* in contrast was slightly, but not significantly, upregulated when unusual high doses of IL-26 (1000 ng/ml and more) were added (*Fig. 13B*). We found that *ICAM1* was also slightly upregulated in the presence of very high amounts of IL-26 (*Fig. 13C*).

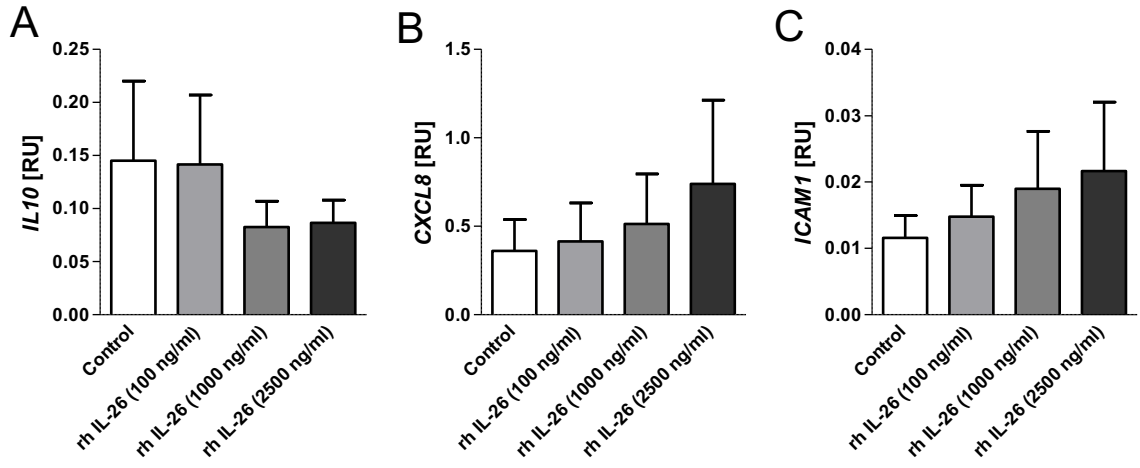

FIGURE 13: Gene expression of *IL10*, *CXCL8* and *ICAM1* in primary human keratinocytes detected via RT-qPCR. A) *IL10* gene expression appears to be downregulated when IL-26 is added (n=5-6). B) *CXCL8* gene expression is slightly induced in keratinocytes when high doses of IL-26 are added and incubated for 24h (n=5). C) *ICAM1* gene expression is induced when IL-26 is added for 24h (n=3-5).

As we were unable to reproduce the findings from the literature in our primary keratinocytes, we tested if our keratinocytes respond to the treatment with other T_H17 cell derived cytokines such as IL-17 and IL-22. We found that both IL-17 and IL-22 minimally induce *IL10* gene expression (*Fig. 14A*). The expression of *CXCL8* was highly induced by IL-17, while basically no induction was seen in the presence of IL-22 (*Fig. 14B*). For *ICAM1*, we saw an induction in the presence of IL-17 and an even stronger induction when keratinocytes were treated with 100 ng/ml IL-22 (*Fig. 14C*).

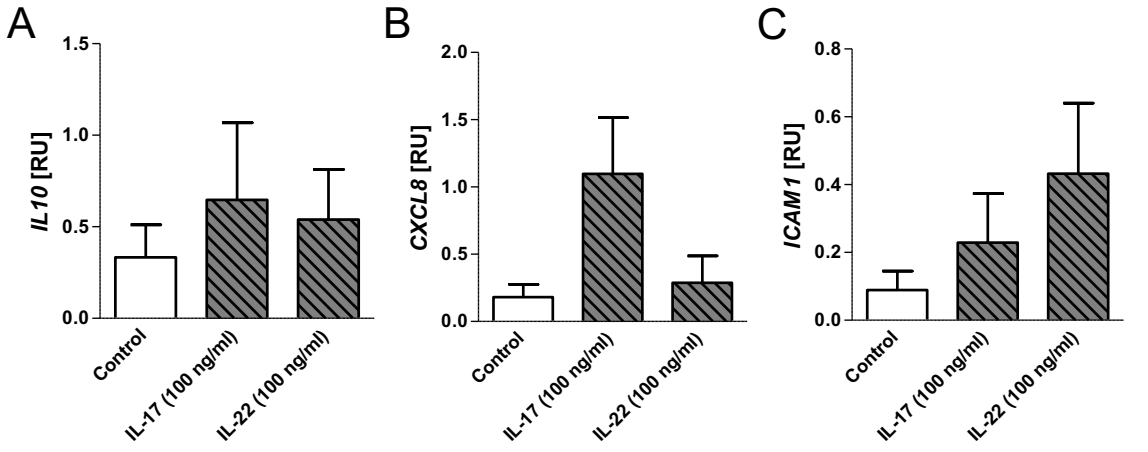

FIGURE 14: Gene expression of *IL10*, *CXCL8* and *ICAM1* (CD54) in primary human keratinocytes treated with the T_H17 cytokines IL-17 and IL-22. *IL10* (A), *CXCL8* (B) and *ICAM1* (C) gene expressions were detected via RT-qPCR in keratinocytes incubated with 100 ng/ml IL-17 or IL-22 (n=4).

As our primary keratinocytes responded to other T_H17 cell-derived interleukins normally, we went back to HaCaT keratinocytes. We wondered if HaCaT keratinocytes expressed a higher amount of receptor heterodimer so they could respond more efficiently to IL-26 treatment. We compared the *IL20R1* and *IL10R2* gene expressions in the epithelial colon cell line Colo-205, the keratinocyte cell line HaCaT, primary keratinocytes, and primary skin fibroblasts. We found that *IL20R1* gene expression is highest in Colo-205 cells followed by HaCaT keratinocytes, primary keratinocytes, and finally fibroblasts (*Fig. 15A*). Gene expression of *IL20R1* was about 100-times higher in Colo-205 and HaCaT keratinocytes as compared to primary keratinocytes and fibroblasts (*Fig. 15A*). Having this rather low gene expression of *IL20R1* in primary keratinocytes might explain the difficulties in stimulating them with IL-26. For *IL10R2*, the relative gene expression units were much lower than *IL20R1*. Here, the highest values were found in primary keratinocytes, followed by Colo-205 cells and HaCaT cells (*Fig. 15B*). Again, primary fibroblasts displayed the lowest *IL10R2* gene expression.

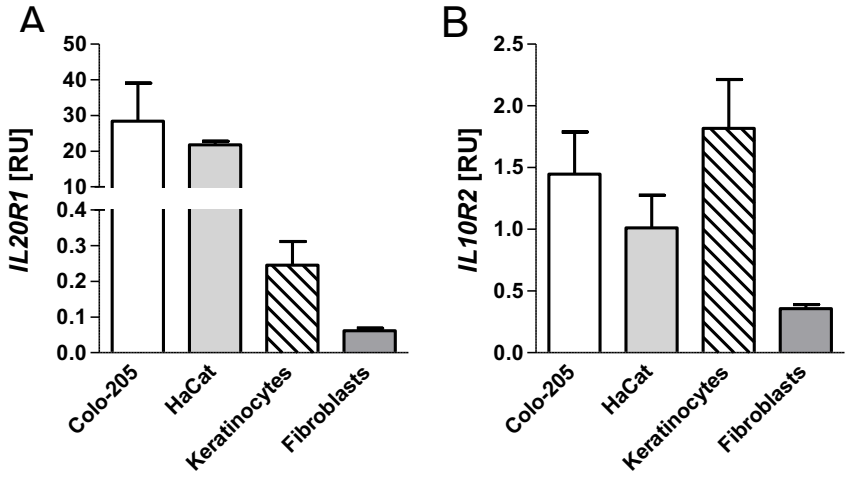

FIGURE 15: Comparison between the *IL20R1* and *IL10R2* gene expression levels of Colo-205 cells, HaCat keratinocyte cell line, primary keratinocytes and primary fibroblasts. Both *IL20R1* (A) and *IL10R2* (B) genes are detected via qPCR in all tested cell types (Colo-205; n=4, HaCaT; n=2, keratinocytes; n=3 and fibroblasts; n=3-4).

We went on to reproduce the data from Hör *et al.*[50], and first investigated *CXCL8*, *IL10*, and *ICAM1* gene expression in IL-26 stimulated HaCaT keratinocytes, and subsequently tested protein secretion via ELISA. We found no effect on *CXCL8* expression (*Fig. 16A*) and secretion (*Fig. 16B*). Looking at IL-10 protein levels, there is absolutely no effect on IL-10 secretion in the presence of IL-26 (*Fig. 16C*).

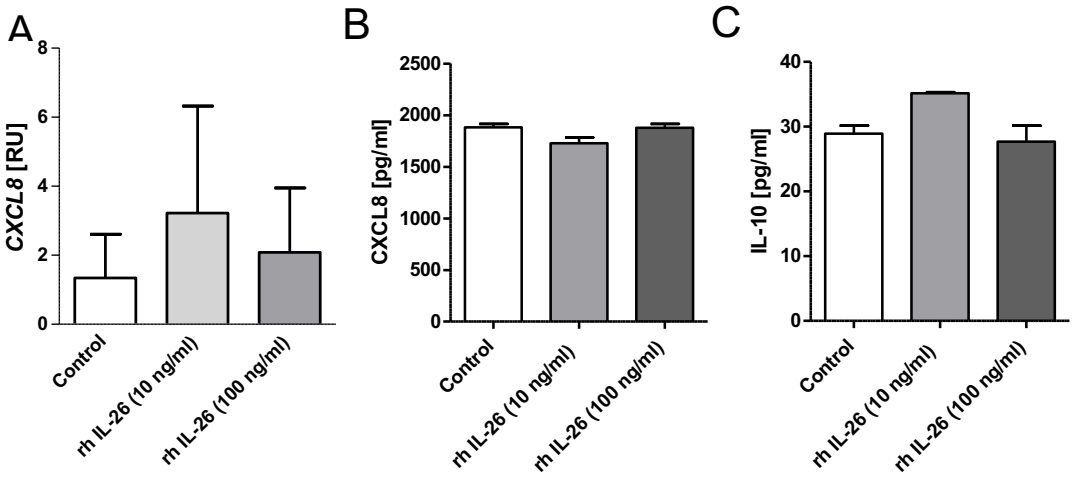

FIGURE 16: Gene expression and protein secretion of IL-10 and CXCL8 in HaCaT keratinocytes treated with 10 and 100 ng/ml IL-26. *CXCL8* (A) gene expression was detected via RT-qPCR in keratinocytes after 24h incubation with IL-26 (n=3). Protein secretion of CXCL8 (B) and IL-10 (C) was detected via ELISA (n=2).

Seeing that HaCaT keratinocytes did not respond to IL-26 stimulation as expected, we tested the stimulation on Colo-205 cells, which should also respond with *CXCL8*, *IL10*, and *ICAM1* upregulation. Furthermore, they are used as positive controls by R&D Systems to prove IL-26's bioactivity. We treated Colo-205 cells analogously to how it is done by R&D Systems, using their bioactivity assay protocol where the cells were adjusted to 2×10^6 cells per ml, incubated for 24h, and subsequently IL-10 secretion is detected via ELISA. We found that *IL10* gene expression was significantly upregulated after stimulation with 100 ng/ml IL-26 (*Supplemental Figure 2A*). *CXCL8* was slightly increased, *IL10* gene expression also resulted in increased IL-10 secretion in presence of IL-26 in the Colo-205 cells (*Supplemental Figure 2B/C*).

To sum this up: the recombinant human IL-26 does fulfill the manufacturer's bioactivity standards and it modulates gene expression in Colo-205 cells, which express the highest amounts of both parts of the receptor heterodimer (*IL20R1* and *IL10R2*). On the other hand, contra the results from Hör et al[50], we were unable to affect gene expression in HaCaT keratinocytes and primary keratinocytes.

3.3 IL-26 in adaptive immunity

3.3.1 IL-26 receptor on immune cells

That immune cells generally express IL-10R2 but not the IL-20R1 of the IL-26 receptor heterodimer consisting of both IL-10R2 and IL-20R1 has been described[42]. To make sure this holds true for our cells of interest, we investigated *IL20R1* and *IL10R2* gene expression on $CD14^+$ monocytes, macrophages and moDCs.

$CD14^+$ monocytes did not express *IL20R1*, but *IL10R2* on mRNA level (*Fig. 17*). The addition of LPS, which was generally used as positive control for induction of an inflammatory response, did not influence the gene expression (*Fig. 17*). The exact mean relative expression units (RU) are provided in table 7. Looking at the protein level using flow cytometry, we have been unable to detect any IL-20R1 expression in $CD14^+$ monocytes (*Supplemental figure 3*).

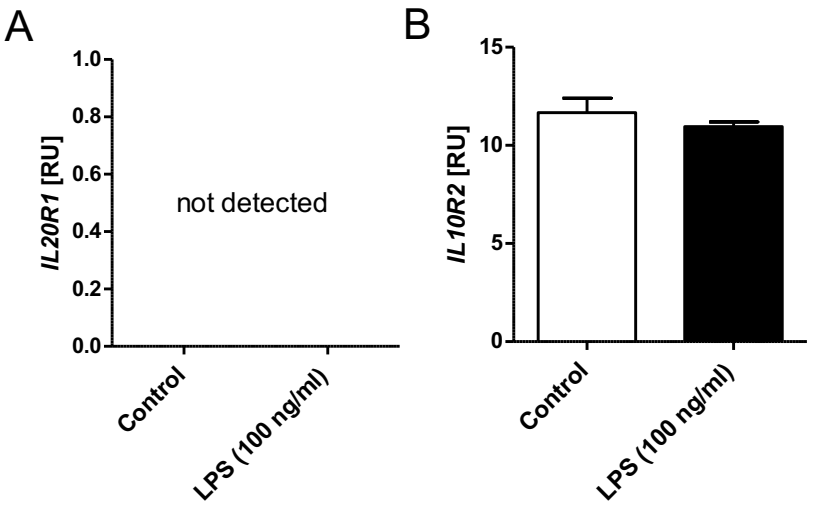

FIGURE 17: CD14$^+$ monocytes do not express *IL20R1* on mRNA level. CD14$^+$ monocytes were incubated 24h in presence or absence of LPS. The isolated RNA was then used for qPCR analysis. qPCR results from gene expression of *IL20R1* (A) and *IL10R2* (B) (n=2) are shown in relative units compared to 18S RNA.

We next investigated the *IL20R1* and *IL10R2* gene expression in monocyte-derived macrophages, a monocytic cell line named THP1 that differentiate into macrophages in the presence of 50 nM PMA and monocyte-derived dendritic cells (moDCs). Like monocytes, macrophages didn't express *IL20R1* at all (*Table 7*). The gene expression of *IL10R2* was approximately at the same level as seen in monocytes, but the addition of LPS slightly increased *IL10R2* in macrophages (*Table 7*). In differentiated THP1 macrophages, negligible expression levels of *IL20R1* were detected. MoDCs didn't express *IL20R1* at mRNA level (*Table 7*), but *IL10R2* was detected at levels similar to monocytes and macrophages and seemed to be induced by LPS (*Table 7*).

TABLE 7: *IL20R1* and *IL10R2* gene expression in different cell types in mean RU. (Ctrl equals "untreated controls", N. D. equals "not detected")

Cell type	***IL20R1* (Ctrl)**	***IL10R2* (Ctrl)**	***IL20R1* (LPS)**	***IL10R2* (LPS)**
CD14+ monocytes	N.D.	11.76	N.D.	10.95
Monocyte-derived macrophage	N.D.	8.77	N. D.	15.76
THP1 Macrophage	0.0015	28.38	0.0045	33.24
moDC	N.D.	8.0	N. D.	27.17

3.3.2 IL-26/nucleic acid binding

IL-26 is a highly cationic protein and it is therefore able to bind anionic nucleic acids such as DNA, which we have shown previously using a nucleic acid condensation assay (similar to *fig. 47*)[19].

Here this finding was confirmed using microscale thermophoresis (MST), a method to investigate molecular interactions in a small volume. Therefore, we subjected a serial dilution of IL-26 or LL37 (as positive control) to a constant amount of 10 nM FAM-labelled single-stranded DNA (ssDNA) or double-stranded DNA (dsDNA). IL-26 bound to both types of DNA in the low micromolar range (*Fig. 18 and Table 8*). LL37 bound much better to ssDNA than IL-26, but on the other hand it had lower affinity to dsDNA than IL-26 (*Fig. 18 and Table 8*). As another control, IL-22 that shares about 25% sequence identity with IL-26 was used[199]. Interestingly, IL-22 also bound to ssDNA and dsDNA, but the affinity was much weaker as K_D values of 16 µM for ssDNA and 19.4 µM for dsDNA were calculated (*Table 8*).

Similarly to LL37/DNA complexes, it has also been found that LL37/RNA complexes activate both pDCs and moDCs[98]. In moDCs, this activation is mediated via endosomal TLR8, which is specialized for detection of intracellular foreign RNA[98]. We next investigated if IL-26 also binds RNA, and in turn activates monocyte-derived dendritic cells (moDCs).

Using MST, we found that IL-26 also bound RNA (*Fig. 18*). IL-26 bound similarly well to RNA as DNA, with a dissociation constant of about 1 µM (see table 8). Comparing the binding affinities to LL37, one can see that LL37 binds with very rather low affinity to RNA (K_D: 7.42 µM, *Table 8*) compared to a K_D of 1.03 µM when IL-26 binds to RNA. Generally, the binding to RNA of both IL-26 and LL37 was weaker than the binding to ssDNA (*Table 8*). When subjecting IL-22 together with RNA to MST, a weak binding with a K_D at 12.5 µM was observed (*Table 8*). Comparing DNA to RNA concerning binding to IL-22, the binding of RNA appeared to be somewhat stronger (*Table 8*).

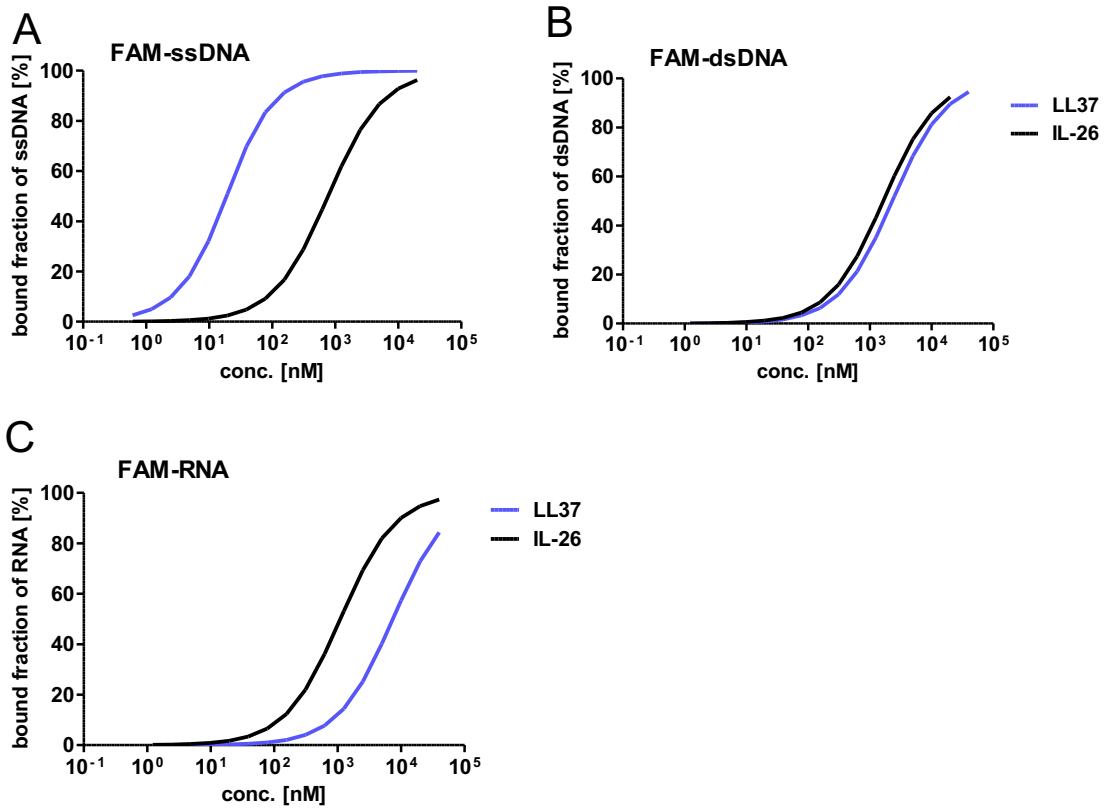

FIGURE 18: IL-26 shows high affinity to double and single stranded DNA as measured with microscale thermophoresis. A constant amount of 10 nM DNA was added to serial dilution of reduced or oxidized IL-26, incubated for 15 min and measured. Graphical depiction of bound fractions of ssDNA (A), dsDNA (B) or RNA (C) to either IL-26 or CAMP.

The exact dissociation constants for the DNA and RNA binding experiments are found in *table 8*.

TABLE 8: Dissociation constants (K_D) of ssDNA, dsDNA or RNA binding.

Protein/ligand	**LL37/DNA (ss)**	**IL-26/DNA (ss)**	**IL-22/DNA (ss)**
K_D (mean ± SD)	13.9 nM ± 0.971	0.750 µM ± 0.059	16.0 µM ± 0.576
Protein/ligand	**LL37/DNA (ds)**	**IL-26/DNA (ds)**	**IL-22/DNA (ds)**
K_D (mean ± SD)	2.31 µM ± 0.299	1.54 µM ± 0.115	19.4 µM ± 0.606
Protein/ligand	**LL37/RNA**	**IL-26/RNA**	**IL-22/RNA**
KD (mean ± SD)	7.42 µM ± 0.322	1.03 µM ± 0.0556	12.8 µM ± 0.222

3.3.3 Effects of IL-26/DNA complexes on monocytes and macrophages

The effects of IL-26/DNA complexes on monocytes have partly been published in Meller *et al.*[19], while the effects of those complexes on macrophages have not been described yet.

3.3.3.1 Induction of cytokines

Monocytes were isolated from buffy coat using a $CD14^+$ cell isolation kit optimized for MACS selection. To generate IL-26/DNA complexes, the DNA was co-incubated with IL-26 in a separate reaction tube for 30 min at RT before addition to the monocyte cell culture. The monocytes were then incubated together with LPS (100 ng/ml, positive control) and IL-26/DNA complexes but also IL-26 and DNA alone for 24 h. The supernatant was then harvested, and the cells were either lysed for subsequent RNA isolation and qPCR analysis or labelled with antibodies for flow cytometry analysis.

$CD14^+$ monocytes responded to IL-26/DNA complexes and to IL-26 alone with the secretion of IL-1β, which was detected via ELISA (*Fig. 19A*). Statistical analysis revealed a p-value of 0.06 between control and IL-26/DNA complexes, and a p-value of 0.11 between control and IL-26 alone. Comparing DNA to IL-26/DNA complexes, there was statistical significance (p= 0.04). LPS served as positive control and was not included in the statistics.

As described in chapter 3.3.1, monocytes do not express the IL-26 receptor. It was therefore surprising that IL-26 alone leads to an increased secretion of IL-1β. To check if this increase might be due to free nucleic acids in the cell culture, we added DNAse and RNAse to inhibit possible binding of IL-26. Furthermore, to investigate the downstream signaling pathway of IL-26/DNA complexes we added chloroquine to the cells before treatment with IL-26/DNA complexes. Chloroquine is a compound that inhibits signaling via endosomal TLRs, mainly blocking the interaction of DNA with TLR9[200]. Adding chloroquine efficiently blocked IL-26/DNA complex mediated IL-1β secretion, and furthermore the added nucleases led to a slight decrease of IL-1β secretion in presence of IL-26 (*Fig. 19B*). Possibly due to low the experiment number (n=3 in *Fig. 19B*), no significance was reached.

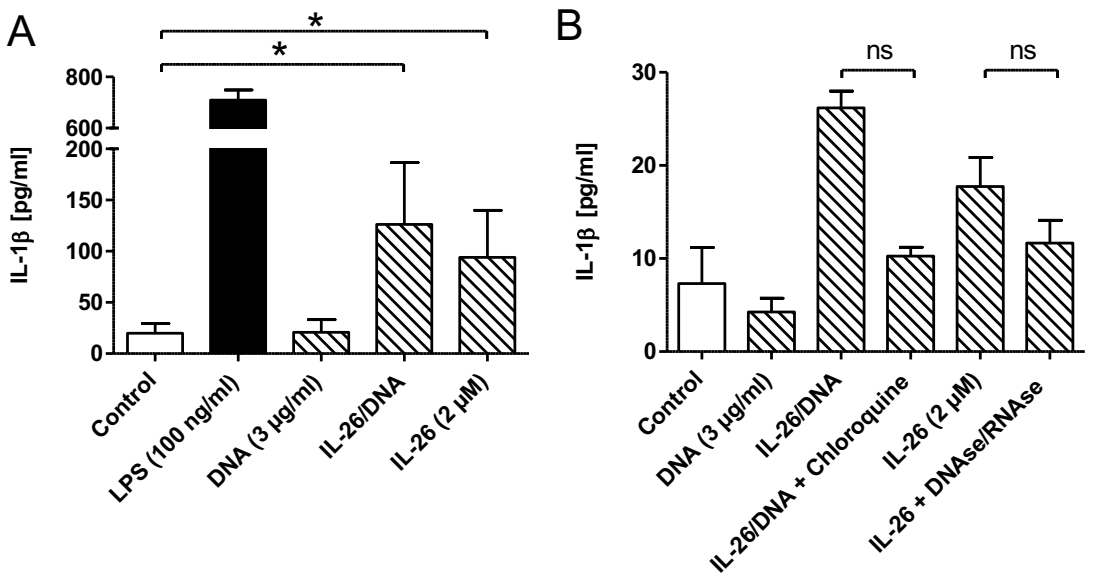

FIGURE 19: CD14$^+$ monocytes respond to IL-26 and IL-26/DNA complex stimulation with IL-1β secretion, but pre-treatment with chloroquine downregulates IL-26/DNA complex induced IL-1β secretion and nucleases slightly reduce the effects of IL-26 alone. CD14$^+$ monocytes were isolated from buffy coats and incubated with the indicated components (A) for 24h or pre-treated with the inhibitors (B) 30 min before addition of IL-26 or IL-26/DNA complexes and then incubated for 24 h before supernatants were harvested and measured with ELISA (A, n=6; B, n=3). Statistical analysis was done using Wilcoxon matched-pairs signed rank test ("ns" equals "not significant", * equals $P \leq 0.05$).

Since monocytes differentiate into either dendritic cells (DCs) or macrophages when they enter the tissue[201,202], we went on to investigate these cell types starting with macrophages.

To differentiate CD14$^+$ monocytes into monocyte-derived macrophages, the monocytes were incubated for six days in presence of 100 ng/ml GM-CSF before they were stimulated with IL-26/DNA complexes and the indicated other components.

CD14$^+$ monocytes responded to both IL-26 and IL-26/DNA complexes with significantly increased gene expression of *IL1B* compared to control cells, which were only incubated with cell culture medium (*Fig. 20B*). Looking at *TNFA* gene expression, IL-26 led to a significant upregulation (*Fig. 20A*). For IL-26/DNA complexes a trend towards increased gene expression was seen but did not reach significance ($p = 0.0556$) (*Fig. 20A*).

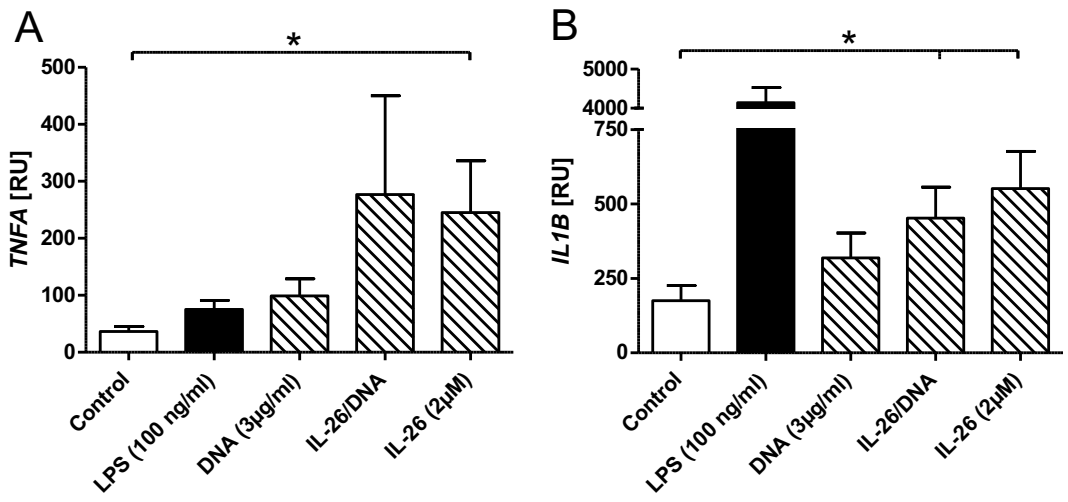

FIGURE 20: Monocyte-derived macrophages respond to IL-26 stimulation with increased *TNFA* and *IL1B* gene expression. The macrophages were differentiated from $CD14^+$ monocytes in presence of GM-CSF for six days and then stimulated with the indicated components for 24h before RNA isolation and qPCR analysis was performed. Gene expressions of *TNFA* (A) and *IL1B* (B) are displayed as relative units compared to 18S gene expression. Statistical evaluation was done using Mann-Whitney U test and indicated as follows: * $P \leq 0.05$ ($n = 5$).

3.3.3.2 Induction of chemokines

In order to attract different cell types to different tissues, the tissue-residing cells produce chemotactic molecules that bind to the respective chemokine receptor on the target cell. As IL-26 expression and secretion is increased during inflammatory diseases, we investigated if it also elicits effects on chemokines and chemokine receptors.

Macrophages express a variety of chemokines and chemokine receptors. Among their repertoire are CXCL2 and CXCL8, which are both ligands that attract neutrophils to infection sites. Furthermore they express CCL20, the ligand for CCR6. Gene expression of *CXCL2* was increased in the presence of IL-26 alone (*Fig. 21A*), but not when the macrophages were incubated with IL-26/DNA complexes. For *CXCL8*, a similar pattern was observed but did not reach significance for either IL-26 or IL-26/DNA complexes (*Fig. 21B*). *CCL20* gene expression was clearly and significantly upregulated in the presence of IL-26/DNA complexes, but also IL-26 alone (*Fig. 21C*). Here, the gene expression of *CCL20* in macrophages treated with IL-26 alone was even higher than the expression measured after treatment with LPS. Having the $CD14^+$ monocytes differentiated towards the M1 macrophage subtype (using GM-CSF instead of

M-CSF)[203], it was interesting to investigate if IL-26 or IL-26/DNA complexes would enhance this polarization or drive it towards an M2 phenotype. Classically, M1 macrophages express CCR7 and are attracted to its ligands CCL19 and CCL21[203]. We found that the incubation with IL-26 or IL-26/nucleic acid complexes led to a slightly increased expression of *CCR7* indicating that the macrophages are likely to stick to their phenotype (*Fig. 21D*).

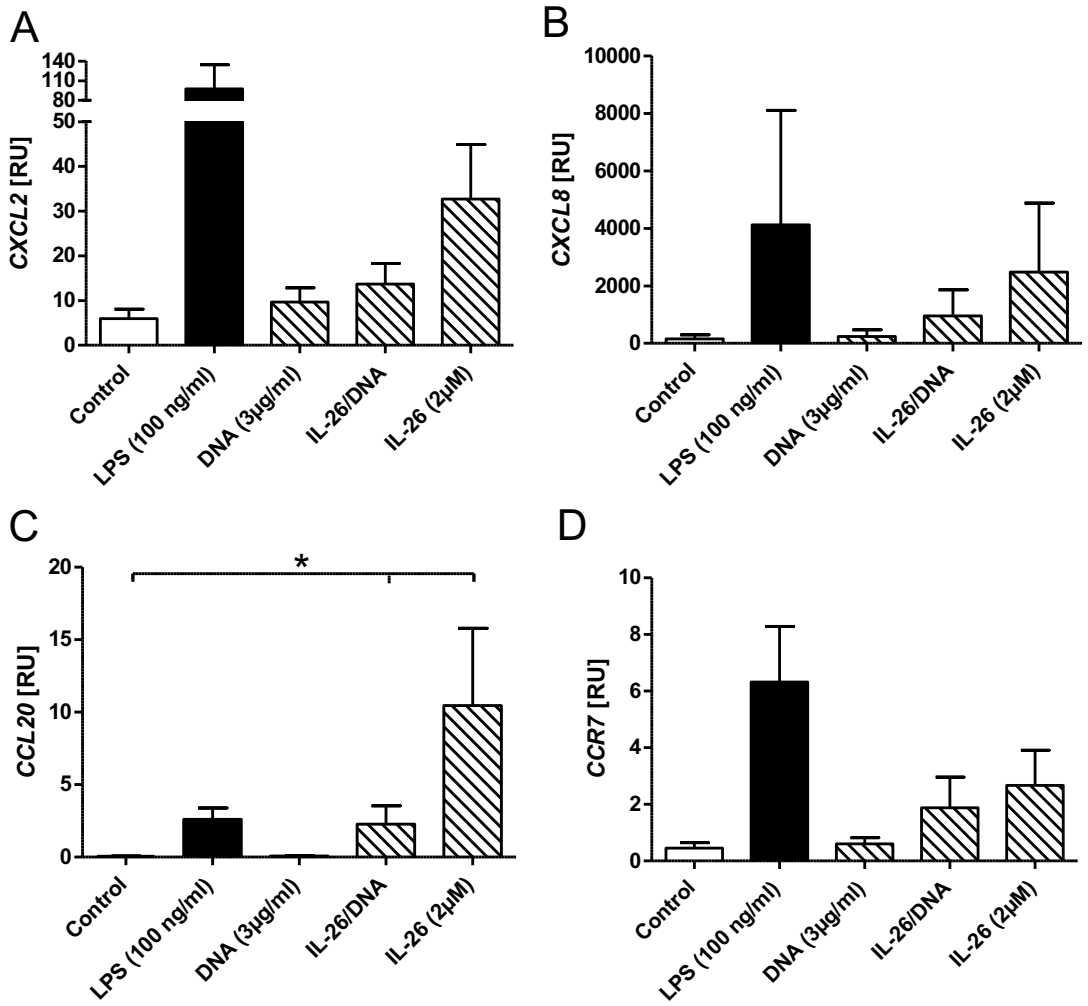

FIGURE 21: Primary macrophages express different chemokines and chemokine receptors in response to IL-26 treatment. Macrophages polarized towards M1 phenotype using GM-CSF show increased gene expression of the chemokines *CXCL2* (A), *CXCL8* (B) and *CCL20* (C). Also chemokine receptor *CCR7* gene expression (D) is enhanced in presence of IL-26 and IL-26/DNA complexes. qPCR values are depicted as relative units compared to 18S gene expression and the statistical significance was calculated using Mann-Whitney U test (***** $P \leq 0.05$; $n = 5$).

As we also used the monocytic cell line THP1 and differentiated those cells into macrophages in the presence of PMA for 24h, we sought to compare their

chemokine and chemokine receptor gene expression in response to IL-26 and IL-26/DNA complexes in comparison to the above-described primary macrophages generated from buffy coat. The THP1 macrophages were stimulated with IL-26 and IL-26/DNA complexes and incubated for 24h before the cells were lysed and RNA was extracted for subsequent qPCR investigations. The gene expression of both *CXCL2* and *CXCL8* were slightly increased when incubated with IL-26 and IL-26/DNA complexes (*Fig. 22A and B*). These finding were similar to the results obtained with primary macrophages. Looking at *CCL20* in THP1 macrophages, it seemed to be only minimally increased when the macrophages were stimulated with IL-26 alone (*Fig. 22C*). Having added IL-26/DNA complexes, no effect on the gene expression of *CCL20* was observed (*Fig. 22C*).

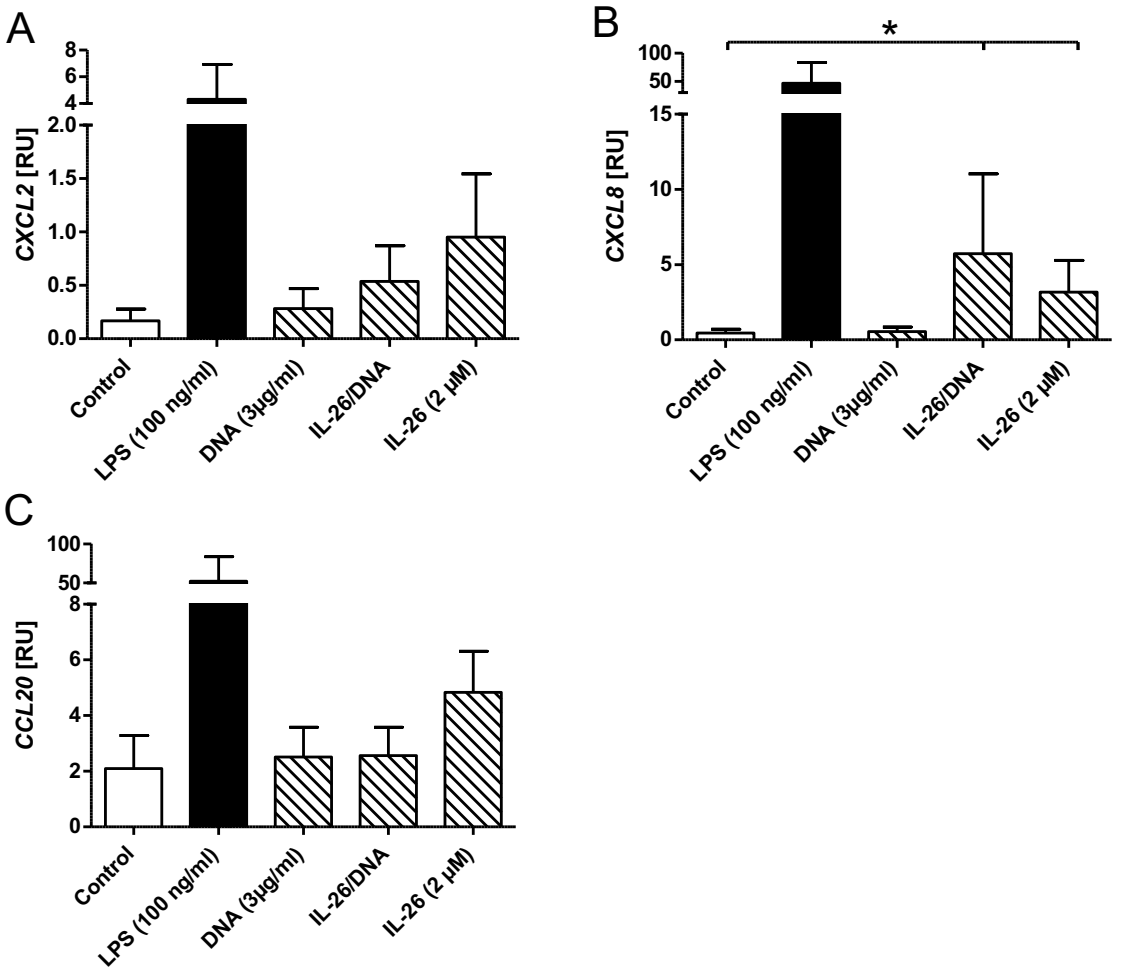

FIGURE 22: THP1 macrophages express the chemokines *CXCL2* and *CXCL8* in response to IL-26 treatment. THP1 monocytes were differentiated into macrophages in presence of PMA for 24h. The resulting THP1 macrophages were then treated with the displayed components and incubated for another 24h. RNA was isolated and the gene expression of *CXCL2* (A, n=5), *CXCL8* (B, n=6) and *CCL20* (C, n=5) was detected via qPCR. The qPCR values are shown

relative to 18S gene expression and statistics were calculated using Wilcoxon matched-pairs signed rank test (* equals P ≤ 0.05).

To conclude, PMA-differentiated THP1 macrophages responded similarly to IL-26 and IL-26/DNA complexes as differentiated primary macrophages from buffy coat.

3.3.4 Effects of IL-26/RNA complexes on moDCs

Having shown that IL-26 binds RNA (chapter 3.3.2), we investigated the effects of IL-26/RNA complexes on moDCs *in vitro*.

3.3.4.1 Induction of cytokines

In the next experiments, we stimulated moDCs with IL-26/RNA complexes overnight, harvested the cell supernatant and lysed the cell pellet for RNA isolation and subsequent qPCR. As expected, moDCs responded to IL-26/RNA complexes with significant secretion of TNF-α, but an increased amount of IL-6 was also detected with ELISA (*Fig. 23*). Furthermore, we found that similar to $CD14^+$ monocytes, moDCs respond to treatment with IL-26 alone. This response to IL-26 was unexpected, as moDCs only express one part of the IL-26 receptor, namely *IL10R2* (*Fig. 17 and table 7*), but an expression of *IL20R1* was not detected via qPCR. This means that, according to the literature on receptor distribution, immune cells should not be able to react to the single treatment with IL-26. Similar to the monocyte culture, we were wondering if there might be a “contamination” of DNA or RNA in the culture derived from another cell that died.

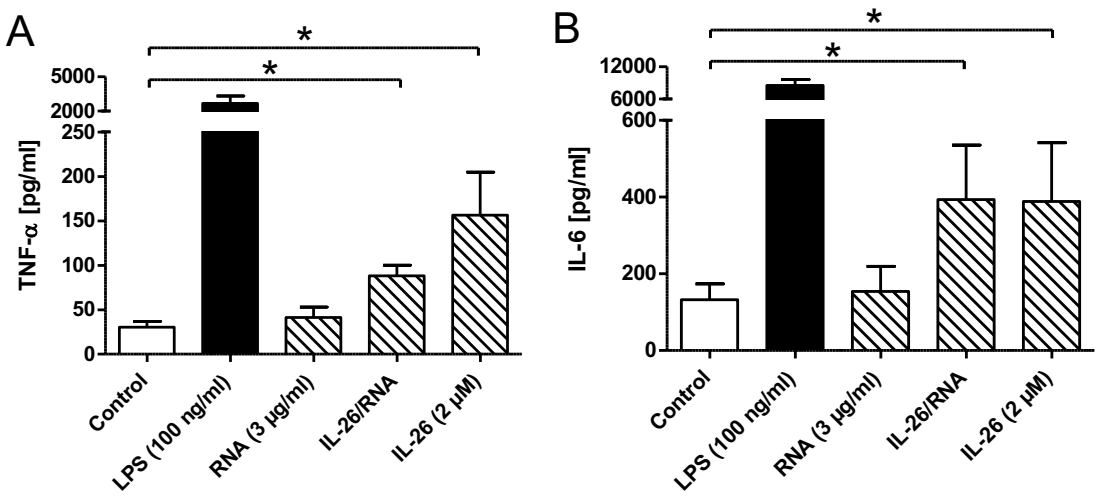

FIGURE 23: MoDCs respond to IL-26 and IL-26/RNA stimulation with increased TNFα and IL-6 secretion as measured by ELISA. $CD14^+$ monocytes were differentiated into moDCs in presence of GM-CSF and IL-4 for six days before the addition of IL-26 and IL-26/RNA complexes and incubated for another 24h. Supernatants were harvested and TNF-α (A) and IL-6 (B) secretion was measured via ELISA (n=6-8). Statistical analysis was performed using Wilcoxon matched-pairs signed rank test and indicated as follows: * $P \leq 0.05$ and ** equals $P \leq 0.01$.

To address this problem, DNAse and RNAse were added to the culture for an incubation time of 30 minutes prior to the addition of IL-26. This treatment led to a slight reduction of TNF-α and IL-6 secretion (*Fig. 24*). Interestingly, the inhibition of endosomal signaling using bafilomycin or chloroquine did not affect the secretion of TNF-α and IL-6 in the presence of IL-26/RNA complexes. This might indicate that those complexes are recognized by cytosolic RNA sensors.

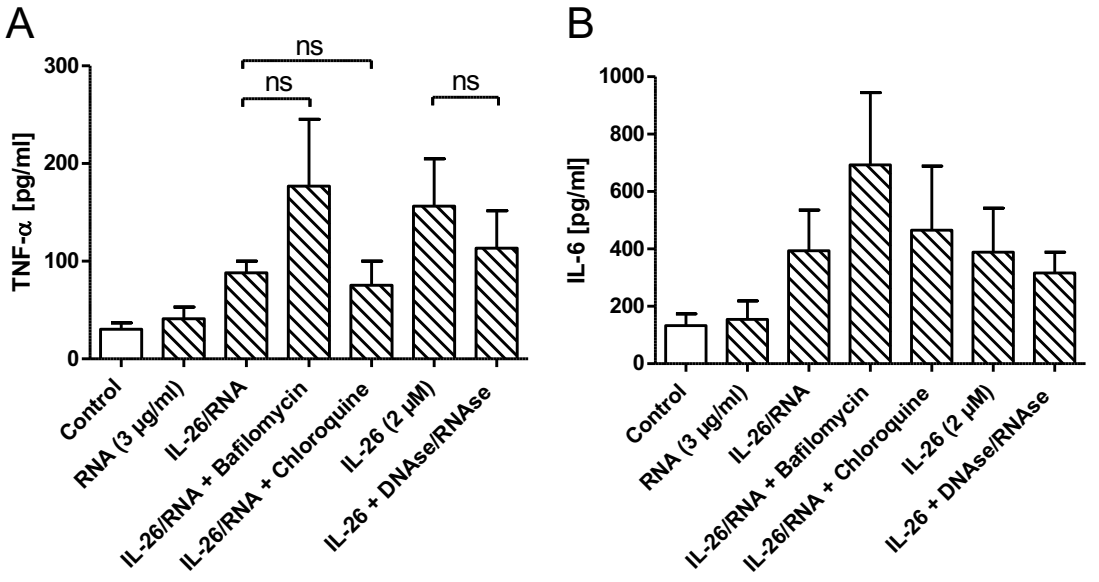

FIGURE 24: MoDCs respond to IL-26 and IL-26/RNA stimulation with increased TNF-α and IL-6 secretion as measured by ELISA. MoDCs generated in presence of GM-CSF and IL-4 for six days were treated with bafilomycin, chloroquine or nucleases before the addition of IL-26 or IL-26/RNA complexes and incubated for another 24h. Supernatants were harvested and TNF-α (A) and IL-6 (B) secretion was measured via ELISA (n=5-8). Statistical analysis was performed using Wilcoxon matched-pairs signed rank test and indicated as follows: ns (P > 0.05; not significant).

3.3.4.2 Induction of chemokines

As IL-26 and IL-26/DNA complexes were able to induce chemokines e.g. CXCL8 in macrophages, we investigated CCR7, a key chemokine receptor in moDCs that is crucial for them to migrate into skin lymphatic tissue[74,75] and secondary lymphoid tissues[75,76]. CCR7 showed a trend towards upregulation in the presence of IL-26/RNA complexes and IL-26 alone (*Fig. 25*). Looking at qPCR (*Fig. 25B*), there was a strong trend (p=0.0571, Mann-Whitney *U* test) towards increased *CCR7* expression when moDCs were treated with IL-26 alone.

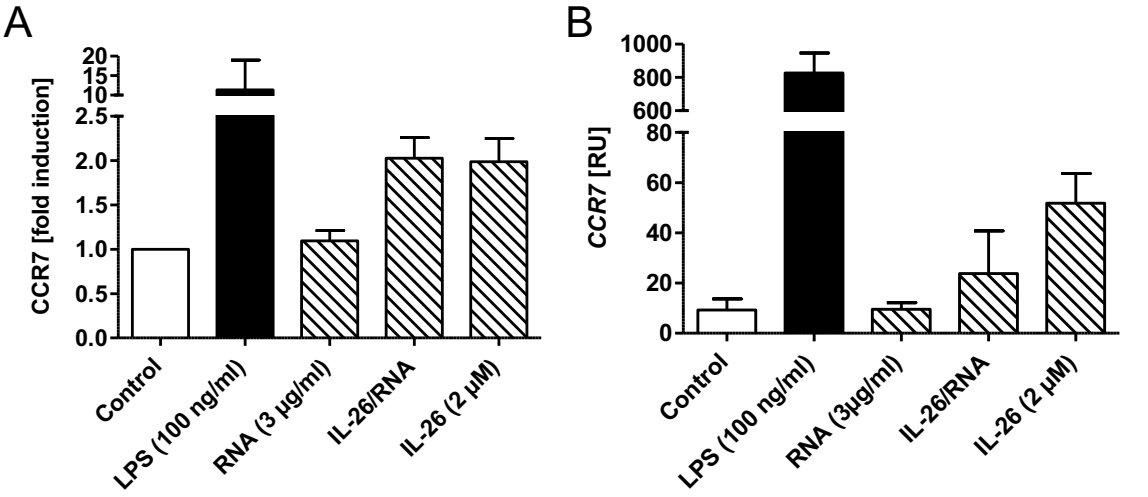

FIGURE 25: MoDCs respond to IL-26 and IL-26/RNA stimulation with CCR7. MoDCs were treated IL-26 or IL-26/RNA complexes and incubated for 24h. LPS was used as positive control. The cells were then stained with an antibody against CCR7 and analyzed via flow cytometry (A) or via qPCR (B). The percentage of CCR7-positive cells were then displayed as fold induction compared to untreated control cells (A, n = 2; B, n=4).

3.3.4.3 Impact on surface markers

Maturation of DC is measured by investigating the expression of different surface markers such as CD83[204] or CD86[205]. Maturation in DC occurs, for example, after contact with LPS, viral nucleic acids but also different cytokines. We found a slight increase of CD83 in presence of IL-26/RNA, which was not seen in presence of RNA alone (*Fig. 26A*). The increase of CD83 expression in the presence of IL-26 alone resulted in a p-value of 0.0556 (*Fig. 26A*). Looking at CD86, the presence of IL-26/RNA complexes in the moDC culture did not change the expression (*Fig. 26B*). Instead, IL-26 alone seemed to increase CD86 expression on moDCs (p=0.1508) (*Fig. 26B*).

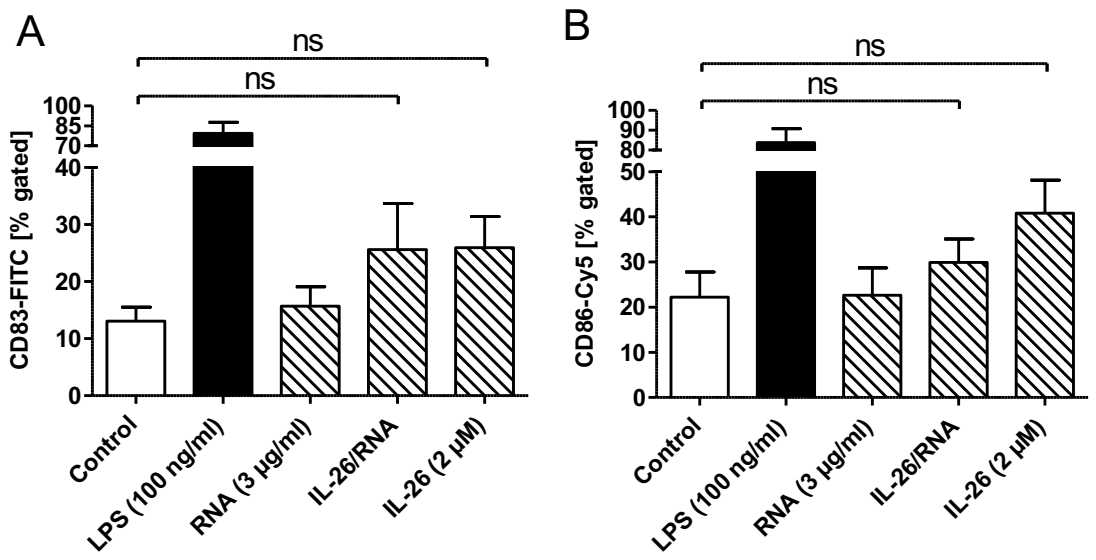

FIGURE 26: Expression of CD83 and CD86 is slightly increased in presence of IL-26 and IL-26/RNA complexes. MoDCs were treated IL-26 or IL-26/RNA complexes and incubated for 24h. The cells were stained with an antibody against the surface markers CD83 and CD86. Analysis was done by flow cytometry. The percentage of CD83-positive (A) and CD86-positive cells (B) were then displayed together with untreated control cells and the LPS-treated positive control (n = 5). Mann-Whitney U test was used to investigate statistical significances (ns equals "not significant").

3.4 Potential receptor for IL-26 on immune cells

3.4.1 IL-26 induces SEAP secretion via TLR2

In the previous chapters, it was shown that IL-26 alone leads to a response in immune cells, such as $CD14^+$ monocytes, primary macrophages, and also moDCs. Surprisingly, another immune cell type, namely plasmacytoid dendritic cells (pDCs), does not respond to treatment with IL-26 (Meller *et al.*[19]). The question arose, what is the difference between pDCs and monocytes, moDCs, and macrophages? $CD14^+$ monocytes, as well as moDCs and macrophages, which are both derived from $CD14^+$ monocytes, belong to the myeloid lineage[206]. PDCs instead derive from a different lineage that is not yet completely defined[207]. PDCs are specialized in responding to viral nucleic acids via their intracellular TLR7 and 9, which are the only TLRs they express. Myeloid lineage cells on the other hand express TLR2, 3, 4, 5, 6, 7, and 8[207]. This variety of expressed TLRs makes the myeloid cells prone to react to a variety of different stimuli ranging from extracellular gram-positive and -negative bacteria to intracellular pathogens. As the TLRs 3 and 7 to 9 are exclusively

found within the endosomal compartment and therefore are unlikely a potential target for IL-26, we sought to investigate the role of TLR2.

First, we determined the *TLR2* expression levels in different immune cells. As shown in *figure 27*, monocytes expressed the highest level of *TLR2* (*Fig. 27A*). It even seemed as if the presence of IL-26 increased the *TLR2* expression in monocytes. Primary macrophages, moDCs, and THP1 macrophages expressed about the same level of *TLR2* (*Fig. 27B to D*). In moDCs, *TLR2* was significantly induced by IL-26, reaching about 4-times the relative expression compared to untreated cells (*Fig. 27B*). Especially in primary macrophages the presence of LPS induced the *TLR2* expression by about 3-fold. On both types of macrophages IL-26 did not affect the *TLR2* expression (*Fig. 27C and D*).

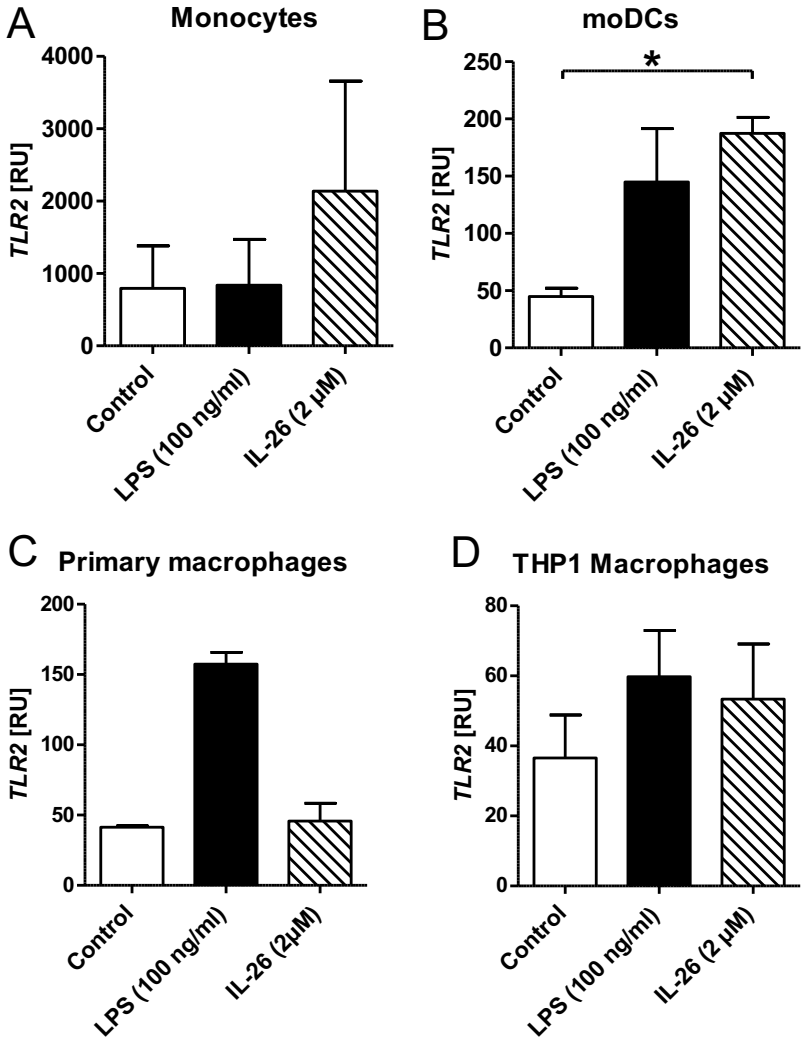

FIGURE 27: Different immune cells express *TLR2*. In monocytes (A) the addition of 2 µM IL-26 enhanced the *TLR2* gene expression (n=2). Monocytes (A), moDCs (B, n=4), primary macrophages (C, n=2) and THP1 macrophages (D, n=3) were incubated with LPS or IL-26 for

24h before the cells were harvested and subjected to qPCR. Statistical analysis was performed using Mann Whitney *U* test (* equals $p<0.05$).

In order to the test the hypothesis that IL-26 might possibly signal via TLR2, we obtained HEK-Blue™ hTLR2 cells. These HEK293 cells are transfected with genes for human TLR2 and secreted embryonic alkaline phosphatase (SEAP). The secretion of SEAP in response to stimulation via TLR2 was then measured as a colour change at an OD of 620nm.

The HEK-Blue™ hTLR2 cells were checked for gene expression of *IL20R1*, *IL10R2*, and *TLR2*. No expression of *IL20R1* was observed, while expression for *IL10R2* and *TLR2* was detected (*Supplemental figure 4*). Incubating HEK-Blue™ hTLR2 cells for 24h with IL-26 (2 µM, n=4), we found a significant increase in SEAP secretion compared to the untreated control (*Fig. 28A*). Both LTA (positive control) and LL37 (negative control, n=3 for 10 µM and n=2 for 2 µM) were used. LTA resulted in a very strong SEAP secretion, while LL37 did not cause any SEAP in the HEK-Blue™ hTLR2 cells (*Fig. 28A*). To validate the results, the HEK-Blue™ hTLR2 cells were pre-incubated for 45 min with an anti-human TLR2 antibody before the addition of IL-26 (*Fig. 28B*). The blocking of TLR2 using this antibody did block the IL-26 induced SEAP secretion at an antibody concentration of 1 µg/ml (n=2) and 10 µg/ml (n=1). The validity of the anti-TLR2 antibody was tested in a separate experiment, where its effectivity in blocking SEAP secretion prior to stimulation with LTA was evaluated (*Supplemental figure 5*). The anti-TLR2 antibody acted in a dose-dependent manner and completely blocked LTA-induced SEAP secretion at a concentration of 10 µg/ml (*Supplemental figure 5*). To exclude any potential effects of IL-26 binding to nucleic acids present in cell culture, the HEK-Blue™ hTLR2 cells were pre-incubated with DNase and RNase before the addition of IL-26. The pre-incubation with DNase/RNase did not change the SEAP secretion (*Fig. 28B*).

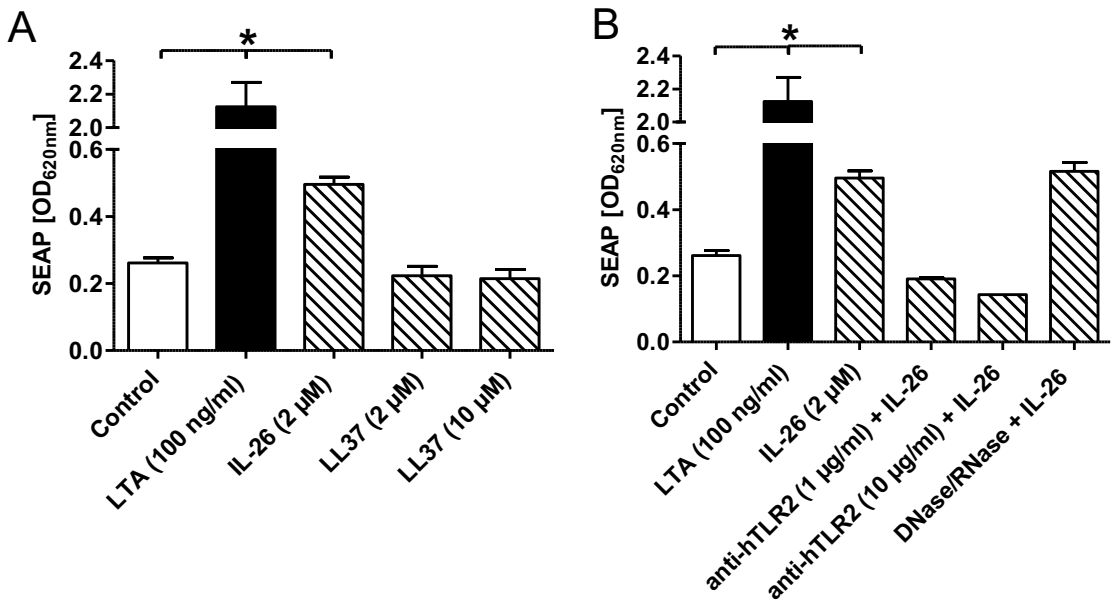

FIGURE 28: IL-26 induces SEAP secretion in HEK Blue hTLR2 cells. A) IL-26 but not LL37 is inducing SEAP secretion in HEK Blue hTLR2 cells. LTA was used as positive control (Mann-Whitney *U* test, n=2-4). B) IL-26 induced SEAP secretion is blocked by anti-hTLR2 antibody, but not by pre-incubation by DNase I and RNase (n=1-4).

In contrast to HEK-Blue™ hTLR2 cells, no differential SEAP secretion after treatment with IL-26 was observed HEK-Blue™ hTLR4 cells (*Supplemental figure 6*).

We went on to investigate if a TLR2 blocking would be inhibiting the direct effects of IL-26 on primary immune cells. Treating moDCs with anti-hTLR2 antibody prior to the addition of IL-26 resulted in a significant reduction of TNF-α secretion after 24h (*Fig. 29A*). Interestingly, treating primary macrophages with anti-hTLR2 did not result in a change in TNF-α secretion (*Fig. 29B*).

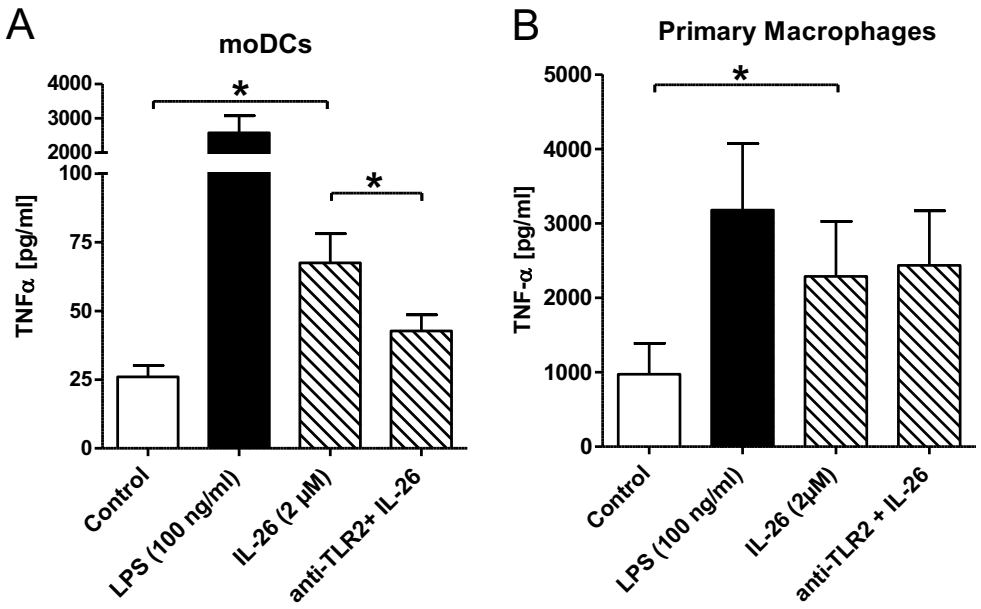

FIGURE 29: Blocking of TLR2 prior to stimulation with IL-26 significantly decreases TNF-α secretion in moDCs. MoDCs (A) or primary macrophages (B) were pre-incubated with 10 µg/ml anti-hTLR2 antibody for 30 min before the addition of IL-26. The cells were then further incubated for 24h before supernatants were harvested and subjected to ELISA. LPS was used as control. Statistical significance was calculated using Wilcoxon's matched-pairs signed rank test (n=6).

3.4.2 Disease association of TLR2

Having found that TLR2 has an importance in the signaling of IL-26, we sought to examine the gene expression of *TLR2* in different skin diseases (*Fig. 30A*) and tuberculosis (*Fig. 30B*). We found a trend towards upregulated gene expression when comparing rosacea and sarcoidosis to healthy control. Comparing healthy skin samples to rosacea using the Mann Whitney U test it resulted in a p-value of 0.0559. Similar results were obtained when comparing sarcoidosis to healthy skin. Here a p-value of 0.0539 was calculated when Mann Whitney *U* test was applied. Performing a multiple comparison as done for *Fig. 30A*, using the Kruskal Wallis test with Dunn's post testing, no significant differences were seen. Investigating the *TLR2* expression in tuberculosis lymph nodes and healthy lymph nodes, we found a generally much higher expression compared to skin samples (*Fig. 30A* versus *B*). More importantly we found that *TLR2* expression was significantly increased in tuberculosis compared to healthy controls (*Fig. 30B*).

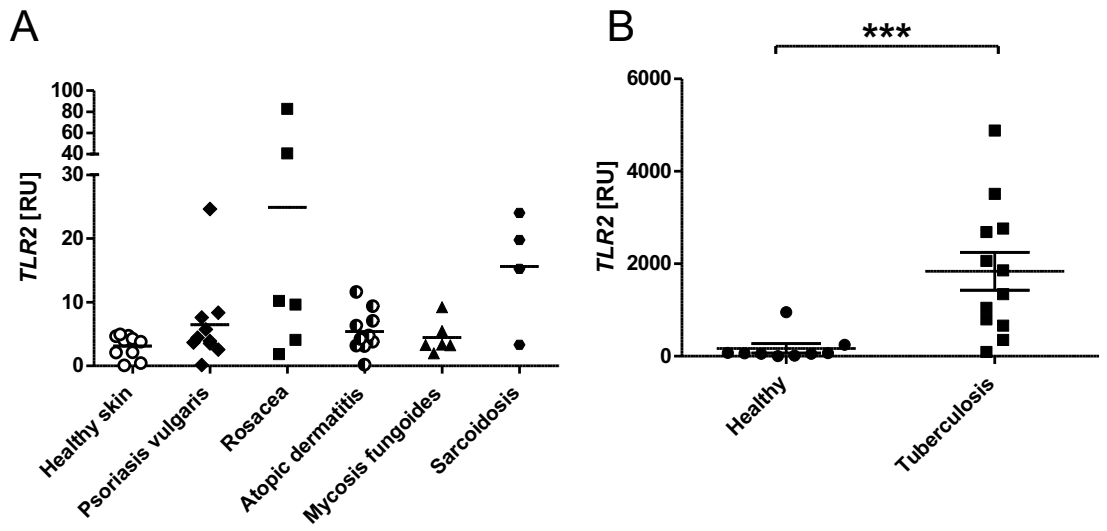

FIGURE 30: The expression of *TLR2* is increased in rosacea, sarcoidosis, and tuberculosis compared to healthy skin. Gene expressions in different skin diseases and healthy skin (A), as well as tuberculosis lymph nodes (B) compared to healthy lymph nodes are depicted in relative expression units compared to 18S ribosomal RNA. Statistical analysis was done using Kruskal-Wallis test with Dunn's posttest (A) or Mann Whitney *U* test (B) and shown as *** equals $P \leq 0.001$.

3.5 IL-26 in innate immunity

3.5.1 Antibacterial properties

3.5.1.1 IL-26/bacterial component binding

We have previously shown with a different method that IL-26 binds anionic bacterial components such as LPS (e.g. from *E. coli*) and LTA (e.g. *S. aureus*)[19]. This finding was confirmed using MST. We see that IL-26 binds both FITC-labelled LPS and Alexa488-labelled LTA (*Fig. 31A and B*). The binding of IL-26 to LTA was about 4-times stronger than the binding to LPS (*Table 9*). Comparing the binding affinity of IL-26 to bacterial surface components to LL37's ability to bind LPS and LTA, we saw that LL37 bound to both LPS and LTA better than IL-26. As a negative control, we used IL-22 that shows high sequence identity and similarity to IL-26. For IL-22 we were unable to measure any interaction (no interaction = NI) which was as expected.

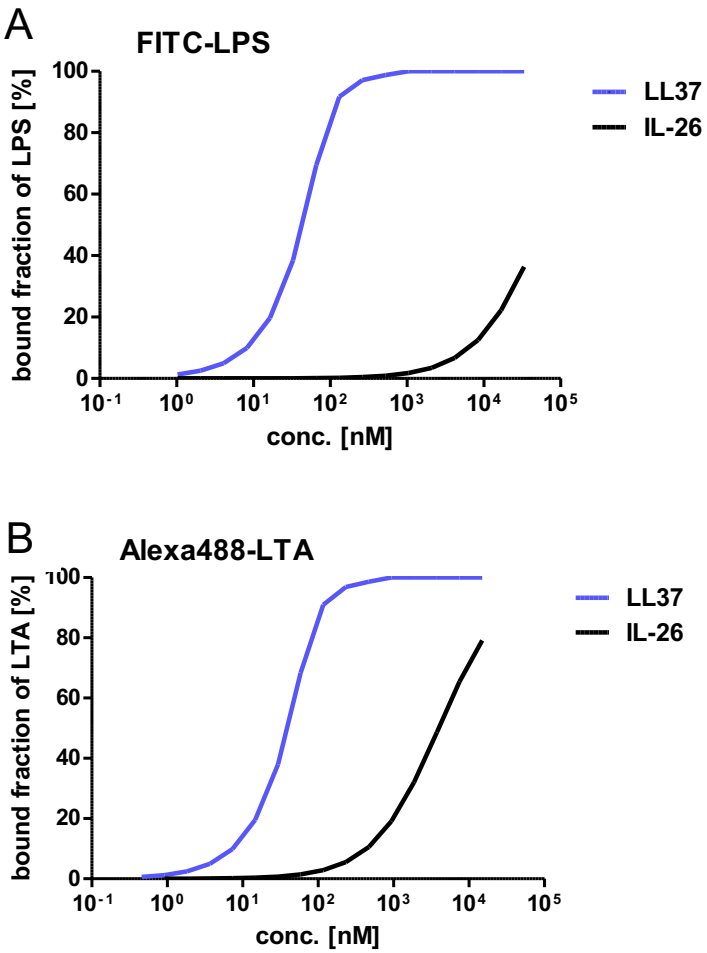

FIGURE 31: IL-26 binds better to LTA than to LPS. Microscale thermophoresis (MST) was used to investigate the protein-protein interactions. The binding of IL-26 and LL37 to LPS is depicted in A) and the binding to LTA is shown in B). LL37 binds to both bacterial components with about the same affinity.

The respective dissociation constants K_D for the above depicted graphs can be extracted from table 9.

TABLE 9: Dissociation constants K_D from MST measurement evaluating the binding of IL-26 to the bacterial surface components LPS and LTA.

Protein/ligand	**LL37/LPS**	**IL-26/LPS**	**IL-22/LPS**
K_D (mean ± SD)	6.57 nM ± 2.2	58.9 µM ± 2.8	NI
Protein/ligand	**LL37/LTA**	**IL-26/LTA**	**IL-22/LTA**
K_D (mean ± SD)	7.33 nM ± 4.6	12.5 µM ± 2.1	NI

3.5.1.2 Efficacy of IL-26 in bacterial killing

The antimicrobial activity of IL-26 was extensively investigated using a microbroth dilution assay in Meller *et al.*[19]. In this type of assay, serial dilutions of the potential antimicrobial substances are prepared in a 96-well format and the bacterial viability is measured after a defined incubation time. *Fig. 32* shows the example of *Pseudomonas aeruginosa (P. aeruginosa*). The bacterial growth was investigated after 18 hours with the measurement of the optical density (OD) at 600 nm. In this representative figure, the minimal inhibitory concentration to achieve 50% killing (MIC_{50}) of *P. aeruginosa* was calculated to be 6.052 µM for LL37 and 13.05 µM for IL-26. This MIC_{50} of IL-26 was slightly above 8.6 µM, which is the published concentration[19].

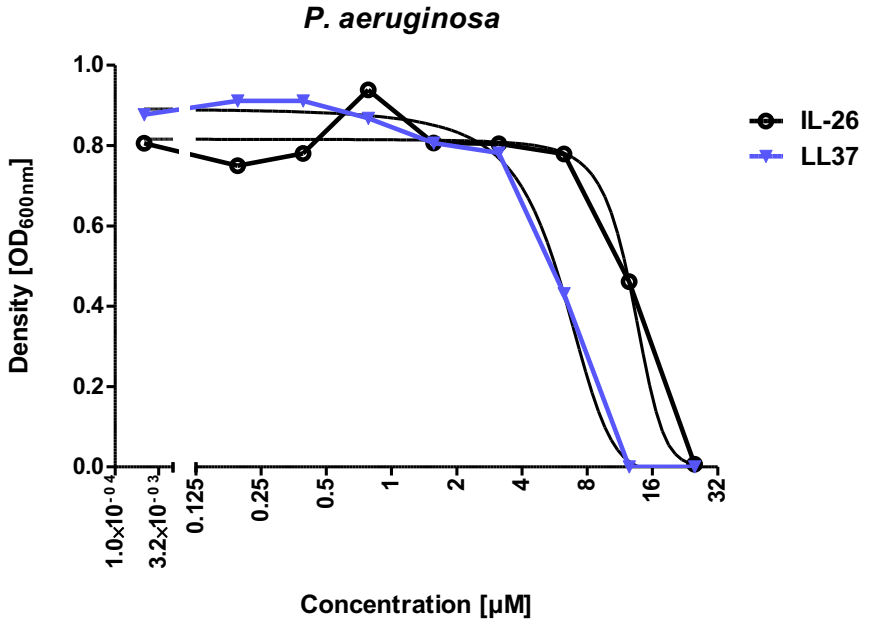

FIGURE 32: IL-26 directly kills P. aeruginosa. P. aeruginosa was cultured in tryptic soy broth (TSB) and incubated with a serial dilution of LL37 or IL-26 for 18h before the OD at 600 nm was measured. One representative experiment is shown.

3.5.1.3 IL-26/mycobacterial component binding

As shown in the previous paragraph, IL-26 binds anionic bacterial components. Seeing that IL-26 has an association with tuberculosis, we asked whether IL-26 also binds to (anionic) mycobacterial components, as mycobacteria are the causative agent of tuberculosis. One major cell wall component found

throughout mycobacterial species is lipoarabinomannan (LAM), or more specifically, mannosylated LAM (manLAM)[208]. Furthermore, LAM (from *M. smegmatis*) is characterized by a negatively charged fraction and shows similarities to LPS[209]. ManLAM from *Mycobacterium smegmatis* and *M. tuberculosis H37Rv* (provided by BEIResources) was fluorescently labelled with Alexa488 and then together with IL-26 subjected to MST. We found that both LL37 and IL-26 bind to LAM from *M. smegmatis* with very high affinity (*Fig. 33 and table 10*). LL37 seemed to bind a little better to LAM from *M. smegmatis* compared to IL-26 (*table 10*). IL-26 bound to LAM from *M. smegmatis* and *Mtb* with the same affinity, but there was no binding observed between LL37 and LAM from *Mtb* (*Fig. 33 and table 10*). Looking at IL-22, which served again as negative control, we could not observe any binding.

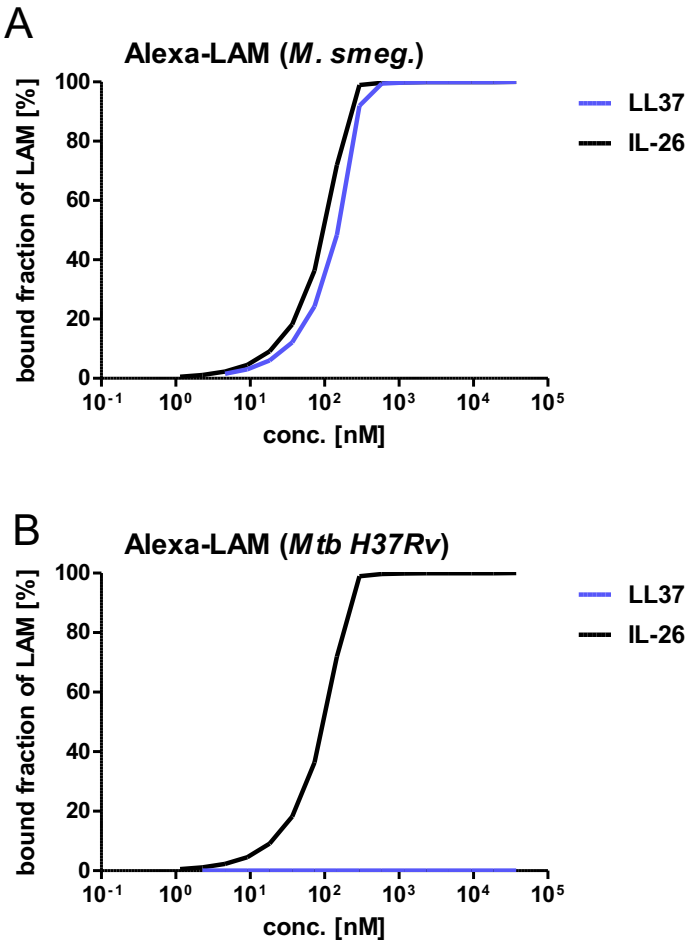

FIGURE 33: IL-26 shows high affinity to lipoarabinomannan (LAM) from both *M. smegmatis* (*M. smeg*) and *Mtb H37Rv* as measured with microscale thermophoresis. The bound fractions of LAM from *M. smegmatis* (A) and *M. tuberculosis H37Rv* (B) to IL-26 and LL37 are displayed.

The respective dissociation constants for LL37 and IL-26 to the different LAMs are displayed in table 10, where the mean dissociation constants together with the standard deviation are shown.

TABLE 10: Dissociation constants K_D from MST measurement evaluating the binding of IL-26 and LL37 to the mycobacterial surface components LAM from *M. smegmatis (M. smeg)* and *Mtb H37Rv*.

Protein/ligand	**LL37/LAM *M. smeg***	**IL-26/LAM *M. smeg***	**IL-22/LAM *M. smeg***
K_D (mean ± SD)	1 nM ± 0.0068	1 nM ± 1.26	NI (166 µM)
Protein/ligand	**LL37/LAM *Mtb***	**IL-26/LAM *Mtb***	**IL-22/LAM *Mtb***
K_D (mean ± SD)	140 µM ± 13.3	1 nM ± 1.45	NI (160µM)

3.5.1.4 Efficacy of IL-26 in mycobacterial inhibition

Mycobacterium tuberculosis (Mtb) H37Rv and *M. bovis BCG* were subjected to a serial dilution of IL-26 (starting at 25 µM) and LL37 (starting at 25 µM) in an H_2O-diluted RPMI medium and incubated for 5 days for *Mtb* and 24h for *M. bovis* in order to determine the MIC_{50}. Here, bacterial growth of *Mtb* was evaluated after the addition of resazurin, which turns from a dark blue colour into a pinkish colour in the presence of viable bacterial cells. The colour change was then measured using a fluorescence reader at an excitation wave length of 540 nm and an emission wave length of 590 nm. For *M. bovis*, a BakTiterGlo assay was applied, where bacterial viability was determined with a luminescence reader.

Both IL-26 and LL37 inhibited *Mtb H37Rv* (*Fig. 34A*) and *M. bovis* (*Fig. 34B*) directly. IL-26 seemed to be a bit more potent in inhibiting *Mtb H37Rv* (MIC_{50} approx. 5 µM) compared to *M. bovis* (MIC_{50}: 7 µM) (*Fig. 34A/B* and *table 11*). This was in contrast to LL37, which appeared to be more potent against *Mtb H37Rv* and less potent against *M. bovis BCG* (*Fig. 34A/B*).

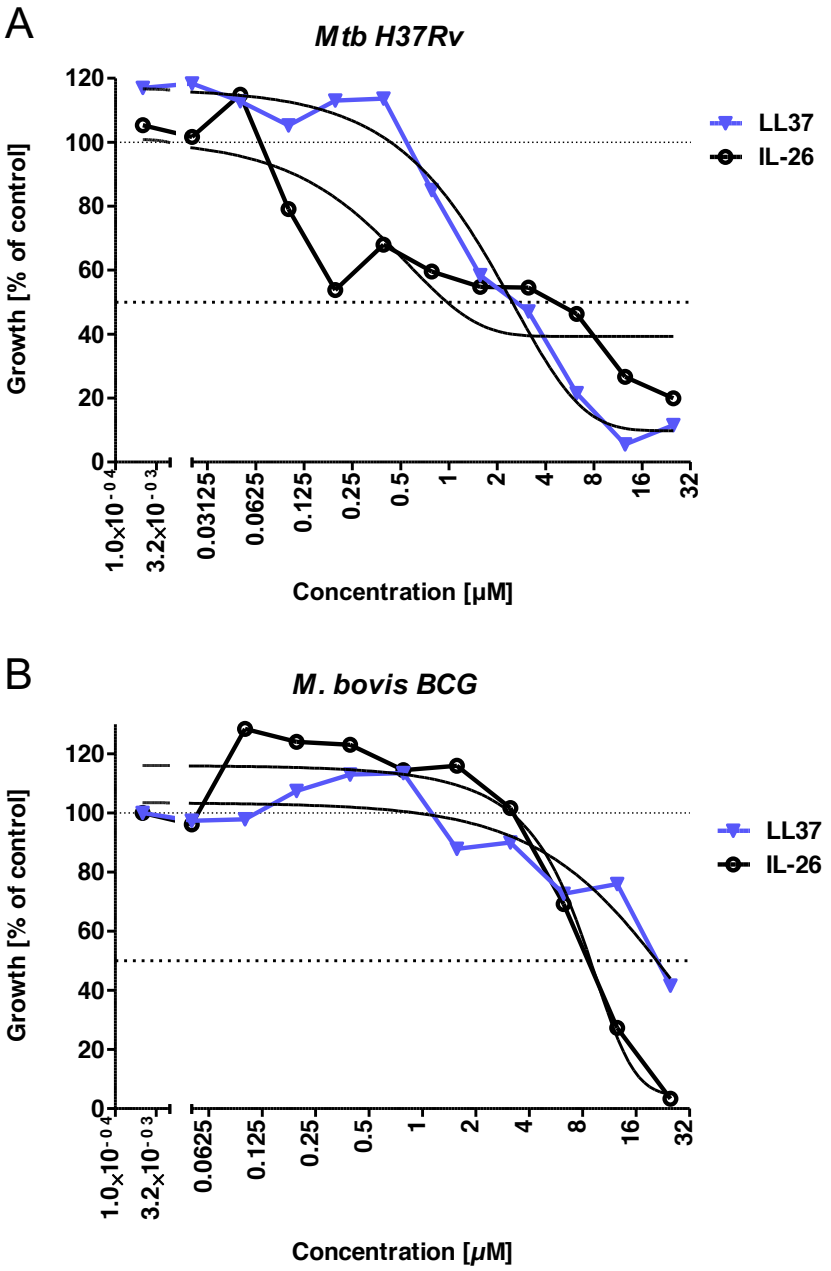

FIGURE 34: IL-26 displays anti-mycobacterial activity against different mycobacteria strains. Determination of MIC of different mycobacteria strains treated with increasing concentrations of IL-26 or LL37. Growth of *Mtb* (A) in % to untreated control was analyzed after 5 days of incubation using resazurin and *M. bovis* (B) was analyzed after 24h using the BakTiterGlo Assay (n=4 for *Mtb* and one pilot experiment for *M. bovis*).

The resulting MIC_{50} from the microbroth dilution assays are displayed in *table 11*.

TABLE 11: MIC_{50} determination of IL-26 on *M. bovis BCG* and *Mtb H37Rv*.

Mycobacterium strain	**IL-26 MIC_{50}**	**LL37 MIC_{50}**
M. tuberculosis H37Rv	Approx. 5 µM	Approx. 2.5 µM
M. bovis BCG	7.046 µM	Approx. 24 µM

Next, we performed scanning electron microscopy (SEM) to reveal how IL-26 (and LL37) is changing the morphology of mycobacteria (here: *Mtb*) and thereby inhibits mycobacterial growth. The mycobacteria were incubated for 24h in the presence or absence of isoniazid (10 µM), IL-26 (12.5 µM) or LL37 (12.5 µM). The fixed mycobacteria were then subjected to critical point drying (CPD).

Untreated mycobacteria were characterized by a rod-like shape with a smooth membrane and a size of approximately 2 µm, as seen in *Fig 35A*. Additionally, the mycobacteria grew in clusters that can also be seen in *Fig 35A*. The potent anti-mycobacterial reagent isoniazid known to affect the mycobacterial cell wall[210] served as positive control. Too high doses of isoniazid led to complete destruction of mycobacterial cells as displayed in (not shown). Comparing IL-26 and LL37, they appeared to have similar effects on the mycobacterial membrane that is shown in *Fig 35B* (for LL37) and *Fig 35C/D* (for IL-26). Large disruptions of the mycobacterial membrane integrity were observed after treatment with LL37 for 24h (*Fig. 35B*). The disruptions potentially led to a release of cellular material into the surrounding space (indicated with an arrow). Mycobacteria treated with IL-26 (12.5 µM) developed several blebs on their membrane as indicated with an arrow (*Fig. 35C/D*). It seemed as if both IL-26 and LL37 prevented the formation of large cell clusters, as clusters like the one depicted in *Fig. 35A* were not found in presence of LL37 or IL-26.

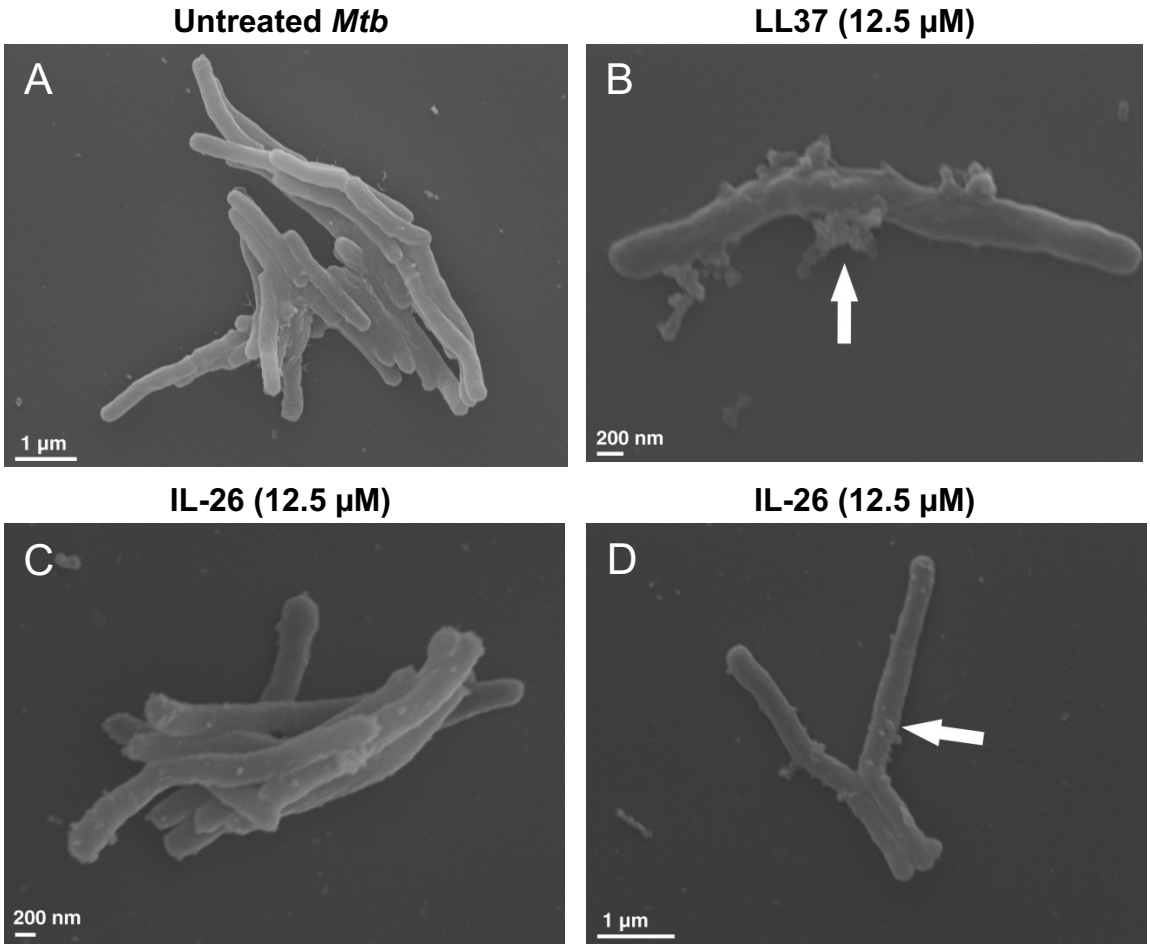

FIGURE 35: IL-26 leads to bleb formation on mycobacterial membrane. *Mtb H37Rv* were incubated in RPMI (A) with LL37 (12.5 µM, B) and IL-26 (12.5 µM, C and D) for 24h on glass cover slides before fixation and critical point drying. Images were taken on a SEM LEO1430 VP (Zeiss).

3.5.1.5 Efficacy of IL-26 in intracellular killing of Mtb

IL-26 is capable of killing mycobacteria when they are outside a host cell. But mycobacteria typically infect alveolar macrophages in the lung. So, we wondered if IL-26 is also able to kill mycobacteria or inhibit mycobacterial growth when they are inside a macrophage. In order to test this idea, we infected THP1 macrophages with *Mycobacterium tuberculosis H37Rv* reporter strain (*Mtb pBEN::mCherry* (Hsp60), that expresses mCherry under a promotor of heat shock protein 60 (Hsp60). Carrying this reporter gene construct the mycobacteria are easily detected and analysed via fluorescent microscopy. An exemplary microscopy series is shown in the panel below where the THP1 macrophages were depicted in bright field, the infecting mycobacteria red

fluorescing in the middle picture and then in C a merged image where it can be seen which macrophage is infected and which not (*Fig. 36*).

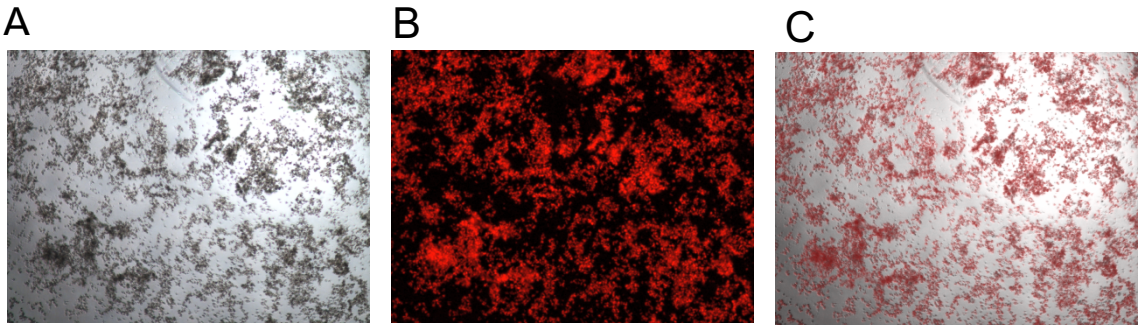

FIGURE 36: Exemplary analysis of intracellular infection assay. A) Bright field microscopy showing only THP1 macrophages. B) *Mtb H37Rv pBEN::mCherry* appears red under the fluorescence light. C) A merged picture of A) and B) created with ImageJ program.

We found that IL-26 seemed to enhance THP1 macrophage defence when infected with mycobacteria. Microscopic analysis revealed that in the presence of 10 µM IL-26, macrophages seem to be much more viable as compared to untreated infected control (*Fig. 37*). This conclusion was drawn as untreated and uninfected macrophages look very much like macrophages treated with 10 µM IL-26 (data not shown). In infected THP1 macrophages a strong red fluorescence was seen, and the macrophages seemed to lose their adherence (*Fig. 37A*). This loss of adherence was also seen for treatment with LL37 and 2 µM IL-26 (*Fig. 37B-D*).

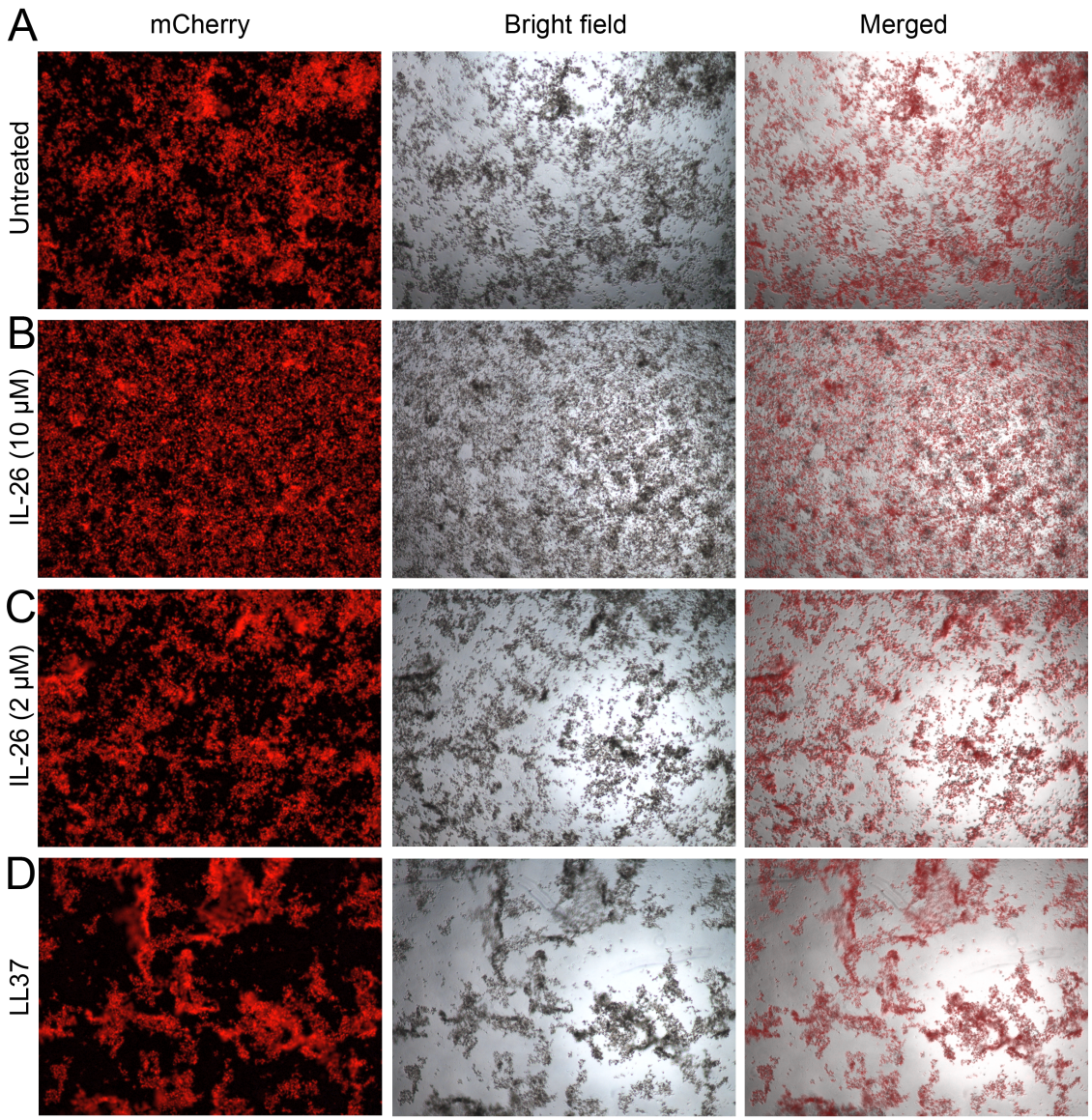

FIGURE 37: IL-26 improves THP1 macrophage defense by improving survival upon infection with mycobacteria. A) Fluorescence detected in untreated control after 3 h infection with *Mtb H37Rv mCherry* subsequent 5 days incubation without further treatment. B) to D) Fluorescence in macrophages after 3 h infection and 5 days incubation with IL-26 (10 µM; B), IL-26 (2 µM; C) or LL37 (10 µM, D). Exemplary images are shown.

The fluorescent images were quantified using the ImageJ program. The area of fluorescence was calculated for each treatment and then displayed as percentage of the image area (*Fig. 38*). It was observed that the presence of rifampicin (Rif), LL37, and IL-26 (2 µM) slightly reduced the fluorescent area compared to untreated control cells. Looking at 10 µM IL-26, the fluorescent area is just as large as from the infected controls. This analysis reflects visual observation in the microscopic images in *Fig. 37*.

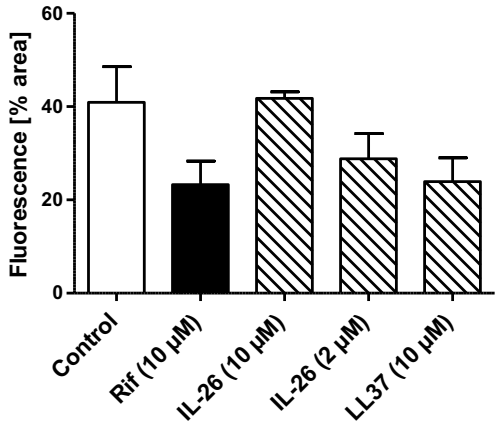

FIGURE 38: IL-26 enhances intracellular killing of intruding mycobacteria in THP1 macrophages. Using the fluorescence images, binary pictures were created with ImageJ and with those binary pictures the originally fluorescing area was calculated and the percentages graphically depicted (n=3).

3.6 Physiological thioredoxin redox system

3.6.1 Skin disease association

Inflammatory disorders of the skin as well as (mycobacterial-induced) granulomas in sarcoidosis and tuberculosis lead to the high influx of immune cells, and the vast amount of immune cells present in the respective lesions these cases involve reducing conditions together with a hypoxic environment[129]. We sought to investigate the physiological conditions in the different diseases and the resulting effects on the structure and chemical properties of IL-26. To start off we investigated the most relevant and prominent physiological redox system known to reduce proteins *in vivo*, namely the thioredoxin (TXN) system[211,212].

Therefore, we first analyzed the gene expression levels of *TXN* and thioredoxin reductase (*TXNRD1*) in different skin diseases as shown in Fig. 39. We found that *TXN* was significantly increased in PV, AD, and MF (*Fig. 39A*). In AD, *TXN* expression was increased compared to healthy skin in about half the tested samples but the other half displayed expression values similar to healthy skin. Some of the highest *TXN* expression values were also found amongst patients suffering from AD. Furthermore, lichen ruber, squamous cell carcinoma (SCC), and prurigo nodularis exhibited increased *TXN* expression compared to healthy control (supplementary figure 7). Investigating *TXNRD1* gene expression (*Fig.*

39B), we found it extremely upregulated in sarcoidosis and MF, whereas PV, rosacea, and AD did not show any differentially regulated *TXNRD1* expression. All other tested skin diseases did not show any differentially regulated *TXNRD1* gene expression (*Fig. 39B and supplementary figure 8*).

In addition, the expression levels of *TXN* and *IL26* in psoriatic skin correlated positively but not significantly. For *TXN* and *IL26* a P-value of 0.0944 and a Spearman correlation value of 0.43 were reached while *TXNRD1* and *IL26* did not correlate in our cohort (*Fig. 39C and D*).

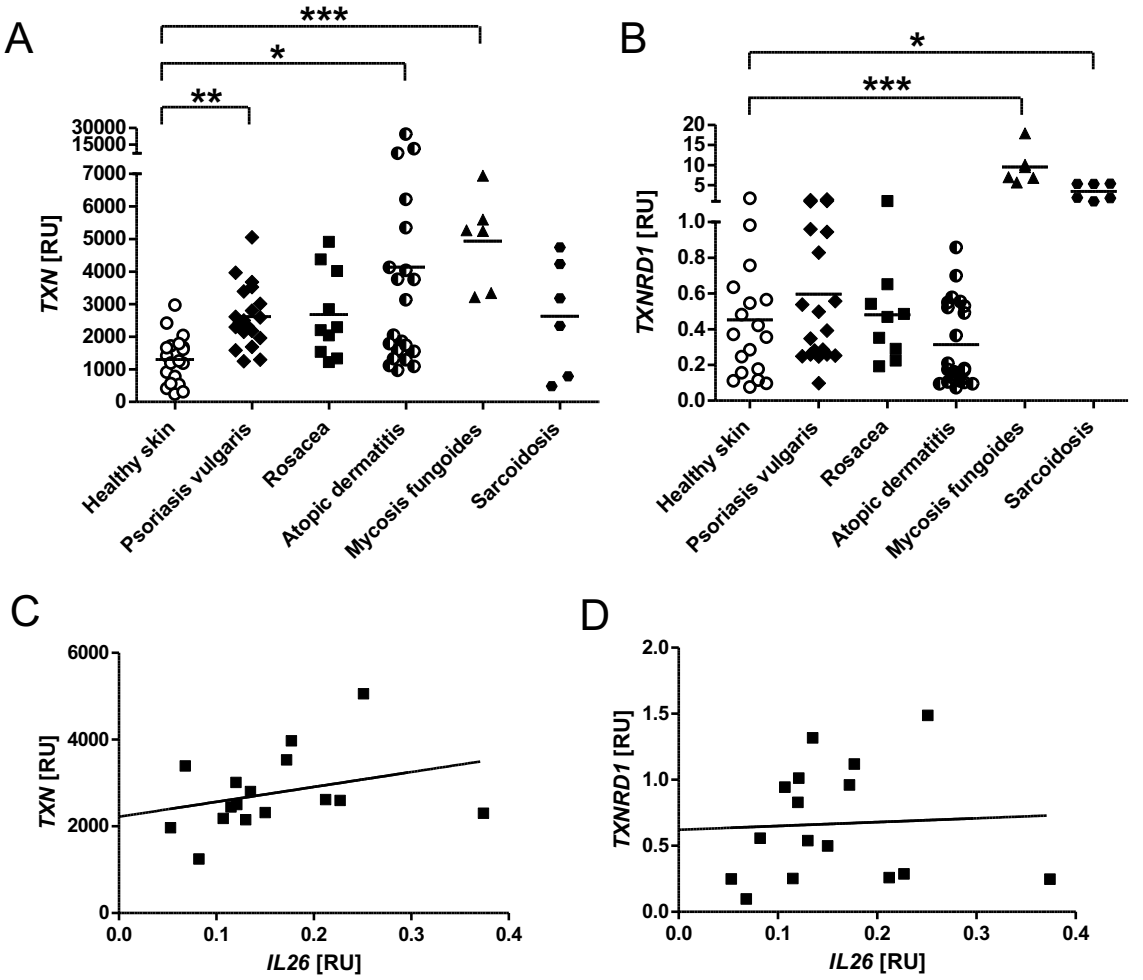

FIGURE 39: TXN and TXNRD1 gene expression in different skin diseases compared to healthy skin. A, B) The graphs depict relative TXN or TXNRD1 gene expression values compared to the 18S gene. Data were analyzed using Kruskal-Wallis test with Dunn's posttest. C,D) TXN and TXNRD1 expression partly correlates with IL-26 expression in psoriasis. Data were analyzed using Spearman correlation analyzes together with two-tailed Student's t test. Statistical significances are depicted as follows; * equals P ≤ 0.05, ** equals P ≤ 0.01 and *** equals P ≤ 0.001.

Next, we aimed to display the increased gene expression of TXN on protein level by performing IHC. In healthy skin sections (*Fig. 40A-C*) we mainly did

TXN staining in the epidermal keratinocyte layer and around the vessels. In psoriasis vulgaris (*Fig. 40D-F*) and rosacea (*Fig. 40J-K*) the keratinocyte layer was approximately as strongly stained as in the healthy control. In both psoriasis vulgaris (*Fig. 40D-F*) and psoriasis pustulosa (*Fig. 40G-I*) the outermost keratinocyte layers have not been stained.

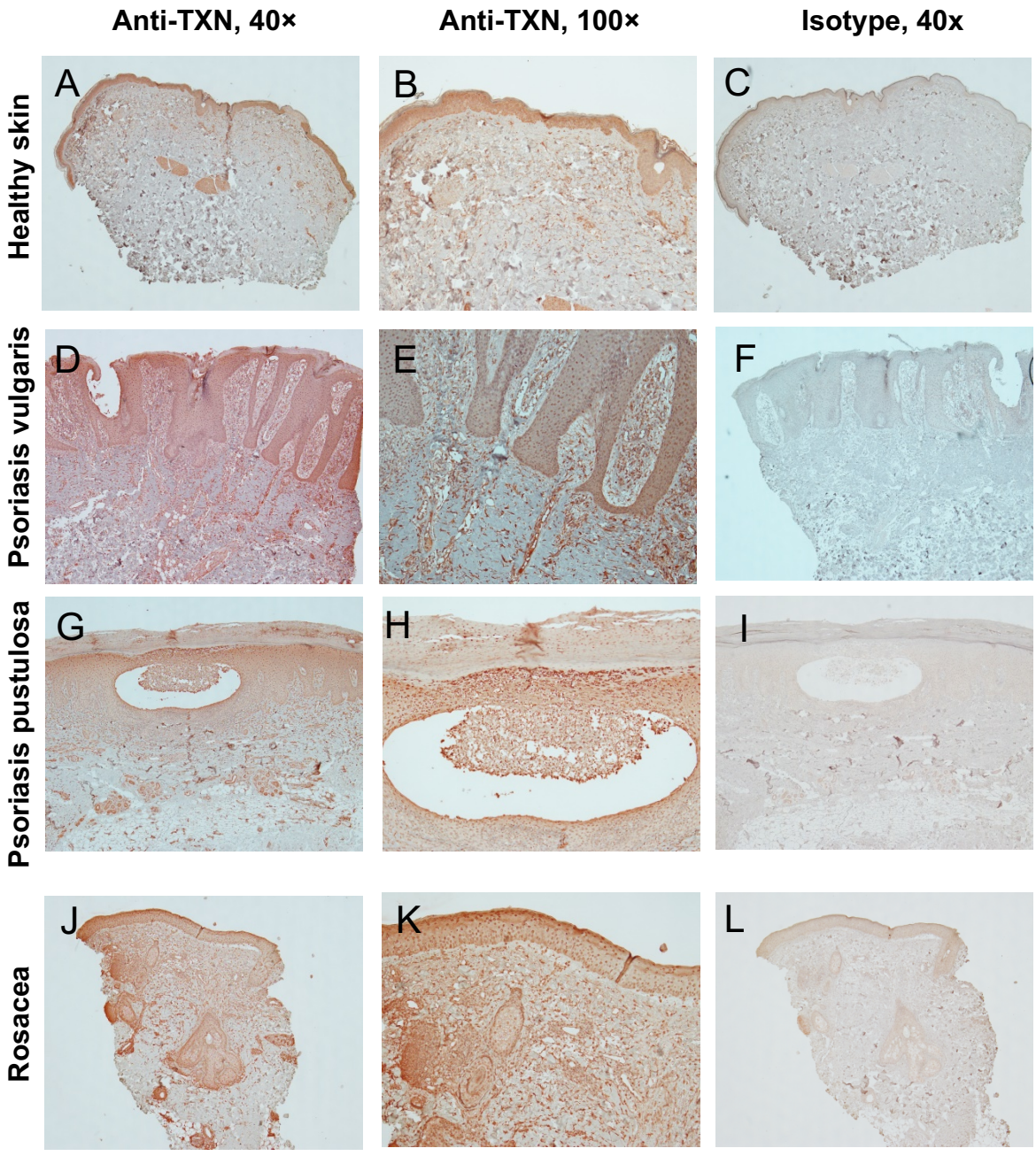

FIGURE 40: Thioredoxin staining via IHC in skin diseases in comparison to healthy skin. The first column represents the staining with an anti-TXN-antibody at a magnification of 40, the second column shows anti-TXN at a magnification of 100, while the last column shows images of the isotype control (Magnification: 40×). A-C) healthy skin, D-F) psoriasis vulgaris, G-I) psoriasis pustulosa and J-L) rosacea. Representative pictures are shown.

3.6.2 Infectious disease association

As just reported, we found an extremely upregulated expression of *TXNRD1* in sarcoidosis together with a significant upregulation of *TXN*. We then also investigated this gene expression in tuberculosis. Here we found significant upregulated gene expression of *TXN* (P= 0.0001) in tuberculosis lymph nodes compared to healthy lymph nodes (*Fig. 41A*). For *TXNRD1* we also found an upregulation in the tuberculosis lymph nodes (P= 0.0051) (*Fig. 41B*).

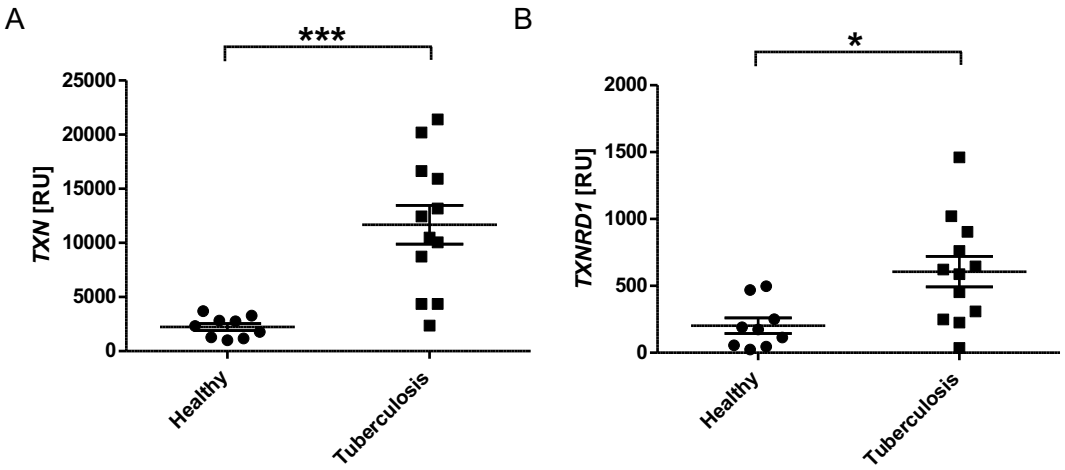

FIGURE 41: TXN and TXNRD1 gene expression in tuberculosis lymph nodes. A) TXN gene expression in tuberculosis lymph nodes (n=9) compared to healthy lymph nodes (n=12). B) TXNRD1 gene expression. Data depicted in relative expression units compared to 18S. Statistical analysis was done using Mann Whitney *U* test and the significances are depicted as * equals $P \leq 0.05$.

Also here, the TXN protein expression was investigated via IHC. Looking at sarcoidosis (*Fig. 42D-F*), a homogenous staining throughout the section was observed. Looking at lymph nodes from healthy donor (*Fig. 42G-I*) and TB sample (*Fig. 42J-L*), no difference in staining could be observed.

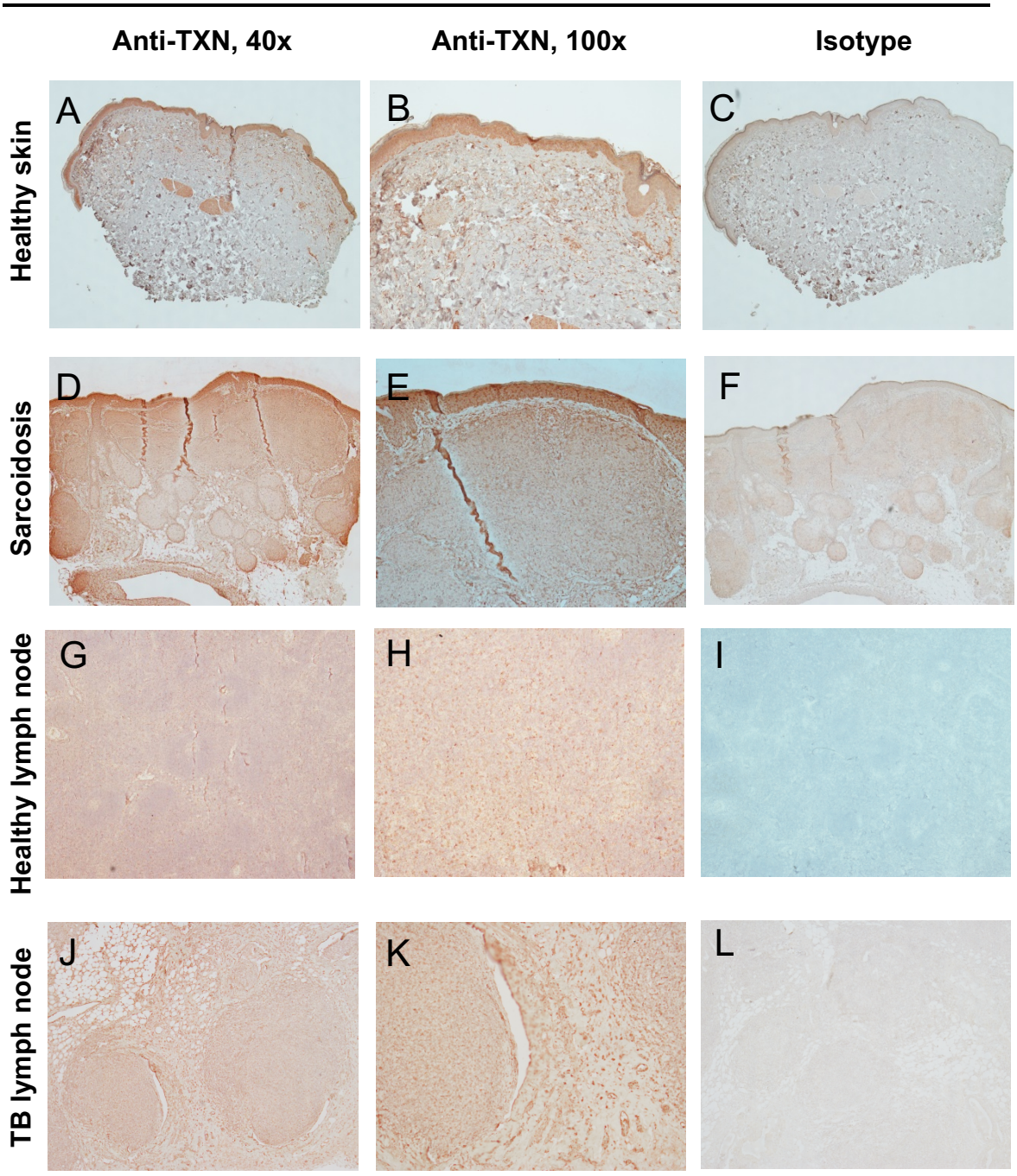

FIGURE 42: TXN protein expression in tuberculous diseases in comparison to healthy skin or healthy lymph node. The first column represents the staining with anti-TXN at a magnification of 40, the second column shows anti-TXN at a magnification of 100, while the last column shows images of the isotype control (Magnification: 40×). A-C) healthy skin, D-F) sarcoidosis, G-I) healthy lymph node and J-L) TB lymph node. Representative pictures are shown.

3.7 Disulphide bond reduction

3.7.1 Physiological reduction of IL-26

We next investigated if the physiological redox system, namely the thioredoxin (TXN) system, is indeed able to reduce of IL-26 *in vitro*. To show this a NADPH,

consumption assay as described by Holmgren *et al.*[193] was performed (*Fig. 43*). In this assay, the consumption of reduction of NADPH to NADP was measured by a decrease of the absorbance at 340 nm. As used and described by Holmgren, insulin was used as a positive control. Furthermore, LL37, which does not have any disulphide bonds, served as a negative control, as well as the TXN system alone without any compound that could be reduced. The reduction in absorbance in the presence of insulin was clearly seen in Fig. 43A. As IL-26 showed nearly the same reduction in delta absorbance (*Fig. 43B*) it indicates that IL-26 can indeed by reduced by the TXN system. In both negative controls (TXN system and LL37; *Fig. 43C* and *D*) no decrease in absorbance was observed.

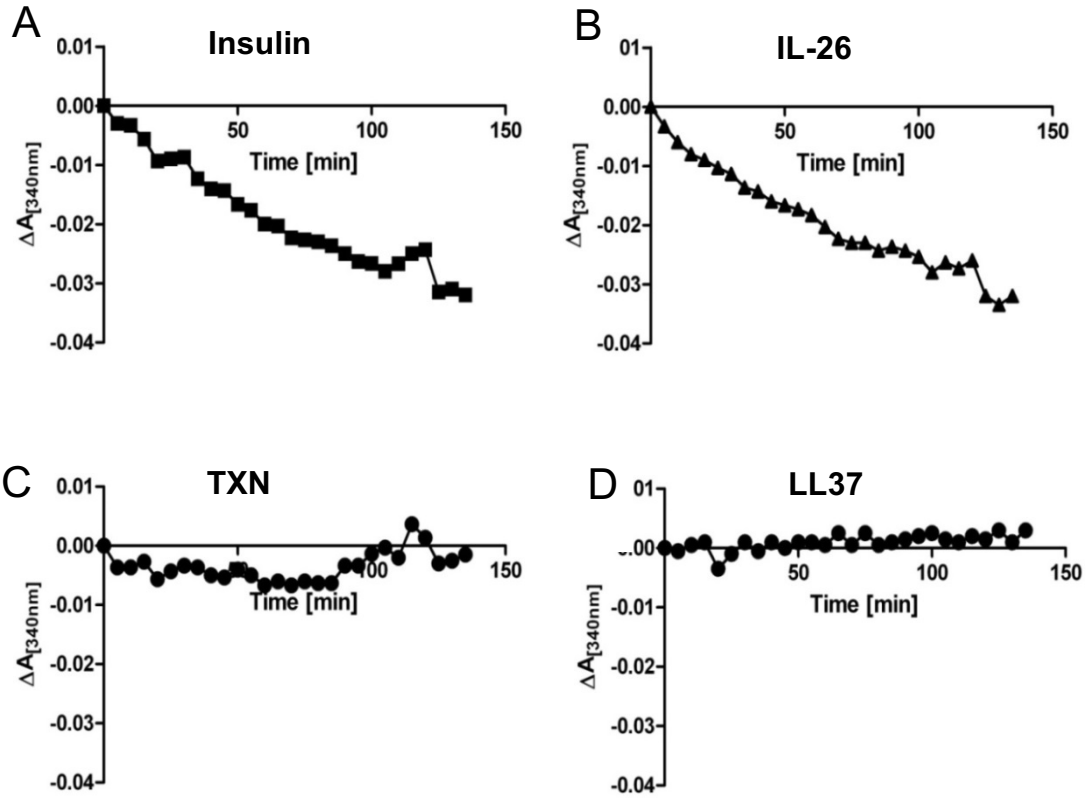

FIGURE 43: IL-26 is efficiently reduced via the TXN system. NADPH consumption assay was performed using 80 µM NADPH, 10 nM TXNRD1 and 0.2 µM TXN together with either 2.5 µM insulin (A), 2.5 µM IL-26 (B) or 2.5 µM LL37 (D). The TXN system alone (C) was used as second negative control besides LL37. NAPDH consumption is indicated with a decrease of the absorbance at 340 nm which was measured repetitively every 5 min for at least 1.5 hours. The measured values were divided by the NADPH values and adjusted to “0” as starting point. The experiment was performed three times.

3.7.2 Chemical reduction of IL-26

To obtain reduced IL-26, we incubated it with 20 mM DTT. This high concentration of DTT would negatively impact all further experiments and so the reduced IL-26 needed to be purified. Reversed phase-HPLC was used to purify highly hydrophobic IL-26 from its reductant DTT. The reduction of IL-26 with DTT resulted in an increase of hydrophobicity and thus resulted in an increased retention time in the HPLC column. This increased time is shown in Fig. 44, where oxidized IL-26 (eluted after 38.86 min, *Fig. 44A*) was compared to reduced IL-26 (eluted after 41.07 min, *Fig. 44B*). To prove that the reduction and the subsequent HPLC purification had really been successful we performed electrospray ionization mass spectrometry (ESI-MS).

Using the ExPASy protein prediction tool (http://web.expasy.org/protparam/), molecular weight was predicted for recombinant oxidized IL-26 (including N-terminal methionine) to be 17,714 Dalton and the respective molecular weight for reduced IL-26 is 17,718 Dalton. This higher weight of reduced IL-26 is due to the four additional hydrogen molecules that attach at the sulphur molecules. The hydrogen molecules have a molecular weight of one Dalton each.

Coming back to the ESI-MS data (*Fig. 44C and D*), we found that recombinant oxidized IL-26 did not at all have the predicted mass of 17,714 Dalton. Instead it has a mass of 18,018 Dalton, which is 304 Daltons higher than calculated. This effect is explained by the chemical addition of glutathione to the free cysteine residue in the oxidized form of the recombinant IL-26 (personal communication with bio-techne/RnD Systems support team). Glutathione has a molecular mass of approximately 300 Dalton, which is the weight that was not considered in the prediction. Looking at the reduced IL-26, it exactly showed the predicted mass of 17,718 Dalton and additionally no remains of oxidized IL-26 where found. Furthermore, the introduced glutathione was detached. This means the reduction using DTT as well as the purification has been successful.

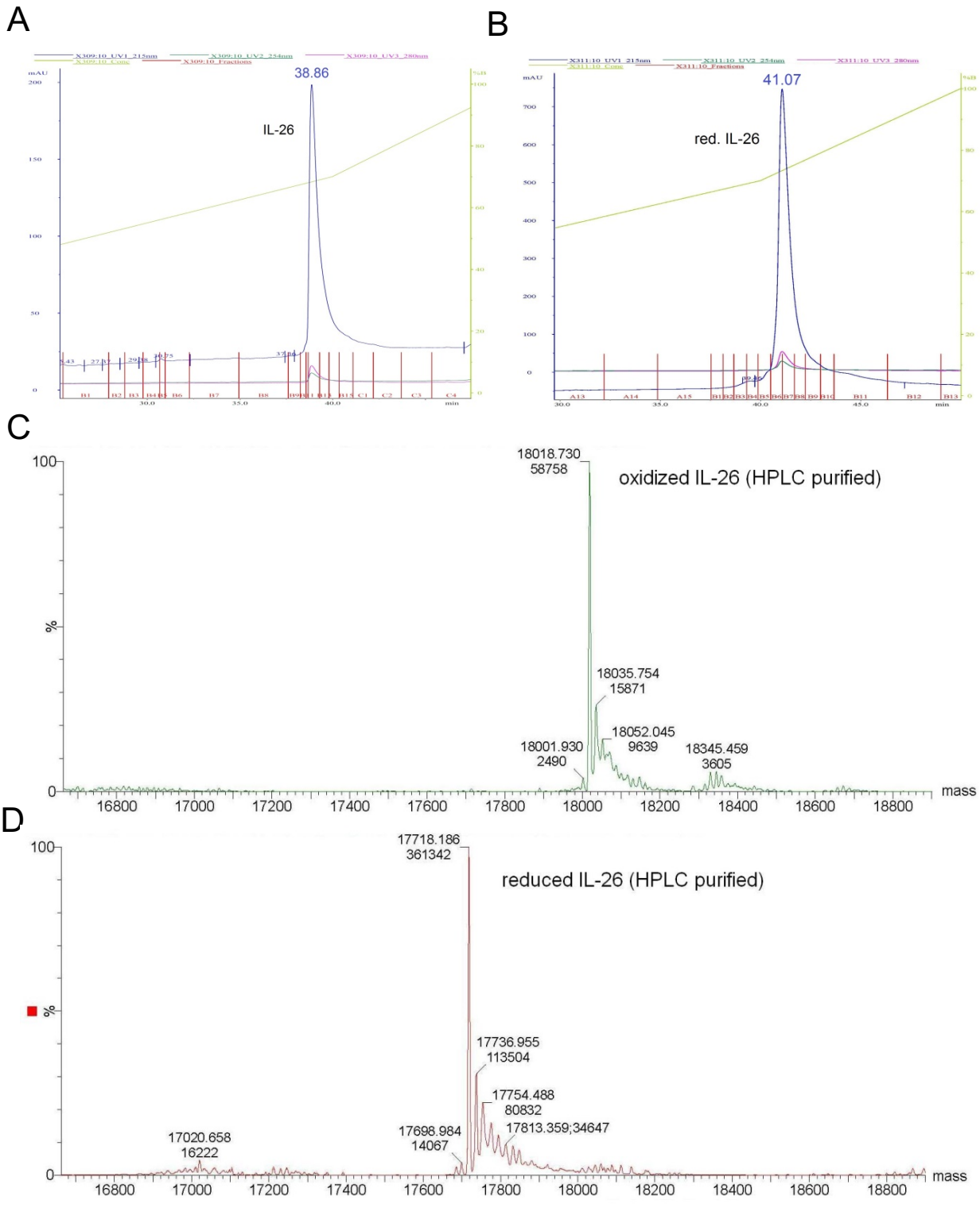

FIGURE 44: RP-HPLC was used to purify IL-26 after DTT-reduction, followed by an ESI-MS Scan to check the efficacy of the reduction. A) Oxidized IL-26 is eluted after 38.86 min and B) reduced IL-26 is eluted approx. 2 min later. C, D) The efficiency of reduction was subsequently evaluated with ESI-MS. C) Oxidized IL-26 and D) reduced IL-26.

The possible change of IL-26 in secondary structure after reduction was investigated using circular dichroism (CD). The results of these CD measurements are depicted in *Fig. 45*. Oxidized IL-26 is shown in black, while reduced TCEP-reduced IL-26 is shown in red. The reason for using TCEP for reduction in CD measurements instead of DTT was due to the fact that DTT interfered negatively with the measurements. Oxidized IL-26 showed a clear α-helical structure as predicted. Reduced IL-26 showed a structure changed from α-helical towards a more “open” protein. As it is clearly seen, the protein did not change its structure drastically and can still be considered to have an α-helical structure.

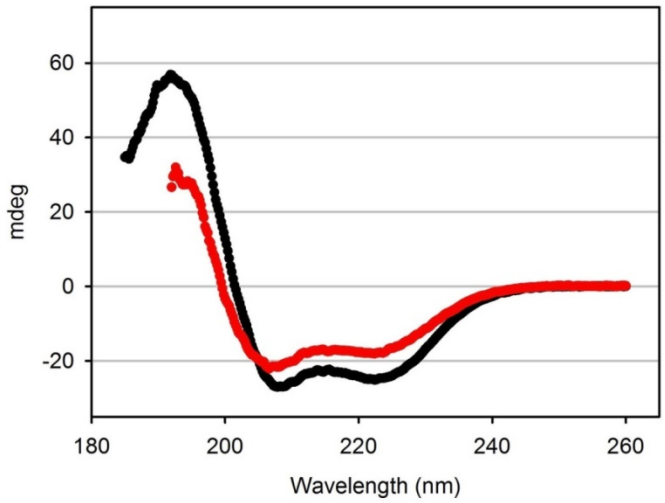

FIGURE 45: Investigations on the secondary structure of IL-26 after reduction were done using circular dichroism (CD). Depicted in black is the oxidized IL-26 (black line) and IL-26 (red line) after reduction with TCEP (10 mM).

3.8 Reduced IL-26 in adaptive immunity

3.8.1 Reduced IL-26/DNA binding

The ability of IL-26 to bind nucleic acids has been demonstrated in chapter 3.3.2, and the binding to DNA is explored in Meller *et al.*[19] using the nucleic acid condensation assay (*see also figure 47*).

We are now exploring whether the reduction of IL-26, and the accompanying change in protein structure, might improve or worsen the capacity of IL-26 to bind DNA RNA. Therefore we objected a serial dilution of reduced or oxidized IL-26 to a constant amount of 10 nM FAM-labelled single-stranded DNA (ssDNA) or double-stranded DNA (dsDNA). Oxidized IL-26 bound to both types

of DNA in the low micromolar range (*Fig. 46 and Table 12*). Reduced IL-26 bound much better to both types of nucleic acids (*Fig. 46A/B*) compared to the oxidized IL-26. Considering dissociation constants, reduced IL-26 bound about 100-times better to ssDNA and about 1,500-times better to dsDNA than oxidized IL-26 (*Table 12*). Reduced IL-26 bound similarly well to RNA as compared to dsDNA with a dissociation constant of about 1 nM (*Table 12*). Also here there was a large difference between the binding of reduced and oxidized IL-26 to RNA (*Fig. 46C*).

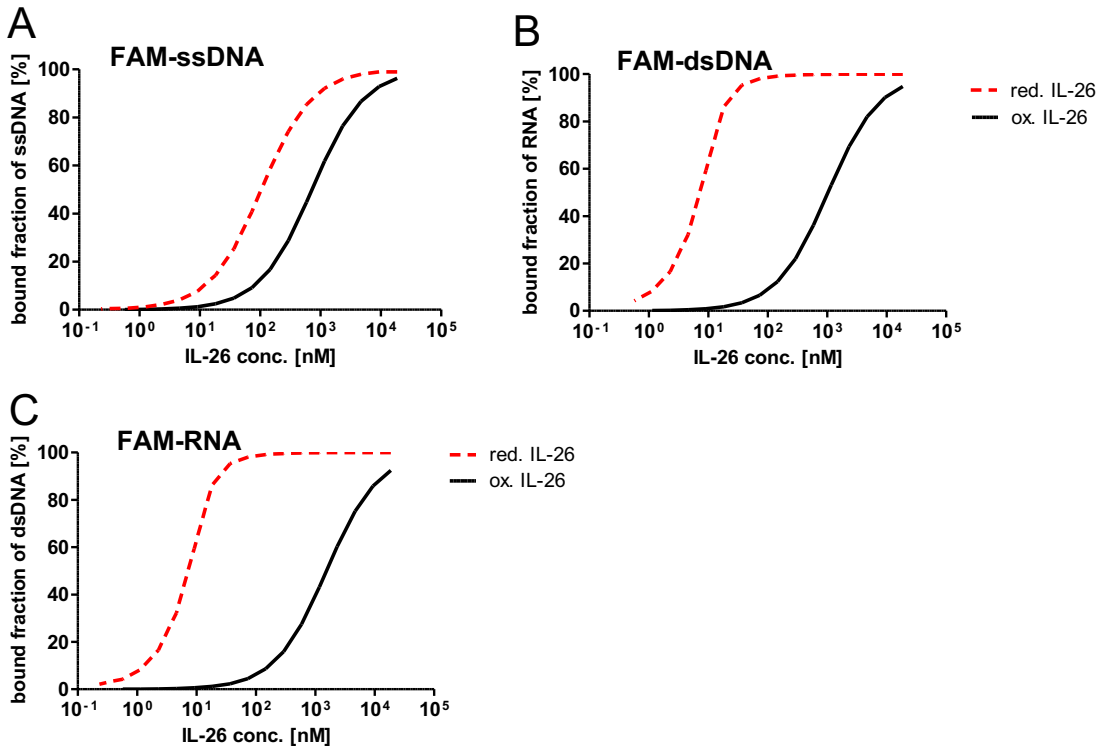

FIGURE 46: Reduced IL-26 shows high affinity to double and single stranded DNA we well as RNA as measured with microscale thermophoresis. A constant amount of 10 nM DNA or RNA was added to serial dilution of reduced or oxidized IL-26, incubated for 15 min and measured. Graphical depiction of bound fractions of ssDNA (A), dsDNA (B) or RNA (C) to either reduced or oxidized IL-26.

The exact dissociation constants for the binding of reduced IL-26 to DNA or RNA are found in *table 12*.

TABLE 12: Dissociation constants (K_D) of ssDNA, dsDNA or RNA binding.

Protein/ligand	**IL-26/DNA (ss)**	**Red. IL-26/DNA**
K_D (mean ± SD)	0.750 µM ± 0.059	80.2 nM ± 0.937
Protein/ligand	**IL-26/DNA (ds)**	**Red. IL-26/DNA**
K_D (mean ± SD)	1.54 µM ± 0.115	1.0 nM ± 0.368
Protein/ligand	**IL-26/RNA**	**Red. IL-26/RNA**
KD (mean ± SD)	1.03 µM ± 0.0556	1.0 nM ± 0.794

The findings of the MST binding experiments were confirmed using a Nucleic Acid Condensation Assay (*Fig. 47A*). Briefly, in this assay different concentrations of IL-26 were first incubated with or without 2 mM DTT before a constant amount of DNA was added for a certain time (see Material and Methods, paragraph 2.11). After the incubation time, the specific DNA dye PicoGreen dye was added and the fluorescence was measured a few minutes later. In dilutions were IL-26 was able to bind and complex DNA, the PicoGreen dye was excluded resulting in a low fluorescence detection. A clear DNA binding was observed in samples with 2 µM and 1.5 µM IL-26 for both non-reducing and reducing conditions. Under reducing conditions, in the presence of 2 mM DTT, DNA binding was observed down to an IL-26 concentration of 0.6 µM. This was a 2.5-times improved binding under reduced conditions compared to non-reducing conditions. DTT itself did not affect the fluorescence detection even at very high concentrations (*Supplemental Fig. 9*). Looking at the MST results with the 10-times difference for reduced versus oxidized IL-26/ssDNA binding or the 1000-times higher affinity when comparing reduced and oxidized IL-26 and the binding to dsDNA, one might expect greater differences in nucleic acid condensation assay but these differences might be due to the experimental setup and the differences in the used DNA.

The findings of the RNA binding assay could not be confirmed using a Nucleic Acid Condensation Assay (*Fig. 47B*). Here the assay was performed analogously to the one with DNA, but instead of PicoGreen dye, a specific RNA dye namely RiboGreen was added.

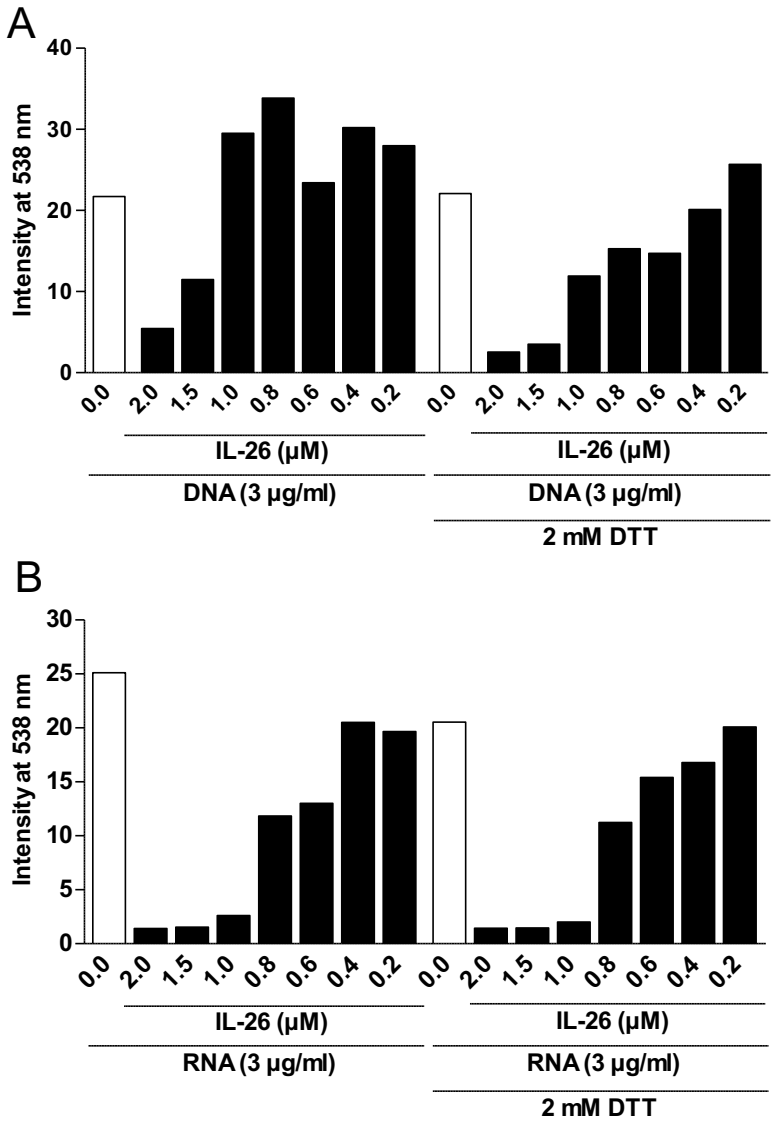

FIGURE 47: Reduction improves IL-26 binding to DNA, but not RNA binding when using a nucleic acid condensation assay. A dilution of IL-26 was incubated with or without 2 mM DTT before the addition of DNA (A) or RNA (B). After another 30 min of incubation PicoGreen dye (for DNA) or RiboGreen dye (for RNA) was added and the fluorescence at 538 nm was measured. White bars display DNA or RNA only and black bars where IL-26 was added. Mean values are depicted (A, n=3-4; B, n=2).

3.8.2 Effects of reduction on monocytes and macrophages

3.8.2.1 Induction of cytokines and chemokines

In order to generate and maintain reducing conditions we added 2 mM DTT to the cell culture prior to the addition of reduced IL-26. The presence of 2 mM DTT did not affect cell viability in primary macrophages, but viability of THP1 macrophages appears to be decreased in a dose dependent manner (*Supplemental figure 10*).

In a pilot experiment, it was seen that the addition of 2 mM DTT completely blocks TNF-α secretion in all samples except the positive control (*Fig. 48*). The TNF-α secretion in the DTT-treated positive control was about 24-times less than in LPS-treated macrophages under standard conditions (*Fig. 48*).

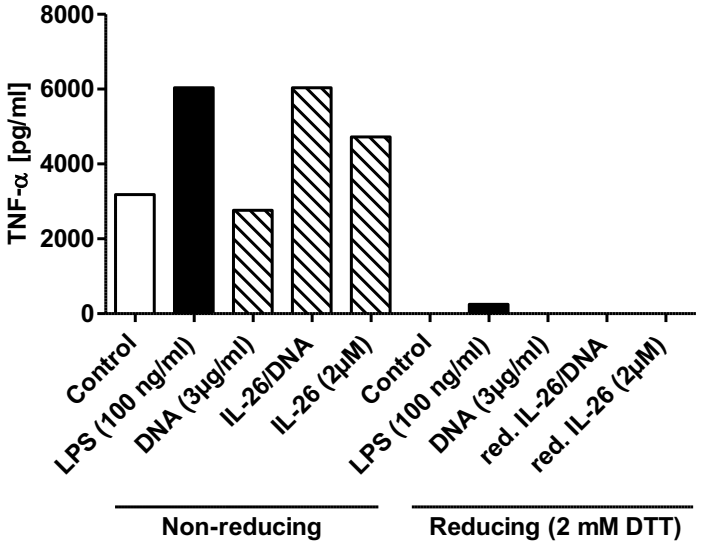

FIGURE 48: Primary macrophages respond to reducing conditions a complete block of TNF-α secretion. Macrophages were kept under standard conditions (non-reducing) or with 2 mM DTT to simulate reducing conditions. Then the stimulants LPS, DNA and reduced or oxidized IL-26 with or without complexed DNA were added and incubated for 24h. The harvested supernatants were subjected to TNF-α ELISA (n=1).

Interestingly, gene expression in these primary monocyte-derived macrophages was not as drastically affected as cytokine secretion. When looking at chemokines such as *CCL20* (*Fig. 49A*), *CXCL2* (*Fig. 49B*), and *CXCL8* (*Fig. 49C*), increased expression under reducing conditions was found in macrophages treated with IL-26 alone. The baseline expression levels of these chemokines in untreated controls cells were similar in non-reducing and reducing conditions. In contrast, a strong decrease of the expression of all tested chemokines was found under reducing conditions in response to LPS.

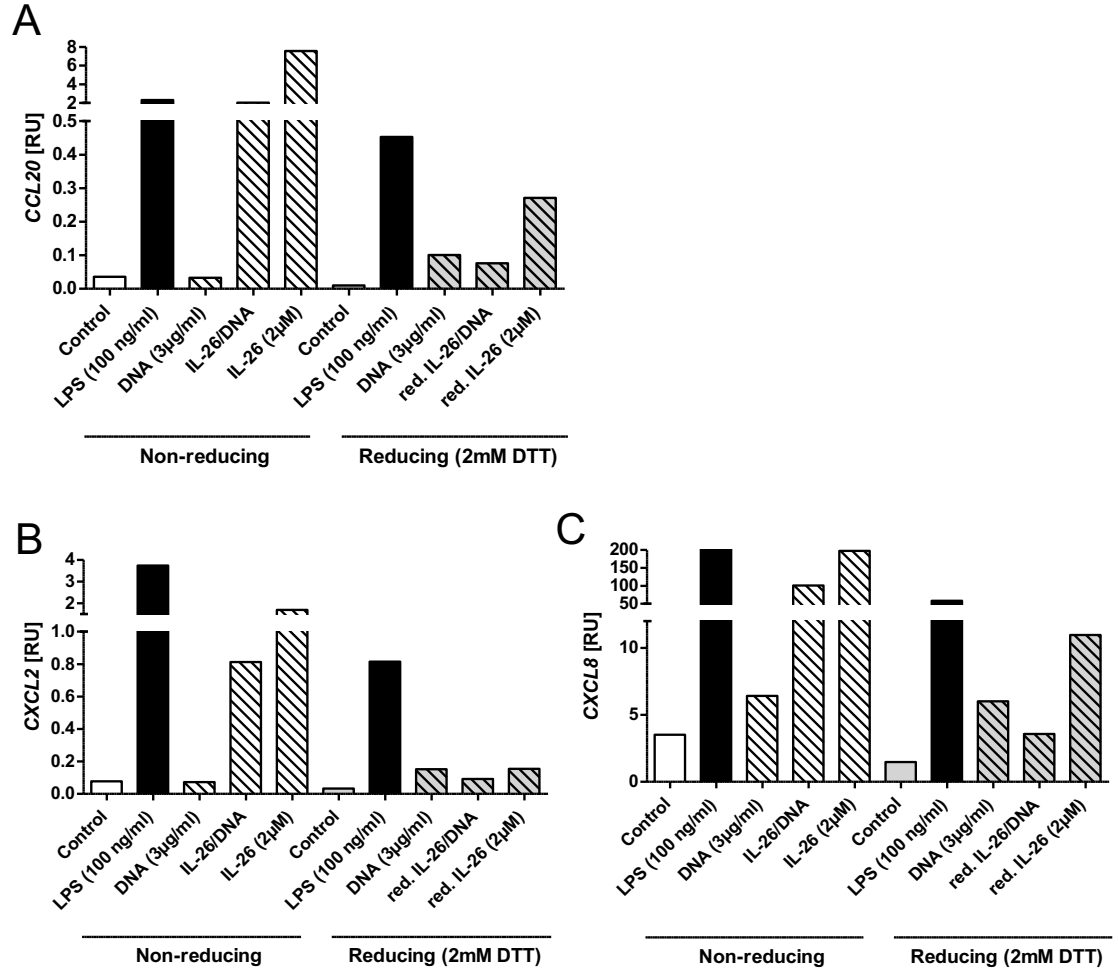

FIGURE 49: Chemokine gene expression in primary macrophages is down-regulated in the positive control. Gene expression of *CCL20* (A), *CXCL2* (B) and *CXCL8* (C) was analyzed via qPCR in primary macrophages in presence or absence of 2 mM DTT. Values depicted as relative units compared to 18 ribosomal gene (n=1).

3.8.2.2 Induction of cytokine and chemokines under hypoxia

Simulating reducing conditions using 2 mM DTT has some severe drawbacks as displayed in the previous chapter.

As there is a relation between reducing conditions and hypoxia, we went on to simulate reducing conditions by incubating the cells under hypoxic conditions (1% O_2) compared to normoxic conditions with about 20% O_2.

Hypoxia, in contrast to DTT-mediated reduction, did not block cytokine secretion (*Fig. 50*). $CD14^+$ monocytes responded with the same amount of cytokine secretion after LPS treatment regardless if they have been cultured under normoxic or hypoxic conditions (*Fig. 50*). IL-1β secretion was lower under hypoxic conditions in presence of reduced IL-26 in complex with DNA as

compared to standard conditions and oxidized IL-26/DNA complexes. When looking at IL-26 alone, the IL-1β secretion was somewhat higher when monocytes were stimulated with reduced IL-26 under hypoxia (*Fig. 50*).

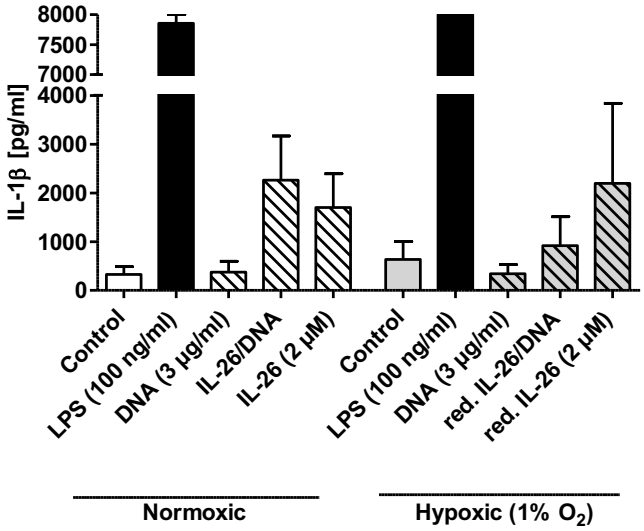

FIGURE 50: CD14$^+$ monocytes secrete less IL-1β in response to red.IL-26/DNA complexes in hypoxia. CD14$^+$ monocytes were isolated from buffy coat, stimulated with oxidized or reduced IL-26 or IL-26/DNA complexes. The cell culture was then incubated either in normoxic (20% O2) or hypoxic (1% O2) conditions. Supernatants were collected after 24h of incubation and the IL-1β secretion was evaluated via ELISA (n=3).

A key molecule in hypoxia is the hypoxia-inducible factor 1 alpha (HIF1α). Therefore, we investigated its expression in monocytes under both normoxic and hypoxic conditions. *HIF1A* was induced by IL-26 and IL-26/DNA complexes even under standard normoxic conditions (*Fig. 51*). The *HIF1A* levels reached in presence of IL-26 and IL-26/DNA complexes under standard treatment are a little higher as in hypoxia. Furthermore, treatment with reduced IL-26 alone resulted in less *HIF1A* gene expression as compared to oxidized IL-26 under standard conditions (*Fig. 51*).

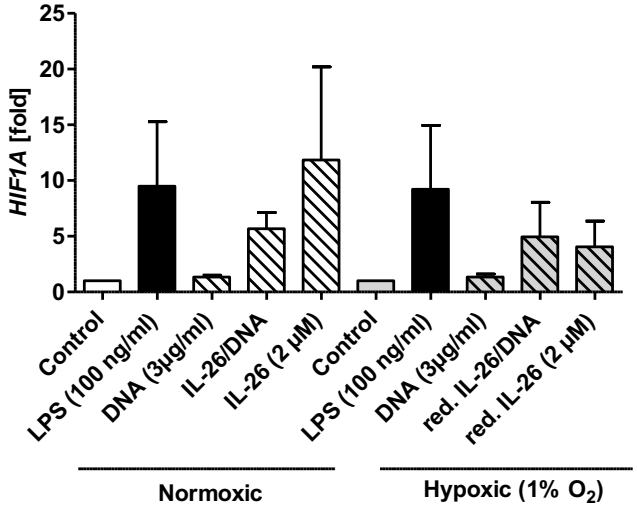

FIGURE 51: *HIF1A* expression is increased in CD14$^+$ monocytes after IL-26 and IL-26/DNA stimulation under normoxic and hypoxic conditions. Monocytes were stimulated with oxidized or reduced IL-26 or IL-26/DNA complexes. *HIF1A* gene expression was analyzed after 24h of cell incubation and displayed as fold increase of relative units (RU) compared to 18 ribosomal reference gene and to the respective untreated control (n=3).

The results from primary macrophages under hypoxic conditions were more evident: TNF-α secretion in response to LPS were similar in macrophages cultured under hypoxic or normoxic conditions (*Fig. 52*). Under standard conditions a strong secretion of TNF in presence of both IL-26 and IL-26/DNA complexes was seen (*Fig. 52*). This was in strong contrast to the hypoxic conditions where reduced IL-26 and reduced IL-26 in complex with DNA did not enhance TNF-α secretion (*Fig. 52*).

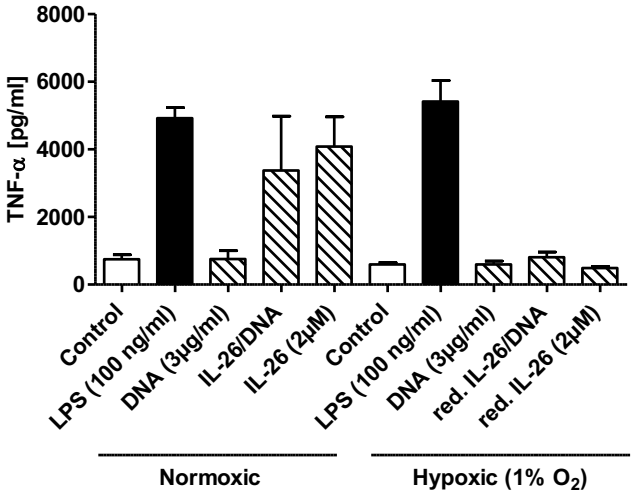

FIGURE 52: Primary macrophages do not respond to reduced IL-26 and reduced IL-26/DNA complexes under hypoxia. TNF-α secretion in primary macrophages that were kept under standard conditions (normoxic) or hypoxic conditions (1% O_2) and stimulated with LPS, DNA and reduced or oxidized IL-26 with or without complexed DNA were measured via ELISA (n=2).

3.8.3 Effects of reduction on moDCs

3.8.3.1 Induction of cytokines and chemokines under hypoxia

Seeing an improved binding of reduced IL-26 to RNA, we aimed to prove this effect *in vitro*. Here, we stimulated moDCs with IL-26/RNA complexes and IL-26 alone under hypoxic conditions and compared TNF-α and IL-6 secretion to the same cells that were kept under normoxic conditions. In our pilot experiments, we found that TNF-α secretion in moDCs was down-regulated in presence of reduced IL-26 under hypoxia (*Fig. 53A*). Investigating IL-6 we saw an increased secretion when moDCs were treated with reduced IL-26/RNA complexes in comparison to oxidized IL-26/RNA complexes (*Fig. 53B*). As an increased IL-6 secretion was already detected at baseline level, this finding needs to be reconsidered after investigating an increased number of experiments.

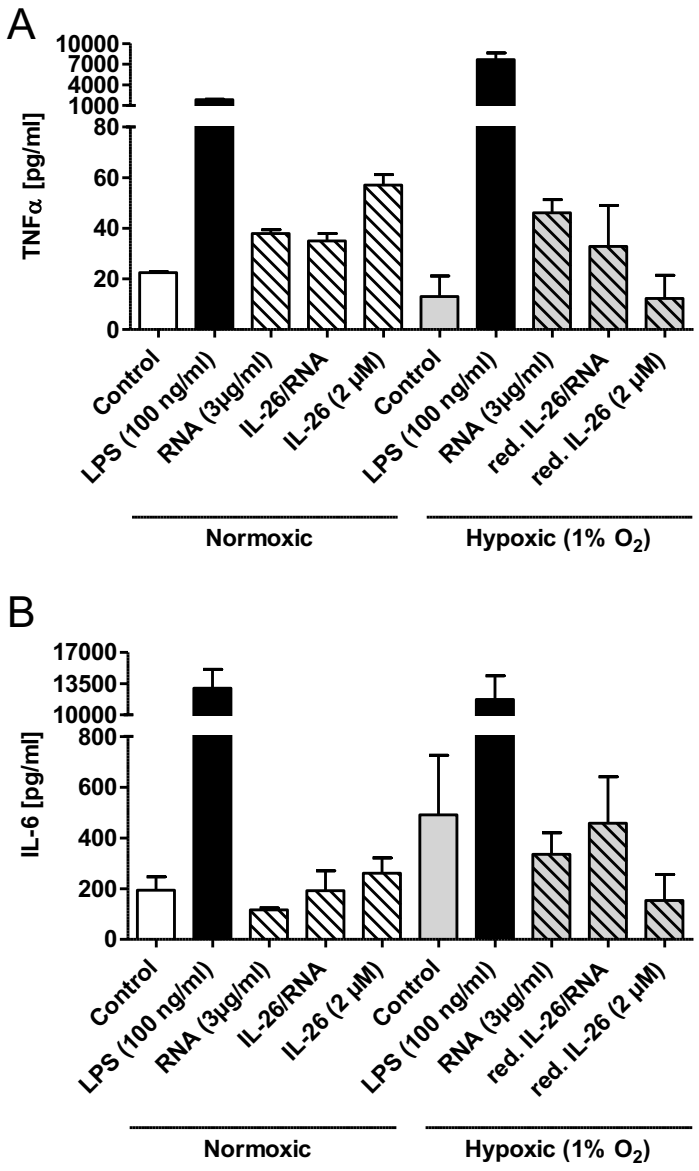

FIGURE 53: MoDCs tend to elicit a decreased response to IL-26 under hypoxia. TNF-α secretion (A) and IL-6 (B) in moDCs that were kept under standard conditions (normoxic) or hypoxic conditions (1% O_2) and stimulated with LPS, RNA and reduced or oxidized IL-26 with or without complexed RNA were measured via ELISA (n=2).

Having found that IL-26 leads to increased chemokine receptor CCR7 expression in moDCs (*Fig. 25*), we investigated how this is affected by reduced IL-26 and reduced IL-26/RNA complexes under hypoxia. Hypoxia, in general, led to a lower *CCR7* gene expression as response to LPS (*Fig. 54*). Baseline *CCR7* expression levels in untreated control cells were comparable between normoxia and hypoxia. Interestingly, the increased *CCR7* expression that was found in IL-26-treated moDCs under standard conditions was strongly diminished in moDCs treated with reduced IL-26 under hypoxia (*Fig. 54*).

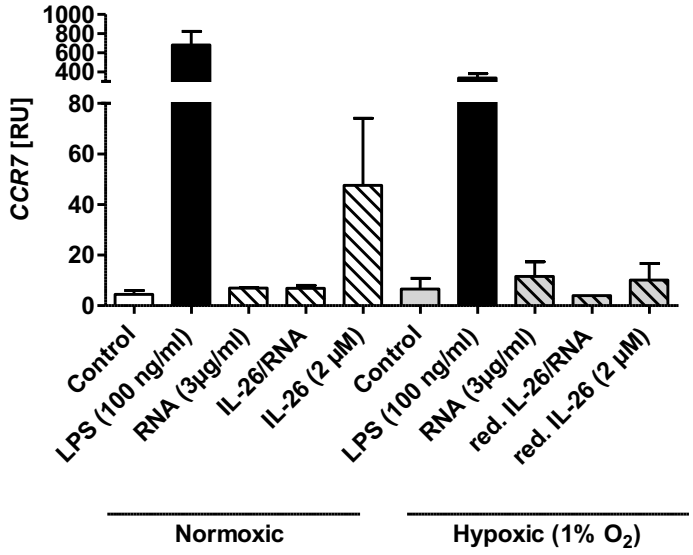

FIGURE 54: *CCR7* expression in moDCs as response to IL-26 is blocked under hypoxic conditions. MoDCs were incubated under standard conditions (normoxic) or hypoxic conditions (1% O_2) and stimulated with LPS, RNA and reduced or oxidized IL-26 with or without complexed RNA. Relative *CCR7* gene expression values are shown compared to the 18S ribosomal gene in moDCs under standard and hypoxic conditions (n=2).

3.8.4 Disease association of hypoxia-inducible factor

As hypoxia is linked to disulphide bond reduction[134] and seen in different diseases especially cancers[132], we investigated the gene expression of the major hypoxia factor, HIF1α, in more detail relative to the different skin diseases. We found that *HIF1A* was significantly increased in psoriasis vulgaris and mycosis fungoides (*Fig. 55A*). Performing a Mann Whitney *U* test, a significant increase from control samples to rosacea can also be reported. Looking at skin disease that did not show an increased *IL26* gene expression, a significant induction of gene expression of *HIF1A* was found in squamous cell carcinomas (*Supplemental figure 11*). Comparing *HIF1A* gene expression in tuberculosis lymph nodes to healthy lymph nodes also revealed a significantly higher gene expression (p= 0.0428 calculated with Mann-Whitney *U* test) (*Fig. 55B*).

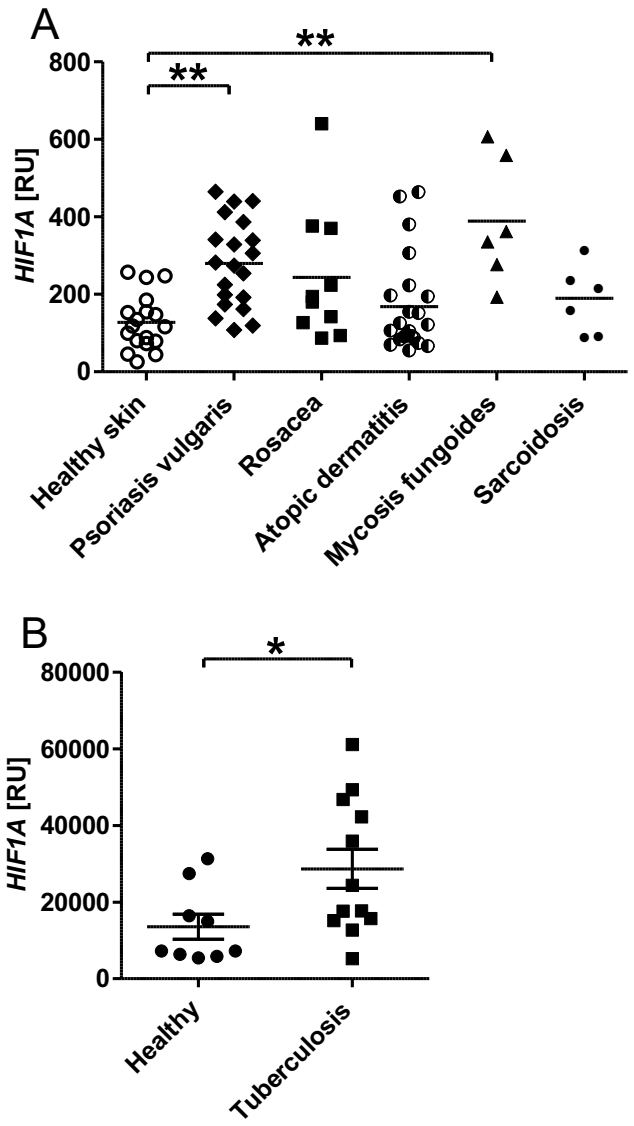

FIGURE 55: *HIF1A* gene expression in different diseases and healthy controls. A) relative gene expression of *HIF1A* in different skin diseases compared to healthy skin samples. B) relative *HIF1A* gene expression values compared to the 18S ribosomal gene in healthy lymph nodes and tuberculosis lymph nodes. Data were analyzed using Kruskal-Wallis test with Dunn's posttest or Mann-Whitney *U* test for tuberculosis. Statistical significances are as follows; ** equals $P \leq 0.01$.

Considering possible gene expression correlation in psoriasis, we found that gene expression levels of *IL26* and *HIF1A* positively correlated (Spearman correlation value 0.47) with a strong trend towards significance (p-value 0.0658) (*Fig. 56A*). Further, a correlation analysis between *HIF1A* and *TXN* (*Fig. 56B*) and *HIF1A* and *TXNRD1* (*Fig. 56C*) in our psoriasis cohort was performed. The expression levels of *HIF1A* and *TXN* correlated significantly and positively with

a calculated p-value of 0.0350 and a Spearman rho of 0.53 (*Fig. 56B*). For *TXNRD1* and *HIF1A*, a slightly positive but not significant correlation was seen (*Fig. 56C*), with Spearman value of 0.36.

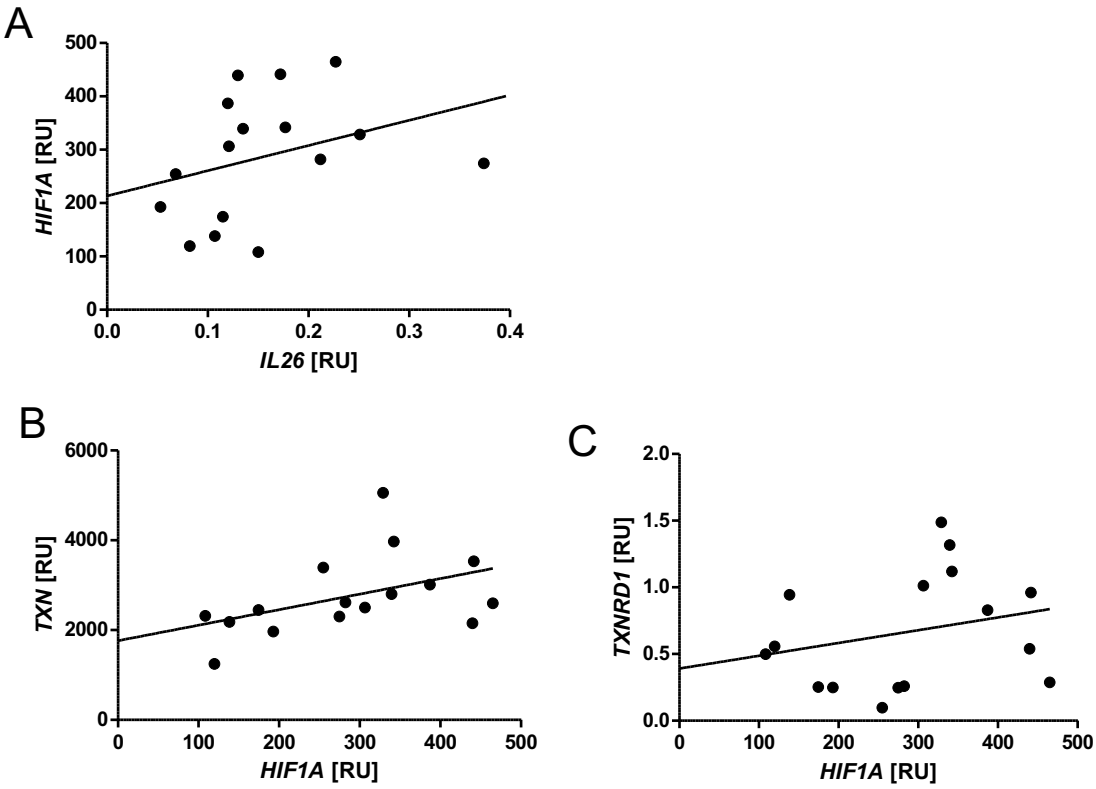

FIGURE 56: Correlation between *IL26*, *HIF1A*, *TXN* and *TXNRD1* gene expression in psoriasis vulgaris. A) *IL26* and *HIF1A* gene expression correlates positively in psoriasis. B,C) *TXN* and *TXNRD1* expressions correlate with *HIF1A* expression in psoriasis. Data were analyzed using Spearman correlation analyzes together with two-tailed Student's t test.

3.9 Reduced IL-26 in innate immunity

3.9.1 Antibacterial properties

3.9.1.1 Reduced IL-26/bacterial component binding

We found that oxidized IL-26 binds both FITC-labelled LPS and Alexa488-labelled LTA (*Fig. 57*). Reduced IL-26 showed higher affinity towards LPS and LTA compared to oxidized IL-26 (*Fig. 57A and B*). Reduced IL-26 bound about twice as well to LPS compared to oxidized IL-26, while the binding of reduced IL-26 to LTA was about 350-times better compared to oxidized IL-26 (*Table 13*). The strong affinity of reduced IL-26 to both bacterial surface components did not exceed the very strong affinity in the nanomolar range that was seen for the antimicrobial peptide LL37 (*Table 9*).

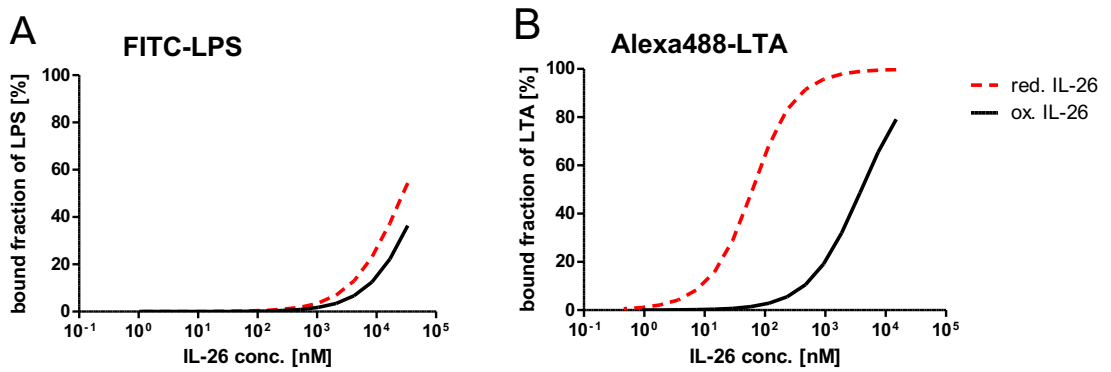

FIGURE 57: Reduced IL-26 binds much stronger to bacterial surface molecules compared to oxidized IL-26. Microscale thermophoresis (MST) was used to investigate the protein-protein interactions. The binding of IL-26 (reduced and oxidized) to LPS is depicted in A). A very big difference in binding affinities is seen for LTA (B).

The respective dissociation constants K_D for the above depicted graphs can be extracted from table 13.

TABLE 13: Dissociation constants K_D from MST measurement evaluating the binding of reduced and oxidized IL-26 to the bacterial surface components LPS and LTA.

Protein/ligand	**IL-26/LPS**	**Red. IL-26/LPS**
K_D (mean ± SD)	58.9 µM ± 2.8	28.2 µM ± 0.58
Protein/ligand	**IL-26/LTA**	**Red. IL-26/LTA**
K_D (mean ± SD)	12.5 µM ± 2.1	35.5 nM ± 0.2

3.9.1.2 Reduced IL-26/mycobacterial component binding

Lipoarabinomannan (LAM) from *Mycobacterium smegmatis* and *M. tuberculosis H37Rv* (provided by BEIResources) was fluorescently labelled with Alexa488 and then, together with reduced or oxidized IL-26, subjected to MST.

Comparing oxidized and reduced IL-26, they both bound to LAM very strongly, but it appeared as if reduced IL-26 did bind to LAM from *M. smegmatis* a little bit better, as the standard deviation was much smaller for reduced IL-26 as for oxidized IL-26 (*Fig. 58A* and *Table 14*). Very similar results were obtained when investigating the binding to LAM from *MtbH37Rv* (*Fig. 58B* and *Table 14*). As the dissociation constants between both types of LAM and both version of IL-26 differed only minimally, the graphs indicating the bound fraction were basically identical (*Fig. 58*).

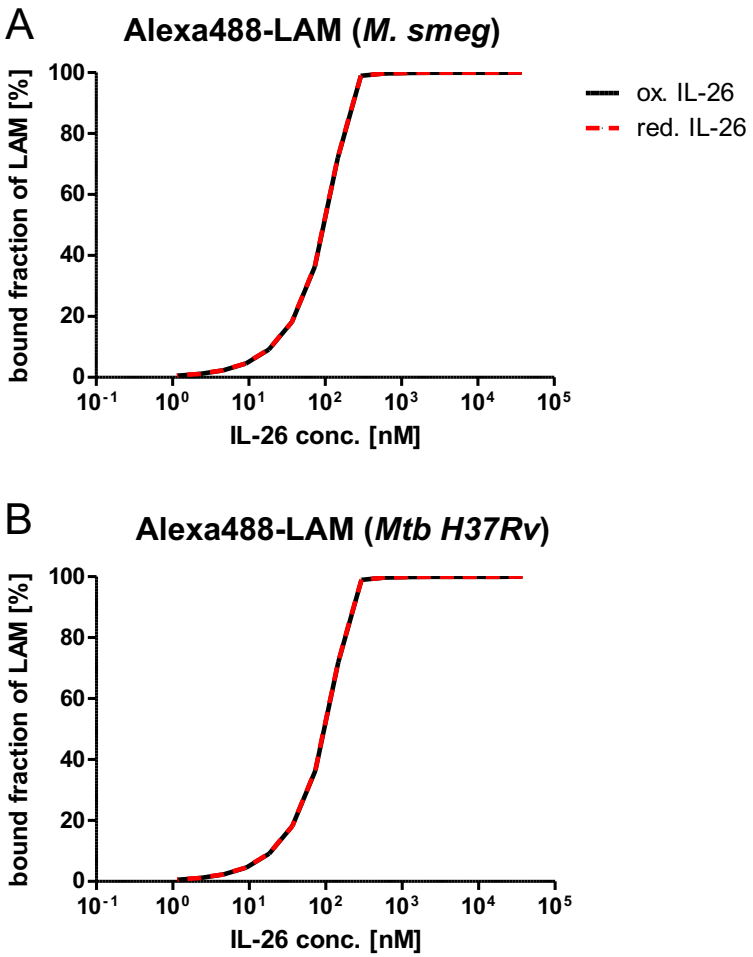

FIGURE 58: IL-26 shows high affinity to lipoarabinomannan (LAM) protein as measured with microscale thermophoresis. Graphical depiction of bound fractions of LAM from *M. smegmatis* (A) or *M. tuberculosis H37Rv* (B) to either reduced or oxidized IL-26.

The respective dissociation constants for oxidized or reduced IL-26 to the different LAMs are displayed in table 14, where the mean dissociation constants together with the standard deviation are shown.

TABLE 14: Dissociation constants K_D from MST measurement evaluating the binding of reduced and oxidized IL-26 to the mycobacterial surface components LAM from *M. smegmatis* and *Mtb H37Rv*.

Protein/ligand	**IL-26/LAM *Mtb***	**Red. IL-26/LAM *Mtb***
K_D (mean ± SD)	1 nM ±1.45	1 nM ± 0.000765
Protein/ligand	**IL-26/LAM *M. smeg.***	**Red. IL-26/LAM *M. smeg.***
K_D (mean ± SD)	1 nM ± 1.26	1 nM ± 0.000984

3.9.1.3 Reduced IL-26 in bacterial and mycobacterial killing

In bacteria and mycobacteria, we started off exploring their tolerance towards DTT. We found that *P. aeruginosa* was extremely sensitive to 2 mM DTT (*Fig. 59A*). Using concentrations less than 2 mM DTT seemed not to affect *P. aeruginosa* growth in this pilot experiment. Looking at *Mtb H37Rv*, a concentration of 2 mM DTT only inhibited the mycobacterial growth by about 20% (*Fig. 59B*). The minimal inhibitory concentration, where 50% of the mycobacteria are killed, is around 3 mM DTT. Generating reducing conditions using DTT did not appear to be a suitable method in both tested germs. Of note: an investigation of *P. aeruginosa* and *Mtb H37Rv* under hypoxic conditions in comparison to standard conditions could not be implemented.

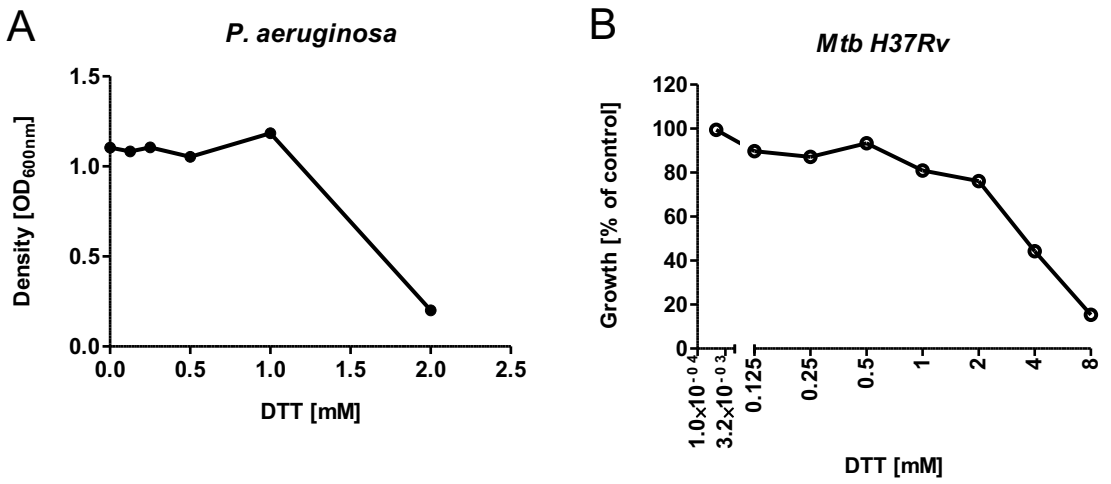

FIGURE 59: Both *P. aeruginosa* and *Mtb H37Rv* are sensitive towards DTT, but at different concentrations. A) Density of *P. aeruginosa* measured at an OD of 600nm in presence of different concentrations of DTT and incubated for 18h (n=1). B) Growth curve of *Mtb H37Rv* treated with increasing concentrations of DTT for 5 days (n=4).

3.10 IL-26 in the interface between innate and adaptive immunity

3.10.1 IL-26 scavenges and neutralizes bacterial components

As demonstrated in chapters 3.4.1.1 and 3.8.1.1, IL-26 binds to both LPS and LTA. This made us wonder if IL-26 is able to scavenge or neutralize these bacterial compounds and thereby prevent immune cells from activation. A similar feature has been reported for LL37[213,214].

We found that IL-26 indeed neutralized LPS in the sense that LPS was not able to induce maturation markers such as CD83 and CD86 on moDCs as strongly

as in absence of IL-26 (*Fig. 60A and B*). Comparing IL-26 to LL37: IL-26 neutralizes LPS to the same extent as LPS was neutralized by LL37. LPS induced CD83 induction was downregulated by a factor of about 3.5, when LPS was pre-incubated with IL-26 (*Fig. 60A*). The CD86 expression was reduced by about half when LPS was scavenged with IL-26 (*Fig. 60B*).

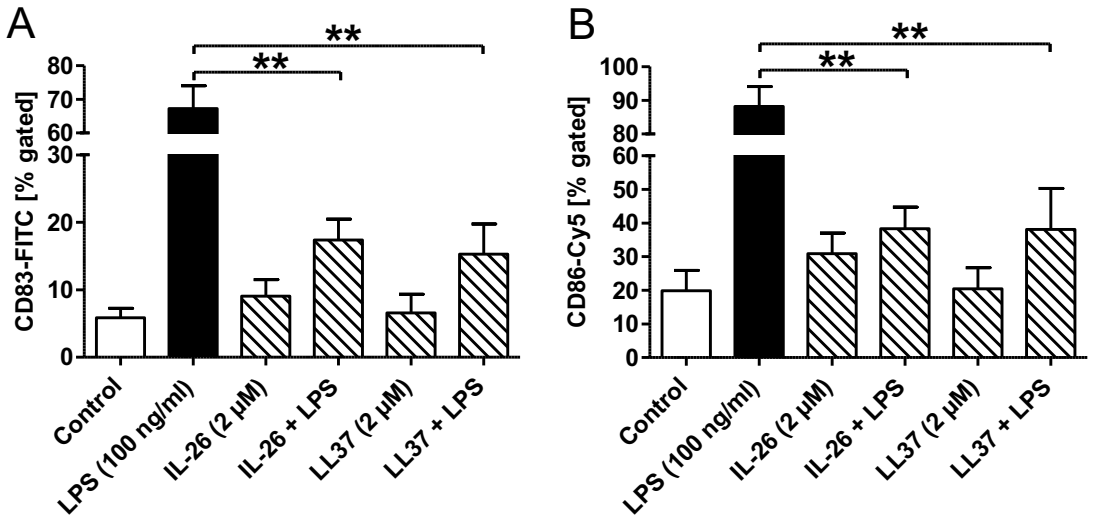

FIGURE 60: IL-26 and LL37 significantly inhibit LPS induced upregulation of both CD83 and CD86 on moDCs. IL-26 and LL37 were individually incubated together with LPS for 30 min before addition to moDC culture and incubation for 24 h. The cells were then subjected to flow cytometry analysis after surface staining with anti-CD83 and anti-CD86 antibodies. Results depicted as mean + SEM of % CD83 (A) or CD86 (B) positive cells (n=5-6). Statistical analysis was performed using Mann Whitney *U* test (** equals $p<0.01$).

Next, we investigated if the neutralization of LPS also works on chemokine receptor expression. We found that IL-26 significantly blocked the LPS induced CCR7 surface expression (*Fig. 61*). Also, a similar trend ($p=0.0667$) was seen when LPS was pre-incubated with LL37 prior to the addition to the cell culture.

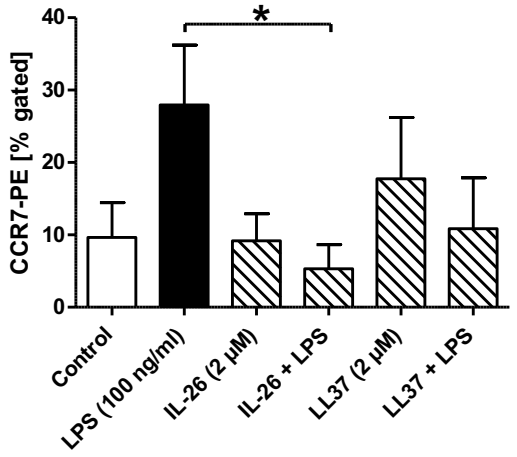

FIGURE 61: IL-26 scavenges LPS and downregulates LPS induced CCR7 expression. MoDCs were stimulated with IL-26 or LL37 which have both been pre-incubated together with LPS for 30 min before addition to the cell culture and incubated for another 24h. The cells were then stained with an antibody against CCR7 and analyzed via flow cytometry. The percentage of CCR7-positive cells were then displayed and Mann-Whitney *U* test was applied to calculate significant differences (* equals $p<0.05$) (n = 4-6).

It was additionally investigated if similar effects were seen for LTA and LAM, but these components did not induce CD83, CD86, and CCR7 to a sufficiently strong extent (*supplemental figures 12 and 13*).

We then examined if the neutralizing effect of IL-26 was also seen on secreted pro-inflammatory mediators, such as TNF-α. IL-26 and LL37 efficiently downregulated LPS or LTA induced TNF-α secretion (*Fig. 62A and B*). The downregulation of LPS induced TNF-α was close to significance ($p= 0.0571$). Mycobacterial LAM did not induce TNF-α secretion by itself on moDCs, and therefore a potential inhibition in presence of IL-26 could not be evaluated using this assay (*supplemental figure 14*).

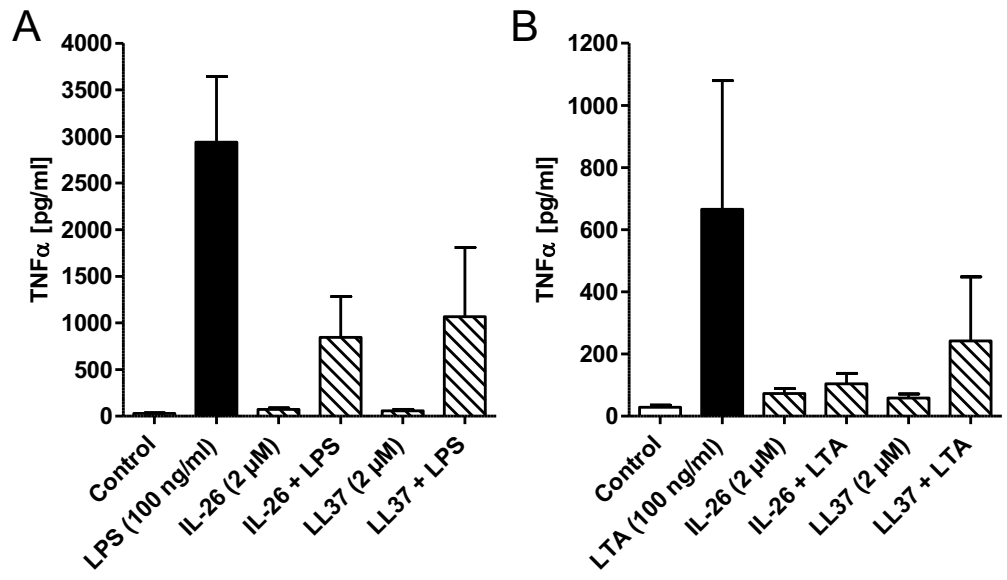

FIGURE 62: IL-26 and LL37 scavenge LPS and LTA and thereby inhibit TNF-α secretion. IL-26 and LL37 were incubated together with LPS (A) or LTA (B) for 30 min before addition to moDC culture and incubation for 24 h. The harvested supernatants were then subjected to TNF-α ELISA (n=3-4). Data depicted as mean + SEM and statistical analysis was performed using Mann-Whitney *U* test.

3.11 Feedback loop of IL-26 on immune cells

T cells, especially the subsets T_H1 and T_H17, are likely the main source of IL-26[19]. Here we show that IL-26 induced its own gene expression in monocytes, moDCs, and macrophages (*Fig. 63*). It thereby elicits potential new sources of IL-26, particularly in diseases. The gene expression of *IL26* showed a highly significant increase in $CD14^+$ monocytes after treatment with IL-26/DNA complexes and IL-26 alone (*Fig. 63A*). Also, moDCs revealed a significant increase of *IL26* gene expression in the presence of both IL-26/RNA complexes and IL-26 alone (*Fig. 63B*). Probably due to the low n-number of 3 experiments, a statistical significance was not seen (p-values for both IL-26/DNA complexes and IL-26 compared to control were 0.0536). In contrast to $CD14^+$ monocytes, an *IL26* expression was not detected in the untreated controls (*Fig. 63A* versus *63B*). Additionally, the relative gene expression was about 10-times lower in moDCs compared to $CD14^+$ monocytes. Looking at primary macrophages, a marginal increase in *IL26* gene expression after IL-26 stimulation was observed (Fig. 63C). The gene expression appeared to be highly induced in the presence of IL-26/DNA complexes. This lowest increase of *IL26* gene expression was found in THP1 macrophages when looking at relative units (*Fig. 63D*).

Furthermore, in contrast to primary macrophages, the higher gene expression levels were found in the presence of IL-26 alone, while IL-26/DNA complexes only slightly enhanced *IL26* gene expression in THP1 macrophages (*Fig. 63D*).

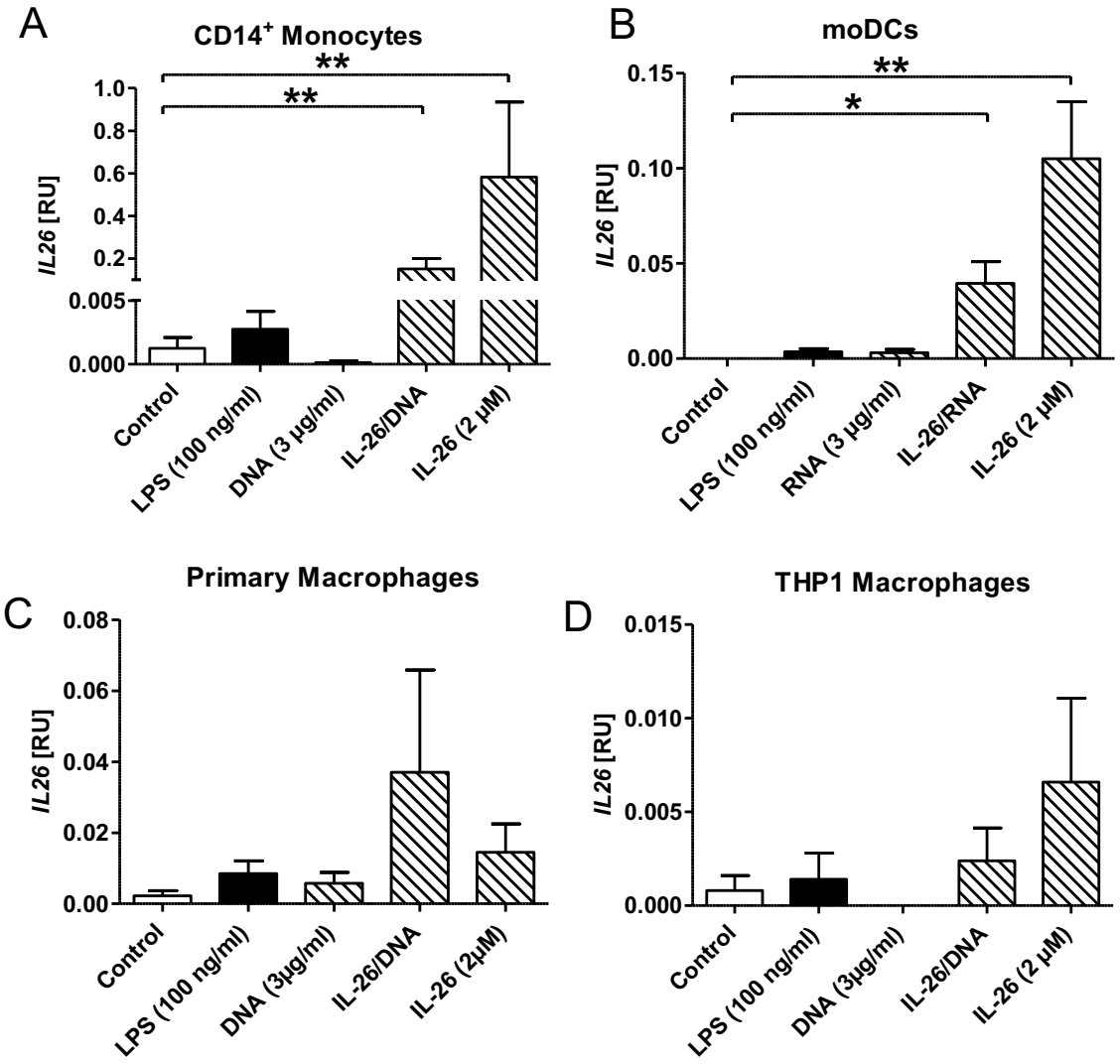

FIGURE 63: All tested immune cell types respond to IL-26 with increased *IL26* gene expression. CD14$^+$ monocytes (A, n=8), monocyte-derived DCs (moDCs) (B, n=5), monocyte-derived (primary) macrophages (C, n=4) and THP1 macrophages (D, n=5) respond to IL-26 alone and IL-26 in complex with nucleic acids with *IL26* gene expression after 24h stimulation. QPCR analysis was performed to evaluate the gene expression of *IL26* using Mann-Whitney *U* test for calculation of significance (* equals $p<0.05$, ** equals $p<0.01$).

4 Discussion

4.1 IL-26 in inflammatory and infectious diseases

We presented an increased gene expression of *IL26* for the following skin diseases: psoriasis vulgaris (PV), psoriasis pustulosa, atopic dermatitis (AD), rosacea, mycosis fungoides (MF), and sarcoidosis (*Fig. 6*). This increase in gene expression was also translated to the protein level, which we demonstrated for PV, PP, rosacea, and sarcoidosis. PV, PP as well as rosacea are chronic inflammatory diseases that are characterized by the presence of T_H17 cells[159,162,163,191]. As T_H17 cells are considered one of the main producers of IL-26[19], an increased gene expression of *IL26* in PV, psoriasis pustulosa, and rosacea is not very surprising.

The lack of *IL26* gene expression in healthy skin is consistent with the first paper describing IL-26 (previously AK155)[40] and other publications[47]. In this publication by Kunz *et al.*[47], they could not detect IL-26 in skin biopsy cells from four donors via RT-PCR.

The reported increase in *IL26* gene expression in AD is somewhat surprising as the predominant T cell type in AD are long thought to be T_H2 cells that are mainly associated with allergic reactions[172]. On the other hand, IFN-γ, the signature cytokine of T_H1 cells, has also been reported to have a role in AD[173,174]. Increased *IL26* gene expression in AD and psoriasis has already been described by Kunz *et al.*[47]. These results are in accordance with our finding. It generally suggests that IL-26 in AD is likely produced by T_H1 cells. There might even be a direct correlation between IFN-γ and IL-26 expressions as these patients as the gene for IFNG is located in close proximity to *IL26* [40] and could therefore be transcribed simultaneously. Another theory could be that the IL-26 in AD comes from T_H22 cells that are the key producers of IL-22 in AD[215]. These T_H22 that lack IL-17 production could also be the source of IL-26.

MF is a form of cutaneous T cell lymphoma (CTCL)[178,179]. There are similarities between MF and AD such as the predominance of T_H2 cells[179], the susceptibility for infections[169] and pruritus[216]. We found that *IL26* gene expression is significantly increased in MF, which is similar to our finding for AD, and surprising at first glance. As for AD, a substantial amount of IL-22,

potentially produced by T_H22 cells, has also been reported in MF[183]. The hypothesis that at least a proportion of IL-26 in AD might be produced by T_H22 cells can therefore also be applied for MF. Our data showing significantly increased *IL26* gene expression in MF patients is consistent with the literature: Wolk *et al.*[182] found that the *IL26* gene expression in MF patients is about as high as in psoriasis patients. There has also been another study by Litvinov and colleagues where *IL26* was also found to be differentially regulated between CTCL patients and controls[217]. In this large cohort study (110 patients with all sorts of CTCL at different stages and 29 controls samples with benign inflammatory dermatoses), the researchers performed a TruSeq targeted RNA expression analysis. They found that *IL26* is significantly more expressed in all CTCL samples compared to their control samples that are benign inflammatory skin diseases[217]. Due to comparably small cohort size, we cannot see a higher *IL26* gene expression when comparing MF, e.g. to psoriasis. But potentially relatable to their data, we report that the highest *IL26* gene expressions detected in our samples are found among the MF samples.

Another study investigating anaplastic large cell lymphomas that also presents a subtype of non-hodgekin T cell lymphomas found *IL26* upregulated[218]. The authors of the study analyzed further genes and concluded that the recently defined innate lymphoid cells type 3 (ILC3) might play a substantial role as originating cell types for some anaplastic large cell lymphomas. The data from our MF cohort is also in line with data found on the gene expression database Genevisible (https://genevisible.com/cell-lines/HS/UniProt/Q9NPH9). The database collects microarray samples performed with Affymetrix Human Genome U133 Plus 2.0 Array and compares their expression levels of the target protein. For *IL26* expression in cell lines, the top three cells were lymphoma cell lines, the next six cell lines were neoplastic cell lines from the nervous system, and the last (Psychiatry and Psychology) were dermal/skin fibroblast cell lines. Even though cell lines from the nervous system pop up here, an association between *IL26* and multiple sclerosis – a disease of the nervous system - has not been identified yet[219].

Looking at *IL26* expression in cancers in the Genevisible database, T cell lymphomas were again the top hit followed by Hodgekin's disease (Hodgekin

lymphomas). This is even more suitable to our data than the above displayed *IL26* expressing lymphoma cell lines as we measured *IL26* gene expression in skin biopsies *ex vivo*.

Sarcoidosis is a disease that affects multiple organs, including the skin in about one fourth of all cases[220,221]. The disease is characterized by the formation of granulomas that involve macrophages and T_H1 cells[220] as well as T_H17 cells[222]. Due to the fact that the granulomas found in sarcoidosis patients very much resemble the granulomas that are found in patients suffering from tuberculosis, sarcoidosis was for a long time falsely diagnosed as tuberculosis, and mycobacteria were thought to be the causative agent for the disease[223]. The true causative agent has not yet been found, but mycobacteria cannot be excluded completely as there are reports that demonstrate mycobacterial DNA in some of the sarcoidosis patients[224,225]. Another interesting finding linking sarcoidosis to tuberculosis is that T_H17 cells in sarcoidosis have been found to be specific for the mycobacterial antigen ESAT-6[226]. Our reported increase in *IL26* gene expression in cutaneous sarcoidosis could most likely be attributed to an increased total number of T_H17 cells in sarcoidosis[226]. Having an increased number of T_H17 cells, and thereby increased IL-17 secretion, might also be the cause for increased levels of the antimicrobial LL37 in bronchoalveolar lavage fluid from sarcoidosis patients compared to healthy controls[227].

Consulting again the Genevisible database for the *IL26* expression in different diseases, or as they call it “perturbations”, it is clearly seen that the top hits resemble our results. *IL26* is more expressed in rosacea as compared to normal skin tissue. In different psoriasis studies and cutaneous sarcoidosis studies, where lesional and non-lesional skin was compared, the lesional one always had higher *IL26* expression compared to non-lesional skin. Here it would be interesting to see the differences in expression when lesional and non-lesional skin is compared to normal healthy skin.

Looking at tuberculosis (TB) that appears to have some histological similarities to sarcoidosis, we also found increased IL-26 on both gene but also protein level (*Fig. 9*). TB is caused by *Mycobacterium tuberculosis* (*Mtb*) and in order to fight the mycobacteria the immune system generates granulomas encapsulating the intruder[228]. A role for IL-26 in TB has been described by Guerra-Laso *et al.*

who found that IL-26 might be susceptibility factor in TB[229]. A study investigating the levels of IL-10 family cytokines in plasma or lymph node supernatants in patients suffering from tuberculous lymphadenitis did not find any difference in IL-26 protein levels in their cohort compared to healthy control[230]. IL-26 levels in both plasma and LN supernatant were similar. This group also showed that anti-tuberculosis treatment (not described more closely) significantly reduces the plasma levels of IL-26[230]. A possible explanation of this contrasting finding might lie in the methodological procedure applied by the authors. They have chopped the respective lymph nodes into small pieces and have then applied enzymes and DNase for digestion of the tissue. Thereafter the resulting single cells were incubated, and the culture supernatant was used for ELISA. This standard procedure is probably suitable for all their tested cytokines except IL-26. As IL-26 is highly cationic it will probably bind to the released DNA (due to chopping) before the DNase will be added. IL-26/DNA complexes might negatively influence the detection efficiency of the IL-26 ELISA. Additionally, a compound such as a high salt concentration should have been added to prevent binding of IL-26 to other negatively charged substances or glycosaminoglycans on cell surfaces[51]. Considering these points, the published results in tuberculous lymphadenitis might be a false negative.

Besides increased *IL26* gene expression (*Fig. 9A*), we observed increased *IL22* expression and *IFNG* expression (data for the latter not shown) but we could not detect increased gene expression of *IL17A* (*Fig. 9C*) in our TB lymph nodes implying that T_H1 cells are the main source of IL-26 in our TB cohort. Furthermore, the novel T_H22 cells might play and important role here. Our results are consistent with findings from Qiao *et al.*[231], showing high levels of IFN-γ and IL-22 in tubercular pleural fluid while IL-17 could not be detected at all. This publication, together with others[232-234], suggests that T_H22 cells might play a novel and important role here. The lack of *IL17A* is most likely a result of the granulomatous stage of the investigated lymph nodes, as T_H17 cells and IL-17 is assumed to play an important role in the early infection with Mtb[235,236].

4.2 IL-26's effects on skin cells

The proposed IL-26 receptor consisting of IL-20R1 and IL-10R2 is found in skin[47] or more precisely in keratinocytes[42,50]. This was confirmed by our own

gene expression data (*Fig. 12* and *Fig.15*). Unfortunately, we were not able to reproduce the results of Hör *et al.*[50], showing that the HaCaT keratinocyte cell line responds to IL-26 concentrations as little as 10 ng/ml with significant secretion of IL-10 and CXCL8 (IL-8) (compare *Fig. 16*). The main reason for the lacking reproducibility might be the fact that they have been using N-terminally histidine-tagged IL-26, while we are using commercially available untagged recombinant IL-26. Due to the tag, the protein structure is different and it therefore might bind better to its proposed receptor inducing gene expression changes in low concentrations. Furthermore, the research group isolated the IL-26 from supernatants from a virus-transformed cell line; there might still be some effects due to the viral infection.

Even tough keratinocytes are one of the few cell types that express that unique receptor heterodimer combination, there are only two publications[42,50] (both from 2004), where the researchers have been focusing on the effects of IL-26 on (HaCaT) keratinocytes. Seeing our own difficulties in getting keratinocytes to respond to IL-26, the lack of original research publications can possibly be explained. Furthermore, when comparing the gene expressions of the IL-26 receptor heterodimer between Colo-205 cells, HaCaT keratinocytes, primary keratinocytes, and primary fibroblasts, we see that primary keratinocytes have the lowest *IL20R1* gene expression of all tested cell types (*Fig. 15*). This detected gene expression in turn does not automatically lead to a surface expression of IL-20R1 protein. This might further explain the difficulties we were facing with primary keratinocytes. As keratinocytes are adherent cells, they are further complicated to process for experiments to directly investigate IL-20R1 surface expression, for example, flow cytometry. In line with the literature, Corvaisier *et al.* reported that they also do not see a response in keratinocytes to IL-26[62]. On the other hand, similar phenomenon has been reported for IFN-λ. Its receptor heterodimer IFN-λR1 and IL-10R2 is found on keratinocytes and different immune cells, but still the immune cells do not even respond to high concentrations (1 µg/ml) of IFN-λ[237]. The keratinocytes in this case respond as expected. In fact, it was shown that immune cells express a shorter IFN-λR1 splice variant that is active as a soluble single receptor[237].

Simulating pro-inflammatory conditions via pre-stimulation of primary human keratinocytes with TNF-α and IL-1β did not affect the subsequent stimulation with IL-26 (data not shown). It might therefore be interesting to stimulate keratinocytes isolated from a psoriatic plaque skin biopsy and see if they respond to IL-26. Additionally, considering the high amount of IL-26 protein in psoriasis there could be a certain threshold needed to stimulate cytokine secretion or gene expression in primary keratinocytes meaning that higher concentrations of IL-26 would give a desired result. Another option could be the stimulation of keratinocytes with IL-26 in combination with different T_H17 cytokines, such as IL-17 and IL-22. On one hand, this could simulate a psoriatic milieu, but it has also been shown that IL-17 and IL-22 act synergistically together to induce gene expression of antimicrobial peptides in keratinocytes[238]. If one of these options would work, it could be interesting to investigate if IL-26/DNA complexes have an effect on keratinocytes and if TLRs (especially TLR9) are differentially regulated by IL-26. An analog effect has been published regarding LL37[239].

Our results showing no IL-20R1 on immune cells (*Fig. 17* and *table 7*) is in accordance with Kunz *et al.*[47], that also could not detect any expression of this IL-26 receptor component on monocytes, NK cells, B cells, and T cells.

4.3 IL-26/nucleic acid complex formation

Our findings about IL-26/DNA complex formation (chapter 3.3.2) have in large parts been published in Meller *et al.*[19]. Previous to that publication, nucleic acid complex formation has only been described for peptides but not for larger proteins such as interleukins. For the cationic LL37, DNA complex formation had first been reported by Sandgren and colleagues[94], where they showed that LL37 is transferring bacterial DNA plasmids into mammalian cells. Later, Lande *et al.*[96] unraveled an important pathomechanism in psoriasis showing that LL37 binds self-DNA and subsequently the complex is taken up by, and activates, pDCs to secrete type I interferons that are usually a response to viral infections. This finding was also applied to monocytes, which in contrast to pDCs do not sense the LL37/DNA complexes via TLRs but with cytosolic nucleic acid sensors instead[97]. LL37 does bind to self-RNA and activates moDCs via endosomal TLR8 to secrete TNF-α and IL-6 while pDCs respond to LL37/RNA

complexes with secretion of IFN-α but mediated via TLR7[98]. Our results indicate that IL-26 is also able to bind RNA and then activates moDCs to secrete TNF-α and IL-6 (*Fig. 23*).

As human β-defensins are also cationic antimicrobial peptides it would be natural that they are also forming complexes with anionic nucleic acids. Indeed the complex forming capability has been shown for DEFB4A (also known as hBD2) and DEFB103A (also known as hBD3)[240]. The defensin/self-DNA complexes even induce inflammatory skin symptoms in a murine model. Other researchers reported the complex formation of DEFB103A with bacterial DNA[241].

Interestingly, we also detected an interaction of IL-22 with both DNA and RNA. Using https://pepcalc.com/protein-calculator.php, IL-22 has a calculated net charge at pH7 of +0.1, meaning it is basically neutral, while for IL-26 a charge of +18 is calculated. This implies that further factors need to be taken into consideration when it comes to nucleic acid complex formation. In case of IL-22 there might be the sequence homologies or percentage of identity to IL-26 that facilitate binding to nucleic acids even though it has been shown that in contrast to IL-26 all charged amino acids are distributed evenly throughout the IL-22 protein[19,242].

4.4 Signaling via TLR2

As shown in all experiments involving immune cells, IL-26 elicits effects in absence of nucleic acids and the proposed receptor complex IL-20R1 and IL-10R2. In $CD14^+$ monocytes we showed that the IL-26 mediated induction of IL-1β is downregulated by the combined addition of RNase and DNase (*Fig. 19*). The same effect was expected when moDCs were pre-treated with RNase and DNase prior to the addition of IL-26. But here the nucleic acid degrading enzymes were completely ineffective (*Fig. 24*). Of note, in moDCs we found a slightly increased TNF-α secretion when the endosomal inhibitor bafilomycin together with IL-26/RNA complexes was present (*Fig. 24*). This indicates that cytosolic RNA sensors might possibly be involved in signal transduction. It has been reported for monocytes that the LL37/DNA complex induced IFN-α

secretion is independent from TLR9 and furthermore also there the addition of bafilomycin even led to significant increase in IFN-α secretion[97].

During the search for a possible receptor for IL-26 on immune cells, we found TLR2. Classically, TLR2 recognizes bacterial LTA[110]. Interestingly, the cytotoxic T cell derived antimicrobial peptide granulysin is also able to signal via a TLR that is TLR4 in this case[243]. Another endogenous ligand shown to activate dendritic cells via TLR4 is the antimicrobial murine BD-2[244]. Also, heat shock proteins (HSPs) have been shown to signal via TLR4[245,246]. For TLR2, compounds of necrotic cells have been found to act as endogenous ligands[247]. The exact compound of necrotic cells has not been identified in this study. In this case it would be interesting to further evaluate which intracellular component in fact causes the TLR2 activation. Using specially engineered HEK cells that express human TLR2, we found that IL-26 induces SEAP secretion in these cells that only occurs when signaling via TLR2 is taking place (*Fig. 28*). In the next step, we investigated if the blocking of TLR2 could block the IL-26-induced TNF-α in primary cells. Here, TNF-α secretion is indeed blocked with a neutralizing TLR2 antibody, but this effect can only be seen in moDCs (*Fig. 29*). In macrophages, the blockade of TLR2 signaling does not affect IL-26-induced TNF-α secretion. These results indicate that IL-26 adds to the list of putative endogenous ligands for TLR2.

According to the literature, TLR2 is expressed in monocytes[248,249], macrophages[250], and moDCs[249]. This is also what we could confirm using qPCR (*Fig. 27*). Furthermore, our results show that TLR2 expression is significantly induced in moDCs by the presence of IL-26. This phenomenon was not seen for the other tested cell types (mentioned above). Having only moDCs that respond to IL-26 with significantly increased TLR2 gene expression, and on the other hand being the only cell type that responds to TLR2 blockade with a reduced TNF-α secretion in the presence of IL-26, the hypothesis arose that there might be a certain threshold of TLR2 protein to be reached in order to induce signaling.

We reported a strong trend towards an upregulation of *TLR2* in rosacea (*Fig. 30*). This is in line with results from Yamasaki *et al.*, who indeed found an increased TLR2 expression in their rosacea samples[188]. This then goes along

with an increased serine protease production that in turn cleaves LL37 to make it a functional protein. We also found a trending upregulation of *TLR2* gene expression compared to healthy control in sarcoidosis. Studies on TLR2 in sarcoidosis are limited, but it seems as if the increased gene expression that we found does not translate to surface expression. It rather has been hypothesized that the TLR2 in sarcoidosis might be malfunctioning[251]. In contrast to that hypothesis, a group found that on the surface of monocytes from sarcoidosis patients there is a significantly higher expression of TLR2[252]. Additionally, in their results, TLR2 seems to work as effectively as TLR2 on monocytes of healthy controls in regard to response to suitable ligands[252].

4.5 Antimycobacterial activity

We have shown previously that IL-26 is able to directly kill several types of bacteria[19]. This finding that has also been confirmed by others[253]. We now report that IL-26 also has direct antimycobacterial capabilities and is able to inhibit 50% of *Mycobacterium tuberculosis* (*Mtb*) at concentrations higher than 5 µM (*Fig. 34* and *Table 11*). In addition, we showed that IL-26 at a concentration of 10 µM improves survival of infected macrophages. The overall infection rate does not seem to be affected by the presence of IL-26.

It has been reported that *Mtb*-infected monocytes from elderly people secrete less IL-26 into the supernatant as compared to the non-infected control[229]. This might imply that infected monocytes secrete less IL-26 in order to maintain and transport it into lysosomes and subsequently facilitate intracellular mycobacterial killing. *IL26* gene expression in these monocytes did not differ between adults or elderly study subjects. The addition of IL-26 (in this publication: 25 ng/ml) did inhibit the killing activity normally performed by blood components in whole blood from tuberculosis infected patients[229]. This is surprising, as we report that IL-26 itself mediates direct antimycobacterial activity (*Fig. 34*). Looking closer at the whole blood assay performed, there might be a technical issue possibly leading to this debatable result: In order to prevent whole blood from coagulation, collection tubes containing heparin are used, which prevents the clotting. It has been shown by Hör *et al.*[50] that IL-26 binds to heparin. This then leads to the assumption that in the performed whole

blood assay the IL-26 might by blocked and the IL-26/heparin complexes could further hinder the monocytes in their antimycobacterial activity.

Treating uninfected THP1 macrophages with IL-26 we found an increased expression of the chemokines *CXCL2*, *CXCL8*, and *CCL20* (*Fig. 22*). This implies that even though IL-26 might not directly kill mycobacteria inside macrophages, it is still able to induce chemokines like CXCL8 and CXCL2 that attract neutrophils[79,81] or CCL20 that attracts T_H17 cells[65] to the site of infection. Recruiting T_H17 cells to the side of infections would also lead to a further increased amount of IL-26. Looking at CXCL8, it has been shown to affect mycobacterial growth negatively[82].

In addition to the chemokines, we found that IL-26 induces the gene expression and secretion of TNF-α in macrophages and moDCs (*Fig. 20* and *Fig. 23*). This TNF-α production might contribute to detected amounts of TNF-α in PBMCs from tuberculosis patients[254]. TNF-α seems to have very opposing effects in tuberculosis. On the protective side, it helps in maintenance of granulomas and a latent stage of the disease[255]. On the other hand, TNF-α needs to be tightly controlled as too little TNF leads to an impaired granuloma formation and too high TNF levels lead to an overactivation of macrophage and eventually cell killing and thereby release of mycobacteria and potentially reactivation of the disease[256]. This is also in line with data showing that patients suffering from latent tuberculosis and are receiving with anti-TNF treatment often face a reactivation of the disease[257].

4.6 Reducing conditions

It was shown by Schroeder and colleagues that hBD1 elicits much stronger antimicrobial effects when its disulphide bonds were reduced[123]. As we have shown, IL-26 also has antimicrobial properties and contains disulphide bonds[19], and so we hypothesized that reduction of these disulphide bonds could improve the functionality of IL-26.

As disulphide bonds can be reduced physiologically by the TXN system, we first investigated the major compounds of this system. We found a significantly increased gene expression of *TXN* in PV, AD, MF, and TB (*Fig. 39* and *Fig. 41*). For PV this is in line with the literature showing an increased protein expression

in psoriatic plaques[258]. Considering AD, MF and TB, to our knowledge, there is no data available describing *TXN* on any level or any role in these diseases. The expression of *TXN* positively correlates with *IL26* gene expression in our psoriasis cohort. This might indicate an additional role for TXN than the importance as part of the cellular redox systems. It might therefore be interesting to investigate the effects of IL-26 in cells pre-treated with an inhibitor of TXN activity such as dimethyl fumarate[259]. As this compound has only recently been introduced as a drug in the treatment of psoriasis[260], it further supports that there might also be effects on IL-26.

Similar to TXN, the significantly increased gene expression of *TXNRD1* in MF has not, to our knowledge, been reported before, as there is no literature about it. Looking at the broader picture, especially of solid cancers in general, the TXN system has been extensively studied[261]. Here the main research interest was in TXN, as it functions as growth factor and plays a role in the inhibition of the programmed cell death, namely apoptosis, leading to the development of a number of drugs to target TXN[262].

In sarcoidosis, we found a significant increase of TXNRD1 gene expression (*Fig. 39B*). In a study by Tiitto *et al.*[263] investigating lung diseases including pulmonary sarcoidosis and different tissues as well as cell types, an increased TXNRD1 protein expression in alveolar macrophages[263] and a strong increase of TXN protein in lung granulomas[263,264] and lymph nodes[264] was reported. The fact that we don't see an increase in *TXN* gene expression in our cohort might be due to the different location and to the low sample size, as four of the six samples indeed do show higher *TXN* gene expression compared to the mean of the healthy controls. The high TXN in sarcoidosis granulomas reported by others[263,264] could possibly be connected to the increased *TXN* gene expression in TB granulomas within lymph nodes that we are reporting here (*Fig. 41*).

TXNRD1 gene expression in lymph nodes from TB patients is greatly increased compared to healthy controls (*Fig. 41*). Also here it is nearly impossible to find supporting literature. There has been a study investigating TXNRD1 polymorphisms in TB patients under drug therapy[265], but as this study only focused on genetic polymorphisms no overall gene expression was analyzed and additionally no healthy controls were included. An analogue to dimethyl

fumarate that acts on TXN, namely manumycin A, has just recently been described to have inhibitory effect on TXNRD1 by irreversibly blocking its activity[266].

Using circular dichroism, we investigated the structural change of IL-26 in presence of the reductant TCEP. We observed only a slight change in structure from a classical α-helical structure towards a more open protein (*Fig. 45*). The overall structure seemed to be conserved under reducing conditions. Analogously to the study by Schroeder *et al.*[123] we investigated if IL-26 is reduced by physiological TXN system and found that it indeed can be reduced by this system and thus might play a role *in vivo* (*Fig. 43*). Next, we performed antimicrobial assays where the reduced IL-26 was supposed to be added in parallel to the oxidized IL-26. In order to prevent the reduced IL-26 from being oxidized, a reducing component such as DTT was added.

Unfortunately, DTT in concentrations necessary to maintain the redox status of IL-26 did severely negatively impact the experiment as DTT was killing the bacteria in absence of IL-26 (*Fig. 59*). In cell-free assays we found that reduced IL-26 was binding better to all tested components (LPS, LTA, LAM, DNA, and RNA; *Fig. 46, Fig. 57, Fig. 58* and *Table 12 to 14*) compared to the oxidized counterpart. As human primary cells have shown not to be sensitive to DTT at a concentration of 2 mM, we performed experiments where half the cells were treated with DTT and reduced IL-26 or reduced IL-26/nucleic acid complexes. Even though cell viability did not seem to be affected by 2 mM DTT, cytokine secretion (TNF-α) or gene expressions in presence of DTT are much lower compared to standard conditions (*Fig. 48* and *Fig. 49*). As this effect did not only occur in cells with reduced IL-26 but also in cells treated with the positive control LPS, we concluded that it must be a direct negative effect of DTT. Consulting literature, to our knowledge DTT as reducing agent on cells has only been successfully used in the publication about reduced hBD1 by Schroeder *et al.*[123]. Additionally, a drastically positive effect using DTT as reducing agent has only been reported for hBD1. An interesting feature of this reduced hBD1 is the formation of net-like structures around bacteria that prevent bacterial mobility and thereby present another sort of antimicrobial action[267].

To address the problem with simulating reducing conditions, cells were cultured under hypoxia (1% O_2) when stimulated with reduced IL-26 or under normoxic conditions when treated with oxidized IL-26. In this case, the lack of oxygen was meant to prevent the reduced IL-26 from transitioning into the oxidized state. Hypoxia did not negatively influence the cellular response towards the positive control, LPS, with regards to either cytokine secretion or tested gene expression (*Fig. 50* and *Fig. 52*). Surprisingly, we could not detect an increased expression of *HIF1A* the main inducible factor during hypoxia (*Fig. 51*). Maybe the gene expression level is not the most suitable read-out for effects on HIF1A as the protein itself gets rapidly degraded in presence of oxygen by prolyl hydroxylases (PHDs) and is therefore stabilized only in absence of oxygen[132]. In contrast to our expectations, we could not observe an increased cellular response towards reduced IL-26 or reduced IL-26/nucleic acid complexes compared to the oxidized controls under normoxic conditions. Gene expressions or cytokine secretions in response to reduced IL-26 and reduced IL-26/nucleic acid complexes under hypoxic conditions tended to be lower compared to oxidized counterpart.

We found an increased expression of *HIF1A* in psoriasis and also in TB (*Fig. 55*). In psoriasis, an upregulated HIF1A protein expression has already been seen by Rosenberger and colleagues[268]. Furthermore, a hypoxic environment can easily be imagined when considering that high proliferation of keratinocytes and thickening of the epidermis is as a hallmark of the disease[159,161]. We further found a positive correlation between the expression of *IL26* and *HIF1A* in psoriasis (*Fig. 56*), which further implies a connection between those two even though we could not prove this on a cellular level using blood cells. Here the investigation of psoriatic keratinocytes or *ex vivo* skin explants could be an interesting option. In TB, our detected significantly increased *HIF1A* gene expression in granulomas of TB lymph nodes is in line with literature as it has been found that granulomas present a hypoxic environment and an increased expression of HIF1A expression has thus been reported in pulmonary TB granulomas[269]. The researchers found that IL-17 decreases HIF1A expression, which can be adapted to our results, as we did not see any *IL17A* expression (*Fig. 9C*) but a high *HIF1A* expression (*Fig. 55*).

Generally, most experiments involving human cells are performed under normoxic conditions with about 21% athmosperic oxygen[129]. This oxygen level is above the oxygen level in most tissues and blood[129], the latter where most of the used cells are isolated from. Thus, one probably should rethink all results gained under normoxic conditions due to limited transferability into the human or mammalian system.

Overall, more research is needed to better evaluate the role of IL-26 in both reducing and hypoxic environments. This research should then consider the relevant HIF1A associated target genes.

4.7 Neutralization of LPS

Our data also shows that LL37 forms complexes with LPS (*Fig. 31*), a feature that has been known for some time[270,271]. Building these complexes with LPS, LL37 is further able to drastically reduce the signaling of LPS via TLR4[272]. We here report that similar to LL37 also IL-26 binds to LPS (published in Meller *et al.*[19] and *Fig. 31*). So far for IL-26, the binding to LPS was thought to mediate and facilitate bacterial killing. As anti-septic effects were shown for LL37 (as just described) we were wondering if this is also the case for IL-26. Treating moDCs with IL-26 prior to the addition of LPS, we report here that IL-26 efficiently neutralizes LPS and this neutralization subsequently leads to a reduced secretion and expression of pro-inflammatory cytokines by moDCs (*Fig. 60* to *Fig. 62*). This neutralization effect has also been studied on LTA and LAM, but here the applied concentrations of LTA or LAM have most likely been too low (compare with[272]). In turn, the activation of moDCs was too little and a potential neutralization was therefore either overlooked or simply did not occur. Considering LAM, there is a variety of molecular differences in the structure of LAMs between different mycobacterial strains and it has been shown that LAM from non-virulent strains are recognized via TLR2, but ManLAM (used here) from virulent *Mtb H37Rv* is not recognized via TLR2 nor TLR4[156,273]. Further research is necessary to solve the question whether and how IL-26 influences LTA and LAM signaling.

There has been a study in mice where the effects of IL-26 in presence of LPS were investigated[274]. The animals received intranasal instillation of LPS prior to

the addition of recombinant human IL-26. The researchers then reported that the presence of IL-26 has an additive effect on the LPS-induced secretion of TNF-α, IL-6 and different chemokines[274]. This is in contrast to our results where LPS-mediated effects are significantly downregulated when cells were pre-incubated with IL-26. As we have added IL-26 to the cell culture prior to LPS, it would be interesting to see how this would change the mouse data or how a change in protocol would modify our findings if LPS would have been added before IL-26. Besides their contrasting results, this study can be considered controversial as IL-26 is not found in mice and this study does not include any data from human immune cells to explain if the results are transferable. To prove their concept, the researchers show that the IL-20R1 is expressed in mouse lung tissue.

4.8 Positive feedback loop

We report here that IL-26 induces its own gene expression in all tested immune cell types such as monocytes, moDCs and macrophages (*Fig. 63*). Our data goes in line with results from Che *et al.*[53] showing that human alveolar macrophages express and release IL-26. As we only show this change in expression on the mRNA level, studies on protein level including e.g. ELISAs should be implemented to confirm that this increased gene expression indeed results in an increase of secreted IL-26 protein. Positive feedback loops have been described for other interleukins such as IL-6[275,276] or IL-1β[277]. For IL-6, the authors showed in a mouse model that IL-6 is triggered by IL-17 and in turn IL-6 plays an important role in the development of T_H17 cells which again will produce IL-17[275]. Looking at IL-26, acting via a direct positive feedback loop on a variety of immune cells possibly explains how high levels of IL-26 are reached within certain diseased tissues *in vivo*. Furthermore, we showed that IL-26 also leads to an increased secretion of IL-6 in some immune cells, which then possibly fuels into the described feedback loop with T_H17 cells thereby further accelerating IL-26 secretion.

4.9 Proposed model in inflammatory skin diseases

The proposed model for the role of IL-26 in inflammatory skin diseases is displayed in *Fig. 64*. We found that IL-26 is overexpressed in inflammatory skin

conditions such as PV, rosacea, AD, and cutaneous sarcoidosis but also in the cutaneous T cell lymphoma abbreviated MF. We hypothesize that either T_H1 or T_H17 cells are likely to be the main source of IL-26 in those diseases. IL-26 was able to act as antimicrobial agent on *S. aureus* or *P. aeruginosa* via binding to lipoteichoic acid (LTA) or LPS respectively. Due to its cationic amphipathic structure, IL-26 can also bind to nucleic acids. The binding of IL-26 to nucleic acids seems much stronger compared to LTA or LPS considering dissociation constants. These results in combination with the higher concentration of IL-26 needed to kill bacteria than to bind nucleic acids, implies that IL-26 could have a more important role in autoimmune diseases and adaptive immunity as in bacterial defense and innate immunity. Having IL-26 in complex with DNA, macrophages (MΦ) can be activated and express the chemokines CXCL2 and CXCL8 which both recruit neutrophils to the site of inflammation. IL-26/DNA complexes also stimulate monocytes to secrete IL-1β and to express CCL20. CCL20 in turn can attract T_H17 cells which are then possibly supplying more IL-26. The amount of IL-26 in those inflammatory disorders is probably further accelerated by attracted immune cells such as monocytes, macrophages, and monocyte-derived dendritic cells (moDCs) that express *IL26* in response to IL-26 protein. Immune cells do not carry the heterodimeric IL-26 receptor complex of IL-20R1 and IL-10R2 that is mainly found on epithelial cells. We therefore propose that IL-26 might act as an endogenous ligand for Toll like-receptor (TLR) 2 to stimulate moDCs. To conclude, even though IL-26 appears to have stronger effects in adaptive immunity – such as the binding to nucleic acids – and especially in autoimmunity, it affects also innate immunity as it is able to signal via TLR2 and on the other hand it attracts innate cells such as neutrophils to the inflammatory site.

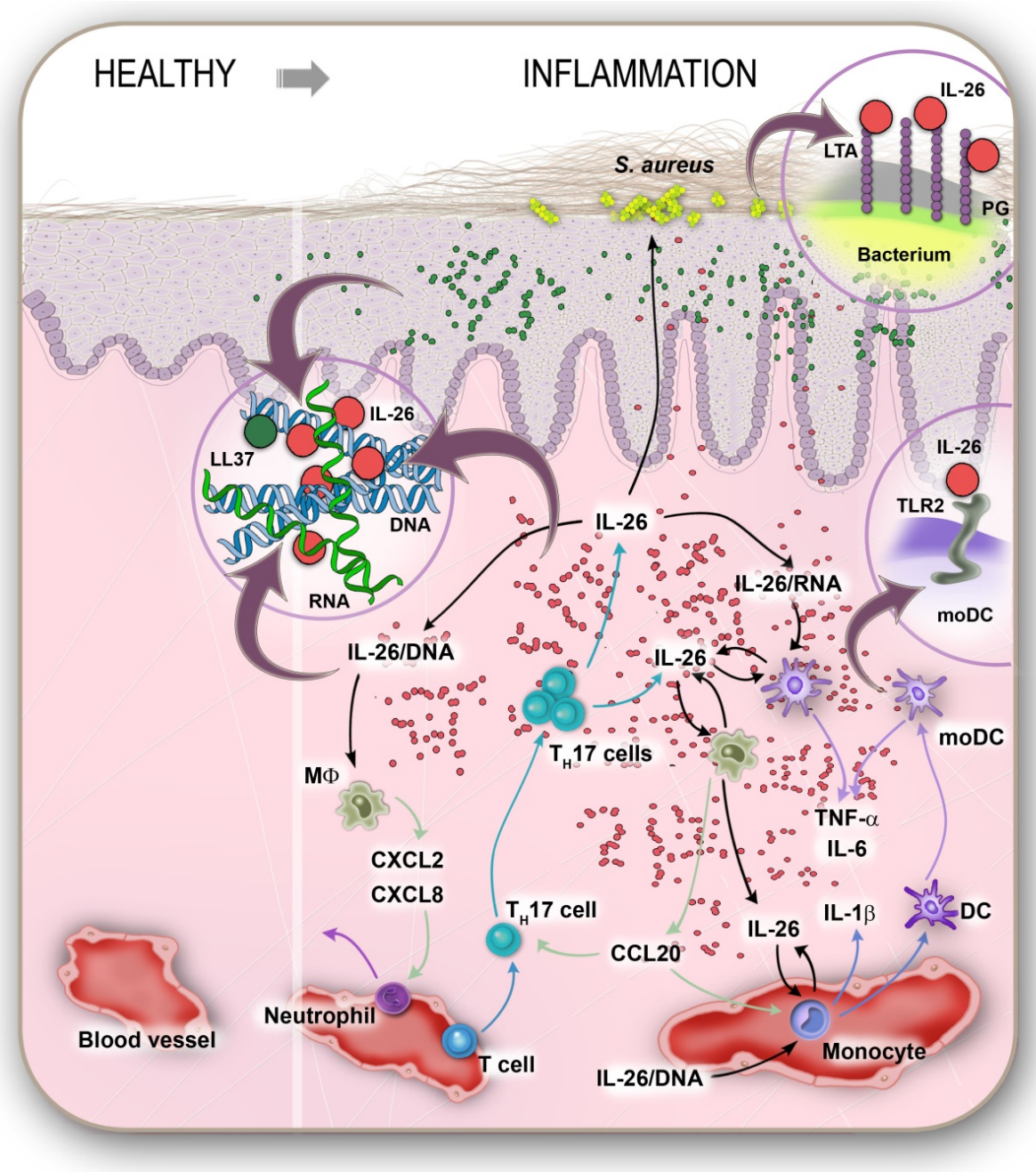

FIGURE 64: Model of the hypothesis for IL-26-mediated actions in inflammatory skin diseases. T_H17 cells produce IL-26 that can then inhibit bacteria e.g. *S. aureus* via binding to their cell surface lipoteichoic acid (LTA). On the other hand, due to its cationic charge IL-26 binds to nucleic acids. IL-26 complexed with DNA is able to activate macrophages (MΦ) to express the chemokines CXCL2 and CXCL8 that in turn recruit neutrophils to the inflammatory site. IL-26/DNA complexes can also activate monocytes to secrete IL-1β and CCL20. CCL20 is a key factor in recruiting T_H17 cells completing a loop towards even higher IL-26 secretion. Additionally, the presence of IL-26 results in an *IL26* gene expression by monocytes, macrophages and monocyte-derived dendritic cells (moDCs), further enhancing local IL-26 concentrations. IL-26 also binds RNA and these complexes activate moDCs to secrete proinflammatory cytokines such as TNF-α and IL-6. In moDCs IL-26 is suggested to be an endogenous ligand of Toll-like receptor (TLR) 2.

4.10 Proposed model in tuberculosis

After seeing that IL-26 is induced in sarcoidosis, we investigated tuberculosis (TB) another disease with a granulomatous presentation and found IL-26 highly expressed in granulomatous lymph nodes of TB patients. The main producers of IL-26 are suspected to be T_H1 cells here, as a strong upregulation of IFNG gene expression is also seen (data not shown). IL-26 was able to directly inhibit *Mtb* probably via binding to LAM and it also improved viability of infected macrophages (*Fig. 65*). But IL-26 has been additionally able to induce TNF-α in macrophages and the expression of different chemokines such as CXCL2, CXCL8 and CCL20. An increased amount of CXCL2 and CXCL8 attracts neutrophils to the side of infection. Furthermore, CXCL8 is able modify intracellular killing of the macrophages[82]. CCL20 interacts with receptors found on T_H17 cells and attracts them to the center of inflammation. As they in turn secrete IL-26 a circle of defense is completed and acts together to stabilize the granuloma and thereby maintaining a latent disease.

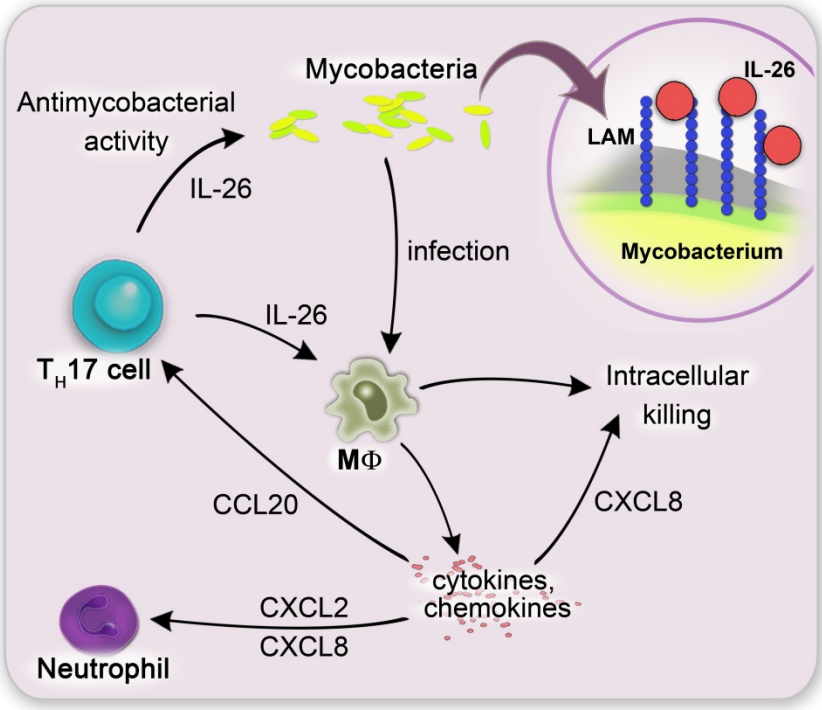

FIGURE 65: Model of the hypothesis for the role of IL-26 in tuberculosis. IL-26 is produced by T_H1 and T_H17 cells and acts directly on mycobacteria in limiting their survival. This is achieved by binding to LAM on the mycobacterial surface. In infected macrophages IL-26 leads to improved survival of the host cell. Non-infected macrophages respond to IL-26 with TNF-α secretion, CXCL2, CXCL8 and CCL20 expression. Inducing CXCL8, IL-26 has an indirect effect on mycobacterial killing, as CXCL8, on one hand, recruits neutrophils and enhances intracellular killing itself. CCL20 then attracts further T_H17 cells to the inflammation and in this way maintains IL-26 levels.

5 References

1. Salmon, J.K., Armstrong, C.A. & Ansel, J.C. The skin as an immune organ. *Western Journal of Medicine* **160**, 146-152 (1994).
2. Eyerich, S., Eyerich, K., Traidl-Hoffmann, C. & Biedermann, T. Cutaneous Barriers and Skin Immunity: Differentiating A Connected Network. *Trends Immunol* **39**, 315-327 (2018).
3. Nestle, F.O., Di Meglio, P., Qin, J.Z. & Nickoloff, B.J. Skin immune sentinels in health and disease. *Nature reviews. Immunology* **9**, 679-691 (2009).
4. Heath, W.R. & Carbone, F.R. The skin-resident and migratory immune system in steady state and memory: innate lymphocytes, dendritic cells and T cells. *Nat Immunol* **14**, 978-985 (2013).
5. Thulabandu, V., Chen, D. & Atit, R.P. Dermal fibroblast in cutaneous development and healing. *Wiley Interdisciplinary Reviews: Developmental Biology*, e307-n/a.
6. Hirobe, T. Keratinocytes regulate the function of melanocytes. *Dermatologica Sinica* **32**, 200-204 (2014).
7. Sorrell, J.M. & Caplan, A.I. Fibroblast heterogeneity: more than skin deep. *Journal of Cell Science* **117**, 667-675 (2004).
8. Tracy, L.E., Minasian, R.A. & Caterson, E.J. Extracellular Matrix and Dermal Fibroblast Function in the Healing Wound. *Advances in wound care* **5**, 119-136 (2016).
9. Alberts B, J.A., Lewis J. *Molecular Biology of the Cell. Innate Immunity.*, (Garland Science, New York, 2002).
10. Janeway CA Jr., T.P., Walport M. *Immunobiology: The Immune System in Health and Disease. Principles of innate and adaptive immunity.*, (Garland Science, New York, 2001).
11. Alberts B, J.A., Lewis J. *Molecular Biology of the Cell. Lymphocytes and the Cellular Basis of Adaptive Immunity.*, (Garland Science, New York, 2002).
12. Ziegler-Heitbrock, L.*, et al.* Nomenclature of monocytes and dendritic cells in blood. *Blood* **116**, e74-e80 (2010).
13. Luis, T.C., Killmann, N.M.B. & Staal, F.J.T. Signal transduction pathways regulating hematopoietic stem cell biology: Introduction to a series of Spotlight Reviews. *Leukemia* **26**, 86 (2012).
14. Zhu, J. & Paul, W.E. CD4 T cells: fates, functions, and faults. *Blood* **112**, 1557-1569 (2008).
15. Luckheeram, R.V., Zhou, R., Verma, A.D. & Xia, B. CD4+T Cells: Differentiation and Functions. *Clinical and Developmental Immunology* **2012**, 12 (2012).
16. Hsieh, C.-S.*, et al.* Pillars Article: Development of T_H1 CD4⁺ T Cells Through IL-12 Produced by Listeria-Induced Macrophages. 1993. Science 260(5107): 547–549. *The Journal of Immunology* **181**, 4437-4439 (2008).
17. Lentjes, M.H.F.M.*, et al.* The emerging role of GATA transcription factors in development and disease. *Expert Reviews in Molecular Medicine* **18**, e3 (2016).
18. Karthikeyan, B., Talwar, Arun, K.V. & Kalaivani, S. Evaluation of transcription factor that regulates T helper 17 and regulatory T cells function in periodontal health and disease. *Journal of pharmacy & bioallied sciences* **7**, S672-676 (2015).
19. Meller, S.*, et al.* T(H)17 cells promote microbial killing and innate immune sensing of DNA via interleukin 26. *Nat Immunol* **16**, 970-979 (2015).
20. Wolk, K.*, et al.* IL-29 Is Produced by TH17 Cells and Mediates the Cutaneous Antiviral Competence in Psoriasis. *Science Translational Medicine* **5**, 204ra129-204ra129 (2013).
21. Kaplan, M.H. Th9 cells: differentiation and disease. *Immunological reviews* **252**, 104-115 (2013).
22. Kaplan, M.H., Hufford, M.M. & Olson, M.R. The Development and in vivo function of T(H)9 cells. *Nature reviews. Immunology* **15**, 295-307 (2015).
23. Schmitt, E., Klein, M. & Bopp, T. Th9 cells, new players in adaptive immunity. *Trends in Immunology* **35**, 61-68.
24. Eyerich, S.*, et al.* Th22 cells represent a distinct human T cell subset involved in epidermal immunity and remodeling. *The Journal of Clinical Investigation* **119**, 3573-3585 (2009).

25. Fujita, H. The role of IL-22 and Th22 cells in human skin diseases. *Journal of Dermatological Science* **72**, 3-8 (2013).
26. Gordon, S. & Taylor, P.R. Monocyte and macrophage heterogeneity. *Nat Rev Immunol* **5**, 953-964 (2005).
27. Zhang, Y., Morgan, M.J., Chen, K., Choksi, S. & Liu, Z.-g. Induction of autophagy is essential for monocyte-macrophage differentiation. *Blood* **119**, 2895-2905 (2012).
28. Geissmann, F.*, et al.* Development of Monocytes, Macrophages, and Dendritic Cells. *Science* **327**, 656-661 (2010).
29. Geissmann, F.*, et al.* Blood monocytes: distinct subsets, how they relate to dendritic cells, and their possible roles in the regulation of T-cell responses. *Immunology And Cell Biology* **86**, 398 (2008).
30. Stockwin, L.H., McGonagle, D., Martin, I.G. & Blair, G.E. Dendritic cells: immunological sentinels with a central role in health and disease. *Immunol Cell Biol* **78**, 91-102 (2000).
31. Merad, M., Sathe, P., Helft, J., Miller, J. & Mortha, A. The dendritic cell lineage: ontogeny and function of dendritic cells and their subsets in the steady state and the inflamed setting. *Annual review of immunology* **31**, 563-604 (2013).
32. Reizis, B., Bunin, A., Ghosh, H.S., Lewis, K.L. & Sisirak, V. Plasmacytoid dendritic cells: recent progress and open questions. *Annual review of immunology* **29**, 163-183 (2011).
33. Gregorio, J.*, et al.* Plasmacytoid dendritic cells sense skin injury and promote wound healing through type I interferons. *The Journal of Experimental Medicine* **207**, 2921-2930 (2010).
34. Gilliet, M., Cao, W. & Liu, Y.J. Plasmacytoid dendritic cells: sensing nucleic acids in viral infection and autoimmune diseases. *Nature reviews. Immunology* **8**, 594-606 (2008).
35. Conrad, C., Meller, S. & Gilliet, M. Plasmacytoid dendritic cells in the skin: to sense or not to sense nucleic acids. *Seminars in immunology* **21**, 101-109 (2009).
36. Sozzani, S., Vermi, W., Del Prete, A. & Facchetti, F. Trafficking properties of plasmacytoid dendritic cells in health and disease. *Trends Immunol* **31**, 270-277 (2010).
37. Akdis, M.*, et al.* Interleukins (from IL-1 to IL-38), interferons, transforming growth factor beta, and TNF-alpha: Receptors, functions, and roles in diseases. *The Journal of allergy and clinical immunology* **138**, 984-1010 (2016).
38. Wang, X.*, et al.* A novel IL-23p19/Ebi3 (IL-39) cytokine mediates inflammation in Lupus-like mice. *European journal of immunology* **46**, 1343-1350 (2016).
39. Catalan-Dibene, J.*, et al.* Identification of IL-40, a Novel B Cell–Associated Cytokine. *The Journal of Immunology* (2017).
40. Knappe, A., Hor, S., Wittmann, S. & Fickenscher, H. Induction of a novel cellular homolog of interleukin-10, AK155, by transformation of T lymphocytes with herpesvirus saimiri. *J Virol* **74**, 3881-3887 (2000).
41. Truong, A.D., Hong, Y., Hoang, C.T., Lee, J. & Hong, Y.H. Chicken IL-26 regulates immune responses through the JAK/STAT and NF-κB signaling pathways. *Developmental & Comparative Immunology* **73**, 10-20 (2017).
42. Sheikh, F.*, et al.* Cutting Edge: IL-26 Signals through a Novel Receptor Complex Composed of IL-20 Receptor 1 and IL-10 Receptor 2. *The Journal of Immunology* **172**, 2006-2010 (2004).
43. Wolk, K.*, et al.* IL-22 regulates the expression of genes responsible for antimicrobial defense, cellular differentiation, and mobility in keratinocytes: a potential role in psoriasis. *European journal of immunology* **36**, 1309-1323 (2006).
44. Kotenko, S.V. & Pestka, S. Jak-Stat signal transduction pathway through the eyes of cytokine class II receptor complexes. *Oncogene* **19**, 2557-2565 (2000).
45. Wolk, K., Kunz, S., Asadullah, K. & Sabat, R. Cutting edge: immune cells as sources and targets of the IL-10 family members? *Journal of immunology (Baltimore, Md. : 1950)* **168**, 5397-5402 (2002).
46. Sa, S.M.*, et al.* The effects of IL-20 subfamily cytokines on reconstituted human epidermis suggest potential roles in cutaneous innate defense and pathogenic adaptive immunity in psoriasis. *Journal of immunology (Baltimore, Md. : 1950)* **178**, 2229-2240 (2007).
47. Kunz, S.*, et al.* Interleukin (IL)-19, IL-20 and IL-24 are produced by and act on keratinocytes and are distinct from classical ILs. *Experimental dermatology* **15**, 991-1004 (2006).
48. Sakurai, N.*, et al.* Expression of IL-19 and its receptors in RA: potential role for synovial hyperplasia formation. *Rheumatology (Oxford, England)* **47**, 815-820 (2008).

49. Blumberg, H.*, et al.* Interleukin 20: Discovery, Receptor Identification, and Role in Epidermal Function. *Cell* **104**, 9-19 (2001).
50. Hor, S.*, et al.* The T-cell lymphokine interleukin-26 targets epithelial cells through the interleukin-20 receptor 1 and interleukin-10 receptor 2 chains. *The Journal of biological chemistry* **279**, 33343-33351 (2004).
51. Braum, O., Pirzer, H. & Fickenscher, H. Interleukin-26, a highly cationic T-cell cytokine targeting epithelial cells. *Anti-inflammatory & anti-allergy agents in medicinal chemistry* **11**, 221-229 (2012).
52. Bech, R.*, et al.* Interleukin 20 regulates dendritic cell migration and expression of co-stimulatory molecules. *Molecular and Cellular Therapies* **4**, 1 (2016).
53. Che, K.F.*, et al.* Interleukin-26 in antibacterial host defense of human lungs. Effects on neutrophil mobilization. *American journal of respiratory and critical care medicine* **190**, 1022-1031 (2014).
54. Dambacher, J.*, et al.* The role of the novel Th17 cytokine IL-26 in intestinal inflammation. *Gut* **58**, 1207-1217 (2009).
55. Fujii, M.*, et al.* Expression of Interleukin-26 is upregulated in inflammatory bowel disease. *World Journal of Gastroenterology* **23**, 5519-5529 (2017).
56. You, W.*, et al.* IL-26 promotes the proliferation and survival of human gastric cancer cells by regulating the balance of STAT1 and STAT3 activation. *PLoS One* **8**, e63588 (2013).
57. Che, K.F.*, et al.* Interleukin-26 Production in Human Primary Bronchial Epithelial Cells in Response to Viral Stimulation: Modulation by Th17 cytokines. *Molecular medicine (Cambridge, Mass.)* **23**(2017).
58. Sato, K. & Takayanagi, H. Osteoclasts, rheumatoid arthritis, and osteoimmunology. *Current opinion in rheumatology* **18**, 419-426 (2006).
59. Peng, Y.-J.*, et al.* Interleukin 26 suppresses receptor activator of nuclear factor κB ligand induced osteoclastogenesis via down-regulation of nuclear factor of activated T-cells, cytoplasmic 1 and nuclear factor κB activity. *Rheumatology* **55**, 2074-2083 (2016).
60. Hsu, Y.-H.*, et al.* Anti–IL-20 monoclonal antibody inhibits the differentiation of osteoclasts and protects against osteoporotic bone loss. *The Journal of Experimental Medicine* **208**, 1849-1861 (2011).
61. Heftdal, L.D.*, et al.* Synovial cell production of IL-26 induces bone mineralization in spondyloarthritis. *Journal of Molecular Medicine* **95**, 779-787 (2017).
62. Corvaisier, M.*, et al.* IL-26 Is Overexpressed in Rheumatoid Arthritis and Induces Proinflammatory Cytokine Production and Th17 Cell Generation. *PLoS Biol* **10**, e1001395 (2012).
63. Turner, M.D., Nedjai, B., Hurst, T. & Pennington, D.J. Cytokines and chemokines: At the crossroads of cell signalling and inflammatory disease. *Biochimica et Biophysica Acta (BBA) - Molecular Cell Research* **1843**, 2563-2582 (2014).
64. Moser, B., Wolf, M., Walz, A. & Loetscher, P. Chemokines: multiple levels of leukocyte migration control☆. *Trends in Immunology* **25**, 75-84 (2004).
65. Harper, E.G.*, et al.* Th17 cytokines stimulate CCL20 expression in keratinocytes in vitro and in vivo: implications for psoriasis pathogenesis. *The Journal of investigative dermatology* **129**, 2175-2183 (2009).
66. Le Borgne, M.*, et al.* Dendritic cells rapidly recruited into epithelial tissues via CCR6/CCL20 are responsible for CD8+ T cell crosspriming in vivo. *Immunity* **24**, 191-201 (2006).
67. Homey, B.*, et al.* Up-regulation of macrophage inflammatory protein-3 alpha/CCL20 and CC chemokine receptor 6 in psoriasis. *Journal of immunology (Baltimore, Md. : 1950)* **164**, 6621-6632 (2000).
68. Olaru, F. & Jensen, L.E. Chemokine expression by human keratinocyte cell lines after activation of Toll-like receptors. *Experimental dermatology* **19**, e314-316 (2010).
69. Giustizieri, M.L.*, et al.* Keratinocytes from patients with atopic dermatitis and psoriasis show a distinct chemokine production profile in response to T cell-derived cytokines. *The Journal of allergy and clinical immunology* **107**, 871-877 (2001).
70. Homey, B. & Meller, S. Chemokines and other mediators as therapeutic targets in psoriasis vulgaris. *Clinics in dermatology* **26**, 539-545 (2008).
71. Deshmane, S.L., Kremlev, S., Amini, S. & Sawaya, B.E. Monocyte chemoattractant protein-1 (MCP-1): an overview. *Journal of interferon & cytokine research : the official*

journal of the International Society for Interferon and Cytokine Research **29**, 313-326 (2009).
72. Shi, C. & Pamer, E.G. Monocyte recruitment during infection and inflammation. *Nature reviews. Immunology* **11**, 762-774 (2011).
73. Tsou, C.L.*, et al.* Critical roles for CCR2 and MCP-3 in monocyte mobilization from bone marrow and recruitment to inflammatory sites. *J Clin Invest* **117**, 902-909 (2007).
74. Ohl, L.*, et al.* CCR7 governs skin dendritic cell migration under inflammatory and steady-state conditions. *Immunity* **21**, 279-288 (2004).
75. McColl, S.R. Chemokines and dendritic cells: a crucial alliance. *Immunol Cell Biol* **80**, 489-496 (2002).
76. Ardeshna, K.M., Pizzey, A.R., Walker, S.J., Devereux, S. & Khwaja, A. The upregulation of CC chemokine receptor 7 and the increased migration of maturing dendritic cells to macrophage inflammatory protein 3beta and secondary lymphoid chemokine is mediated by the p38 stress-activated protein kinase pathway. *British journal of haematology* **119**, 826-829 (2002).
77. Verani, A.*, et al.* C-C chemokines released by lipopolysaccharide (LPS)-stimulated human macrophages suppress HIV-1 infection in both macrophages and T cells. *J Exp Med* **185**, 805-816 (1997).
78. Arango Duque, G. & Descoteaux, A. Macrophage cytokines: involvement in immunity and infectious diseases. *Frontiers in immunology* **5**, 491 (2014).
79. De Filippo, K.*, et al.* Mast cell and macrophage chemokines CXCL1/CXCL2 control the early stage of neutrophil recruitment during tissue inflammation. *Blood* **121**, 4930-4937 (2013).
80. Zhang, Y.*, et al.* Enhanced interleukin-8 release and gene expression in macrophages after exposure to Mycobacterium tuberculosis and its components. *J Clin Invest* **95**, 586-592 (1995).
81. Zheng, L. & Martins-Green, M. Molecular mechanisms of thrombin-induced interleukin-8 (IL-8/CXCL8) expression in THP-1-derived and primary human macrophages. *Journal of leukocyte biology* **82**, 619-629 (2007).
82. O'Kane, C.M., Boyle, J.J., Horncastle, D.E., Elkington, P.T. & Friedland, J.S. Monocyte-dependent fibroblast CXCL8 secretion occurs in tuberculosis and limits survival of mycobacteria within macrophages. *Journal of immunology (Baltimore, Md. : 1950)* **178**, 3767-3776 (2007).
83. Zasloff, M. Antimicrobial peptides of multicellular organisms. *Nature* **415**, 389-395 (2002).
84. De Smet, K. & Contreras, R. Human antimicrobial peptides: defensins, cathelicidins and histatins. *Biotechnol Lett* **27**, 1337-1347 (2005).
85. Ganz, T. Defensins: antimicrobial peptides of innate immunity. *Nature reviews. Immunology* **3**, 710-720 (2003).
86. Zasloff, M. Antimicrobial peptides of multicellular organisms. *Nature* **415**, 389-395 (2002).
87. Gudmundsson, G.H.*, et al.* The Human Gene FALL39 and Processing of the Cathelin Precursor to the Antibacterial Peptide LL-37 in Granulocytes. *European Journal of Biochemistry* **238**, 325-332 (1996).
88. López-García, B., Lee, P.H.A., Yamasaki, K. & Gallo, R.L. Anti-Fungal Activity of Cathelicidins and their Potential Role in Candida albicans Skin Infection. *Journal of Investigative Dermatology* **125**, 108-115 (2005).
89. Noore, J., Noore, A. & Li, B. Cationic antimicrobial peptide LL-37 is effective against both extra- and intracellular Staphylococcus aureus. *Antimicrob Agents Chemother* **57**, 1283-1290 (2013).
90. Scott, M.G., Davidson, D.J., Gold, M.R., Bowdish, D. & Hancock, R.E.W. The Human Antimicrobial Peptide LL-37 Is a Multifunctional Modulator of Innate Immune Responses. *The Journal of Immunology* **169**, 3883-3891 (2002).
91. Bergman, P., Walter-Jallow, L., Broliden, K., Agerberth, B. & Soderlund, J. The antimicrobial peptide LL-37 inhibits HIV-1 replication. *Current HIV research* **5**, 410-415 (2007).
92. Kahlenberg, J.M. & Kaplan, M.J. Little peptide, big effects: the role of LL-37 in inflammation and autoimmune disease. (2013).

93. Davidson, D.J.*, et al.* The cationic antimicrobial peptide LL-37 modulates dendritic cell differentiation and dendritic cell-induced T cell polarization. *Journal of immunology (Baltimore, Md. : 1950)* **172**, 1146-1156 (2004).
94. Sandgren, S.*, et al.* The human antimicrobial peptide LL-37 transfers extracellular DNA plasmid to the nuclear compartment of mammalian cells via lipid rafts and proteoglycan-dependent endocytosis. *The Journal of biological chemistry* **279**, 17951-17956 (2004).
95. Ruoslahti, E. & Yamaguchi, Y. Proteoglycans as modulators of growth factor activities. *Cell* **64**, 867-869 (1991).
96. Lande, R.*, et al.* Plasmacytoid dendritic cells sense self-DNA coupled with antimicrobial peptide. *Nature* **449**, 564-569 (2007).
97. Chamilos, G.*, et al.* Cytosolic sensing of extracellular self-DNA transported into monocytes by the antimicrobial peptide LL37. *Blood* **120**, 3699-3707 (2012).
98. Ganguly, D.*, et al.* Self-RNA-antimicrobial peptide complexes activate human dendritic cells through TLR7 and TLR8. *J Exp Med* **206**, 1983-1994 (2009).
99. Stephen-Victor, E., Fickenscher, H. & Bayry, J. IL-26: An Emerging Proinflammatory Member of the IL-10 Cytokine Family with Multifaceted Actions in Antiviral, Antimicrobial, and Autoimmune Responses. *PLoS pathogens* **12**, e1005624 (2016).
100. Braum, O., Klages, M. & Fickenscher, H. The cationic cytokine IL-26 differentially modulates virus infection in culture. *PLoS One* **8**, e70281 (2013).
101. Miot, C.*, et al.* IL-26 is overexpressed in chronically HCV-infected patients and enhances TRAIL-mediated cytotoxicity and interferon production by human NK cells. *Gut* **64**, 1466-1475 (2015).
102. Poli, C.*, et al.* IL-26 Confers Proinflammatory Properties to Extracellular DNA. *Journal of immunology (Baltimore, Md. : 1950)* **198**, 3650-3661 (2017).
103. Takeda, K., Kaisho, T. & Akira, S. TOLL-LIKE RECEPTORS. *Annual review of immunology* **21**, 335-376 (2003).
104. Moresco, E.M.Y., LaVine, D. & Beutler, B. Toll-like receptors. *Current Biology* **21**, R488-R493 (2011).
105. Hornung, V.*, et al.* Quantitative expression of toll-like receptor 1-10 mRNA in cellular subsets of human peripheral blood mononuclear cells and sensitivity to CpG oligodeoxynucleotides. *Journal of immunology (Baltimore, Md. : 1950)* **168**, 4531-4537 (2002).
106. Akira, S., Takeda, K. & Kaisho, T. Toll-like receptors: critical proteins linking innate and acquired immunity. *Nat Immunol* **2**, 675-680 (2001).
107. Baker, B.S., Ovigne, J.M., Powles, A.V., Corcoran, S. & Fry, L. Normal keratinocytes express Toll-like receptors (TLRs) 1, 2 and 5: modulation of TLR expression in chronic plaque psoriasis. *The British journal of dermatology* **148**, 670-679 (2003).
108. Moresco, E.M., LaVine, D. & Beutler, B. Toll-like receptors. *Current biology : CB* **21**, R488-493 (2011).
109. Schwandner, R., Dziarski, R., Wesche, H., Rothe, M. & Kirschning, C.J. Peptidoglycan- and lipoteichoic acid-induced cell activation is mediated by toll-like receptor 2. *The Journal of biological chemistry* **274**, 17406-17409 (1999).
110. Han, S.H., Kim, J.H., Martin, M., Michalek, S.M. & Nahm, M.H. Pneumococcal lipoteichoic acid (LTA) is not as potent as staphylococcal LTA in stimulating Toll-like receptor 2. *Infection and immunity* **71**, 5541-5548 (2003).
111. Chow, J.C., Young, D.W., Golenbock, D.T., Christ, W.J. & Gusovsky, F. Toll-like receptor-4 mediates lipopolysaccharide-induced signal transduction. *The Journal of biological chemistry* **274**, 10689-10692 (1999).
112. Alexopoulou, L., Holt, A.C., Medzhitov, R. & Flavell, R.A. Recognition of double-stranded RNA and activation of NF-kappaB by Toll-like receptor 3. *Nature* **413**, 732-738 (2001).
113. Heil, F.*, et al.* Species-specific recognition of single-stranded RNA via toll-like receptor 7 and 8. *Science (New York, N.Y.)* **303**, 1526-1529 (2004).
114. Hemmi, H.*, et al.* A Toll-like receptor recognizes bacterial DNA. *Nature* **408**, 740-745 (2000).
115. Hasan, U.*, et al.* Human TLR10 is a functional receptor, expressed by B cells and plasmacytoid dendritic cells, which activates gene transcription through MyD88. *Journal of immunology (Baltimore, Md. : 1950)* **174**, 2942-2950 (2005).

116. Oosting, M.*, et al.* Human TLR10 is an anti-inflammatory pattern-recognition receptor. *Proceedings of the National Academy of Sciences of the United States of America* **111**, E4478-4484 (2014).
117. Lebre, M.C.*, et al.* Human Keratinocytes Express Functional Toll-Like Receptor 3, 4, 5, and 9. *Journal of Investigative Dermatology* **127**, 331-341 (2007).
118. Pivarcsi, A.*, et al.* Expression and function of Toll-like receptors 2 and 4 in human keratinocytes. *International Immunology* **15**, 721-730 (2003).
119. Kawai, K.*, et al.* Expression of functional Toll-like receptor 2 on human epidermal keratinocytes. *J Dermatol Sci* **30**, 185-194 (2002).
120. Song, P.I.*, et al.* Human keratinocytes express functional CD14 and toll-like receptor 4. *The Journal of investigative dermatology* **119**, 424-432 (2002).
121. Melmed, G.*, et al.* Human intestinal epithelial cells are broadly unresponsive to Toll-like receptor 2-dependent bacterial ligands: implications for host-microbial interactions in the gut. *Journal of immunology (Baltimore, Md. : 1950)* **170**, 1406-1415 (2003).
122. Martelli, P.L., Fariselli P Fau - Casadio, R. & Casadio, R. Prediction of disulfide-bonded cysteines in proteomes with a hidden neural network. (2012).
123. Schroeder, B.O.*, et al.* Reduction of disulphide bonds unmasks potent antimicrobial activity of human beta-defensin 1. *Nature* **469**, 419-423 (2011).
124. Nizet, V. & Johnson, R.S. Interdependence of hypoxic and innate immune responses. *Nature reviews. Immunology* **9**, 609-617 (2009).
125. Cleland, W.W. Dithiotreitol, a New Protective Agent for SH Groups. *Biochemistry* **3**, 480-482 (1964).
126. Burns, J.A., Butler, J.C., Moran, J. & Whitesides, G.M. Selective reduction of disulfides by tris(2-carboxyethyl)phosphine. *The Journal of Organic Chemistry* **56**, 2648-2650 (1991).
127. Getz, E.B., Xiao, M., Chakrabarty, T., Cooke, R. & Selvin, P.R. A Comparison between the Sulfhydryl Reductants Tris(2-carboxyethyl)phosphine and Dithiothreitol for Use in Protein Biochemistry. *Analytical Biochemistry* **273**, 73-80 (1999).
128. Lukesh, J.C., 3rd, Palte Mj Fau - Raines, R.T. & Raines, R.T. A potent, versatile disulfide-reducing agent from aspartic acid. (2012).
129. Carreau, A., Hafny-Rahbi, B.E., Matejuk, A., Grillon, C. & Kieda, C. Why is the partial oxygen pressure of human tissues a crucial parameter? Small molecules and hypoxia. *Journal of Cellular and Molecular Medicine* **15**, 1239-1253 (2011).
130. Wang, W., Winlove, C.P. & Michel, C.C. Oxygen partial pressure in outer layers of skin of human finger nail folds. *The Journal of physiology* **549**, 855-863 (2003).
131. Wigerup, C., Pahlman, S. & Bexell, D. Therapeutic targeting of hypoxia and hypoxia-inducible factors in cancer. *Pharmacology & therapeutics* **164**, 152-169 (2016).
132. Palazon, A., Goldrath, A.W., Nizet, V. & Johnson, R.S. HIF transcription factors, inflammation, and immunity. *Immunity* **41**, 518-528 (2014).
133. Palazon, A., Aragones, J., Morales-Kastresana, A., de Landazuri, M.O. & Melero, I. Molecular pathways: hypoxia response in immune cells fighting or promoting cancer. *Clinical cancer research : an official journal of the American Association for Cancer Research* **18**, 1207-1213 (2012).
134. Koritzinsky, M.*, et al.* Two phases of disulfide bond formation have differing requirements for oxygen. *The Journal of cell biology* **203**, 615-627 (2013).
135. Tanaka, S., Uehara, T. & Nomura, Y. Up-regulation of protein-disulfide isomerase in response to hypoxia/brain ischemia and its protective effect against apoptotic cell death. *The Journal of biological chemistry* **275**, 10388-10393 (2000).
136. Welsh, S.J., Bellamy, W.T., Briehl, M.M. & Powis, G. The redox protein thioredoxin-1 (Trx-1) increases hypoxia-inducible factor 1alpha protein expression: Trx-1 overexpression results in increased vascular endothelial growth factor production and enhanced tumor angiogenesis. *Cancer research* **62**, 5089-5095 (2002).
137. Takagi, Y.*, et al.* Expression of thioredoxin-1 and hypoxia inducible factor-1alpha in cerebral arteriovenous malformations: Possible role of redox regulatory factor in neoangiogenic property. *Surgical neurology international* **2**, 61 (2011).
138. Wirth, T.*, et al.* Origin, Spread and Demography of the Mycobacterium tuberculosis Complex. *PLoS pathogens* **4**, e1000160 (2008).
139. Gagneux, S. Host-pathogen coevolution in human tuberculosis. *Philosophical transactions of the Royal Society of London. Series B, Biological sciences* **367**, 850-859 (2012).

140. Esmail, H., Barry, C.E., Young, D.B. & Wilkinson, R.J. The ongoing challenge of latent tuberculosis. *Philosophical Transactions of the Royal Society B: Biological Sciences* **369**, 20130437 (2014).
141. Organization, W.H. Global tuberculosis report 2017. (2017).
142. Lagranderie, M.R., Balazuc, A.M., Deriaud, E., Leclerc, C.D. & Gheorghiu, M. Comparison of immune responses of mice immunized with five different Mycobacterium bovis BCG vaccine strains. *Infection and Immunity* **64**, 1-9 (1996).
143. Sehgal, V.N., Bhattacharya, S.N., Jain, S. & Logani, K. Cutaneous tuberculosis: the evolving scenario. *International journal of dermatology* **33**, 97-104 (1994).
144. Lai-Cheong, J.E.*, et al.* Cutaneous manifestations of tuberculosis. *Clinical and experimental dermatology* **32**, 461-466 (2007).
145. Kivanc-Altunay, I., Baysal, Z., Ekmekci, T.R. & Koslu, A. Incidence of cutaneous tuberculosis in patients with organ tuberculosis. *International journal of dermatology* **42**, 197-200 (2003).
146. Denholm, J.T. & McBryde, E.S. The use of anti-tuberculosis therapy for latent TB infection. *Infection and drug resistance* **3**, 63-72 (2010).
147. Gumbo, T.*, et al.* Isoniazid's bactericidal activity ceases because of the emergence of resistance, not depletion of Mycobacterium tuberculosis in the log phase of growth. *The Journal of infectious diseases* **195**, 194-201 (2007).
148. van Ingen, J.*, et al.* Why Do We Use 600 mg of Rifampicin in Tuberculosis Treatment? *Clinical infectious diseases : an official publication of the Infectious Diseases Society of America* **52**, e194-199 (2011).
149. Stenger, S.*, et al.* An Antimicrobial Activity of Cytolytic T Cells Mediated by Granulysin. *Science (New York, N.Y.)* **282**, 121-125 (1998).
150. Rivas-Santiago, B.*, et al.* Human β-Defensin 2 Is Expressed and Associated with Mycobacterium tuberculosis during Infection of Human Alveolar Epithelial Cells. *Infection and immunity* **73**, 4505-4511 (2005).
151. Nickel, D.*, et al.* Hypoxia Triggers the Expression of Human β Defensin 2 and Antimicrobial Activity against Mycobacterium tuberculosis in Human Macrophages. *The Journal of Immunology* **188**, 4001-4007 (2012).
152. Rivas-Santiago, B.*, et al.* Activity of LL-37, CRAMP and antimicrobial peptide-derived compounds E2, E6 and CP26 against Mycobacterium tuberculosis. *International Journal of Antimicrobial Agents* **41**, 143-148 (2013).
153. Liu, P.T.*, et al.* Toll-Like Receptor Triggering of a Vitamin D-Mediated Human Antimicrobial Response. *Science* **311**, 1770-1773 (2006).
154. Brown, L., Wolf, J.M., Prados-Rosales, R. & Casadevall, A. Through the wall: extracellular vesicles in Gram-positive bacteria, mycobacteria and fungi. *Nat Rev Micro* **13**, 620-630 (2015).
155. Brightbill, H.D.*, et al.* Host defense mechanisms triggered by microbial lipoproteins through toll-like receptors. *Science (New York, N.Y.)* **285**, 732-736 (1999).
156. Stenger, S. & Modlin, R.L. Control of Mycobacterium tuberculosis through mammalian Toll-like receptors. *Current opinion in immunology* **14**, 452-457 (2002).
157. Tapping, R.I. & Tobias, P.S. Mycobacterial lipoarabinomannan mediates physical interactions between TLR1 and TLR2 to induce signaling. *Journal of endotoxin research* **9**, 264-268 (2003).
158. Thoma-Uszynski, S.*, et al.* Induction of Direct Antimicrobial Activity Through Mammalian Toll-Like Receptors. *Science (New York, N.Y.)* **291**, 1544-1547 (2001).
159. Lowes, M.A., Bowcock, A.M. & Krueger, J.G. Pathogenesis and therapy of psoriasis. *Nature* **445**, 866 (2007).
160. Henseler, T. & Christophers, E. Disease concomitance in psoriasis. *Journal of the American Academy of Dermatology* **32**, 982-986 (1995).
161. Griffiths, C.E.M. & Barker, J.N.W.N. Pathogenesis and clinical features of psoriasis. *The Lancet* **370**, 263-271.
162. Lowes, M.A.*, et al.* Psoriasis vulgaris lesions contain discrete populations of Th1 and Th17 T cells. *The Journal of investigative dermatology* **128**, 1207-1211 (2008).
163. Wilson, N.J.*, et al.* Development, cytokine profile and function of human interleukin 17-producing helper T cells. *Nat Immunol* **8**, 950-957 (2007).
164. Boniface, K.*, et al.* IL-22 Inhibits Epidermal Differentiation and Induces Proinflammatory Gene Expression and Migration of Human Keratinocytes. *The Journal of Immunology* **174**, 3695-3702 (2005).

165. Van Belle, A.B.*, et al.* IL-22 Is Required for Imiquimod-Induced Psoriasiform Skin Inflammation in Mice. *The Journal of Immunology* **188**, 462-469 (2012).
166. Wolk, K.*, et al.* IL-22 and IL-20 are key mediators of the epidermal alterations in psoriasis while IL-17 and IFN-γ are not. *Journal of Molecular Medicine* **87**, 523-536 (2009).
167. Leung, D.Y.M. & Bieber, T. Atopic dermatitis. *The Lancet* **361**, 151-160.
168. Leung, D.Y., Boguniewicz, M., Howell, M.D., Nomura, I. & Hamid, Q.A. New insights into atopic dermatitis. *J Clin Invest* **113**, 651-657 (2004).
169. Leung, D.Y. New insights into atopic dermatitis: role of skin barrier and immune dysregulation. *Allergology international : official journal of the Japanese Society of Allergology* **62**, 151-161 (2013).
170. Novak, N., Bieber, T. & Leung, D.Y.M. Immune mechanisms leading to atopic dermatitis. *Journal of Allergy and Clinical Immunology* **112**, S128-S139.
171. Weidinger, S. & Novak, N. Atopic dermatitis. *The Lancet* **387**, 1109-1122 (2016).
172. Hamid, Q., Boguniewicz, M. & Leung, D.Y. Differential in situ cytokine gene expression in acute versus chronic atopic dermatitis. *J Clin Invest* **94**, 870-876 (1994).
173. Grewe, M., Gyufko, K., Schopf, E. & Krutmann, J. Lesional expression of interferon-gamma in atopic eczema. *Lancet (London, England)* **343**, 25-26 (1994).
174. Grewe, M.*, et al.* A role for Th1 and Th2 cells in the immunopathogenesis of atopic dermatitis. *Immunology Today* **19**, 359-361 (1998).
175. Leyden, J.J., Marples, R.R. & Kligman, A.M. Staphylococcus aureus in the lesions of atopic dermatitis. *The British journal of dermatology* **90**, 525-530 (1974).
176. de Jongh, G.J.*, et al.* High Expression Levels of Keratinocyte Antimicrobial Proteins in Psoriasis Compared with Atopic Dermatitis. *Journal of Investigative Dermatology* **125**, 1163-1173 (2005).
177. Ong , P.Y.*, et al.* Endogenous Antimicrobial Peptides and Skin Infections in Atopic Dermatitis. *New England Journal of Medicine* **347**, 1151-1160 (2002).
178. Hwang, S.T., Janik, J.E., Jaffe, E.S. & Wilson, W.H. Mycosis fungoides and Sézary syndrome. *The Lancet* **371**, 945-957 (2008).
179. Yamashita, T., Abbade, L.P., Marques, M.E. & Marques, S.A. Mycosis fungoides and Sezary syndrome: clinical, histopathological and immunohistochemical review and update. *Anais brasileiros de dermatologia* **87**, 817-828; quiz 829-830 (2012).
180. Hoppe, R.T., Wood, G.S. & Abel, E.A. Mycosis fungoides and the Sézary syndrome: Pathology, staging, and treatment. *Current Problems in Cancer* **14**, 297-361 (1990).
181. Rappaport, H. & Thomas, L.B. Mycosis fungoides: the pathology of extracutaneous involvement. *Cancer* **34**, 1198-1229 (1974).
182. Wolk, K.*, et al.* Deficient cutaneous antibacterial competence in cutaneous T-cell lymphomas: role of Th2-mediated biased Th17 function. *Clinical cancer research : an official journal of the American Association for Cancer Research* **20**, 5507-5516 (2014).
183. Miyagaki, T.*, et al.* IL-22, but not IL-17, dominant environment in cutaneous T-cell lymphoma. *Clinical cancer research : an official journal of the American Association for Cancer Research* **17**, 7529-7538 (2011).
184. Steinhoff, M.*, et al.* Clinical, cellular, and molecular aspects in the pathophysiology of rosacea. *J Investig Dermatol Symp Proc* **15**, 2-11 (2011).
185. Powell, F.C. Clinical practice. Rosacea. *The New England journal of medicine* **352**, 793-803 (2005).
186. Crawford, G.H., Pelle, M.T. & James, W.D. Rosacea: I. Etiology, pathogenesis, and subtype classification. *Journal of the American Academy of Dermatology* **51**, 327-341 (2004).
187. Holmes, A.D. Potential role of microorganisms in the pathogenesis of rosacea. *Journal of the American Academy of Dermatology* **69**, 1025-1032 (2013).
188. Yamasaki, K.*, et al.* TLR2 expression is increased in rosacea and stimulates enhanced serine protease production by keratinocytes. *The Journal of investigative dermatology* **131**, 688-697 (2011).
189. Yamasaki, K. & Gallo, R.L. Rosacea as a disease of cathelicidins and skin innate immunity. *J Investig Dermatol Symp Proc* **15**, 12-15 (2011).
190. Yamasaki, K.*, et al.* Increased serine protease activity and cathelicidin promotes skin inflammation in rosacea. *Nat Med* **13**, 975-980 (2007).

191. Buhl, T.*, et al.* Molecular and Morphological Characterization of Inflammatory Infiltrate in Rosacea Reveals Activation of Th1/Th17 Pathways. *The Journal of investigative dermatology* **135**, 2198-2208 (2015).
192. Li, Q.F., Wang, X.R., Yang, Y.W. & Lin, H. Hypoxia upregulates hypoxia inducible factor (HIF)-3[alpha] expression in lung epithelial cells: characterization and comparison with HIF-1[alpha]. *Cell Res* **16**, 548-558 (2006).
193. Holmgren, A. Enzymatic reduction-oxidation of protein disulfides by thioredoxin. *Methods Enzymol* **107**, 295-300 (1984).
194. Boukamp, P.*, et al.* Normal keratinization in a spontaneously immortalized aneuploid human keratinocyte cell line. *The Journal of cell biology* **106**, 761-771 (1988).
195. Mosmann, T. Rapid colorimetric assay for cellular growth and survival: application to proliferation and cytotoxicity assays. *J Immunol Methods* **65**, 55-63 (1983).
196. Wienken, C.J., Baaske, P., Rothbauer, U., Braun, D. & Duhr, S. Protein-binding assays in biological liquids using microscale thermophoresis. *Nat Commun* **1**, 100 (2010).
197. Crouser, E.D.*, et al.* Gene expression profiling identifies MMP-12 and ADAMDEC1 as potential pathogenic mediators of pulmonary sarcoidosis. *American journal of respiratory and critical care medicine* **179**, 929-938 (2009).
198. Cai, Y.*, et al.* Increased complement C1q level marks active disease in human tuberculosis. *PLoS One* **9**, e92340 (2014).
199. Donnelly, R.P.*, et al.* Interleukin-26: an IL-10-related cytokine produced by Th17 cells. *Cytokine Growth Factor Rev* **21**, 393-401 (2010).
200. Rutz, M.*, et al.* Toll-like receptor 9 binds single-stranded CpG-DNA in a sequence- and pH-dependent manner. *European journal of immunology* **34**, 2541-2550 (2004).
201. Yang, J., Zhang, L., Yu, C., Yang, X.-F. & Wang, H. Monocyte and macrophage differentiation: circulation inflammatory monocyte as biomarker for inflammatory diseases. *Biomarker Research* **2**, 1-1 (2014).
202. Ohradanova-Repic, A., Machacek, C., Fischer, M.B. & Stockinger, H. Differentiation of human monocytes and derived subsets of macrophages and dendritic cells by the HLDA10 monoclonal antibody panel. *Clinical & Translational Immunology* **5**, e55 (2016).
203. Xuan, W., Qu, Q., Zheng, B., Xiong, S. & Fan, G.H. The chemotaxis of M1 and M2 macrophages is regulated by different chemokines. *Journal of leukocyte biology* **97**, 61-69 (2015).
204. Aerts-Toegaert, C.*, et al.* CD83 expression on dendritic cells and T cells: correlation with effective immune responses. *European journal of immunology* **37**, 686-695 (2007).
205. Lanier, L.L.*, et al.* CD80 (B7) and CD86 (B70) provide similar costimulatory signals for T cell proliferation, cytokine production, and generation of CTL. *The Journal of Immunology* **154**, 97 (1995).
206. Landmann, R., Muller, B. & Zimmerli, W. CD14, new aspects of ligand and signal diversity. *Microbes Infect* **2**, 295-304 (2000).
207. McKenna, K., Beignon, A.-S. & Bhardwaj, N. Plasmacytoid Dendritic Cells: Linking Innate and Adaptive Immunity. *Journal of Virology* **79**, 17-27 (2005).
208. Fukuda, T.*, et al.* Critical roles for lipomannan and lipoarabinomannan in cell wall integrity of mycobacteria and pathogenesis of tuberculosis. *mBio* **4**, e00472-00412 (2013).
209. Dhiman, R.K.*, et al.* Lipoarabinomannan Localization and Abundance during Growth of Mycobacterium smegmatis. *Journal of Bacteriology* **193**, 5802-5809 (2011).
210. Goldberg, Daniel E., Siliciano, Robert F. & Jacobs, William R., Jr. Outwitting Evolution: Fighting Drug-Resistant TB, Malaria, and HIV. *Cell* **148**, 1271-1283 (2012).
211. Koharyova, M. & Kolarova, M. Oxidative stress and thioredoxin system. *General physiology and biophysics* **27**, 71-84 (2008).
212. Arnér, E.S.J. & Holmgren, A. Physiological functions of thioredoxin and thioredoxin reductase. *European Journal of Biochemistry* **267**, 6102-6109 (2000).
213. Scott, A.*, et al.* Evaluation of the ability of LL-37 to neutralise LPS in vitro and ex vivo. *PLoS One* **6**, e26525 (2011).
214. Golec, M. Cathelicidin LL-37: LPS-neutralizing, pleiotropic peptide. *Annals of agricultural and environmental medicine : AAEM* **14**, 1-4 (2007).
215. Nograles, K.E.*, et al.* IL-22-producing "T22" T cells account for upregulated IL-22 in atopic dermatitis despite reduced IL-17-producing TH17 T cells. *The Journal of allergy and clinical immunology* **123**, 1244-1252.e1242 (2009).

216. Vonderheid, E.C.*, et al.* Update on erythrodermic cutaneous T-cell lymphoma: report of the International Society for Cutaneous Lymphomas. *Journal of the American Academy of Dermatology* **46**, 95-106 (2002).
217. Litvinov, I.V.*, et al.* Gene expression analysis in Cutaneous T-Cell Lymphomas (CTCL) highlights disease heterogeneity and potential diagnostic and prognostic indicators. *OncoImmunology* **6**, e1306618 (2017).
218. Schleussner, N.*, et al.* The AP-1-BATF and -BATF3 module is essential for growth, survival and TH17/ILC3 skewing of anaplastic large cell lymphoma. *Leukemia* **32**, 1994-2007 (2018).
219. Muls, N., Nasr, Z., Dang, H.A., Sindic, C. & van Pesch, V. IL-22, GM-CSF and IL-17 in peripheral CD4+ T cell subpopulations during multiple sclerosis relapses and remission. Impact of corticosteroid therapy. *PLOS ONE* **12**, e0173780 (2017).
220. Tchernev, G. Cutaneous Sarcoidosis: The 'Great Imitator'. *American Journal of Clinical Dermatology* **7**, 375-382 (2006).
221. Fernandez-Faith, E. & McDonnell, J. Cutaneous sarcoidosis: differential diagnosis. *Clinics in dermatology* **25**, 276-287 (2007).
222. Facco, M.*, et al.* Sarcoidosis is a Th1/Th17 multisystem disorder. *Thorax* (2010).
223. Gupta, D., Agarwal, R., Aggarwal, A.N. & Jindal, S.K. Molecular evidence for the role of mycobacteria in sarcoidosis: a meta-analysis. *European Respiratory Journal* **30**, 508 (2007).
224. Eishi, Y.*, et al.* Quantitative Analysis of Mycobacterial and Propionibacterial DNA in Lymph Nodes of Japanese and European Patients with Sarcoidosis. *Journal of Clinical Microbiology* **40**, 198-204 (2002).
225. Saboor, S.A., Saboor, S.A., McFadden, J. & Johnson, N.M. Detection of mycobacterial DNA in sarcoidosis and tuberculosis with polymerase chain reaction. *The Lancet* **339**, 1012-1015 (1992).
226. Richmond, B.W.*, et al.* Sarcoidosis Th17 Cells are ESAT-6 Antigen Specific but Demonstrate Reduced IFN-γ Expression. *Journal of Clinical Immunology* **33**, 446-455 (2013).
227. Agerberth, B.*, et al.* Antibacterial components in bronchoalveolar lavage fluid from healthy individuals and sarcoidosis patients. *American journal of respiratory and critical care medicine* **160**(1999).
228. Guirado, E. & Schlesinger, L.S. Modeling the Mycobacterium tuberculosis Granuloma - the Critical Battlefield in Host Immunity and Disease. *Frontiers in immunology* **4**, 98 (2013).
229. Guerra-Laso, J.M., Raposo-García, S., García-García, S., Diez-Tascón, C. & Rivero-Lezcano, O.M. Microarray analysis of Mycobacterium tuberculosis-infected monocytes reveals IL26 as a new candidate gene for tuberculosis susceptibility. *Immunology* **144**, 291-301 (2015).
230. Kathamuthu, G.R.*, et al.* Diminished circulating plasma and elevated lymph node culture supernatant levels of IL-10 family cytokines in tuberculous lymphadenitis. *Cytokine* (2018).
231. Qiao, D.*, et al.* ESAT-6- and CFP-10-specific Th1, Th22 and Th17 cells in tuberculous pleurisy may contribute to the local immune response against Mycobacterium tuberculosis infection. *Scandinavian journal of immunology* **73**, 330-337 (2011).
232. Yao, S.*, et al.* Differentiation, distribution and gammadelta T cell-driven regulation of IL-22-producing T cells in tuberculosis. *PLoS pathogens* **6**, e1000789 (2010).
233. Scriba, T.J.*, et al.* Distinct, specific IL-17- and IL-22-producing CD4+ T cell subsets contribute to the human anti-mycobacterial immune response. *Journal of immunology (Baltimore, Md. : 1950)* **180**, 1962-1970 (2008).
234. Ye, Z.J.*, et al.* Differentiation and recruitment of IL-22-producing helper T cells stimulated by pleural mesothelial cells in tuberculous pleurisy. *American journal of respiratory and critical care medicine* **185**, 660-669 (2012).
235. Lyadova, I.V. & Panteleev, A.V. Th1 and Th17 Cells in Tuberculosis: Protection, Pathology, and Biomarkers. *Mediators of Inflammation* **2015**, 13 (2015).
236. Torrado, E. & Cooper, A.M. IL-17 and Th17 cells in tuberculosis. *Cytokine & Growth Factor Reviews* **21**, 455-462 (2010).
237. Witte, K.*, et al.* Despite IFN-lambda receptor expression, blood immune cells, but not keratinocytes or melanocytes, have an impaired response to type III interferons:

implications for therapeutic applications of these cytokines. *Genes and immunity* **10**, 702-714 (2009).
238. Liang, S.C.*, et al.* Interleukin (IL)-22 and IL-17 are coexpressed by Th17 cells and cooperatively enhance expression of antimicrobial peptides. *The Journal of Experimental Medicine* **203**, 2271-2279 (2006).
239. Morizane, S.*, et al.* Cathelicidin antimicrobial peptide LL-37 in psoriasis enables keratinocyte reactivity against TLR9 ligands. *The Journal of investigative dermatology* **132**, 135-143 (2012).
240. Tewary, P.*, et al.* β-Defensin 2 and 3 Promote the Uptake of Self or CpG DNA, Enhance IFN-α Production by Human Plasmacytoid Dendritic Cells, and Promote Inflammation. *The Journal of Immunology* **191**, 865-874 (2013).
241. McGlasson, S.L.*, et al.* Human beta-defensin 3 increases the TLR9-dependent response to bacterial DNA. *European journal of immunology* **47**, 658-664 (2017).
242. Nagem, R.A.P.*, et al.* Crystal Structure of Recombinant Human Interleukin-22. *Structure* **10**, 1051-1062 (2002).
243. Tewary, P.*, et al.* Granulysin activates antigen-presenting cells through TLR4 and acts as an immune alarmin. *Blood* **116**, 3465-3474 (2010).
244. Biragyn, A.*, et al.* Toll-Like Receptor 4-Dependent Activation of Dendritic Cells by β-Defensin 2. *Science (New York, N.Y.)* **298**, 1025-1029 (2002).
245. Ohashi, K., Burkart, V., Flohé, S. & Kolb, H. Cutting Edge: Heat Shock Protein 60 Is a Putative Endogenous Ligand of the Toll-Like Receptor-4 Complex. *The Journal of Immunology* **164**, 558 (2000).
246. Beg, A.A. Endogenous ligands of Toll-like receptors: implications for regulating inflammatory and immune responses. *Trends in Immunology* **23**, 509-512 (2002).
247. Li, M.*, et al.* An Essential Role of the NF-κB/Toll-Like Receptor Pathway in Induction of Inflammatory and Tissue-Repair Gene Expression by Necrotic Cells. *The Journal of Immunology* **166**, 7128-7135 (2001).
248. Sabroe, I., Jones, E.C., Usher, L.R., Whyte, M.K.B. & Dower, S.K. Toll-Like Receptor (TLR)2 and TLR4 in Human Peripheral Blood Granulocytes: A Critical Role for Monocytes in Leukocyte Lipopolysaccharide Responses. *The Journal of Immunology* **168**, 4701 (2002).
249. Thoma-Uszynski, S.*, et al.* Activation of Toll-Like Receptor 2 on Human Dendritic Cells Triggers Induction of IL-12, But Not IL-10. *The Journal of Immunology* **165**, 3804 (2000).
250. Schlaepfer, E., Rochat, M.-A., Duo, L. & Speck, R.F. Triggering TLR2, -3, -4, -5, and -8 Reinforces the Restrictive Nature of M1- and M2-Polarized Macrophages to HIV. *Journal of Virology* **88**, 9769 (2014).
251. Gabrilovich, M.I.*, et al.* Disordered Toll-like receptor 2 responses in the pathogenesis of pulmonary sarcoidosis. *Clinical and experimental immunology* **173**, 512-522 (2013).
252. Wikén, M., Grunewald, J., Eklund, A. & Wahlström, J. Higher Monocyte Expression of TLR2 and TLR4, and Enhanced Pro-inflammatory Synergy of TLR2 with NOD2 Stimulation in Sarcoidosis. *Journal of Clinical Immunology* **29**, 78 (2008).
253. Woetmann, A.*, et al.* Interleukin-26 (IL-26) is a novel anti-microbial peptide produced by T cells in response to staphylococcal enterotoxin. *Oncotarget* **9**, 19481-19489 (2018).
254. Al-Attiyah, R., El-Shazly, A. & Mustafa, A.S. Comparative Analysis of Spontaneous and Mycobacterial Antigen-Induced Secretion of Th1, Th2 and Pro-Inflammatory Cytokines by Peripheral Blood Mononuclear Cells of Tuberculosis Patients. *Scandinavian journal of immunology* **75**, 623-632 (2012).
255. Lin, P.L., Plessner, H.L., Voitenok, N.N. & Flynn, J.L. Tumor Necrosis Factor and Tuberculosis. *Journal of Investigative Dermatology Symposium Proceedings* **12**, 22-25 (2007).
256. Dorhoi, A. & Kaufmann, S.H. Tumor necrosis factor alpha in mycobacterial infection. *Seminars in immunology* **26**, 203-209 (2014).
257. Wallis, R.S., Broder, M., Wong, J., Lee, A. & Hoq, L. Reactivation of Latent Granulomatous Infections by Infliximab. *Clinical Infectious Diseases* **41**, S194-S198 (2005).
258. Lee , J.-B.*, et al.* Expression of peroxiredoxin and thioredoxin in dermatological disorders. *British Journal of Dermatology* **146**, 710-712 (2002).

259. Schroeder, A.*, et al.* Targeting Thioredoxin-1 by dimethyl fumarate induces ripoptosome-mediated cell death. *Scientific reports* **7**, 43168 (2017).
260. Blair, H.A. Dimethyl Fumarate: A Review in Moderate to Severe Plaque Psoriasis. *Drugs* **78**, 123-130 (2018).
261. Arnér, E.S.J. & Holmgren, A. The thioredoxin system in cancer. *Seminars in Cancer Biology* **16**, 420-426 (2006).
262. Powis, G. & Kirkpatrick, D.L. Thioredoxin signaling as a target for cancer therapy. *Current Opinion in Pharmacology* **7**, 392-397 (2007).
263. Tiitto, L.*, et al.* Expression of the thioredoxin system in interstitial lung disease. *The Journal of Pathology* **201**, 363-370 (2003).
264. Koura, T.*, et al.* Expression of thioredoxin in granulomas of sarcoidosis: possible role in the development of T lymphocyte activation. *Thorax* **55**, 755 (2000).
265. Ji, G.Y.*, et al.* Association between TXNRD1 polymorphisms and anti-tuberculosis drug-induced hepatotoxicity in a prospective study. *Genetics and molecular research : GMR* **15**(2016).
266. Tuladhar, A. & Rein, K.S. Manumycin A Is a Potent Inhibitor of Mammalian Thioredoxin Reductase-1 (TrxR-1). *ACS medicinal chemistry letters* **9**, 318-322 (2018).
267. Raschig, J.*, et al.* Ubiquitously expressed Human Beta Defensin 1 (hBD1) forms bacteria-entrapping nets in a redox dependent mode of action. *PLoS pathogens* **13**, e1006261 (2017).
268. Rosenberger, C.*, et al.* Upregulation of Hypoxia-Inducible Factors in Normal and Psoriatic Skin. *The Journal of investigative dermatology* **127**, 2445-2452 (2007).
269. Domingo-Gonzalez, R.*, et al.* Interleukin-17 limits hypoxia-inducible factor 1alpha and development of hypoxic granulomas during tuberculosis. *JCI insight* **2**(2017).
270. Larrick, J.W.*, et al.* Human CAP18: a novel antimicrobial lipopolysaccharide-binding protein. *Infection and immunity* **63**, 1291-1297 (1995).
271. Wang, G., Mishra, B., Epand, R.F. & Epand, R.M. High-quality 3D structures shine light on antibacterial, anti-biofilm and antiviral activities of human cathelicidin LL-37 and its fragments. *Biochimica et biophysica acta* **1838**, 2160-2172 (2014).
272. Kandler, K.*, et al.* The anti-microbial peptide LL-37 inhibits the activation of dendritic cells by TLR ligands. *International Immunology* **18**, 1729-1736 (2006).
273. Means, T.K.*, et al.* The CD14 ligands lipoarabinomannan and lipopolysaccharide differ in their requirement for Toll-like receptors. *Journal of immunology (Baltimore, Md. : 1950)* **163**, 6748-6755 (1999).
274. Bao, A.*, et al.* Recombinant human IL-26 facilitates the innate immune response to endotoxin in the bronchoalveolar space of mice in vivo. *PLOS ONE* **12**, e0188909 (2017).
275. Ogura, H.*, et al.* Interleukin-17 Promotes Autoimmunity by Triggering a Positive-Feedback Loop via Interleukin-6 Induction. *Immunity* **29**, 628-636 (2008).
276. Camporeale, A. & Poli, V. IL-6, IL-17 and STAT3: a holy trinity in auto-immunity? *Frontiers in bioscience (Landmark edition)* **17**, 2306-2326 (2012).
277. Jimbo, K., Park, J.S., Yokosuka, K., Sato, K. & Nagata, K. Positive feedback loop of interleukin-1β upregulating production of inflammatory mediators in human intervertebral disc cells in vitro. *Journal of Neurosurgery: Spine* **2**, 589-595 (2005).

6 Appendix

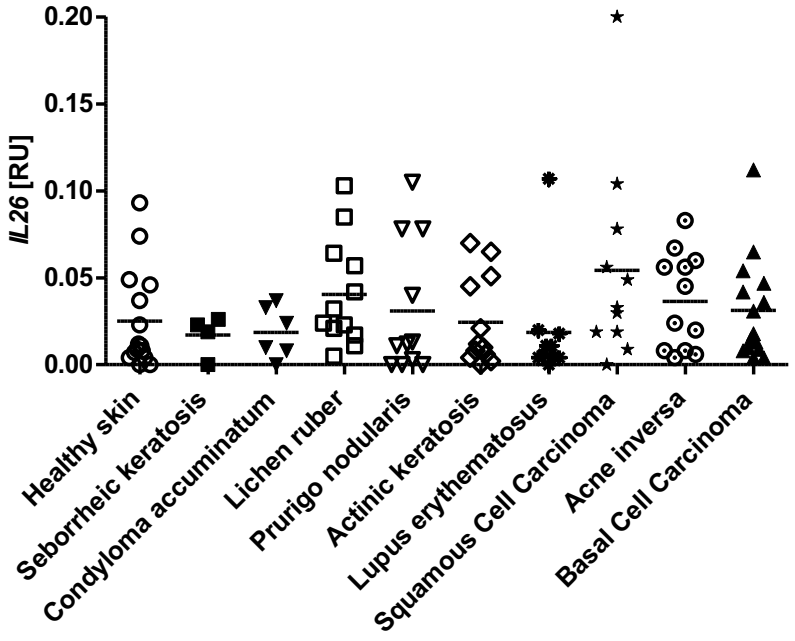

SUPPLEMENTAL FIGURE 1: Non-significant *IL26* expression in different skin diseases compared to healthy skin.

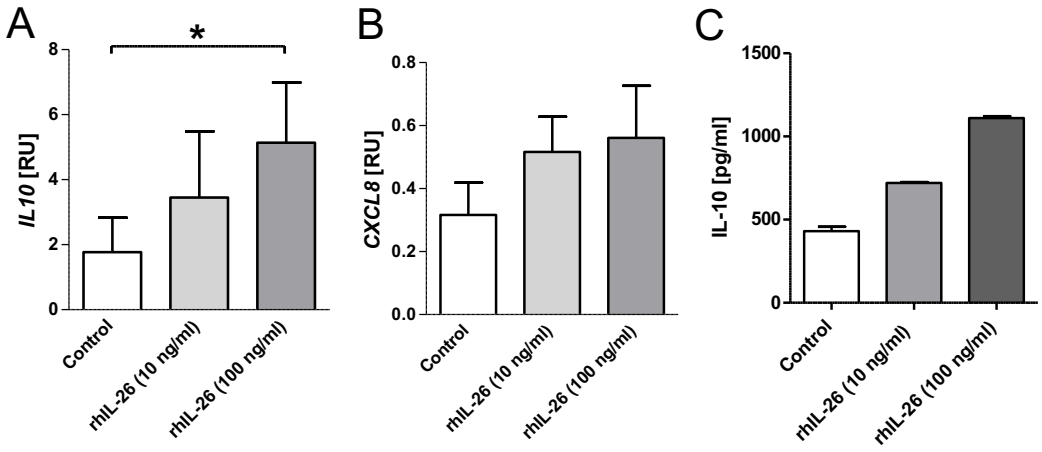

SUPPLEMENTAL FIGURE 2: Bioactivity assay of recombinant human IL-26 protein performed according to R&D Systems' bioassay protocol. IL-26 induces both *IL10* (A) and *CXCL8* (B) gene expression in Colo-205 cell line (n=6). The increased *IL10* expression also leads to an increased IL-10 secretion (C) detected via ELISA (n=1). Statistical significance was calculated using Kruskal-Wallis with Dunn's post-hoc test (* equals $P \leq 0.05$).

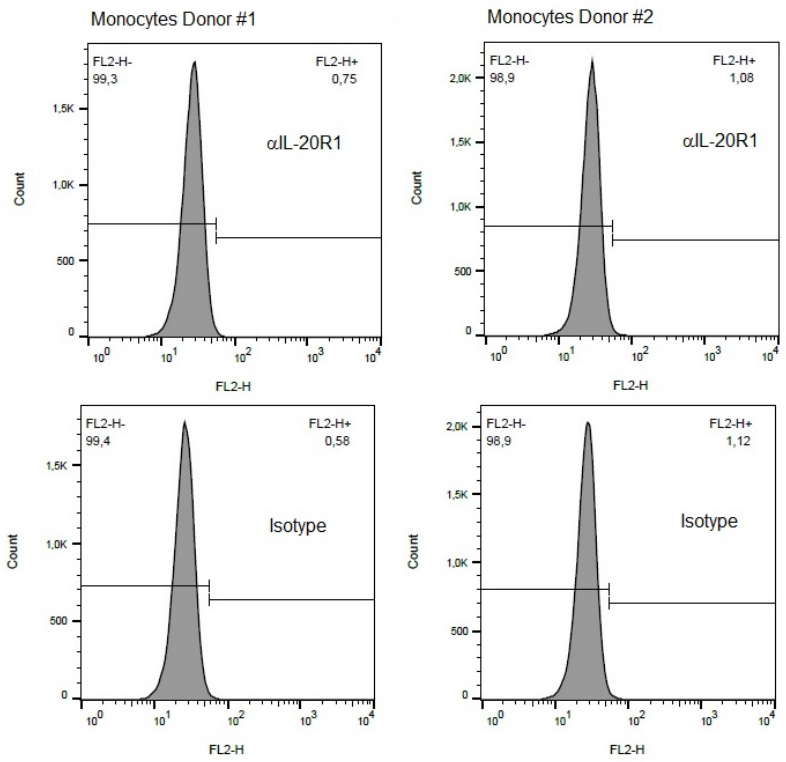

SUPPLEMENTAL FIGURE 3: $CD14^+$ monocytes do not express IL-20R1 protein on the surface. Flow cytometry results from two different buffy coat donors are depicted using anti-IL-20R1 antibody (A, B) and compared to isotype control (C, D).

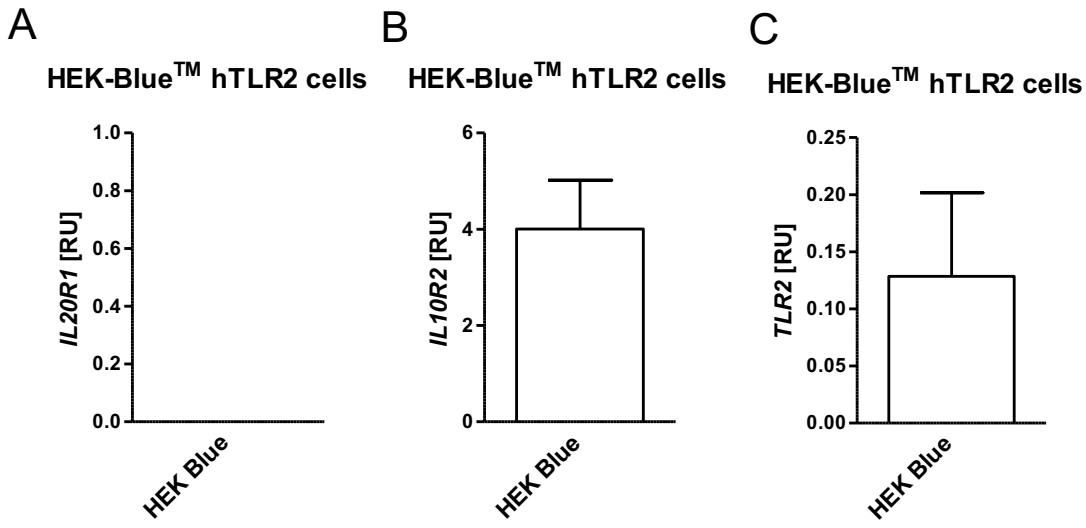

SUPPLEMENTAL FIGURE 4: HEK-Blue™ hTLR2 cells do not express *IL20R1*, but *IL10R2* and *TLR2*. QPCR results from four separate cell passages are depicted.

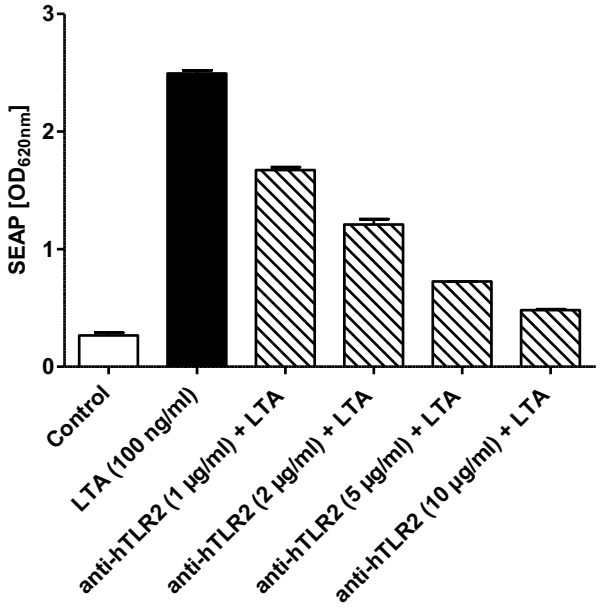

SUPPLEMENTAL FIGURE 5: Anti-TLR2 is working well, as it blocks the SEAP secretion from HEK-Blue™ hTLR2 cells stimulated with LTA nearly completely at a concentration of 10 µg/ml (n=1).

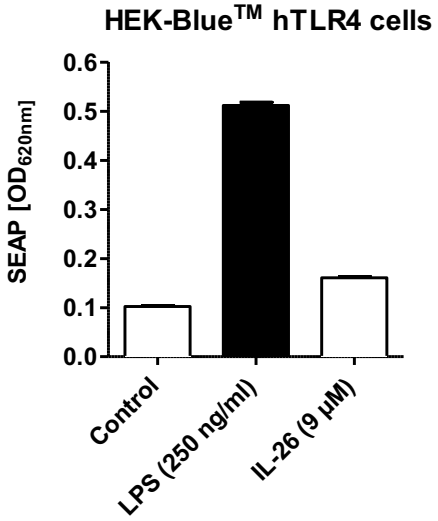

SUPPLEMENTAL FIGURE 6: IL-26 does not signal via TLR4. SEAP secretion in HEK-Blue™ hTLR4 cells expressing human TLR4 is not induced with IL-26, not even at high concentrations of 9 µM (n=1).

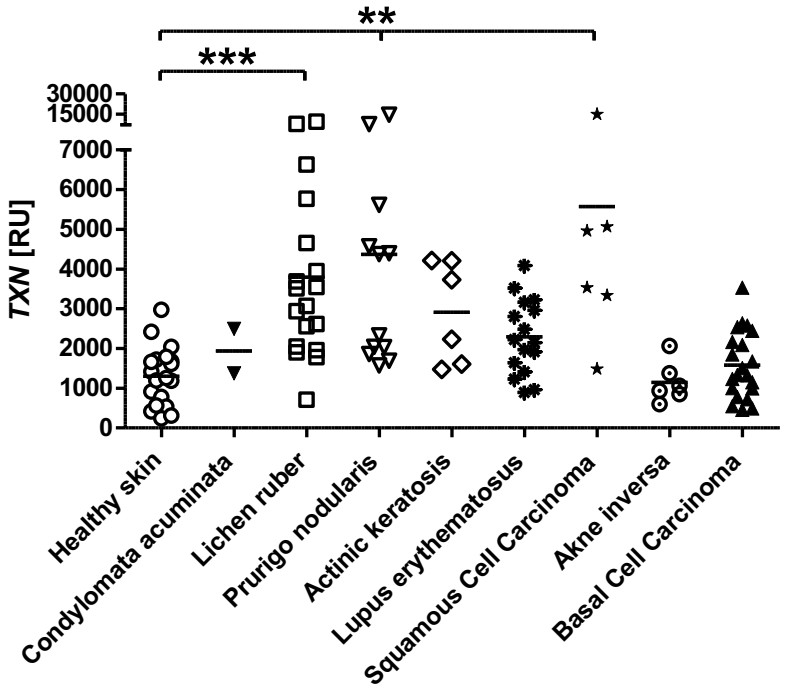

SUPPLEMENTAL FIGURE 7: *TXN* expression in different skin diseases compared to healthy skin. Kruskal Wallis test was used to calculate statistical significances.

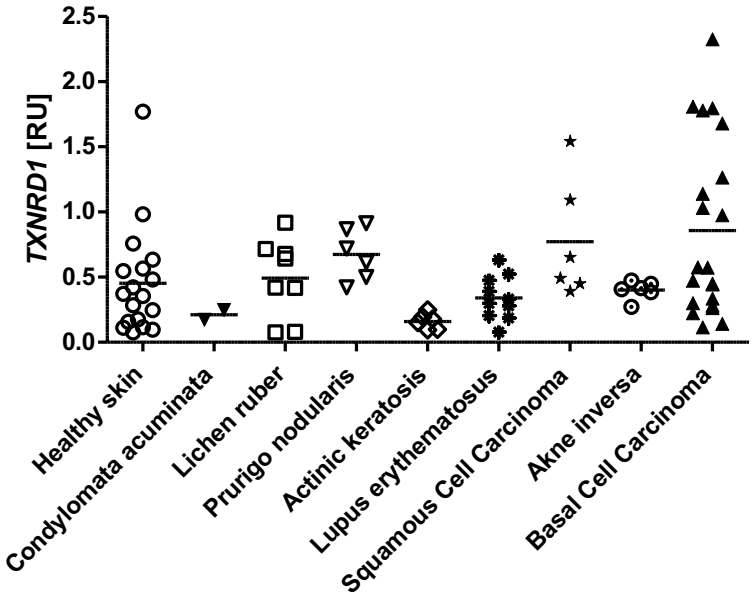

SUPPLEMENTAL FIGURE 8: *TXNRD1* expression in different skin diseases compared to healthy skin.

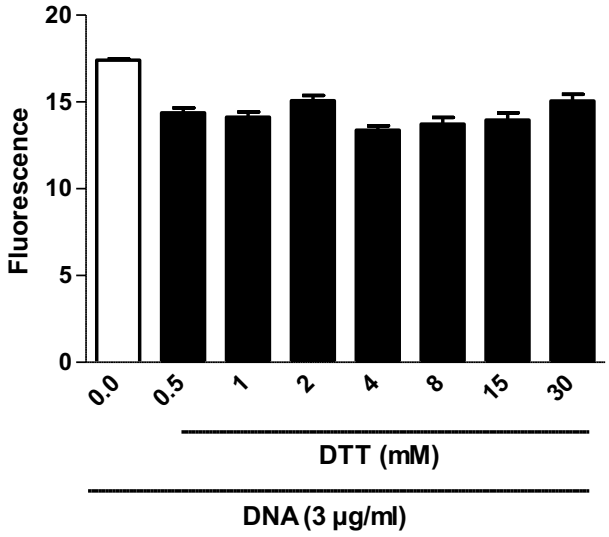

SUPPLEMENTAL FIGURE 9: DTT does not affect the nucleic acid condensation assay. Three µg/ml DNA were incubated with increasing concentration of DTT for 30 min before addition of PicoGreen dye. Fluorescence intensity at 538 nm is depicted (n=1).

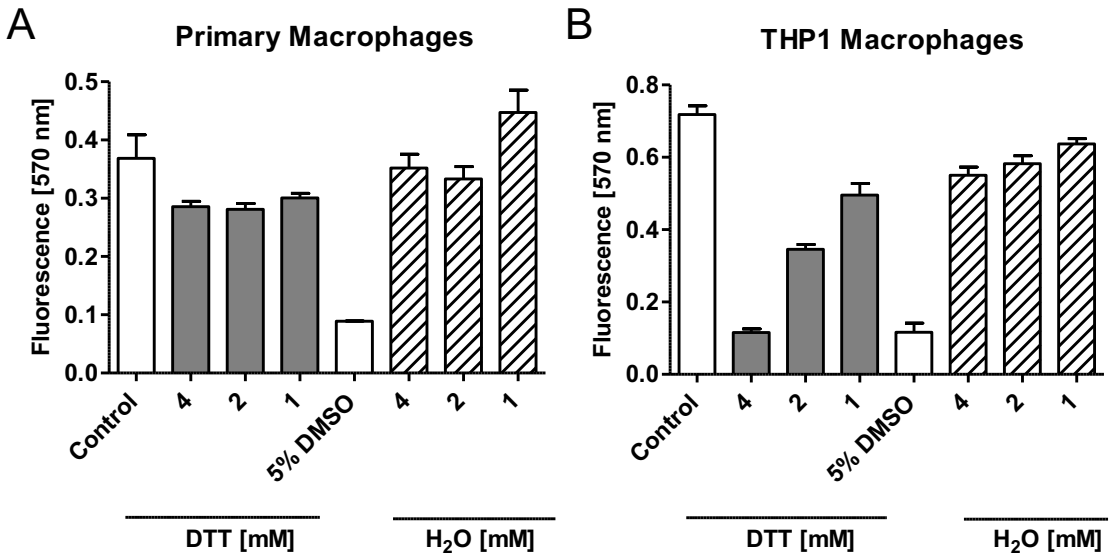

SUPPLEMENTAL FIGURE 10: DTT does not affect the viability of primary macrophages. Increasing concentration of DTT were added to primary macrophages (A) or THP1 macrophages (B) and incubated for 24h before MTT viability assay was performed. Fluorescence intensity at 570 nm is depicted (n=1).

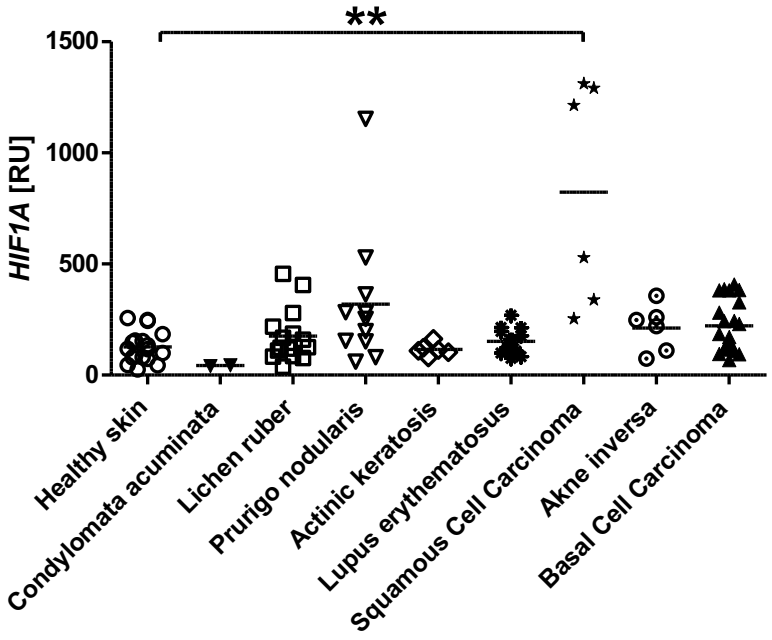

SUPPLEMENTAL FIGURE 11: *HIF1A* expression in different skin diseases compared to healthy skin. Kruskal Wallis test was used to calculate statistical significances.

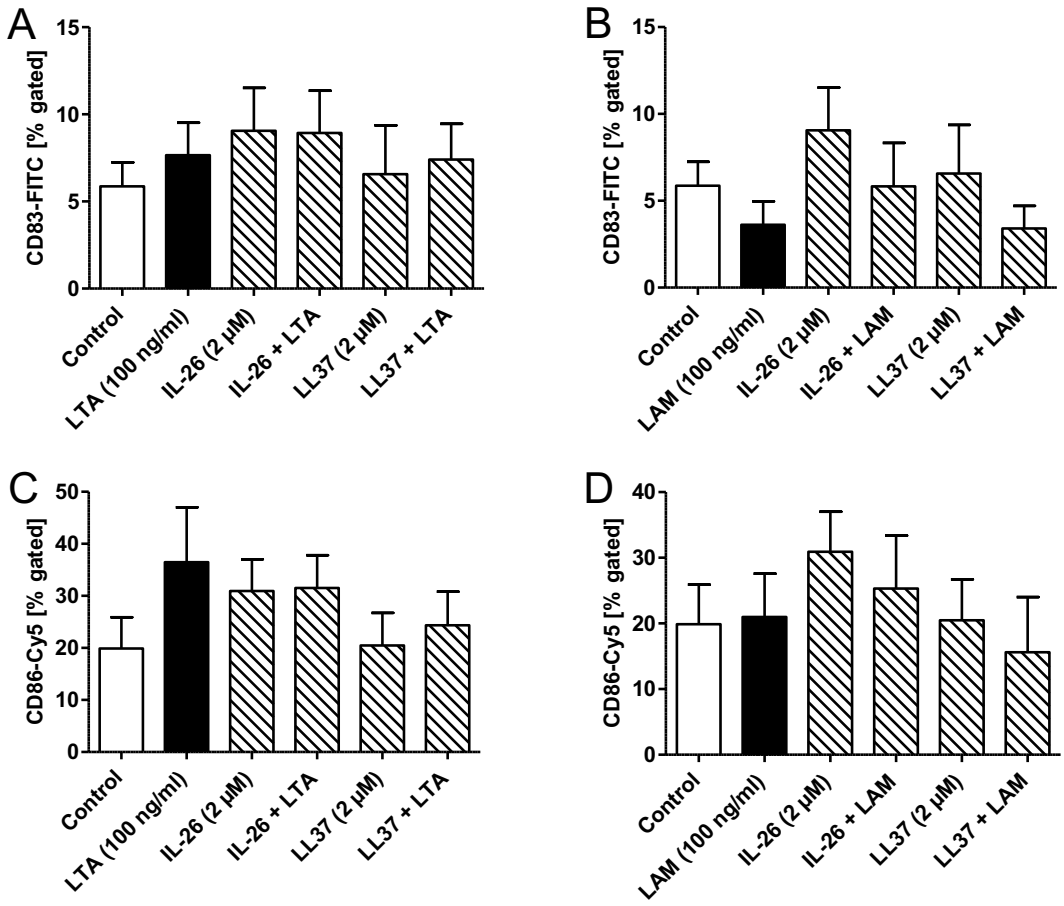

SUPPLEMENTAL FIGURE 12: LTA and LAM do not induce CD83 and CD86 surface expression. IL-26 and LL37 were individually incubated together with LTA (A, C) or LAM (B, D) for 30 min before addition to moDC culture and incubation for 24 h. The cells were then subjected to flow cytometry analysis after surface staining with anti-CD83 and anti-CD86 antibodies. Results depicted as mean + SEM of % CD83 (A, B) or CD86 (C, D) positive cells (n=3-4).

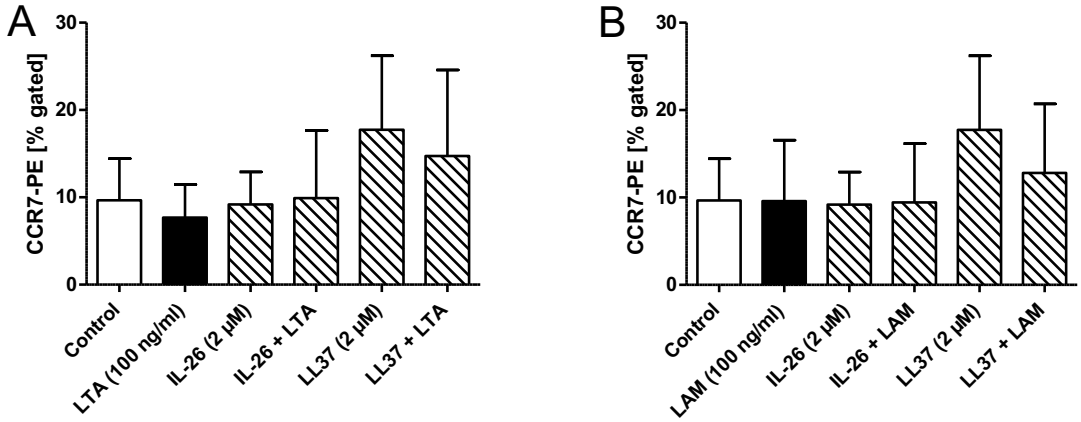

SUPPLEMENTAL FIGURE 13: LTA and LAM do not induce CCR7 on the surface of moDCs. IL-26 and LL37 were individually incubated together with LTA (A) or LAM (B) for 30 min before addition to moDC culture and incubation for 24 h. The cells were stained with anti-CCR7 antibody and analyzed via flow cytometry analysis. Results depicted as mean + SEM of % CCR7 positive cells (n=3).

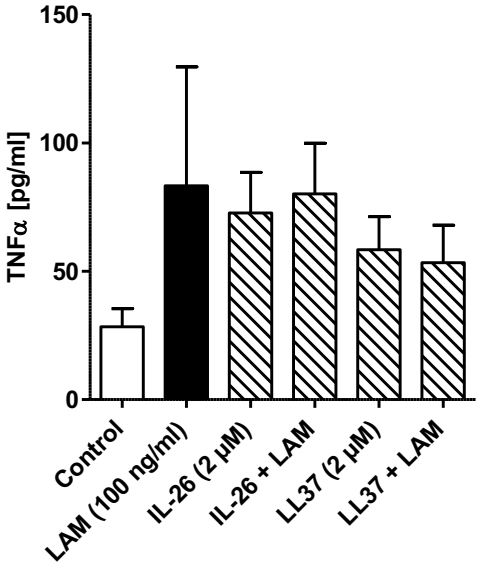

SUPPLEMENTAL FIGURE 14: LAM does not induce a strong TNF-α secretion by moDCs. IL-26 and LL37 were individually incubated together with LAM for 30 min before addition to moDC culture and incubation for 24 h. The cells supernatant was used to perform TNF-α ELISA (n=3).

7 Curriculum Vitae

The Curriculum Vitae was removed for data protection reasons.

8 Acknowledgements

First and particularly, I would like to thank PD Dr. Stephan Meller and Prof. Homey for giving me the unique opportunity to work on this interesting project for my PhD thesis. Stephan, I thank you for your guidance and patience throughout the past years. You further supported me with a great amount of freedom to try my ideas even though they might have been rather unconventional.

I thank Prof. Johannes Hegemann for the co-supervision and discussion of my thesis.

Huge thanks are dedicated to the lab technicians Micha, Ulrike and Sabine. Your technical expertise has been of priceless value for me and the experimental performance of my thesis.

In addition, I thank Kisi, Flora, Kristin, Steffi and Jule that have developed from colleagues into awesome friends. I thank you for endless vibrant discussions about everything and everybody… including science :). Guys, I think it's time for some soup at Naniwa again.

Further thanks go to my medical students Laura, Anna, Lisa and Alina (aka "the LALA-Lab") for performing their medical theses on interesting projects of which some only have been distantly associated with my PhD thesis. This way I gained deeper knowledge in subjects such as rosacea, chronic spontaneous urticaria but also PDE4- and JAK-Inhibitors. Further, you made me improve my teaching skills. Girls, you did a great job, keep going!

A project like the one present in this thesis can't be accomplished without collaborators who shared their knowledge and equipment with me. I thank Lasse and Jan from AG Kalscheuer for bringing me into the mycobacteria world and Anne Berscheid from AG Brötz-Oesterhelt for teaching me a lot about microbes and their culture. Additionally, I thank Lasse and Marc from former AG Ernst, who taught me how use a hypoxia chamber and how to do microscale thermophoresis. Further, I thank Lothar Gremer together with Prof. Schröder and his technician Jutta for explaining me patiently a lot about reduction of proteins and HPLC.

For successful collaborations on other projects I thank Alessio Mylonas, the skilled bioinformatician Péter Oláh, as well as Marius Pollet and Katharina Rolfes from the AG Haarmann-Stemmann at the IUF Düsseldorf.

I further thank the MOI Graduate School for giving me the possibility to meet great people from different parts of the world and thereby making some of the above-mentioned collaborations possible in the first place.

Not to forget my family, I thank them very much for believing in me even though my work is all Greek to them.

Finally, I cordially thank my husband for being my bastion of calm in hard times and for supporting me unconditionally.

Eidesstattliche Erklärung/Declaration

Ich versichere an Eides Statt, dass die Dissertation von mir selbständig und ohne unzulässige fremde Hilfe unter Beachtung der “Grundsatze zur Sicherung guter wissenschaftlicher Praxis an der Heinrich-Heine-Universität Düsseldorf“ erstellt worden ist. Die Dissertation wurde in der vorgelegten oder in ähnlicher Form noch bei keiner anderen Institution eingereicht. Ich habe keinen Doktorgrad an einer anderen Hochschule erworben oder zu erwerben versucht. Zitate wurden kenntlich gemacht.

I declare under oath that I have compiled my dissertation independently and without any undue assistance by third parties under consideration of the ‘Principles for the Safeguarding of Good Scientific Practice at Heinrich Heine University Düsseldorf’. This dissertation has not been submitted in the same or similar form to other institutions. I have not previously failed a doctoral examination procedure. Citations are marked.

Düsseldorf, _____ _____

(Heike Hawerkamp)